



SWITCHABLE AND TUNABLE LIGANDS FOR HOMOGENEOUS CATALYSIS
Maria Dolores Segarra Maset

ISBN: 978-84-693-7666-9
Dipòsit Legal: T-1755-2010

ADVERTIMENT. La consulta d'aquesta tesi queda condicionada a l'acceptació de les següents condicions d'ús: La difusió d'aquesta tesi per mitjà del servei TDX (www.tesisenxarxa.net) ha estat autoritzada pels titulars dels drets de propietat intel·lectual únicament per a usos privats emmarcats en activitats d'investigació i docència. No s'autoritza la seva reproducció amb finalitats de lucre ni la seva difusió i posada a disposició des d'un lloc aliè al servei TDX. No s'autoritza la presentació del seu contingut en una finestra o marc aliè a TDX (framing). Aquesta reserva de drets afecta tant al resum de presentació de la tesi com als seus continguts. En la utilització o cita de parts de la tesi és obligat indicar el nom de la persona autora.

ADVERTENCIA. La consulta de esta tesis queda condicionada a la aceptación de las siguientes condiciones de uso: La difusión de esta tesis por medio del servicio TDR (www.tesisenred.net) ha sido autorizada por los titulares de los derechos de propiedad intelectual únicamente para usos privados enmarcados en actividades de investigación y docencia. No se autoriza su reproducción con finalidades de lucro ni su difusión y puesta a disposición desde un sitio ajeno al servicio TDR. No se autoriza la presentación de su contenido en una ventana o marco ajeno a TDR (framing). Esta reserva de derechos afecta tanto al resumen de presentación de la tesis como a sus contenidos. En la utilización o cita de partes de la tesis es obligado indicar el nombre de la persona autora.

WARNING. On having consulted this thesis you're accepting the following use conditions: Spreading this thesis by the TDX (www.tesisenxarxa.net) service has been authorized by the titular of the intellectual property rights only for private uses placed in investigation and teaching activities. Reproduction with lucrative aims is not authorized neither its spreading and availability from a site foreign to the TDX service. Introducing its content in a window or frame foreign to the TDX service is not authorized (framing). This rights affect to the presentation summary of the thesis as well as to its contents. In the using or citation of parts of the thesis it's obliged to indicate the name of the author.

UNIVERSITAT ROVIRA I VIRGILI
SWITCHABLE AND TUNABLE LIGANDS FOR HOMOGENEOUS CATALYSIS
Maria Dolores Segarra Maset
ISBN:978-84-693-7666-9/DL:T-1755-2010

UNIVERSITAT ROVIRA I VIRGILI
SWITCHABLE AND TUNABLE LIGANDS FOR HOMOGENEOUS CATALYSIS
Maria Dolores Segarra Maset
ISBN:978-84-693-7666-9/DL:T-1755-2010

María Dolores Segarra Maset

**SWITCHABLE AND TUNABLE LIGANDS FOR
HOMOGENEOUS CATALYSIS**

PHD THESIS

Supervised by:

Dr. Piet W. N. M. van Leeuwen

Dr. Zoraida Freixa Fernandez

(ICIQ-Universitat Rovira i Virgili)

Tarragona

2010



UNIVERSITAT ROVIRA I VIRGILI

UNIVERSITAT ROVIRA I VIRGILI
SWITCHABLE AND TUNABLE LIGANDS FOR HOMOGENEOUS CATALYSIS
Maria Dolores Segarra Maset
ISBN:978-84-693-7666-9/DL:T-1755-2010



UNIVERSITAT ROVIRA I VIRGILI

Dr. Piet W. N. M. van Leeuwen, “Group Leader” en el Instituto Catalán de Investigación Química (ICIQ), y

Dr. Zoraida Freixa Fernandez, “Group Coordinator” en el Instituto Catalán de Investigación Química (ICIQ),

CERTIFICAN:

Que el presente trabajo, titulado “Switchable and Tunable Ligands for Homogeneous Catalysis”, que presenta María Dolores Segarra Maset para la obtención del título de Doctor, ha sido realizado bajo nuestra dirección en el grupo de investigación correspondiente en el Instituto Catalán de Investigación Química (ICIQ-URV), y que cumple los requisitos para poder optar a la Mención Europea.

Tarragona, Julio 2010

Dr. P.W.N.M. van Leeuwen

Dr. Z. Freixa

UNIVERSITAT ROVIRA I VIRGILI
SWITCHABLE AND TUNABLE LIGANDS FOR HOMOGENEOUS CATALYSIS
Maria Dolores Segarra Maset
ISBN:978-84-693-7666-9/DL:T-1755-2010

AGRADECIMIENTOS

ACKNOWLEDGEMENTS

Son muchas las personas que, a lo largo de estos años, han contribuido de algún modo al desarrollo de esta tesis. A todas ellas, quisiera darles mi más sincero agradecimiento. Espero no olvidar a nadie.

En primer lugar a mis directores de tesis por su dedicación y darme la oportunidad de realizar esta tesis bajo su supervisión.

Gracias Piet por permitirme aprender a tu lado, por tener siempre la puerta abierta para nosotros y hacer posible la llegada de este día.

A Zoraida. Son muchas, muchísimas cosas las que hemos vivido desde el inicio de esta aventura. Has sido mi guía, y no imagino una persona más adecuada para tal cometido. Gracias por enseñarme, animarme en los malos momentos, hacerme disfrutar en los buenos, y creer en mí.

Josep María, te diría tantas cosas por las que estoy agradecida que me he quedado sin palabras. Ya lo sabes, así que simplemente gracias.

A Marta M., por hacerme la escritura más llevadera, y a María José. Gracias por estar siempre dispuestas a ayudar para que los rollos administrativos no sean tan rollos. Sois las mejores “secres” (¡y amigas!).

A todas las personas que han pasado por el laboratorio durante estos años: Sergio, Mathieu, Sara (¡mi “niña”!), Xavi, Pascal, Henrik, David R., David G., Marta S., Angelica, Olivier, Thomas, Nick, Emanuele, Mariu,... ¡Sois los mejores!

Gracias a los técnicos de ICIQ: Enrique, Simona, Fernando, Susana, (y los desayunos, ¡por supuesto! No m’olvido de Laia!) Gabriel, Kerman, Gisela, Mariona, Marta G., Yvette (¡por los buenos momentos de los cursos de doctorado!), Eduardo,

Jordi, Marta M., Noemi, Alba, Jon,...

También quiero agradecer a los compañeros de ICIQ que me han ayudado en momentos críticos. A M^a Ángeles, Ana y Héctor, siempre dispuestos a echar una mano. Especialmente a Eli que me redescubrió el gNMR. A Silvia (y Rafa), por hacerme sentir como en casa. A Loli, Juana, Sadey, por hacer más llevaderas las “horas extra”.

Todo esto empezó mucho antes de mi llegada a ICIQ. No puedo olvidarme de las personas con las que comencé en el mundo de la investigación, sobre todo, a quién me dio la oportunidad de entrar en su laboratorio, e iniciar la carrera investigadora: gracias, Rosa, por aceptarme en tu grupo y aconsejarme siempre sabiamente.

Eva, contigo he compartido la química más tiempo que con nadie, ¡y espero que sigamos compartiendo muchas más experiencias! A Marta, Sonia (te echaré mucho de menos este día), Cristian, Sergey,... . A Sixte, gràcies per enviar-me un poc de la terreta cada setmana.

I am very grateful to Prof. Chris Hunter for giving me the opportunity to learn about supramolecular chemistry at his group. Thanks also to all the people in his lab: Cristina y Rafel, gracias por ayudarme a comprender un poco más “la supra” (and Lisa!). Simon, Lorna, Jo, Daniele, Marina, Basirat, Fede, Jordan,... Thanks to make my stay in Sheffield unforgettable!

Y siguiendo con la química supramolecular, quisiera agradecer también al Prof. Pau Ballester, por su paciencia al resolver mis dudas sobre esta área a la que nos hemos querido asomar en esta tesis.

I cannot forget the “delighting” week in Eindhoven. Thanks a lot to Dr. Christian Müller for your advices, the fantastic results that we achieved, and for discovering me the amazing raclette! Thanks to Dr. Martin Lutz from Utrecht University (The Netherlands) for the X-Ray measurements.

No podría haber llegado aquí sin la ayuda de mi familia y amigos. Aunque en la distancia, siempre me han animado y apoyado a seguir adelante. Muchas gracias a todos por estar ahí cuando regreso a casa.

Nadie me comprende mejor que Marta. Siempre estás dispuesta a escucharme, y

te estoy eternamente agradecida por todo tu apoyo. Aunque estemos lejos, estaremos siempre unidas.

Gracias a mi sobrina Sara, por su paciencia conmigo durante el diseño de la portada, ¡y el mejor de los resultados! Te has convertido en una mujer extraordinaria, y estoy muy orgullosa de ti.

A mis hermanas, porque soy un poquito de las dos, y son mis pilares en la vida.

A la persona más valiente y luchadora que conozco: mi madre. Ha sido el mejor ejemplo a seguir para no rendirme ante las adversidades. Gracias por tus siempre acertadas palabras.

Por último, a Guzman, gracias por venir a vivir mi sueño. Gracias por ayudarme a seguir adelante cuando creía que ya no podía caminar. Por animarme, por darme ilusión. No podría haber llegado hasta aquí sin ti.

María Dolores

El trabajo desarrollado en la presente Tesis Doctoral ha sido posible gracias a la financiación del Institut Català d'Investigació Química (ICIQ), el Ministerio de Educación y Ciencia (Programas FPU AP2005-3339, Ramón y Cajal), y se ha desarrollado dentro del marco de los proyectos BAECH CTQ2005-03416/BQU, INNOCAT CTQ2008-00683 e INTECAT (CSD2006-003) perteneciente al programa Consolider Ingenio 2010.



UNIVERSITAT ROVIRA I VIRGILI



UNIVERSITAT ROVIRA I VIRGILI
SWITCHABLE AND TUNABLE LIGANDS FOR HOMOGENEOUS CATALYSIS
Maria Dolores Segarra Maset
ISBN:978-84-693-7666-9/DL:T-1755-2010

UNIVERSITAT ROVIRA I VIRGILI
SWITCHABLE AND TUNABLE LIGANDS FOR HOMOGENEOUS CATALYSIS
Maria Dolores Segarra Maset
ISBN:978-84-693-7666-9/DL:T-1755-2010

*A mi madre
... y a mis hermanas*

UNIVERSITAT ROVIRA I VIRGILI
SWITCHABLE AND TUNABLE LIGANDS FOR HOMOGENEOUS CATALYSIS
Maria Dolores Segarra Maset
ISBN:978-84-693-7666-9/DL:T-1755-2010

CONTENTS

	Preface: structure of the thesis	v
	Objectives of the thesis	1
Part I	Light Switchable Phosphines	
Chapter 1	Introduction	5
Chapter 2	Design, synthesis and proof of concept	25
	2.1. Introduction and objectives	25
	2.2. Synthesis	30
	2.3. Switchable behaviour	39
	2.4. Concluding remarks	48
Chapter 3	Catalysis	53
	3.1. Introduction and objectives	53
	3.2. Catalysis	55
	3.2.1. Palladium catalyzed Suzuki cross-coupling	55
	3.2.2. Rhodium catalyzed hydrosilylation of ketones	60
	3.2.3. Palladium catalyzed allylic alkylation	67
	3.2.4. Rhodium catalyzed hydroformylation	76
	3.3. Concluding remarks	95
Chapter 4	Experimental	103
	4.1. General procedures	103
	4.2. Synthesis	104
	4.3. Photochemical processes	111
	4.4. UV-vis studies	111
	4.5. Catalysis	111
	4.6. HP-NMR	116

Part II Supramolecular, Tunable Diphosphines

Chapter 5	Introduction	121
Chapter 6	Results and discussion	143
	6.1. Introduction and objectives	143
	6.2. Results and discussion	146
	6.2.1. Synthesis of the functionalized biaryl phosphines	146
	6.2.2. Supramolecular studies	149
	6.2.3. Catalysis: asymmetric hydrogenation	167
	6.3. Concluding remarks	181
Chapter 7	Experimental	187
	7.1. General procedures	187
	7.2. Synthesis	188
	7.3. NMR titrations	191
	7.4. Catalysis: asymmetric hydrogenation	192

Part III *trans*-Bidentate Supramolecular and Switchable Ligands

Chapter 8	Introduction	197
Chapter 9	Results and discussion	213
	9.1. Introduction and objectives	213
	9.2. Synthesis	216
	9.2.1. Synthesis of the supramolecular ligands	216
	9.2.2. Synthesis of the switchable ligands	220
	9.3. Concluding remarks	225

Chapter 10	Experimental	227
	10.1. General procedures	227
	10.2. Synthesis	228
	Concluding remarks of the thesis	237
	Appendix I: MM2 Structure optimizations	239
	Appendix II: Compounds index	243
	Abbreviations	249

UNIVERSITAT ROVIRA I VIRGILI
SWITCHABLE AND TUNABLE LIGANDS FOR HOMOGENEOUS CATALYSIS
Maria Dolores Segarra Maset
ISBN:978-84-693-7666-9/DL:T-1755-2010

PREFACE

STRUCTURE OF THE THESIS

*T*hose who have followed the research during my PhD will be surprised not to find the initial projects that we started some years ago. This Thesis has evolved along the years, and without those projects, not reflected here, it would have been impossible to arrive at the present stage. Those initial projects helped me to grow as a scientist, solving problems and learning many techniques. After the initial years, we decided to turn our attention to more challenging enterprises, and those latter investigations are the ones reported in this Thesis.

The aim of the research was the design and development of new ligands for homogeneous catalysis. More specifically, we wanted to make ligands with adjustable and/or switchable properties that were unprecedented in literature. To achieve this goal, three major strategies have been adopted. Consequently, the structure of the Thesis has been divided in three main parts, each of them divided in three or four chapters, following the same structure.

Part I is formed by chapters 1, 2, 3 and 4. This part is devoted to the design, synthesis, and catalytic applications of light switchable phosphines. The switchability is accomplished by building an azobenzene moiety in the structure of the phosphines.

Part II consists of chapters 5, 6 and 7. In these chapters the study focuses on the use of supramolecular interactions to induce chirality in diphosphines. The project involves the synthesis of a *tropos* biaryl diphosphine. This diphosphine can be tuned using several chiral modifiers, which are able to interact with the diphosphine via supramolecular interactions. The studies involving supramolecular interactions have been carried out during a three months stage in Prof. Chris Hunter's group (University of Sheffield, UK).

Part III is divided in chapter 8, 9 and 10. This last part describes an ongoing project devoted to the design and synthesis of *trans*-bidentate phosphinines and pyridines. This is achieved incorporating switchable moieties in the structure of the ligands or by means of supramolecular hydrogen bonding interactions. Following a previous open project, this research is done in collaboration with Dr. Christian Müller (Technische Universiteit Eindhoven, The Netherlands).

As explained here, each part of the Thesis is devoted to a different project. For that reason each part contains its own aims and conclusions.

I wish to the reader an exciting and pleasant time while reading this Thesis.

OBJECTIVES OF THE THESIS

The general objectives of this Thesis entitled “Switchable and Tunable Ligands for Homogeneous Catalysis” are:

Part I

- Synthesis of new photosensitive phosphine ligands. To that end the azobenzene function will be incorporated in phosphines.
- Study of the switchability of these ligands and their metal complexes by different techniques.
- Study the effect of the ligands switch triggered by light in several catalytic reactions.

Part II

- Design and synthesis of supramolecular assembled ligands, formed by a generic *tropos* diphosphine backbone and several chiral modifiers, which are expected to induce chirality to the diphosphine.
- Evaluation of the binding constants of the supramolecular systems.
- Test the performance of the supramolecular ligands in asymmetric catalysis.

Part III

- Design and synthesis of bidentate phosphinine and pyridine ligands constructed by hydrogen bonding supramolecular interactions, which give preferentially *trans*-coordination to the metal.
- Design and synthesis of light switchable bidentate phosphinine and pyridine ligands, which give preferentially *trans*-coordination to the metal after isomerization of the azobenzene backbone incorporated in the molecule.

UNIVERSITAT ROVIRA I VIRGILI
SWITCHABLE AND TUNABLE LIGANDS FOR HOMOGENEOUS CATALYSIS
Maria Dolores Segarra Maset
ISBN:978-84-693-7666-9/DL:T-1755-2010

PART I

LIGHT SWITCHABLE PHOSPHINES

UNIVERSITAT ROVIRA I VIRGILI
SWITCHABLE AND TUNABLE LIGANDS FOR HOMOGENEOUS CATALYSIS
Maria Dolores Segarra Maset
ISBN:978-84-693-7666-9/DL:T-1755-2010

CHAPTER 1

INTRODUCTION

Molecular switches and light: azobenzenes

Molecular switches are molecules that can be converted from one (meta)stable state to another and *vice versa*. This change (or switch) can be triggered by external stimuli such as light, heat, pressure, electric or magnetic fields, etc. In particular, nature relies on light induced switches to regulate many biological functions. Numerous examples of synthetic analogues (spiropyrans, azobenzenes, diarylethene, etc.) have been used to modify properties of materials at will by irradiation (Figure 1. 1).¹⁻⁷

Probably, the structurally simplest light-switchable molecules are azobenzene derivatives. Since their discovery almost two centuries ago,⁸ the reddish colour of azobenzenes prompted their use as molecular dyes.⁹⁻¹¹ More recently the number of applications utilizing their photochromic properties has increased enormously. Azobenzenes can be interconverted between two (meta)stable forms: *E* azobenzene and *Z* azobenzene. These structurally different isomers show distinct properties. Switching between the two forms is triggered by irradiation at the appropriate light wavelength. When UV light is used the *E* isomer, the thermodynamically more stable one, undergoes a conformational change to the *Z* isomer. The reverse process can be induced by visible light or heat (Scheme 1. 1).

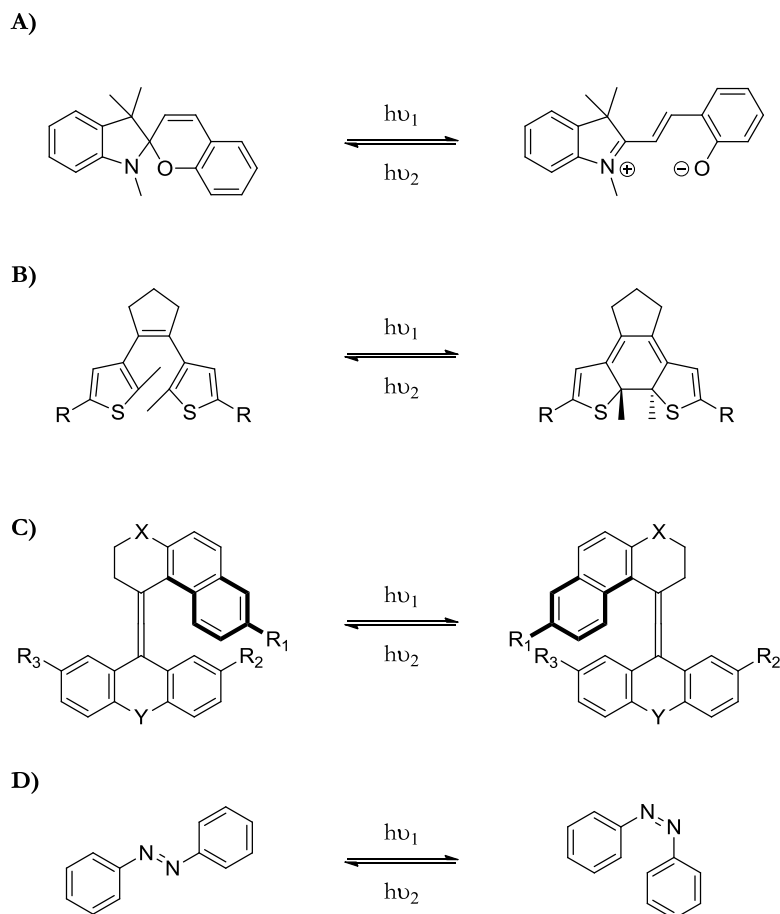
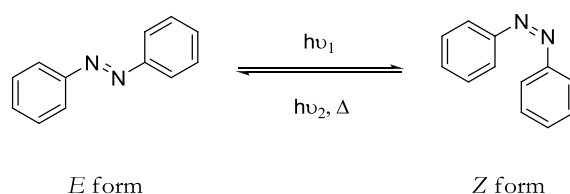


Figure 1. 1. Examples of molecular switches triggered by light: **A)** spiropyran, **B)** diarylethene, **C)** chiroptical switch developed by Feringa *et al.*¹² and **D)** azobenzene.

Several recently reported articles show how this structural change at the molecular level is reflected in macroscopic properties. Thus, the idea of using light to modify properties of materials based on azobenzene moieties has become very attractive nowadays, as for example, for the development of molecular machines.^{13,14}

One of these examples was developed by Baigl *et al.* They were able to photocontrol the motion of a droplet, enabling the development of microsystems for light-driven fluidics.¹⁵ The photoinduced isomerization of azobenzenes can also be applied in the solid state. Koshima *et al.* reported a crystalline azobenzene derivative

that can generate mechanical motion of the entire microcrystal upon irradiation.¹⁶ The same principle was applied in the development of photodriven plastic motors. The examples studied are based on polymers with azobenzenes aligned along the structure able to change the shape of the laminated layer when exposed to the incident light.^{17,18}



Scheme 1. 1. Light mediated azobenzene isomerization.

Nowadays, azobenzene derivatives are also used in molecules with biochemical applications. For example, when incorporated in biological structures, the switch between the two azobenzene isomers can generate a reversible change in the scaffolds of some peptides and DNA, turning on and off their biological functions, or even interrupting DNA transcription.^{19,20} Dohno *et al.* described a photoswitchable azobenzene derivative that acts as a glue to self-assemble DNA (Figure 1. 2).²¹

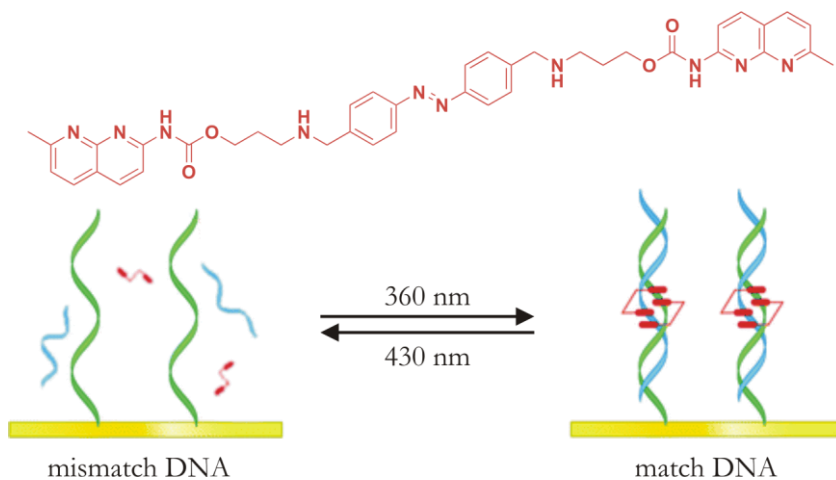


Figure 1. 2. Azobenzene derivative used as DNA glue.

Another biological application that was reported recently is the use of the acrylamide-azo-quaternary ammonium as an amphiphilic molecule that target tetrameric voltage-gated ion channels. The *E* isomer fits in the channel and its ammonium group blocks the transport, while the *Z* isomer does not fit and allows normal transport. The azobenzene derivative acts as a photochromic neuromodulator of the potassium ion channels of the membranes.²²

Studying azobenzene isomerization

Before embarking on the application of azobenzenes it is worth having a look at the studies on their photochemical behaviour.

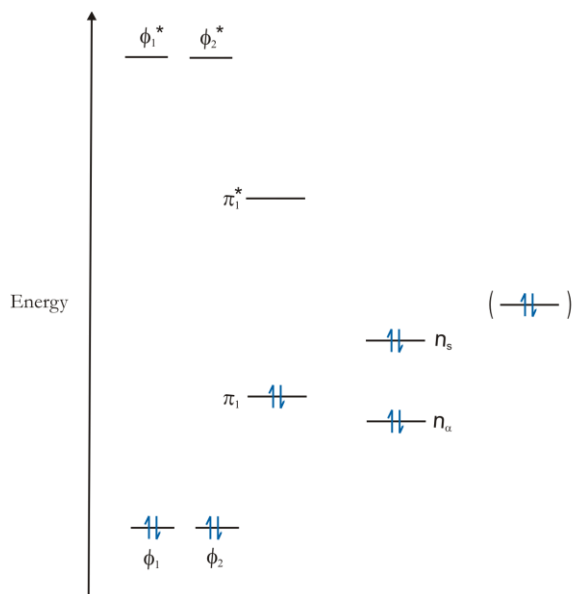


Figure 1. 3. MO Energy diagram for the azobenzene system. The orbital in parentheses is present only in azobenzenes containing a substituent with lone-pair electrons in conjugation with the π -electron system.

Hartley discovered that when a solution of *E* azobenzene was exposed to bright sunlight, a new species was generated, which showed a different melting point and

dipole moment compared to the parent compound.^{23–25} This new species was associated with *Z* azobenzene, the geometrical isomer. It was not until many years later that the influence of the wavelength of the incident light used or the temperature on the isomerization process was studied.^{26–28} Trying to evaluate the reversibility of the process, Zimmerman *et al.* made quantitative measurements to have an idea of the quantum yield as a function of the wavelength used for the irradiation.²⁹

To characterize the behaviour of such molecules towards irradiation, first of all, the excited states of *E* and *Z* azobenzene have to be described. In Figure 1. 3 are presented the molecular orbitals of the azobenzene molecule.³⁰

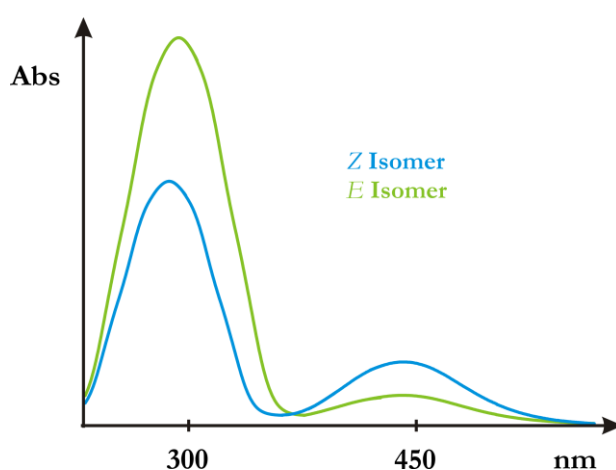
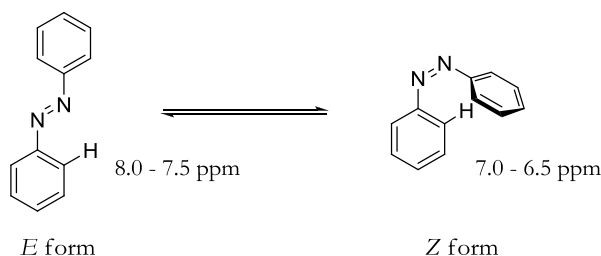


Figure 1. 4. Representation of the change in the UV-vis absorption band for the *E* and *Z* azobenzene isomers.

Two main accessible excited states are observed for the azobenzene molecule, corresponding both to two absorption bands detectable in the visible and near UV spectrum. The less intense transition is observed in the visible region at a wavelength around 430 nm ($\epsilon \sim 1500$) for *Z* azobenzene and around 440 nm ($\epsilon \sim 500$) for the *E* isomer. It corresponds to an $n_s \rightarrow \pi_1^*$, partly forbidden, transition. The highest energy transition occurs in the UV spectra and is observed around 280 nm ($\epsilon \sim 5100$) for *Z* azobenzene and 314 nm ($\epsilon \sim 17000$) for *E* azobenzene. This transition corresponds to an allowed $\pi_1 \rightarrow \pi_1^*$ process. All these transitions are clearly observed when

measuring and comparing the UV-vis spectra for both isomers as depicted in Figure 1. 4.^{26,31}



Scheme 1. 2. Change in the $^1\text{H-NMR}$ chemical shift of the *ortho* proton upon isomerization.

The difference between the spectra of the two isomers is mainly due to the non-planar configuration of the *Z* isomer. In *E* azobenzene, the extended aromaticity of the molecule makes that the whole system adopts a planar conformation. When isomerization occurs, one of the aromatic rings experiments a rotation of 56° with respect to the plane described by the $\text{N}=\text{N}-\text{C}$ moiety. This affects mainly the protons that are positioned *ortho* with respect to the azo double bond, as in the *Z* conformation they are influenced by the electronic system of the other aromatic ring.³² This effect is clearly shown in the $^1\text{H-NMR}$ spectra, because the signal is shifted 1 ppm upfield upon irradiation (Scheme 1. 2). This effect has been widely studied, and techniques were developed by which a laser is applied to irradiate the sample while the NMR spectra are being measured.³³

Azobenzene isomerization mechanisms

In the 70s several studies were devoted to the elucidation of the isomerization mechanism. The way how this twisting of the aromatic ring takes place during the isomerization is still not clear nowadays. Two main approaches are considered (Figure 1. 5).³⁴⁻³⁷

In the first mechanism, named the *inversion mechanism*, the isomerization is supposed to take place by a flip-flop inversion of one of the nitrogen atoms of the

azo double bond. In the transition state calculated for this process, the double bond remains intact, but the nitrogen atom involved undergoes rehybridization from sp^2 to sp . This mechanism is supported by theoretical calculations, and involves the $n_s \rightarrow \pi_1^*$ transition.

The second mechanism, named *rotation mechanism*, involves a rotation around the bond between the two nitrogen atoms and in order to do so, a dipolar transition state needs to be generated. In this case, the presence of push-pull substituents in the 4- and 4'- positions of (the substituted) azobenzene (with strong electron-donating and electron-attracting effects on the molecule) will favour the formation of the dipole, thus decreasing the energy barrier for the isomerization process. In the same manner, the polar character of the solvent used will influence the process. The $\pi_1 \rightarrow \pi_1^*$ transition is involved in this mechanism.

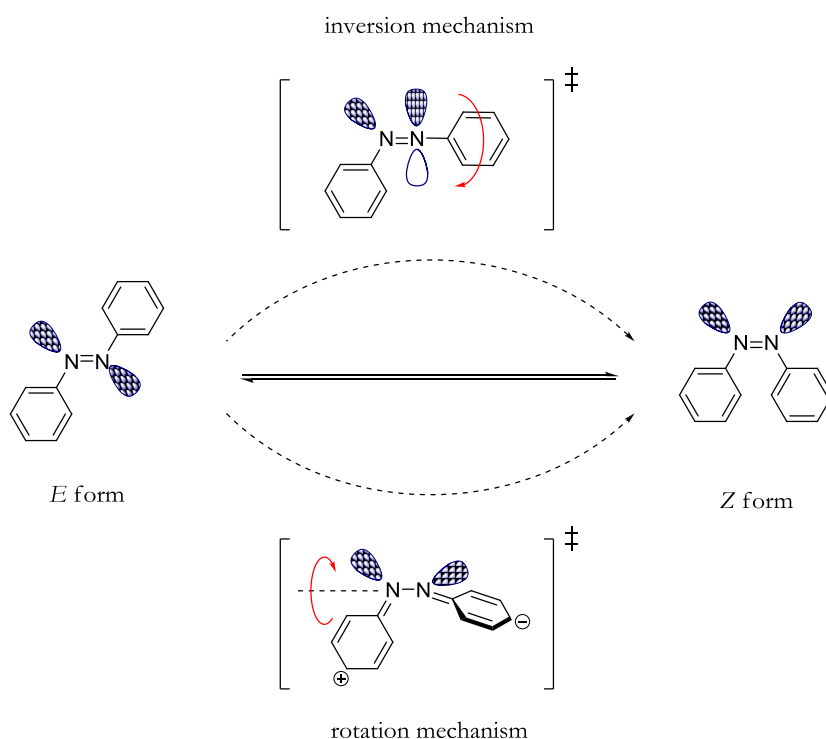


Figure 1. 5. Representation of the two possible mechanisms for the isomerization process of azobenzenes.

The inverse process, (Z to E relaxation) can be reached either thermally, which can last from hours to days, or photochemically, which can be extremely fast (seconds).

Playing with azobenzenes

The range of applications and design of systems that are based on azobenzene moieties are as wide as the imagination of the researchers interested in this field. Although a lot of interesting and elaborated designs can be found in literature, here only a few representative examples will be described to exemplify the many possibilities.

Apart from the nature of the substituents and the polarity of the solvents,^{38,39} many factors can affect the isomerization process (either E to Z or Z to E). Already in the 70s Nakamura *et al.* reported rapid Z to E isomerization of azobenzene catalyzed by metal complexes (*i.e.* $t_{1/2}=1$ min at -20 °C using $\text{Pt}(\text{PPh}_3)_4$ 0.03 mM). Divalent Group 10 metal complexes were found to be inactive.⁴⁰

The opposite effect, inhibition of the Z to E isomerization, is also known. The first example was reported by Shinkai *et al.*⁴¹ They were studying how the change of the conformation in a structure that combines the presence of an azobenzene and a crown ether affected to the binding properties of the last one to cations. They discovered that when the azobenzene is on its Z form, the compound adopts a “basket” conformation that hosts the cation, and this aggregate is more stable than the host alone in an E conformation.

A more recent example makes use of cyclic structures called azobenzenophanes (macrocyclic azobenzene dimers developed to unravel the isomerization mechanism)^{42,43} to stabilize the Z form of both azobenzenes (Figure 1. 6, **A**).⁴⁴ The strain of the structure makes that the ZZ geometrical isomer is the thermodynamically most stable one. It constitutes the first X-Ray structure reported for a Z azobenzene. The same authors described some years before a “molecular hinge” (Figure 1. 6, **B**),⁴⁵ where two xanthene fragments were connected by two azo moieties. The rigidity of this system stabilized the ZZ isomer, with a lifetime of 6.4 years at 303 K, but it was

not yet as stable as the *EE* one.⁴⁶ In both examples the intermediate *EZ* isomer was the less stable one. This effect can be described as a kind of cooperativity in the isomerization of the two azo bonds.

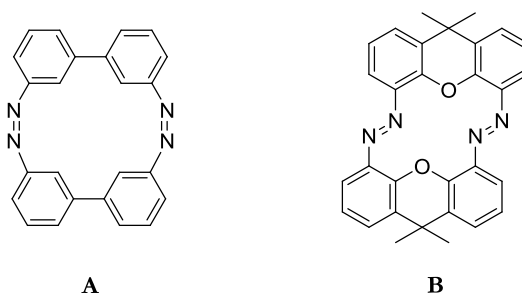
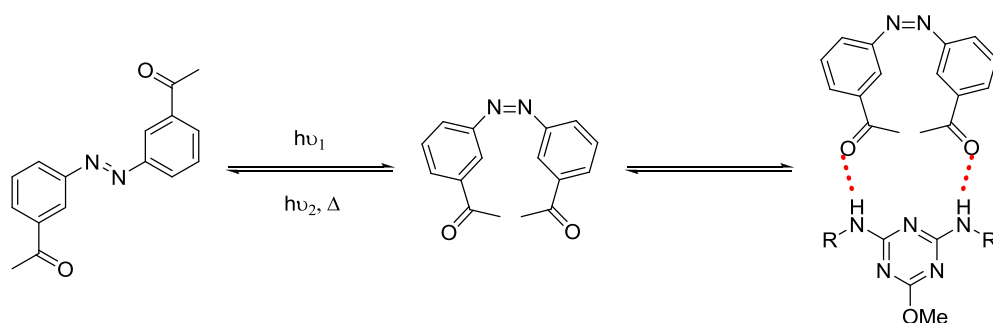


Figure 1. 6. Azobenzenophane type structures designed by Tamaoki *et al.* to stabilize the *Z* conformation of an azobenzene. Biphenyl (**A**) and Xanthene (**B**) based molecular “hinges”.

Alternatively, the *Z* form of an azobenzene can be stabilized by using hydrogen bonding interactions. In 1993 a simple but effective system was described in which 3,3'-diacetyl-*Z*-azobenzene was stabilized by hydrogen bond interactions with 2,4-bis(cyclohexylamino)-6-methoxy-1,3,5-triazine.⁴⁷ The association constant of this assembly was determined as $K_a = 1.2 \cdot 10^6 \text{ M}^{-1}$ (representation in Scheme 1. 3).



Scheme 1. 3. Stabilization of the *Z* form of an azobenzene by interaction through hydrogen bonds.

The same concept (stabilization through hydrogen bonds) was applied some years

later by Rebek *et al.*⁴⁸ to design a photoresponsive synthetic receptor to control the catalytic formation of an amide bond between an adenosine derivative and a *p*-nitrophenyl (PNP) ester. The catalysis involves the use of an azobenzene as a switchable linker that is substituted in both aromatic rings by a carbazole-based supramolecular receptor for adenines by means of hydrogen bonding interactions. The first step is the complexation of azobenzene through the carbazole group to the molecules that contain the adenines. The second step is the irradiation to obtain the *Z* conformation of the azobenzene. This structural change in the system brings the two moieties that are going to form the amide covalent bond in close proximity. Not only is the amide bond formation catalyzed, but also the *Z* form of the azobenzene in the host molecule is stabilized by the strong amide bond formed (Figure 1. 7).

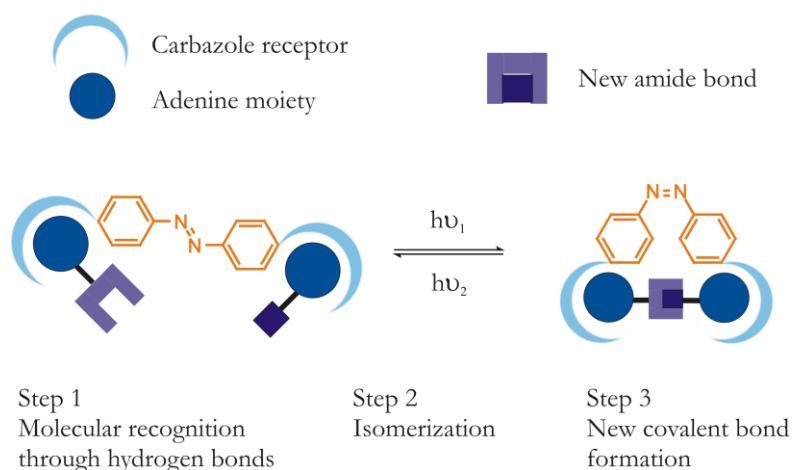


Figure 1. 7. Schematic representation of the system designed by Rebek *et al.*

The previous system explained is just one of the multiple examples in which an azobenzene is integrated in a supramolecular environment.

Porphyrins are among the most commonly used structures in supramolecular arrays. The first system combining azobenzenes and porphyrins was described in 1988.⁴⁹ It consisted of two porphyrins joined by four azobenzene units, creating a cylindrical cavity. The project aimed at the formation of cavities comprising molecular switches. Surprisingly, they did not study the isomerization of the system.

More recently, Hunter *et al.* studied the compatibility of porphyrins with the azobenzene isomerization process.⁵⁰ They designed a system based on the planarity of the porphyrins, which were linked to azobenzenes substituted with functional groups able to interact by means of hydrogen bonds. (Figure 1. 8) Upon irradiation, the isomerization of the azo group should produce a structural change in the molecule that allows molecular recognition of the target molecules. The recognition pocket is created because the H-bond donors are placed close together. This could be applied, for example, in the design of molecular logic gates for molecular data storage. Unfortunately, the study revealed that, although the photochemical properties of the porphyrin were not altered by the presence of the azobenzenes, the photoinduced isomerization of the latter was quenched in this system.

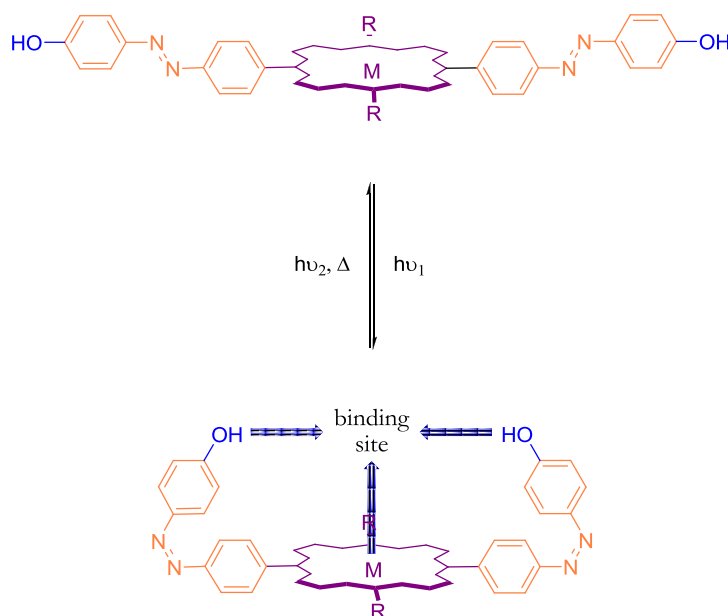


Figure 1. 8. Schematic representation of the porphyrin-azobenzene system designed by Hunter *et al.*

The behaviour of azobenzenes in the presence of porphyrins remains unravelled. In some cases, as in the last example discussed, the photoexcited states were not

accessible and the isomerization was not observed,^{51,52} but in other studies the isomerization of the azo double bond did take place.^{53,54}

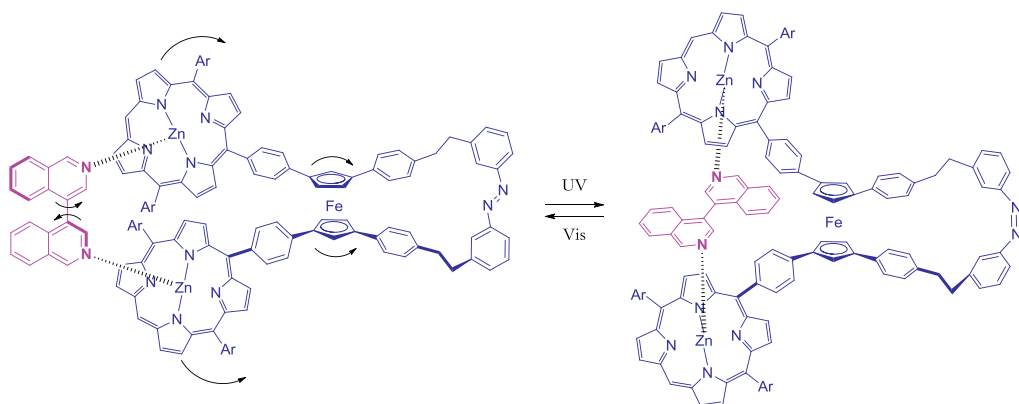
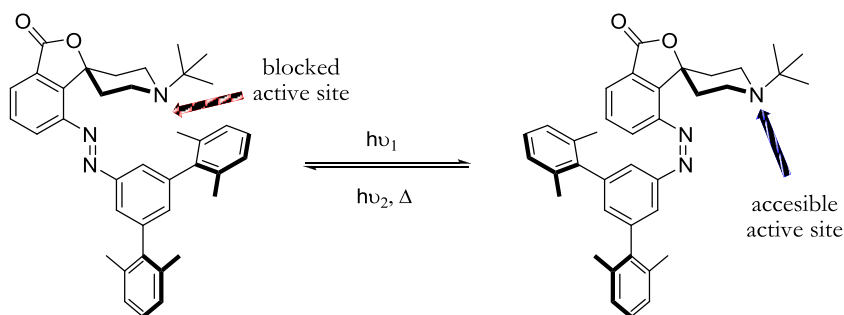


Figure 1. 9. “Molecular scissors” designed by Muraoka *et al.*

In a more complex example, porphyrins were also combined with azobenzenes and ferrocene moieties to generate a pair of “molecular scissors” (Figure 1. 9). In the system designed by Muraoka *et al.*, the switchability of the azobenzene is transferred along the molecule. The structural change of the N=N double bond generates a twisting in the ferrocene unit that displaces the porphyrins. The Zn atoms of the metallated porphyrins are coordinated to the nitrogen atoms that belong to a 4,4'-biisoquinoline molecule, which undergoes a turning of its dihedral angle.⁵⁵

Molecular switches in catalysis

There are many applications of azobenzenes as molecular switches, but surprisingly their use in catalysis has not been widely explored. One of the few recent examples concerns an organocatalyst, whose basic active site (blocked when the molecule is in its *E* form), becomes accessible upon isomerization. In this way irradiation activates the catalytic process (Scheme 1. 4).⁵⁶



Scheme 1. 4. Photoswitchable organocatalyst.

Considering the possibilities how to apply such switches in organometallic catalysis, the simplest strategy is to incorporate the molecular switch into the ligand. For example, the coordination behaviour towards several metals of a phenanthroline ligand linked to a spirooxazine switch has been tested, and it was found that the stability of both isomers depends on the metal used (Figure 1. 10).⁵⁷

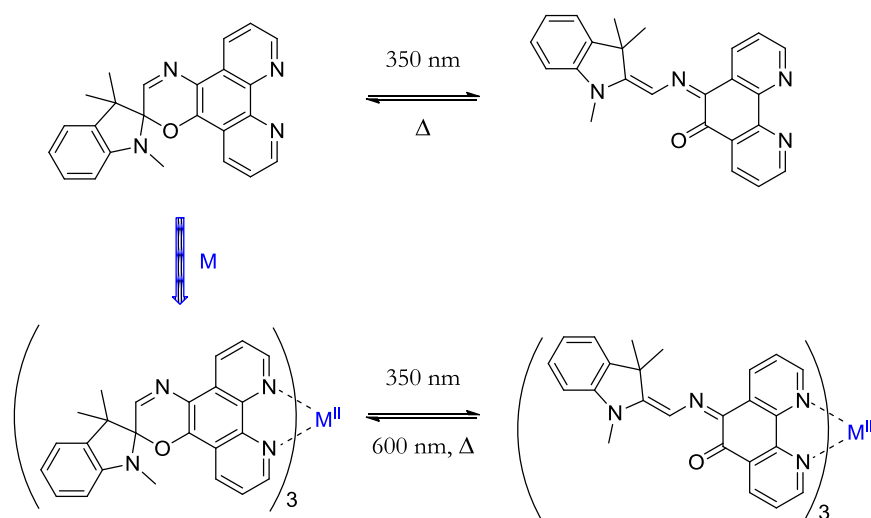


Figure 1. 10. A phenanthroline ligand combined with spirooxazine switch.

There are also several examples of pyridine ligands that contain an azobenzene in their structure.^{58–60} For example Nishihara *et al.* reported an azobipyridine ligand coordinated to cobalt (Figure 1. 11).^{61,62} Combining the electrochemical properties of

the metal complex with the photochemical behaviour of the azobenzene moiety they achieved the *E* to *Z* and the reverse isomerization using single UV light radiation (366 nm) for both processes, depending on the oxidation state of the metal.

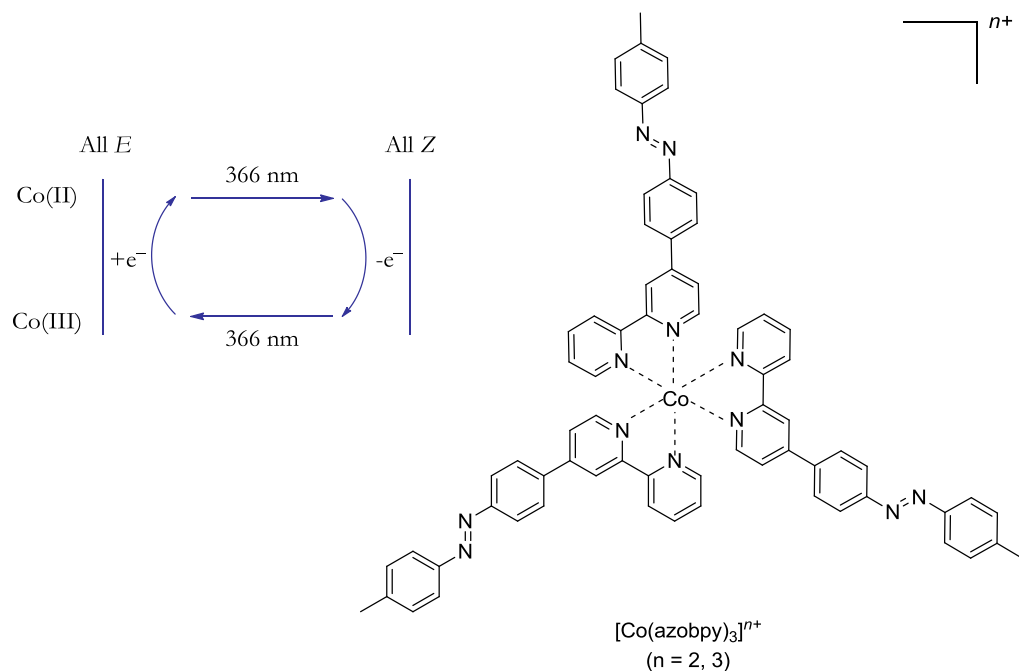


Figure 1. 11. Cobalt system with azopyridine ligands.

The same authors reported similar behaviour for several ferrocenes joined either to an azobenzene switch (Figure 1. 12)⁶³ or to a spiropyrane switch, although the behaviour of the latter system is not the same as the previous ones.⁶⁴

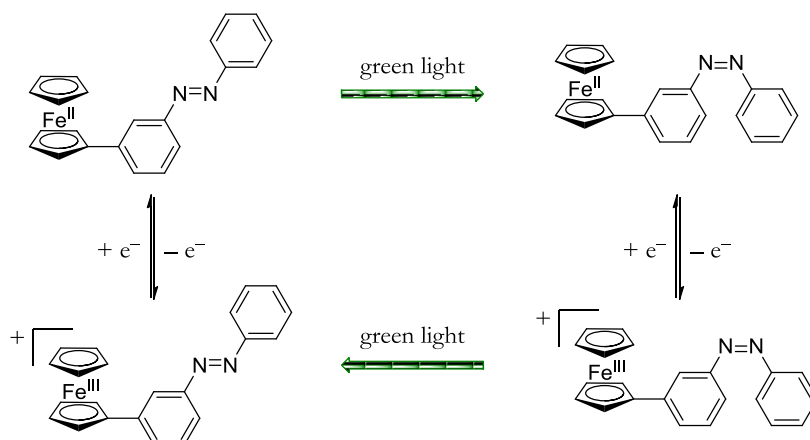
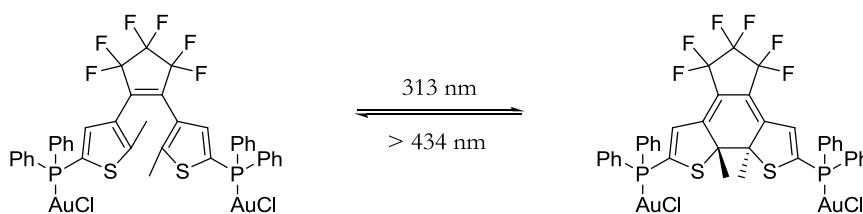


Figure 1. 12. Photo- and electrochemical behaviour of the ferrocene-azobenzene unit.

As regards phosphine ligands there is only one example in literature in which a photoresponsive 1,2-dithienylethene backbone (DTE) is combined with a triarylphosphine to create a ligand.⁶⁵ This phosphine was coordinated to gold and selenium, and then the system was irradiated to check if the switchability of the DTE moiety still takes place in the presence of a metal, gold in this instance (Scheme 1. 5).



Scheme 1. 5. Photoresponsive gold complex of bis(triarylphosphine) based on DTE backbone.

Phosphine ligands have been also combined with azobenzene switches. Flower *et al.*, pioneered the synthesis of a triaryl phosphine incorporating an azo moiety (Figure 1. 13, **A**). They did a complete structural characterization of the molecule, performed some preliminary test in a Heck reaction, and studied its stability under several chemical conditions, but they did not study whether the isomerization of the double

azo bond has an effect on the catalytic performance.⁶⁶⁻⁷¹

Kawashima *et al.* also synthesized an azobenzene containing a phosphine (*ortho* to the nitrogen atom of the azo moiety, Figure 1. 13, **B**). They found that the formation of the tautomeric form of the inner phosphonium salt can take place, interfering with the isomerization process. Their research involved also the study of the reactivity of the molecule and preliminary irradiation studies were done.^{72,73}

Both groups conducted studies of the corresponding derivatives in which the phosphorus atom is oxidized with a chalcogenide (O or S) to P(V).

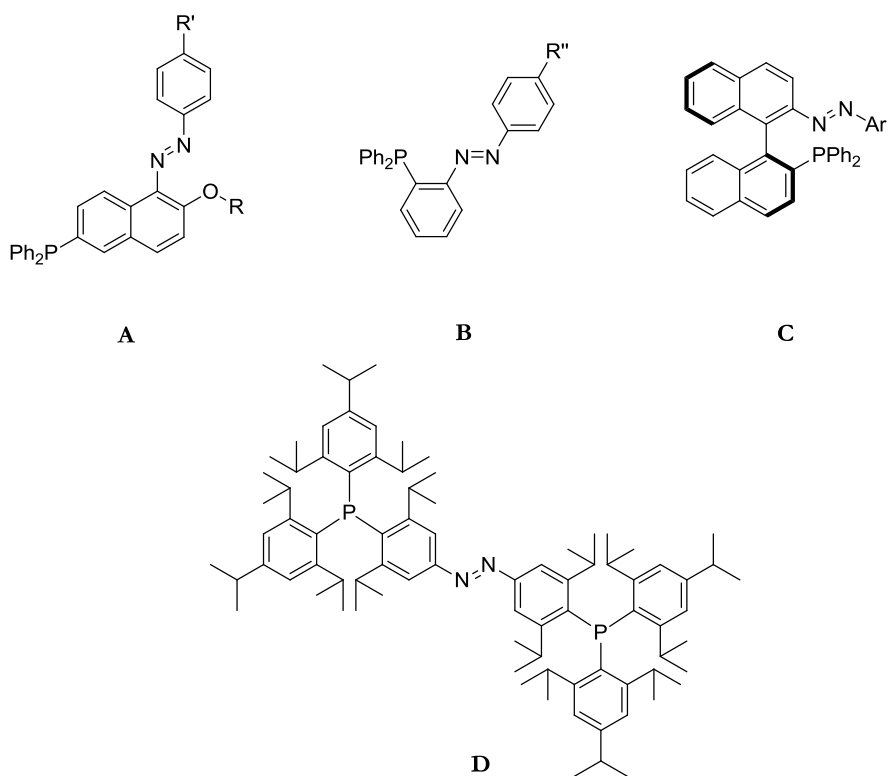


Figure 1. 13. Reported molecules containing a phosphine and an azo double bond.

Another example found in literature of azobenzene containing phosphines was reported by Kudo *et al.* They designed a P,N ligand (Figure 1. 13, **C**),⁷⁴ in which the N-donor atom belongs to an azo double bond. The ligand has a binaphthyl

backbone, responsible for the chirality of the molecule. In this case, the effect of the irradiation in palladium catalyzed asymmetric allylic substitution was studied, but the authors neither observed a change in the yields nor in the enantioselectivity of the catalytic reaction. It should be noted that the authors did not study whether the azo isomerization does not affect the catalysis or whether isomerization does not take place because the metal inhibits the isomerization process by quenching the excited states.

Compound **D**, in Figure 1. 13, can be considered as a very bulky azobenzene diphosphine; it was obtained as a by-product when trying to synthesize crowded triaryl phosphines bearing a nitroxide radical group⁷⁵ and its potential application was never explored.

In conclusion, in spite of the large number of examples of azobenzene containing ligands, the effect of the switchability in catalysis and an explanation of the behaviour when such ligands coordinate to a metal has not been studied in detail.

General objectives of Part I

Keeping in mind all the possibilities of the azobenzene, we thought to combine this molecular switch with phosphine ligands. This combination enables the generation of new ligands with switchable properties. This way, using light as an external stimulus, it can be toggled between two forms of the ligand that will possess, potentially, different properties (or at least, different structures).

Having a look into the published examples of phosphines containing azobenzene moieties in the structure, one can notice that there is little interest in the characterization of the photochromic properties of “azophosphines” (especially when coordinated to metals). We are interested in the metal coordination properties of azophosphines, and the way how the presence of a metal affects the switchability of the system.

Of course, all our studies are directed towards the application of such azophosphines in catalysis, and how the use of the external agent (light) generates ligand changes and therefore, variations in catalytic results.

References and notes

1. Lehn, J. M. *Supramolecular Chemistry: Concepts and Perspectives*; VCH, **1995**.
2. Pieroni, O.; Fissi, A.; Angelini, N.; Lenci, F. *Acc. Chem. Res.* **2001**, *34*, 9.
3. Nayak, A.; Liu, H. W.; Belfort, G. *Angew. Chem., Int. Ed.* **2006**, *45*, 4094.
4. Mayer, G.; Heckel, A. *Angew. Chem., Int. Ed.* **2006**, *45*, 4900.
5. Feringa, B. L. *J. Org. Chem.* **2007**, *72*, 6635.
6. Credi, A. *Angew. Chem., Int. Ed.* **2007**, *46*, 5472.
7. Balzani, V.; Credi, A.; Venturi, M. *Chem. Soc. Rev.* **2009**, *38*, 1542.
8. Noble, A. *Quart. J., Chem. Soc., London* **1856**, *8*, 292.
9. Stebbins, J. H., Jr. *J. Am. Chem. Soc.* **1879**, *1*, 465.
10. Stebbins, J. H., Jr. *J. Am. Chem. Soc.* **1884**, *6*, 117.
11. Stebbins, J. H., Jr. *J. Am. Chem. Soc.* **1884**, *6*, 149.
12. Feringa, B. L.; Koumura, N.; Van Delden, R. A.; Ter Wiel, M. K. J. *Appl. Phys. A: Mater. Sci. Process.* **2002**, *75*, 301.
13. Ballardini, R.; Balzani, V.; Credi, A.; Gandolfi, M. T.; Venturi, M. *Acc. Chem. Res.* **2001**, *34*, 445.
14. Browne, W. R.; Feringa, B. L. *Nat. Nanotechnol.* **2006**, *1*, 25.
15. Diguët, A.; Guillermic, R.-M.; Magome, N.; Saint-Jalmes, A.; Chen, Y.; Yoshikawa, K.; Baigl, D. *Angew. Chem., Int. Ed.* **2009**, *48*, 9281.
16. Koshima, H.; Ojima, N.; Uchimoto, H. *J. Am. Chem. Soc.* **2009**, *131*, 6890.
17. Yu, Y. L.; Nakano, M.; Ikeda, T. *Nature* **2003**, *425*, 145.
18. Yamada, M.; Kondo, M.; Mamiya, J. I.; Yu, Y. L.; Kinoshita, M.; Barrett, C. J.; Ikeda, T. *Angew. Chem., Int. Ed.* **2008**, *47*, 4986.
19. Nomura, A.; Okamoto, A. *Chem. Commun.* **2009**, 1906.
20. Wu, L.; Koumoto, K.; Sugimoto, N. *Chem. Commun.* **2009**, 1915.
21. Dohno, C.; Uno, S. N.; Nakatani, K. *J. Am. Chem. Soc.* **2007**, *129*, 11898.
22. Banghart, M. R.; Mourot, A.; Fortin, D. L.; Yao, J. Z.; Kramer, R. H.; Trauner, D. *Angew. Chem., Int. Ed.* **2009**, *48*, 9097.
23. Hartley, G. S. *Nature* **1937**, *140*, 281.
24. Hartley, G. S. *J. Chem. Soc.* **1938**, 633.
25. Hartley, G. S.; Le Fevre, R. J. W. *J. Chem. Soc.* **1939**, 531.
26. Brode, W. R.; Seldin, I. L.; Spoerri, P. E.; Wyman, G. M. *J. Am. Chem. Soc.* **1955**, *77*, 2762.
27. Fischer, E.; Frankel, M.; Wolovsky, R. *J. Chem. Phys.* **1955**, *23*, 1367.
28. Fischer, E. *J. Am. Chem. Soc.* **1960**, *82*, 3249.
29. Zimmerman, G.; Chow, L. Y.; Paik, U. J. *J. Am. Chem. Soc.* **1958**, *80*, 3528.
30. Griffiths, J. *Chem. Soc. Rev.* **1972**, *1*, 481.
31. Yamashita, S.; Ono, H.; Toyama, O. *Bull. Chem. Soc. Jpn.* **1962**, *35*, 1849.
32. Although we realize that the Z form of the azobenzene is not planar, throughout this document the molecule will be drawn as if it were planar for clarity of the structures.
33. Tait, K. M.; Parkinson, J. A.; Bates, S. P.; Ebenezer, W. J.; Jones, A. C. *J. Photochem. Photobiol., A.* **2003**, *154*, 179.

34. Asano, T.; Okada, T.; Shinkai, S.; Shigematsu, K.; Kusano, Y.; Manabe, O. *J. Am. Chem. Soc.* **1981**, *103*, 5161.
35. Asano, T.; Yano, T.; Okada, T. *J. Am. Chem. Soc.* **1982**, *104*, 4900.
36. Asano, T.; Okada, T. *J. Org. Chem.* **1984**, *49*, 4387.
37. Asano, T.; Okada, T. *J. Org. Chem.* **1986**, *51*, 4454.
38. Wildes, P. D.; Pacifici, J. G.; Irick, G.; Whitten, D. G. *J. Am. Chem. Soc.* **1971**, *93*, 2004.
39. King, N. R.; Whale, E. A.; Davis, F. J.; Gilbert, A.; Mitchell, G. R. *J. Mater. Chem.* **1997**, *7*, 625.
40. Nakamura, A.; Doi, K.; Tatsumi, K.; Otsuka, S. *J. Mol. Catal.* **1976**, *1*, 417.
41. Shinkai, S.; Nakaji, T.; Nishida, Y.; Ogawa, T.; Manabe, O. *J. Am. Chem. Soc.* **1980**, *102*, 5860.
42. Rau, H.; Luddecke, E. *J. Am. Chem. Soc.* **1982**, *104*, 1616.
43. Bassotti, E.; Carbone, P.; Credi, A.; Di Stefano, M.; Masiero, S.; Negri, F.; Orlandi, G.; Spada, G. P. *J. Phys. Chem. A* **2006**, *110*, 12385.
44. Norikane, Y.; Katoh, R.; Tamaoki, N. *Chem. Commun.* **2008**, 1898.
45. Norikane, Y.; Tamaoki, N. *Org. Lett.* **2004**, *6*, 2595.
46. Nagamani, S. A.; Norikane, Y.; Tamaoki, N. *J. Org. Chem.* **2005**, *70*, 9304.
47. Rosengaus, J.; Willner, I. *J. Chem. Soc., Chem. Commun.* **1993**, 1044.
48. Wurthner, F.; Rebek, J. J. *J. Chem. Soc., Perkin Trans. 2* **1995**, 1727.
49. Neumann, K. H.; Vogtle, F. *J. Chem. Soc., Chem. Commun.* **1988**, 520.
50. Hunter, C. A.; Sarson, L. D. *Tetrahedron Lett.* **1996**, *37*, 699.
51. Peters, M. V.; Goddard, R.; Hecht, S. *J. Org. Chem.* **2006**, *71*, 7846.
52. Esdaile, L. J.; Jensen, P.; McMurtrie, J. C.; Arnold, D. P. *Angew. Chem., Int. Ed.* **2007**, *46*, 2090.
53. Tsuchiya, S. *J. Am. Chem. Soc.* **1999**, *121*, 48.
54. Yamamura, T.; Momotake, A.; Arai, T. *Tetrahedron Lett.* **2004**, *45*, 9219.
55. Muraoka, T.; Kinbara, K.; Aida, T. *Nature* **2006**, *440*, 512.
56. Stoll, R. S.; Peters, M. V.; Kuhn, A.; Heiles, S.; Goddard, R.; Buhl, M.; Thiele, C. M.; Hecht, S. *J. Am. Chem. Soc.* **2009**, *131*, 357.
57. Kopelman, R. A.; Snyder, S. M.; Frank, N. L. *J. Am. Chem. Soc.* **2003**, *125*, 13684.
58. Ko, C.-C.; Yam, V. W.-W. *J. Mater. Chem.* **2010**, *20*, 2063.
59. Kume, S.; Nishihara, H. *Dalton Trans.* **2008**, 3260.
60. Sakamoto, R.; Murata, M.; Kume, S.; Sampei, H.; Sugimoto, M.; Nishihara, H. *Chem. Commun.* **2005**, 1215.
61. Nishihara, H. *Coord. Chem. Rev.* **2005**, *249*, 1468.
62. Kume, S.; Kurihara, M.; Nishihara, H. *Chem. Commun.* **2001**, 1656.
63. Kurihara, M.; Hirooka, A.; Kume, S.; Sugimoto, M.; Nishihara, H. *J. Am. Chem. Soc.* **2002**, *124*, 8800.
64. Nagashima, S.; Murata, M.; Nishihara, H. *Angew. Chem., Int. Ed.* **2006**, *45*, 4298.
65. Sud, D.; McDonald, R.; Branda, N. R. *Inorg. Chem.* **2005**, *44*, 5960.
66. Alder, M. J.; Flower, K. R.; Pritchard, R. G. *Tetrahedron Lett.* **1998**, *39*, 3571.

67. Alder, M. J.; Cross, W. I.; Flower, K. R.; Pritchard, R. G. *J. Organomet. Chem.* **1998**, *568*, 279.
68. Alder, M. J.; Cross, W. I.; Flower, K. R.; Pritchard, R. G. *J. Organomet. Chem.* **1999**, *590*, 123.
69. Alder, M. J.; Cross, W. I.; Flower, K. R.; Pritchard, R. G. *J. Chem. Soc., Dalton Trans.* **1999**, 2563.
70. Alder, M. J.; Bates, V. M.; Cross, W. I.; Flower, K. R.; Pritchard, R. G. *J. Chem. Soc., Perkin Trans. 1* **2001**, 2669.
71. Alder, M. J.; Flower, K. R.; Pritchard, R. G. *J. Organomet. Chem.* **2001**, *629*, 153.
72. Yamamura, M.; Kano, N.; Kawashima, T. *J. Am. Chem. Soc.* **2005**, *127*, 11954.
73. Yamamura, M.; Kano, N.; Kawashima, T. *Inorg. Chem.* **2006**, *45*, 6497.
74. Kawamura, M.; Kiyotake, R.; Kudo, K. *Chirality* **2002**, *14*, 724.
75. Sasaki, S.; Kato, K.; Yoshifuji, M. *Bull. Chem. Soc. Jpn.* **2007**, *80*, 1791.

CHAPTER 2

DESIGN, SYNTHESIS AND PROOF OF CONCEPT

This work has been partially published as:

Segarra-Maset, M. D.; van Leeuwen, P.W.N.M.; Freixa Z.

Eur. J. Inorg. Chem. **2010**, 2075.



2.1. INTRODUCTION AND OBJECTIVES

As described in chapter 1, there are very few examples in literature that combine in the same structure a phosphine and an azobenzene moiety. The systems already reported are not characterized in terms of switchability, ligand and metal complex properties.

To start with, we considered a simple design with only one phosphine and one azobenzene moiety, which allows us to study their photochromic properties before considering catalytic applications: azomonophosphines **1** and **2** (Figure 2. 1). Their response to irradiation will be studied, initially as free ligands, but also the compatibility of their photochromic properties with metal coordination and catalytic conditions needs to be unravelled. Azobenzenes have been used frequently as N-based ligands for transition metals.^{1,2} This has to be kept in mind, as for our purposes the coordination through the azo group forming a P,N chelate has to be avoided. For this reason, the *ortho* derivative (known in literature) has not been

considered for our studies.³ Instead, only the *meta* and *para* derivatives will be considered.

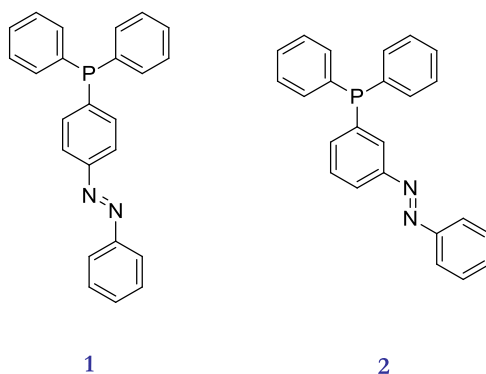


Figure 2. 1. Azomonomophosphines **1** and **2**.

Our challenge was to induce changes in steric effects in phosphine ligands used in metal catalysis by means of irradiation. The most commonly accepted parameter to measure steric properties of monophosphine ligands is Tolman's *cone angle* (θ).^{4,5} For phosphorus ligands the *cone angle* is defined as the apex angle of a cylindrical cone, centred 2.28 Å from the centre of the P atom, which touches the outermost atoms of the ligand (Figure 2. 2, a). *Cone angles* are originally based on a typical Ni(0)–P bond length and therefore the magnitude of a ligand *cone angle* is inherently somewhat dependent on the transition metal involved. Recently, a new family of monophosphines presenting a very large cone angle (larger than 180°!) has been reported (Figure 2. 2, b, c).⁶ These phosphines are the so-called *bowl-shaped phosphines* (BSP), because of the shape of the space confined around the metal. This unusually large *cone angle* confers to their complexes unusual catalytic behaviour.

The question is how to induce large cone angles by *E* to *Z* isomerization of azo groups and to this end phosphine **3** was designed (Figure 2. 3).

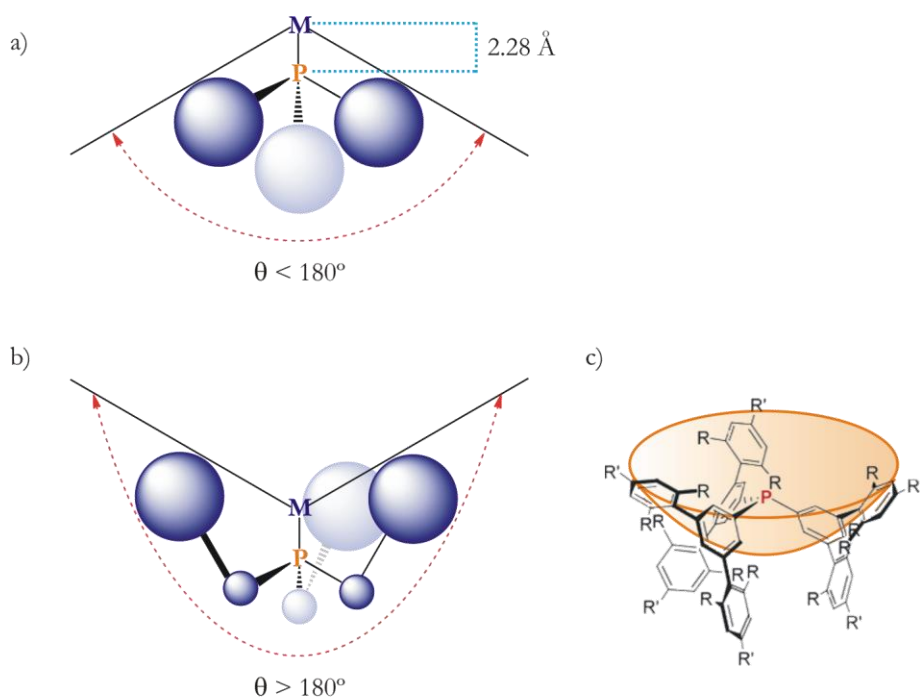


Figure 2. 2. a) Schematic representation of Tolman's *cone angle*. b) Schematic representation of a monophosphine with a concave *cone angle* (larger than 180°). c) BSPs reported by Tsuji *et al.*⁷

As shown by molecular modelling,⁸ one might expect that *E* to *Z* isomerization of the three azo bonds of phosphine **3** generates a structure resembling the reported BSP (Figure 2. 4). It is well established that *E* to *Z* isomerization usually reaches a photostationary equilibrium of ~85 % of *Z* isomers, but also if only one or two of the azo groups in **3** adopt a *Z* conformation, a ligand with steric properties different from those of the tris *E* isomer will be generated. Note that the isomers of ligand **3** can occur in several conformational isomers, obtained by rotation around P–aryl bonds. The differences in energy between the various isomers located are very small (less than 2 kcal mol⁻¹, as calculated by MM2, see appendix I). The isomer for *EEE*-**3**, that is represented in Figure 2. 4, is the one with the smallest *cone angle* from the different conformers located. The one with the largest *cone angle* (in which the aryl rings are

arranged in a similar manner as in the idealized structure of tris *Z*) also resembles a BSP, but the depth of the cone is much smaller than the one observed in the tris *Z* structure.

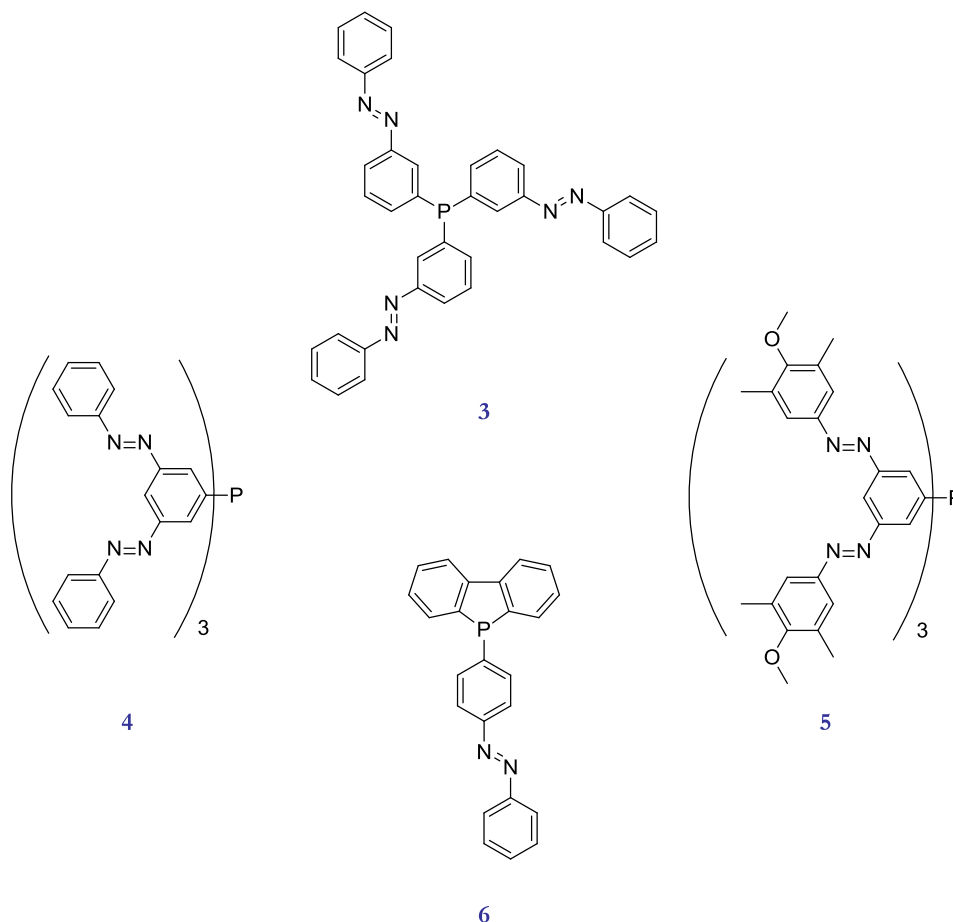


Figure 2. 3. Azomonophosphines designed with restricted geometry around P atom.

To avoid the generation of different isomers by rotation along the P–C bond, derivatives analogous to **3** were designed that incorporate azo functionalities both in 3 and 5 positions on each aryl ring, as for example ligands **4** and **5**, which contain six azo double bonds. Another possibility to restrict the number of conformations is to include the phosphorus atom into a cyclic structure, as for example in phosphine **6**, in

which the azo phenyl group will bend away from the dibenzophosphole plane when it is in the azo *Z* form. The phosphole functionality will also modify the electronic properties of the phosphine.

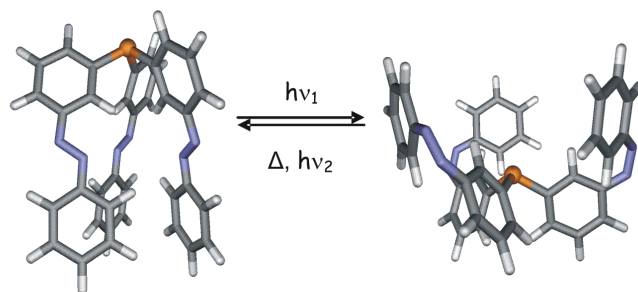


Figure 2. 4. Molecular modelling of trisazophosphine **3** in tris *E* and tris *Z* azo conformations showing maximized steric difference.

Alternatively, in our pursuit of different structural changes upon irradiation, another design was developed. Azodiphosphines **7** and **8** (Figure 2. 5) are expected to present a change in their coordination properties upon irradiation. One can imagine that when the ligand is in its most stable but rigid *E* form, it cannot coordinate as a chelating ligand. In contrast, when the *Z* form of the azobenzene is generated, the ligand can act as a chelating diphosphine.

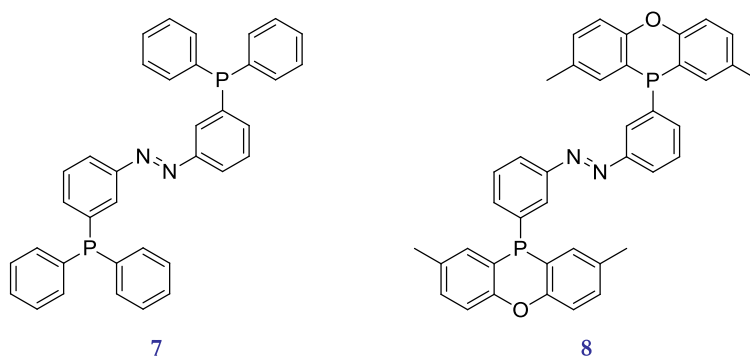
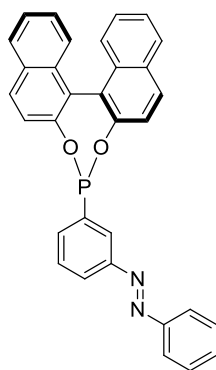


Figure 2. 5. Azodiphosphines designed.

Additionally, one can expand the possibilities in catalysis by incorporating

chirality in the molecules. A very simple example is phosphonite **9** (Figure 2. 6) which includes the chiral binaphthol moiety. Minor changes in such monophos ligands are known to have major effects in enantioselective hydrogenation (the term “monophos” is used to mean a monodentate P-donor rather than the DSM trademarked “MonoPhos” family of phosphoramidite ligands).⁹⁻¹⁴



9

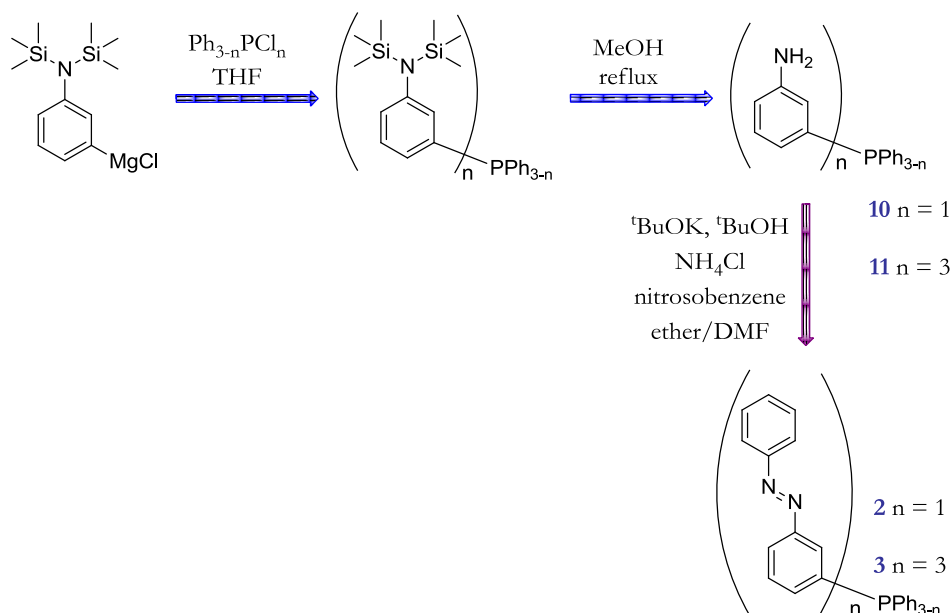
Figure 2. 6. Chiral phosphonite with an azo moiety.

2.2. SYNTHESIS

The synthesis of azophosphines can be performed in two manners: either by forming an azo double bond in a phosphine or by introducing a phosphorus moiety in an azobenzene derivative.

Usually the synthesis of the azo double bond requires harsh acidic conditions, which will lead to oxidation or protonation of the phosphorus if the phosphine is already present. However, there is an example in literature where basic conditions are used (as described by Kudo *et al.* for the synthesis of a P,N type ligand, see Figure 1.13, **C**, chapter 1).¹ For the synthesis of azomonophosphines **2** and **3** (*meta* substituted ones) this method can be applied, as the starting aminophosphines **10** and **11** have been described by Stelzer *et al.*¹⁵ The synthesis of such compounds starts from the Grignard reagent containing the trimethylsilyl protected amine, and making it react with the corresponding chlorophosphine. Intermediate **10** was synthesized in

our group previously for the formation of heterobidentate assembly ligands by ionic interactions.¹⁶ **11** was synthesized with 68 % yield (Scheme 2. 1). Unfortunately, azomonophosphines **2** and **3** were never obtained using this methodology. When aminophosphines **10** and **11** were reacted with an excess of nitrosobenzene, mainly the formation of by-products coming from nitrosobenzene homo-coupling reactions was observed.



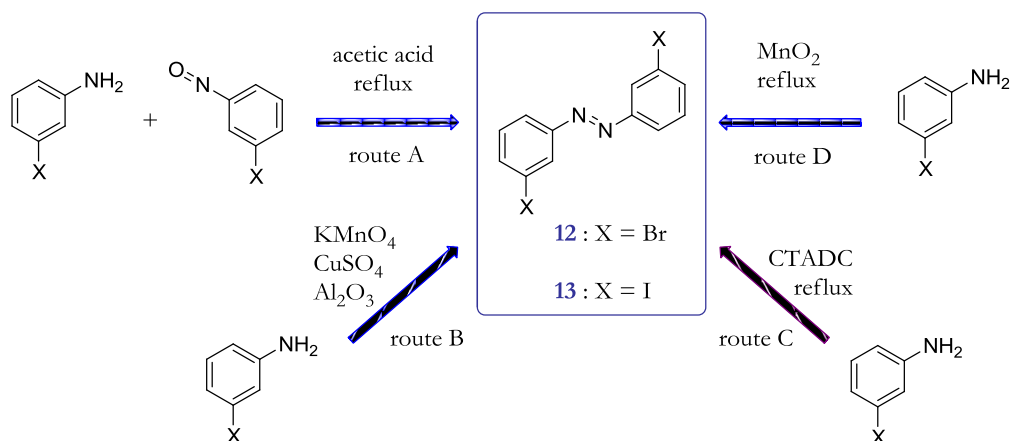
Scheme 2. 1. Proposed synthesis of azophosphines **2** and **3** via aminophosphines **10** and **11**.

After these results a change of strategy was proposed, and the synthesis starting with halogenated azobenzene was attempted. From the bromo- or iodo- compounds there are two possible routes: the phosphine can be introduced either by lithiation and reaction with chlorophosphine or by palladium catalyzed P–C coupling with HPR_2 (*vide infra*). Accordingly, we started with the synthesis of the halogenated azobenzenes.

The first synthesis of an azo compound was carried out probably by Noble in 1856.¹⁷ He discovered a new coloured compound while studying the reaction

conditions described previously by Béchamp to reduce the nitrobenzene to aniline. He found that upon increasing the amount of iron in the reaction mixture with acetic acid, a deep red by-product was obtained that responded to the formula of azobenzene. Since that initial experiment, several general methods have been developed to optimize the synthesis of azo derivatives. Some of them are explained hereafter.

The methods used for the synthesis of azobenzenes depend on whether the final product is symmetric or asymmetric. In our case, when the final product is a diphosphine, a symmetric, dihalogenated azobenzene precursor is needed. Instead, for the synthesis of monophosphines, only one of the rings of the azobenzene needs to be substituted with a halogen atom, *i.e.* an “asymmetric” method is required.



Scheme 2. 2. Routes for the synthesis of the symmetric halogenated azobenzenes.

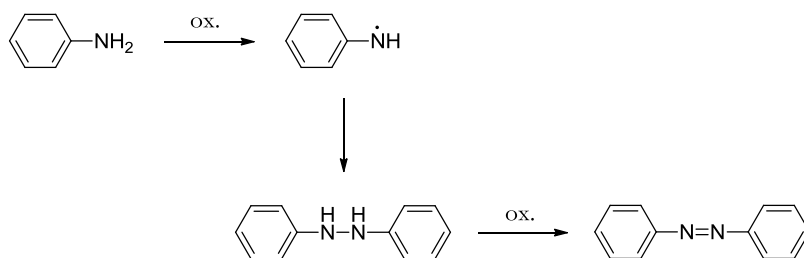
Azodiphosphines **7** and **8** can be obtained from the same dihalogenated azobenzene precursor **12** or **13** (bromo and iodo derivatives respectively). There are several methods that can be used for the synthesis of these symmetric, halogenated azobenzenes starting from anilines with the halogen in the *meta* position, some of them are depicted in Scheme 2. 2.

In the case of route A, the methodology used is clearly different from the other routes proposed. In this case the reaction is a coupling between aniline and nitrosobenzene.¹⁸ It is the well known Mills coupling,¹⁹ in which an intermediate is

formed that upon dehydration gives the azobenzene.

When the desired nitroso compound was not commercially available it was synthesized. Nitrosobenzenes are obtained by oxidation of anilines, and several reaction conditions have been described in literature,²⁰⁻²² among them a recently reported methodology using Oxone[®] as oxidizing reagent ($2 \text{ KHSO}_5 \cdot \text{KHSO}_4 \cdot \text{K}_2\text{SO}_4$).²³ By following this procedure, 1-bromo-3-nitrosobenzene was obtained with a 73 % yield. Unfortunately, the posterior coupling with aniline to obtain 1,2-bis(3-bromophenyl)diazene gave less than 5 % yield.²⁴

The other three routes (B, C and D) involve a coupling of two identical halo-anilines. They make use of an oxidant such as manganese dioxide,²⁵⁻²⁷ potassium permanganate²⁸ or a more recent smooth oxidant, cetyltrimethylammonium dichromate (CTADC).²⁹ In literature there are plenty of other oxidants used (nickel peroxide,³⁰ potassium ferricyanide,³¹⁻³³ cupric chloride,³⁴ etc.), which show different success depending on the substituents on the aromatic ring of the aniline. Wang *et al.* proposed that this reaction starts with the formation of a phenylimino-radical species. The coupling of two of these radical species gives the hydrazobenzene, which converts to azobenzene by dehydrogenation (Scheme 2. 3).³⁵

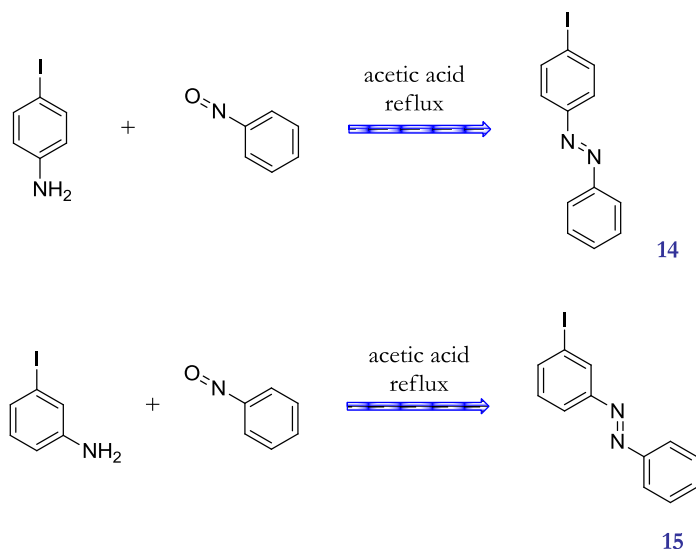


Scheme 2. 3. Mechanism proposed by Wang *et al.* for the synthesis of azobenzenes using an oxidizing agent.

We explored several routes, which are summarized in Scheme 2. 2. The best yields were obtained when MnO_2 (route D) was used as the oxidant, obtaining compounds **12** and **13** with 92 % and 94 % yield respectively.

In contrast, for the synthesis of asymmetric azobenzenes **14** and **15**, the first route described (heterocoupling of a halo-aniline and nitrosobenzene) was employed. Both

anilines and nitrosobenzene are commercially available (Scheme 2. 4). Compounds **14** and **15** were obtained in high yields (around 80 %).³⁶



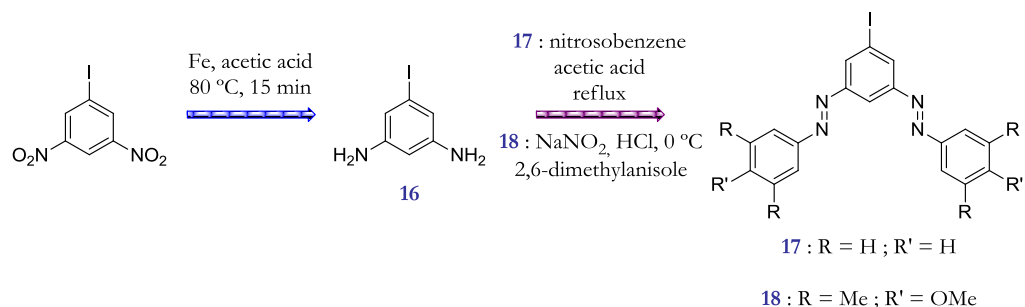
Scheme 2. 4. Synthesis of the asymmetric azobenzenes.

For the synthesis of ligands **4** and **5**, halogenated precursors with more than one azobenzene moiety were required (**17** and **18**, Scheme 2. 5). The synthesis of these compounds was initially planned starting from the commercially available 1-iodo-3,5-dinitrobenzene. The corresponding diamines were obtained by reduction using iron.³⁷ The next step, the functionalization of an aromatic ring with two azo moieties was reported by Hecht *et al.* when pursuing a switchable porphyrin.³⁸ They encountered many problems, which could only be solved by performing the synthesis in a sequential way.

The synthesis of **17** was attempted by reacting the diamine with nitrosobenzene in acetic acid, (method A) but the reaction gave only decomposition products even when performed in a sequential manner.

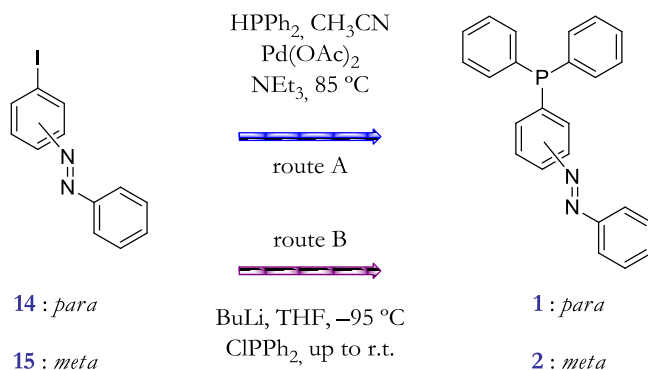
An alternative methodology is the traditional use of NaNO_2 in acidic media for the synthesis via the diazonium salt of the aniline.³⁹ As this salt is not very reactive, the presence of electron-donating groups in the counterpart of the final azobenzene

should increase the conversion. That is why a methoxy group was incorporated in the aromatic ring (product **18**). Unfortunately, via this route the desired bis-azo product was not obtained either.⁴⁰



Scheme 2. 5. Synthesis of molecules with two azobenzene functionalities.

The next step, once the halo-azobenzenes are obtained, is to introduce the phosphine functionality.

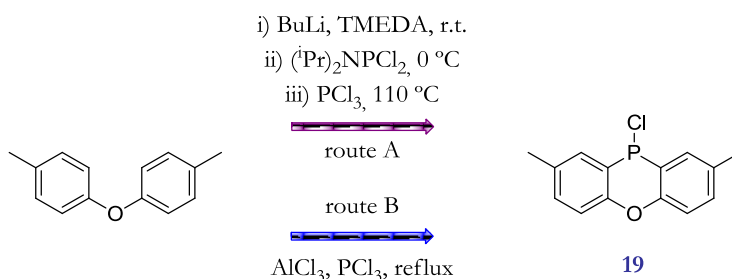


Scheme 2. 6. Synthetic routes employed for the synthesis of the azomonophosphines **1** and **2**.

For the synthesis of the azomonophosphines, two routes were employed (Scheme 2. 6). As described before, route A implies palladium catalyzed P–C bond formation. Route B goes via lithiation and further reaction with the corresponding chlorophosphine. Both routes rendered phosphine **1** from 4-iodoazobenzene (**14**) and

phosphine **2** from 3-iodoazobenzene (**15**). However, when route B was used, the yields obtained were very low (less than 10 %).⁴¹ Yields as high as 74 % for phosphine **1** and 58 % for phosphine **2** were obtained by palladium catalyzed P–C coupling.⁴²

For the synthesis of the diphosphines, two different compounds are used to introduce the phosphorus moiety in the ligands. For azodiphosphine **7**, commercially available chlorodiphenylphosphine was used as phosphorus precursor. For ligand **8** the chlorophosphine (ClMePOP, **19**) needed to be synthesized. According to literature reports, this synthesis can be done in two different manners: via lithiation⁴³ (Scheme 2. 7, route A) or via Friedel–Crafts (Scheme 2. 7, route B).⁴⁴ The second route was used (61 % yield).



Scheme 2. 7. Two possible routes for the synthesis of the ClMePOP.

From the azo compounds **12** and **13**, the only route that worked to obtain the azodiphosphines was the one that employs lithiation (route B, Scheme 2. 6). The reaction conditions described in literature were optimized. Usually, the synthesis of triarylphosphines starting from the bromo substituted aromatic precursor can be accomplished by performing the lithiation at low temperature (generally at -78 °C). When the lithiation is complete (which can be confirmed by GC-MS analysis of a H₂O quenched aliquot), the corresponding chlorodiphenylphosphine is added, and the reaction mixture is allowed to warm up to room temperature. When this procedure was used, starting from **12**, for the synthesis of azodiphosphines, products coming from the lithiation of the azo double bond (aminophosphines) were obtained.⁴⁵ For that reason alternative routes using iodo derivative **13** as precursors were explored. With this more reactive iodine derivative the lithiation can be

performed at lower temperatures. Although the overall yield is not very high for diphosphine **7** (only 55 %), the by-products formation is diminished, and relatively good yield is obtained for diphosphine **8** (84 %).

For diphosphines **7** and **8** crystals suitable for X-ray diffraction were obtained. For compound **7** they were obtained by slow diffusion of ether into a dichloromethane solution of the ligand. In the case of **8**, they were obtained by slow evaporation of the solvent from a dichloromethane solution of phosphine (Figure 2. 7). In both structures high planarity of the structure was noticed.

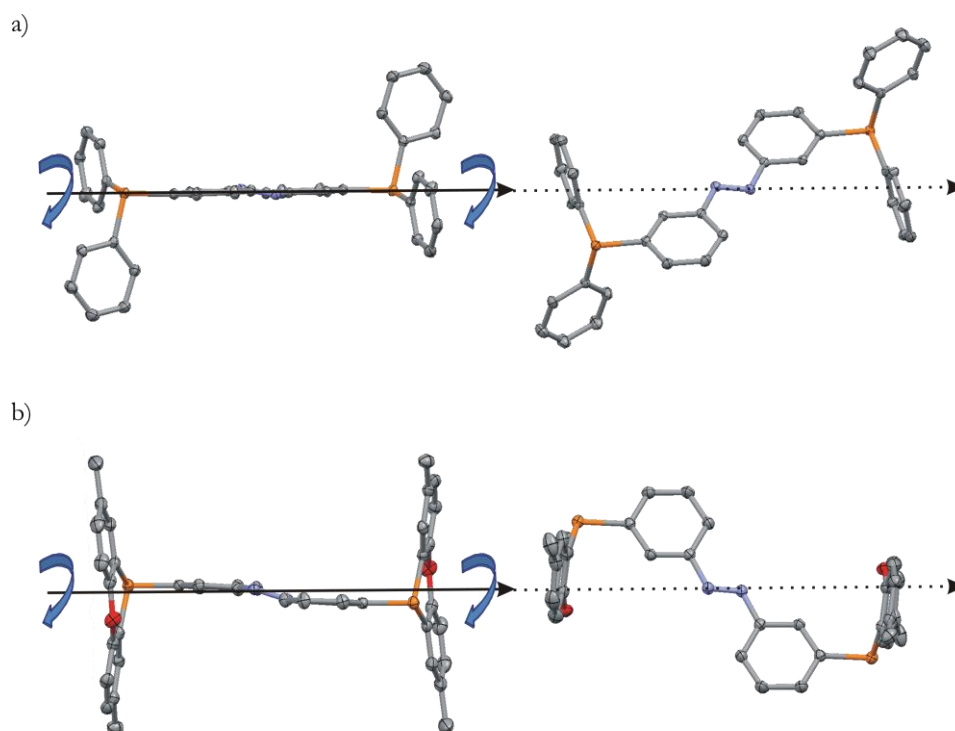
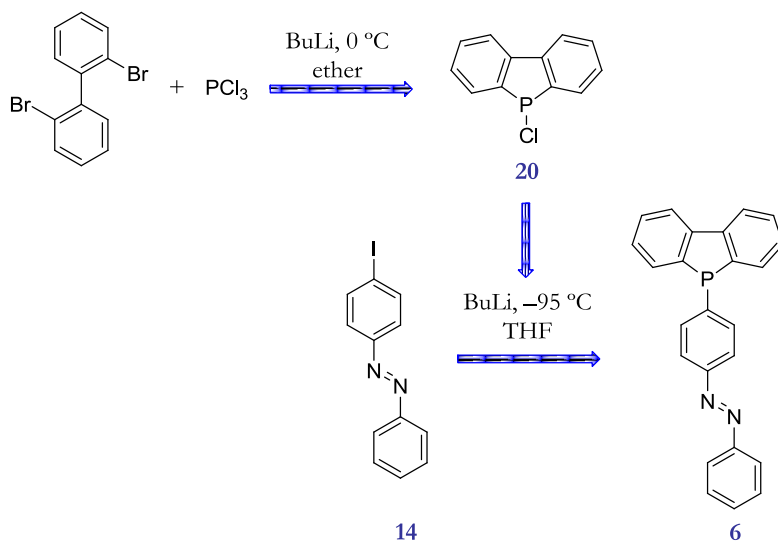


Figure 2. 7. X-Ray structure showing the planarity of the azobenzene a) compound **7**; b) compound **8**.

The synthesis of an azomonophosphine containing dibenzophosphole (DBP) was also attempted (Scheme 2. 8, ligand **6**). The CIDBP (**20**) precursor was synthesized from the 2,2'-dibromobiphenyl via lithiation at 0 °C and PCl_3 .⁴⁶

Unfortunately, the overall yield of the reaction to obtain **6** was extremely low (less than 10 %). Product **6** was obtained in very small amounts and only one complexation test with Pt could be performed.

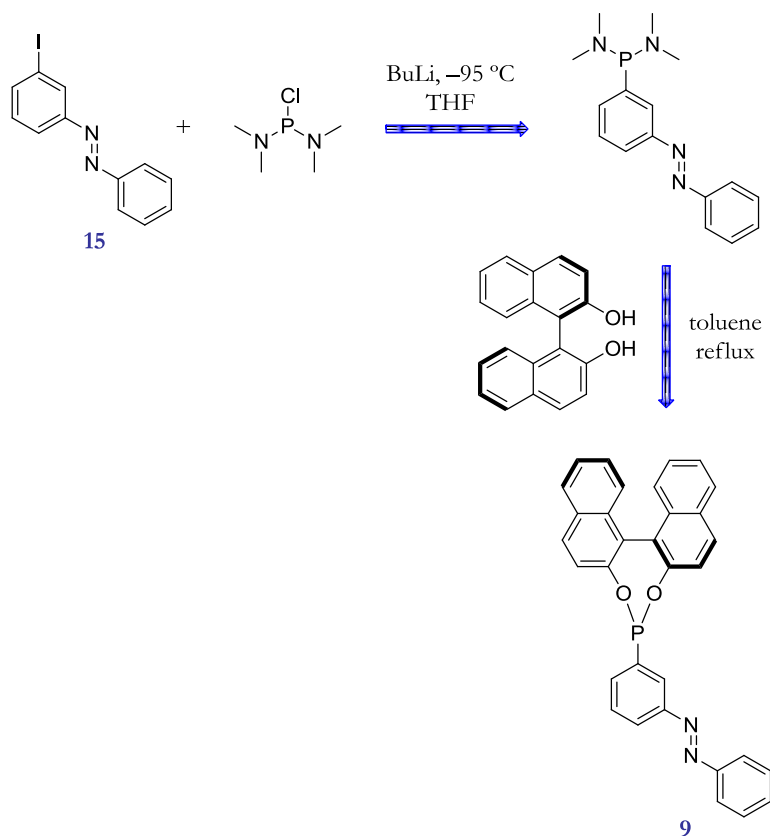


Scheme 2. 8. Synthesis of **6**.

For the synthesis of the more hindered azomonophosphine **3**, the iodinated precursor **15** was used, performing the lithiation at $-95\text{ }^\circ\text{C}$ and using PCl_3 as phosphorus source. Phosphine **3** was obtained in moderate yield (53 %).⁷

As mentioned before, the synthesis of a chiral ligand was also attempted: azophosphonite **9**. The reaction was performed in one pot from 3-iodoazobenzene (**15**), with butyllithium and subsequently with bis(dimethylamino)chlorophosphine. After full conversion to the intermediate was observed, it was reacted with commercially available, enantiopure (*R*)-binaphthol to obtain phosphonite **9** (Scheme 2. 9).^{47,48}

Compound **9** was successfully isolated, but it was synthesized only on a small scale.



Scheme 2. 9. Synthesis of the chiral azo-phosphonite **9**.

2.3. SWITCHABLE BEHAVIOUR

As explained in chapter 1, the switchability of azobenzenes can be easily monitored by using NMR or UV. In the next paragraphs a description of how these techniques were used to study the azophosphine systems is reported.

The switchability of the free ligands was initially studied by $^{31}\text{P}\{^1\text{H}\}$ -NMR spectroscopy. A CDCl_3 solution of phosphine **1** shows a singlet at -1.97 ppm (Figure 2. 8) corresponding to the pure *E* isomer of the double azo bond. After irradiation of the sample at $\lambda = 350$ nm during 1 h, the initial signal at -1.97 ppm decreased in intensity and a new singlet appeared at -2.70 ppm, attributed to the *Z* isomer. When the sample was left in the dark, the reversibility of the process was confirmed; the

original singlet due to the *E* form of the azo bond progressively recovered its original intensity whilst the latter singlet due to the *Z* isomer of the azophosphine disappeared with time.

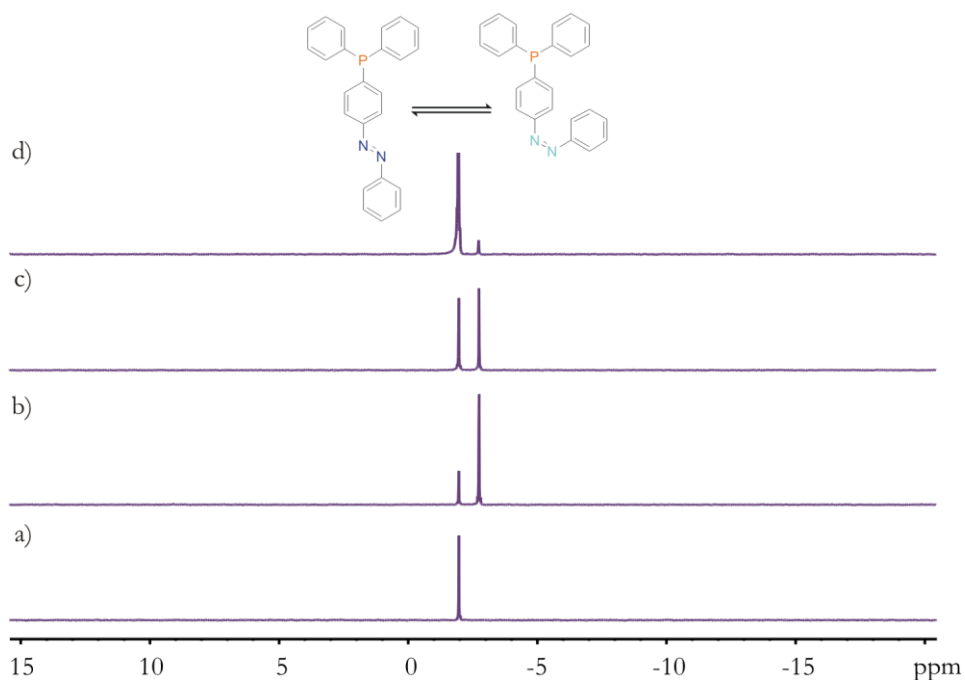


Figure 2. 8. $^{31}\text{P}\{^1\text{H}\}$ -NMR in CDCl_3 of the phosphine **1**: a) before irradiation; b) after 1 h irradiation; c) after 38 h in the dark at r.t.; d) after 9 days in the dark at r.t.

The effect of the light on the ligand can also be observed in the $^1\text{H}\{^{31}\text{P}\}$ -NMR spectra (Figure 2. 9). When the sample was irradiated, a new set of signals appeared, shifted upfield compared to the original ones, in concordance with the trends explained in chapter 1.

The isomerization process and its reversibility were also studied by UV-vis spectroscopy. A solution of the azophosphine **1** in toluene was irradiated at $\lambda = 350$ nm during 1 h, then the sample was placed in the UV-vis quartz cell and spectra were recorded at fixed time intervals to study the *Z* to *E* isomerization process. As expected, two bands were observed; a very intense one at 325 nm due to the transition $\pi_1 \rightarrow \pi_1^*$, characteristic of the *E* azo isomer, and a less intense one at 440

nm, attributed to the partly forbidden transition $n_s \rightarrow \pi_1^*$, typical of a *Z* azo moiety. The former one progressively increases when the irradiated sample is left in the dark. Accordingly, the weak band decreases when the *Z* form returns to the *E* form (Figure 2. 10).

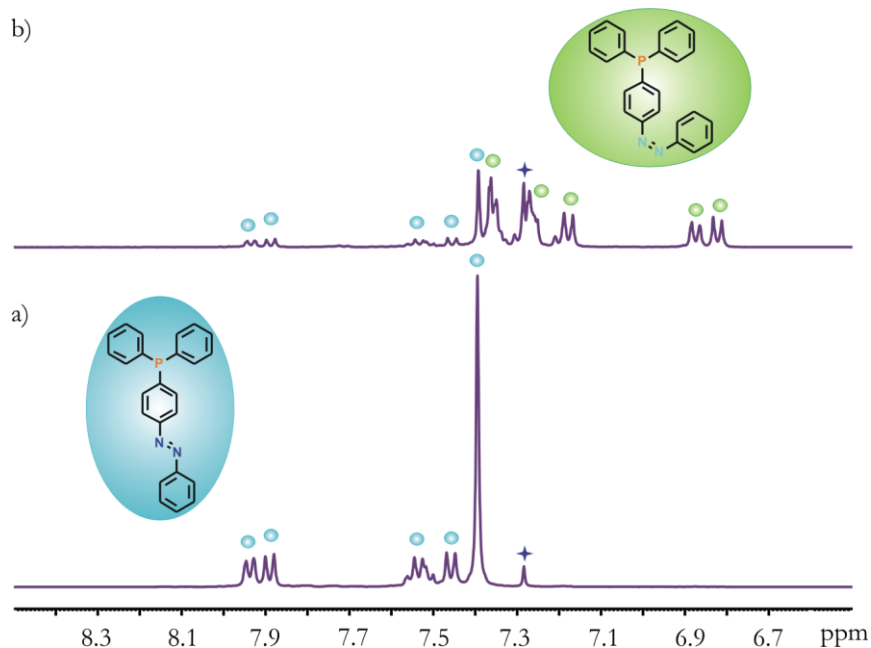


Figure 2. 9. $^1\text{H}\{^{31}\text{P}\}$ -NMR in CDCl_3 of the phosphine **1**: a) before irradiation; b) after 1 h irradiation. The shift of 1 ppm of the signals is clearly appreciated.

The same behaviour was observed for azomonophosphine **2** and diphosphines **7** and **8**, as they all have only one azo moiety in the structure. For example, azodiphosphine **7** shows a singlet in the $^{31}\text{P}\{^1\text{H}\}$ -NMR at -2.16 ppm that disappeared upon irradiation, rendering a new signal at -2.39 ppm. After keeping the sample in the dark, the initial signal was recovered whilst the one associated to the *Z* azobenzene isomer disappeared with time (Figure 2. 11).

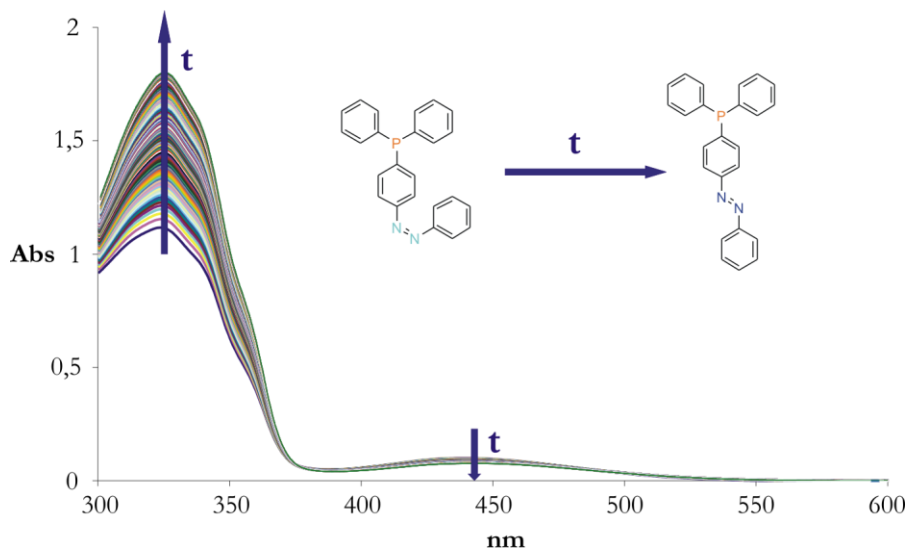


Figure 2. 10. UV-vis absorption spectroscopic change of the phosphine **1** after irradiation of the sample with $\lambda = 350$ nm during 1 h in toluene.

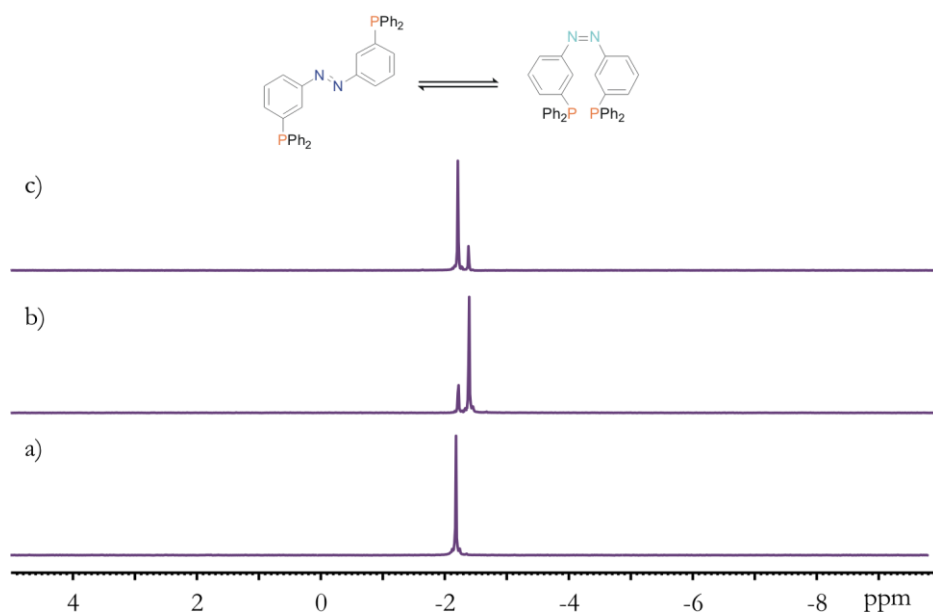


Figure 2. 11. $^{31}\text{P}\{^1\text{H}\}$ -NMR in CDCl_3 of phosphine **7**: a) before irradiation; b) after 1 h irradiation; c) after 3 days in the dark at r.t.

As regards to tris-azophosphine **3**, the situation is slightly more complicated since the three azo groups in the molecule may isomerize independently, rendering up to four different isomers. Depending on the relative configuration of the azo double bonds, *EEE*, *EEZ*, *EZZ* and *ZZZ* isomers are possible. Before irradiation a solution in CDCl_3 of ligand **3** shows one singlet in the $^{31}\text{P}\{^1\text{H}\}$ -NMR spectrum. The signal was attributed to the presence of only one species with the *EEE* conformation. The surprising result is that after irradiation at $\lambda = 350 \text{ nm}$ during 1 h, only two additional signals at -2.48 ppm and -2.84 ppm appeared next to the initial singlet at -1.94 ppm (Figure 2. 12). As observed for the monoazo ligands, the initial singlet was recovered after several days in the dark. It is worth mentioning that the peak distribution did not suffer any variation when the irradiation was prolonged for several hours, and thus a steady state was reached under these conditions. Although kinetic studies for the ligands containing less azo groups have not been performed, it is assumed that 1 h of irradiation is sufficient to reach a steady state. Consequently, this is the irradiation time that will be applied in the studies to induce $E \rightarrow Z$ isomerizations.

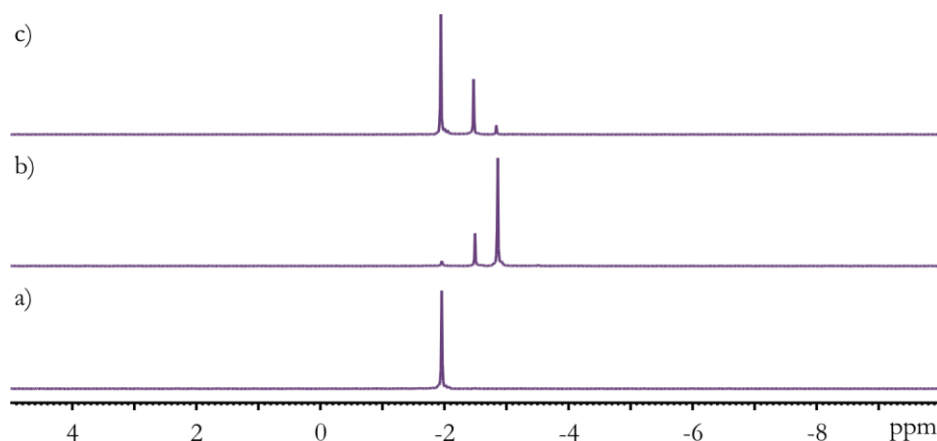


Figure 2. 12. $^{31}\text{P}\{^1\text{H}\}$ -NMR in CDCl_3 of the phosphine **3**: a) before irradiation; b) after 1 h irradiation; c) after 7 days in the dark at r.t. or heating.

The results obtained demonstrated that the presence of a phosphine is compatible with the isomerization processes of the azo group. The next step (on the way to potential catalytic applications) was to study if the presence of a metal

complex or coordination of the phosphines to a metal affects the $E \rightarrow Z \rightarrow E$ isomerization processes.

Initially, the photochemical E to Z isomerization was studied. The coordination properties of the ligands were studied by *in situ* $^{31}\text{P}\{^1\text{H}\}$ -NMR analysis of their platinum dichloride complexes $[\text{PtCl}_2\text{L}_2]$. When two equivalents of the azomonophosphine **1** in E conformation were mixed with the metal precursor $[\text{PtCl}_2(\text{cod})]$ in CDCl_3 , the spectrum shows a singlet at 17.33 ppm. By inspection of the satellites of the signal, the coupling constant between phosphorus and platinum can be measured and it has the value of 3662 Hz, characteristic of a *cis* complex. Hence, this signal is attributed to the formation of the *cis*- $[\text{PtCl}_2\text{P}_E\text{P}_E]$ complex as major compound (Figure 2. 13, Table 2. 1). Around 23 ppm, traces of the *trans*- $[\text{PtCl}_2\text{P}_E\text{P}_E]$ complex are observed.⁴⁹ The sample is then irradiated for 1 h at $\lambda = 350$ nm. The original signal at 17.33 ppm evolves to a pair of doublets at 17.91 ppm and 16.70 ppm, and a new singlet at 17.25 ppm (with their corresponding satellites). The doublets are attributed to *cis*- $[\text{PtCl}_2\text{P}_E\text{P}_Z]$ and the singlet to a *cis* complex in which both ligands were converted to the Z form (*cis*- $[\text{PtCl}_2\text{P}_Z\text{P}_Z]$). As for the free phosphines, the original singlet is recovered after five days, demonstrating that metal coordination inhibits neither E to Z nor Z to E isomerization.

Table 2. 1. $^{31}\text{P}\{^1\text{H}\}$ -NMR spectra data of *cis*- $[\text{PtCl}_2(\mathbf{1})_2]$ complexes in CDCl_3 .

	δ [ppm]	$^1\text{J}(\text{P}_E, \text{Pt})$ [Hz]	$^1\text{J}(\text{P}_Z, \text{Pt})$ [Hz]	$^2\text{J}(\text{P}_E, \text{P}_Z)$ [Hz]
$[\text{PtCl}_2\text{P}_E\text{P}_E]$	17.33	3662	-	-
$[\text{PtCl}_2\text{P}_E\text{P}_Z]$	17.91 16.70	3683 -	- 3640	15.85
$[\text{PtCl}_2\text{P}_Z\text{P}_Z]$	17.25	-	3660	-

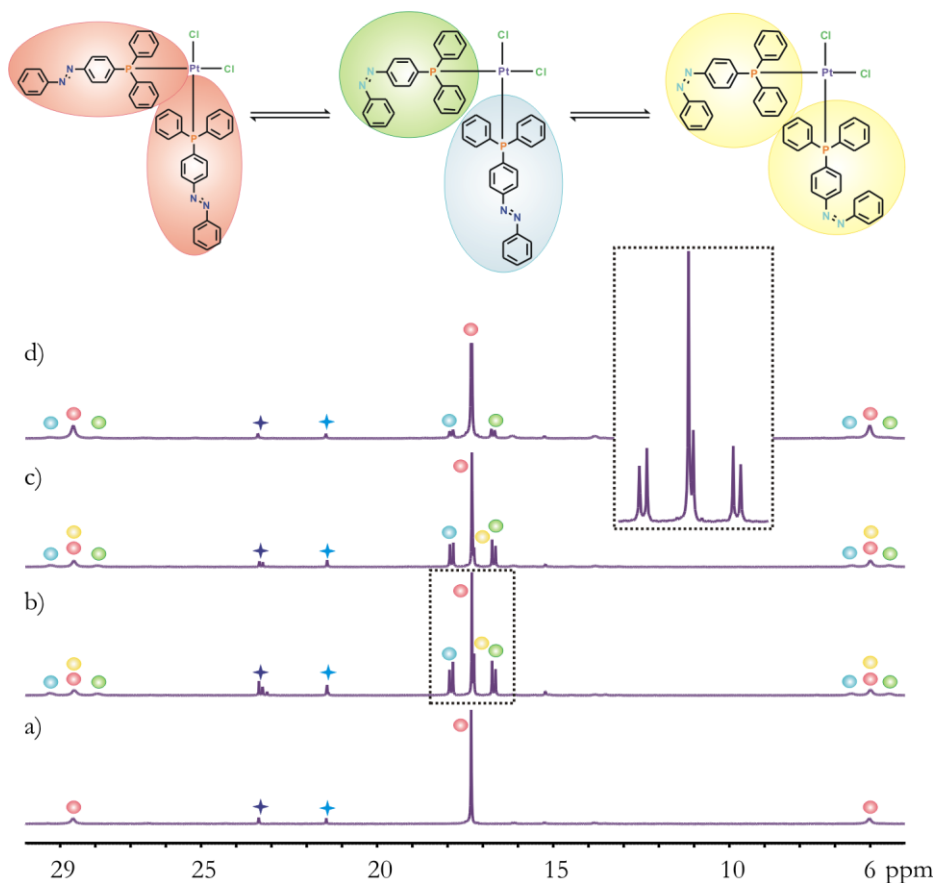


Figure 2. 13. ³¹P{¹H}-NMR in CDCl₃ of the complex *cis*-[PtCl₂(**1**)₂]: a) before irradiation; b) after 1 h irradiation; c) after 14 h in the dark at r.t.; d) after 5 days in the dark at r.t..

Additionally, we can also conclude that the metal complexes do not catalyze *Z* to *E* conversion of the azophosphines either. The latter is somewhat surprising because, as mentioned above, Nakamura *et al.* reported rapid catalytic *Z* to *E* isomerization of azobenzene for several metal complexes. They proposed that back donation from a zero-valent metal to the azo functionality in a transient complex causes the catalytic *Z* to *E* transformation.⁴⁹ In our case, the present complexes are not sufficiently electron-rich to do so. This reversibility can be observed when performing the study by UV-vis, as done previously for the free phosphines. A solution of complex *cis*-[PtCl₂(**1**)₂] in toluene was irradiated at $\lambda = 350$ nm during 1 h, then the sample was

placed in the UV-vis quartz cell and spectra were recorded at fixed time intervals. The two bands observed followed the same trend as the ones for the free ligand; the more intense progressively increased when the irradiated sample was left in the dark, while the weak band decreased when the *Z* form returned to the *E* form.

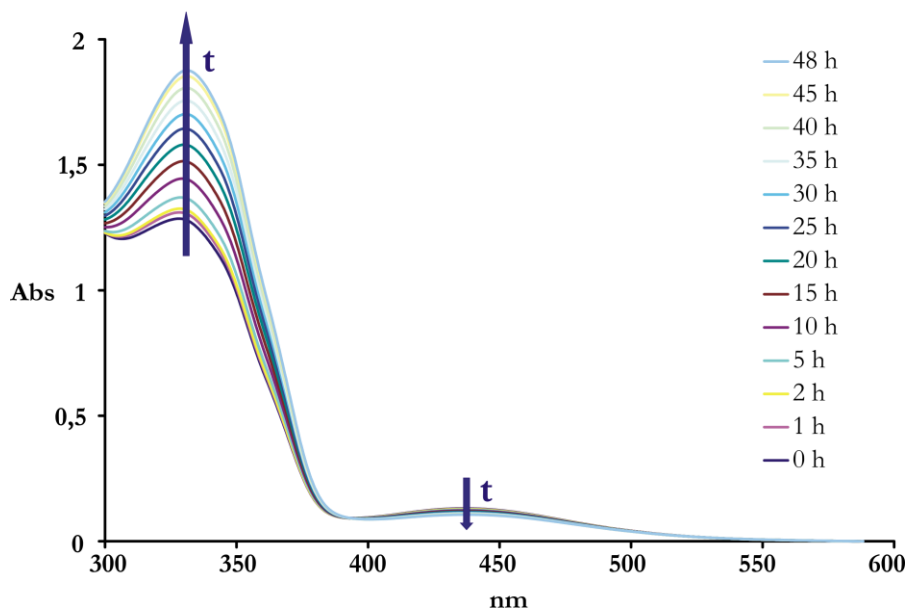


Figure 2. 14. UV-vis absorption spectroscopic change of the complex *cis*-[PtCl₂(**1**)₂] after irradiation of the sample with $\lambda = 350$ nm during 1 h in toluene.

Regarding the study of the complexes of trisazophosphine **3**, the system becomes more complicated. The two phosphines coordinated to the metal present each three azo moieties that can isomerize independently, rendering up to ten possible species (considering only those compounds in which the coordination of the two phosphines to the platinum occurs in a *cis* fashion). In the complexes in which the two phosphines are equivalent, singlets should be observed in the ³¹P{¹H}-NMR spectrum, but if the phosphines are not equivalent, sets of doublets will be observed. The number of signals in the spectrum can be doubled considering the possibility that the phosphines can also coordinate in a *trans* manner to the metal.

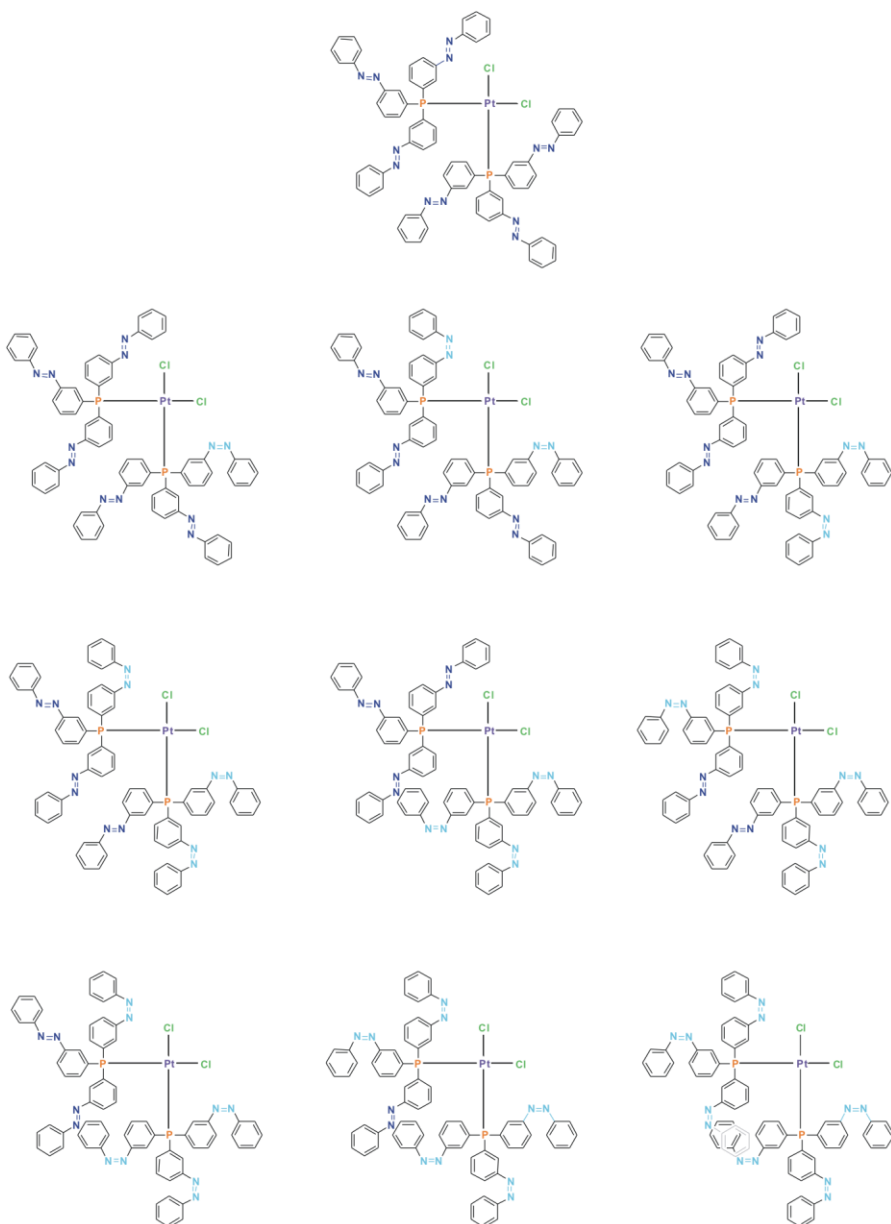


Figure 2. 15. Species that can be present upon irradiation of the $[\text{PtCl}_2(\mathbf{3})_2]$ having the azophosphines **3** coordinated in a *cis* manner to the platinum.

When two equivalents of phosphine **3** in *E* conformation were mixed with the metal precursor $[\text{PtCl}_2(\text{cod})]$ in CDCl_3 , we had initially only one signal present in the

$^{31}\text{P}\{^1\text{H}\}$ -NMR spectrum at 17.45 ppm, attributed to *cis*-[PtCl₂(*EEE-3*)₂]. Due to the complexity of the signal, we were not able to identify all the species present after irradiation (Figure 2. 16), but we can conclude from this experiment that all complexes generated after irradiation are *cis* complexes, since all signals retain a similar chemical shift, and the satellites presented coupling constants $^1\text{J}(\text{P-Pt})$ around 3600 Hz.

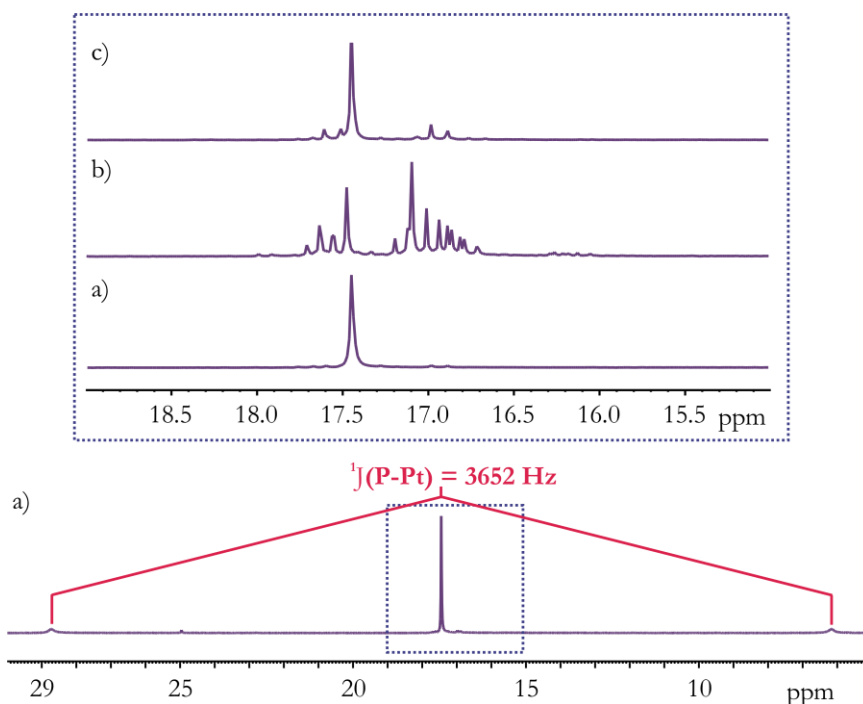


Figure 2. 16. $^{31}\text{P}\{^1\text{H}\}$ -NMR in CDCl_3 of the complex *cis*-[PtCl₂(**3**)₂]: a) before irradiation; b) after 1 h irradiation; c) after 3 days in the dark at r.t..

2.4. CONCLUDING REMARKS

In conclusion, we have designed and synthesized a series of azophosphines with switchable properties.

By using different techniques (UV-vis and NMR spectroscopy) we have corroborated that the phosphorus atom present in the molecule does not influence

the photochemical and thermal isomerization processes.

Furthermore, the same behaviour can be observed when the phosphines were tested upon coordination to a metal, such as platinum. The complexes and their switchability have been studied and characterized by using NMR and UV spectroscopy.

These results encouraged us to design more elaborated systems and preliminary studies under catalytic conditions.

References and notes

1. Kawamura, M.; Kiyotake, R.; Kudo, K. *Chirality* **2002**, *14*, 724.
2. Pasynskii, A. A.; Nefedov, S. E.; Eremenko, I. L.; Kolobkov, B. I.; Yanovsky, A. I.; Struchkov, Y. T. *Bull. Pol. Acad. Sci., Chem.* **1994**, *42*, 23.
3. Yamamura, M.; Kano, N.; Kawashima, T. *J. Am. Chem. Soc.* **2005**, *127*, 11954.
4. Tolman, C. A.; Seidel, W. C.; Gosser, L. W. *J. Am. Chem. Soc.* **1974**, *96*, 53.
5. Tolman, C. A. *Chem. Rev.* **1977**, *77*, 313.
6. Goto, K.; Ohzu, Y.; Sato, H.; Kawashima, T. *Phosphorus, Sulfur Silicon Relat. Elem.* **2002**, *177*, 2179.
7. Niyomura, O.; Iwasawa, T.; Sawada, N.; Tokunaga, M.; Obora, Y.; Tsuji, Y. *Organometallics* **2005**, *24*, 3468.
8. Molecular mechanics calculations have been performed using MM2 force field, as implemented in CAChe v. 6.1.1. Minimum energy conformations were located by using a block diagonal Newton–Raphson algorithm. Optimization continues until the energy change is less than 0.001 kcal/mol. The structures shown in Figure 2.3 are conformations selected from the several local minima observed for the tris *E* and tris *Z* form respectively.
9. Claver, C.; Fernandez, E.; Gillon, A.; Heslop, K.; Hyett, D. J.; Martorell, A.; Orpen, A. G.; Pringle, P. G. *Chem. Commun.* **2000**, 961.
10. Gridnev, I. D.; Fan, C.; Pringle, P. G. *Chem. Commun.* **2007**, 1319.
11. Norman, D. W.; Carraz, C. A.; Hyett, D. J.; Pringle, P. G.; Sweeney, J. B.; Orpen, A. G.; Phetmung, H.; Wingad, R. L. *J. Am. Chem. Soc.* **2008**, *130*, 6840.
12. de Vries, J. G.; Lefort, L. *Chem.–Eur. J.* **2006**, *12*, 4722.
13. Reetz, M. T.; Sell, T. *Tetrahedron Lett.* **2000**, *41*, 6333.
14. Reetz, M. T.; Fu, Y.; Meiswinkel, A. *Angew. Chem., Int. Ed.* **2006**, *45*, 1412.
15. Hessler, A.; Stelzer, O.; Dibowski, H.; Worm, K.; Schmidtchen, F. P. *J. Org. Chem.* **1997**, *62*, 2362.
16. Gulyas, H.; Benet-Buchholz, J.; Escudero-Adan, E. C.; Freixa, Z.; van Leeuwen, P. W. N. M. *Chem.–Eur. J.* **2007**, *13*, 3424.
17. Noble, A. *Quart. J., Chem. Soc., London* **1856**, *8*, 292.
18. Ogata, Y.; Takagi, Y. *J. Am. Chem. Soc.* **1958**, *80*, 3591.
19. Mills, C. J. *Chem. Soc.* **1895**, *67*, 925.
20. Baeyer, A.; Caro, H. *Berichte der Deutschen Chemischen Gesellschaft* **1874**, *7*, 963.
21. Davey, M. H.; Lee, V. Y.; Miller, R. D.; Marks, T. J. *J. Org. Chem.* **1999**, *64*, 4976.
22. Gowenlock, B. G.; Richter-Addo, G. B. *Chem. Rev.* **2004**, *104*, 3315.
23. Prievisch, B.; Rueck-Braun, K. *J. Org. Chem.* **2005**, *70*, 2350.
24. Garlich-Zschoche, F. A.; Doetz, K. H. *Organometallics* **2007**, *26*, 4535.
25. Barakat, M. Z.; Abdelwahab, M. F.; Elsadr, M. M. *J. Chem. Soc.* **1956**, 4685.
26. Shine, H. J.; Zmuda, H.; Kwart, H.; Horgan, A. G.; Brechbiel, M. *J. Am. Chem. Soc.* **1982**, *104*, 5181.
27. Wheeler, O. H.; Gonzalez, D. *Tetrahedron* **1964**, *20*, 189.
28. Shaabani, A.; Lee, D. G. *Tetrahedron Lett.* **2001**, *42*, 5833.

29. Patel, S.; Mishra, B. K. *Tetrahedron Lett.* **2004**, *45*, 1371.
30. Nakagawa, K.; Tsuji, T. *Chem. Pharm. Bull.* **1963**, *11*, 296.
31. Goldstein, S.; McNelis, E. *J. Org. Chem.* **1973**, *38*, 183.
32. Leyva, E.; Monreal, E.; Medina, C.; Leyva, S. *Tetrahedron Lett.* **1997**, *38*, 7847.
33. Wang, X. Y.; Wang, Y. L.; Li, J. P.; Wang, C. L.; Duan, Z. F.; Zhang, Z. Y. *Indian J. Chem., Sect. B: Org. Chem. Incl. Med. Chem.* **2000**, *39*, 545.
34. Zhang, M.; Zhang, R. L.; Zhang, A. Q.; Li, X. F.; Liang, H. H. *Synth. Commun.* **2009**, *39*, 3428.
35. Wang, X. Y.; Wang, Y. L.; Li, J. P.; Sun, L. F.; Zhang, Z. Y. *Chin. Chem. Lett.* **1999**, *10*, 533.
36. Yu, B.-C.; Shirai, Y.; Tour, J. M. *Tetrahedron* **2006**, *62*, 10303.
37. Parlow, J. J.; South, M. S. *Tetrahedron* **2003**, *59*, 7695.
38. Peters, M. V.; Stoll, R. S.; Goddard, R.; Buth, G.; Hecht, S. *J. Org. Chem.* **2006**, *71*, 7840.
39. Mori, Y.; Niwa, T.; Toyoshi, K. *Chem. Pharm. Bull.* **1981**, *29*, 1439.
40. Li, Q.; Green, L.; Venkataraman, N.; Shiyonovskaya, I.; Khan, A.; Urbas, A.; Doane, J. W. *J. Am. Chem. Soc.* **2007**, *129*, 12908.
41. Yamamura, M.; Kano, N.; Kawashima, T. *Inorg. Chem.* **2006**, *45*, 6497.
42. Herd, O.; Hessler, A.; Hingst, M.; Machnitzki, P.; Tepper, M.; Stelzer, O. *Catal. Today* **1998**, *42*, 413.
43. van der Veen, L. A.; Kamer, P. C. J.; van Leeuwen, P. W. N. M. *Organometallics* **1999**, *18*, 4765.
44. Herwig, J.; Bohnen, H.; Skutta, P.; Sturm, S.; Van Leeuwen, P. W. N. M.; Bronger, R.. PCY. Int. Appl. WO Patent 2002-EP1380, **2002** (to Celanese).
45. Fei, Z.; Scopelliti, R.; Dyson, P. J. *Dalton Trans.* **2003**, 2772.
46. Teunissen, H. T.; Hansen, C. B.; Bickelhaupt, F. *Phosphorus, Sulfur Silicon Relat. Elem.* **1996**, *118*, 309.
47. Sirbu, D.; Consiglio, G.; Gischig, S. *J. Organomet. Chem.* **2006**, *691*, 1143.
48. Reetz, M. T.; Maiwald, P. C. R. *Chim.* **2002**, *5*, 341.
49. Nakamura, A.; Doi, K.; Tatsumi, K.; Otsuka, S. *J. Mol. Catal.* **1976**, *1*, 417.

UNIVERSITAT ROVIRA I VIRGILI
SWITCHABLE AND TUNABLE LIGANDS FOR HOMOGENEOUS CATALYSIS
Maria Dolores Segarra Maset
ISBN:978-84-693-7666-9/DL:T-1755-2010

CHAPTER 3

CATALYSIS

3.1. INTRODUCTION AND OBJECTIVES

In the previous chapter it was demonstrated that it is feasible to place an azobenzene moiety in a molecule containing a phosphorus donor ligand, while maintaining access to *Z* and *E* conformations via the azo isomerization process. It was also proved that the azo moiety even retains its photochromic properties when the P-donor is coordinated to a metal. Furthermore, when Pt was used as a model of metallic centre, it was evidenced that the coordination of the ligand takes place through the phosphorus atom and not via the nitrogen atoms present in the structure. Once all these basic requirements were established, in the current chapter several catalytic tests will be presented to study if the isomerization of the azo double bond produces any effective structural change in the phosphines that translates in an effect on catalysis.

Before attempting to use azobenzene containing ligands in catalysis, it is worth to recall some excerpts on the nature of the azobenzene isomerism. At the steady state, the concentration of the *E* and *Z* forms of an azobenzene fragment strongly depends on the temperature. After ligand irradiation at the appropriate wavelength, to obtain a steady state enriched in the *Z* form, the equilibrium reverts to the most thermodynamically stable *E* conformer with time. Moreover, as it is well-known in

literature, and shown in the previous chapter, under irradiation conditions when a steady state is reached, the ligands are never present as pure *Z* isomers, but at best around ~85 % of the azo groups occur in the *Z* form. The reversion from *Z* to *E* is also a photochemical process (using ~430 nm light source, depending on the photochromic properties of each compound), which takes place in addition to the thermal process. The latter continues when the irradiation is stopped. All these factors need to be taken into account when studying the catalysis.

Ideally, one of the two conformers should give a complex that is more active in catalysis. To obtain the highest difference in the catalytic results between a non irradiated azophosphine (*i. e.* the *E* azo isomer) and an irradiated one (*i. e.* the mixture enriched in *Z* azo isomer) the optimal conditions to stabilize (as much as possible) each isomer used during the catalysis have to be found.

For the reasons previously mentioned, it is needed to test the azophosphines in “fast” catalytic reactions to minimize the evolution of the irradiated ligand to the more stable *E* isomer during the reaction. In addition, the reaction temperature should be kept as low as possible to minimize *Z* to *E* thermal isomerization. Finally, to perform the catalysis with “the *Z* isomer” (or an enriched sample of it), the reaction has to be performed in the dark, as sunlight also favours the *E* to *Z* isomerization (as it contains the wavelength light necessary to induce this isomerization process).

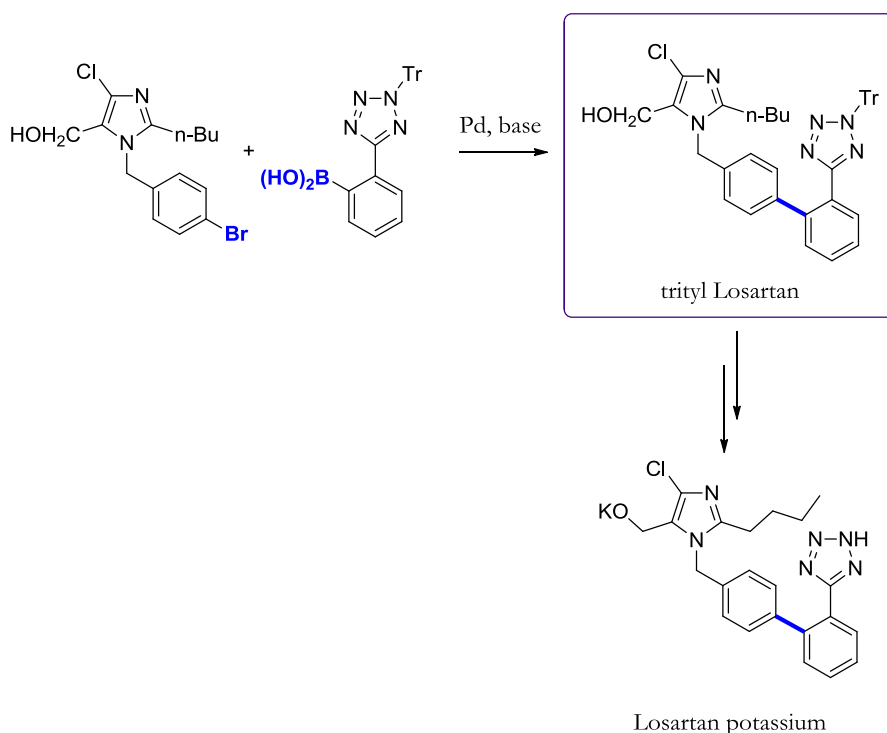
Two methodologies were used to maximize the proportion of catalyst containing the ligand in the *Z* isomeric form. The first one involves a pre-isomerization of the ligand in solution, before incorporating it into the catalytic reaction mixture. The second approach is to construct an experimental setup in which the irradiation of the sample can take place during the catalysis. In that case a cooling system needs to be implemented, as the irradiation of the sample always involves a temperature increase. Quartz vessels are used to irradiate the sample during catalysis. If the presence of a gas is required for the catalytic process, it will be restricted to 1–2 bars, which is the pressure limitation of these reactors.

All these restrictions need to be kept in mind when choosing the catalytic reaction. In the next pages some catalytic studies are presented using azobenzene containing ligands in reactions that, *a priori*, meet these requirements.

3.2. CATALYSIS

3.2.1. PALLADIUM CATALYZED SUZUKI CROSS-COUPLING

The Suzuki reaction is a palladium catalyzed C–C bond formation, between a boronic acid and a halogenated derivate. This reaction has been widely studied^{1–3} and industrially it is applied in the synthesis of several pharmaceutical compounds, for example, Losartan potassium for treatment of high blood pressure and heart failure (Scheme 3. 1);⁴ or Vancomycin, used as antibiotic.⁵



Scheme 3. 1. Palladium Suzuki cross-coupling step involved in the synthesis of Losartan potassium.

There are many parameters that affect the activity (or selectivity) of this reaction depending on the substrate and catalyst, and there is not a simple and general rule to

control this process. Nowadays, the optimization of a certain Suzuki cross-coupling reaction is mainly a matter of trial and error, changing and studying for each case the conditions, such as the ligands employed, solvent, temperature, base, metal precursor, substrates, reaction times, etc.⁶⁻¹⁰

The reaction was discovered in the 70s,¹¹ but some mechanistic aspects are still under discussion.^{1,12,13} The generally accepted mechanism involves oxidative addition of the halide derivative to a Pd(0) complex, then a transmetalation with the arylboronic acid and finally reductive elimination to generate the new C–C bonded product and the initial Pd(0) complex. The step less known is the transmetalation one, for which it seems that a base is required, but its role is not clearly understood. Two main theories have been postulated to describe the transmetalation step. In the first mechanism proposed (Figure 3. 1, A) the base reacts with the boronic acid to form a more reactive boronate that interacts with the Pd center.¹⁴ The second one (Figure 3. 1, B) explains the effect of the base by assuming that it replaces the halide in the coordination sphere of the palladium complex, thereby facilitating the intramolecular transmetalation.¹⁵

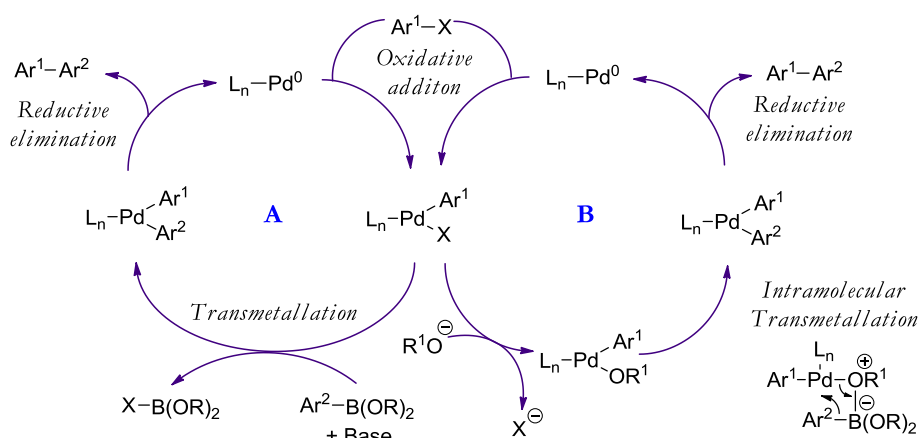


Figure 3. 1. Two catalytic cycles proposed for the mechanism of Suzuki cross-coupling.

The ligands used for this reaction are mainly phosphines. In particular, Fu and Buchwald have shown that bulky and basic monophosphines are effective in the

Suzuki reaction.^{16,17} Later on, Tsuji *et al.* have demonstrated that structural parameters of bowl shaped phosphines (BSP) resulted to be crucial in the activity in palladium catalyzed Suzuki reaction.¹⁸ The authors could not find any relation between the usual parameters used to describe phosphine properties and catalytic activity (*i.e.* basicity and cone angle). They conceived new parameters to describe BSPs. The *depth* (d) and the *diameter* (l) of the BSP (Figure 3. 2) were calculated for several ligands and it was found that the effectiveness of the ligand (in terms of activity) increases with the depth of the bowl for unactivated aryl chlorides.

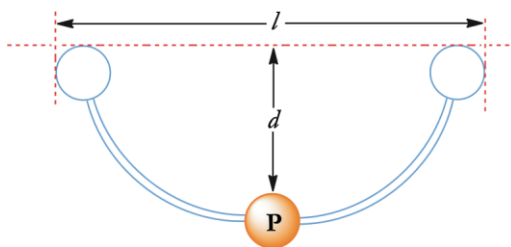
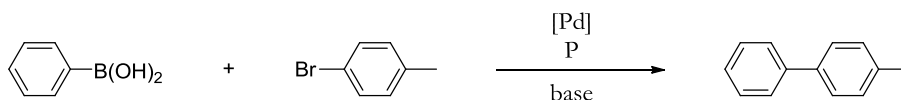


Figure 3. 2. Picture of the BSP showing the parameters *depth* (d) and *diameter* (l) used as descriptors.

As mentioned in the previous chapter, when azophosphine **3** adopts an *E* conformation it should have a catalytic behaviour similar to that of PPh_3 . Instead, in an optimistic view, the *Z* isomer might resemble a BSP. The Suzuki cross-coupling reaction seems then adequate as proof of concept to test the structural change in the azophosphines designed in this thesis.

Few examples are known in literature of Suzuki cross-coupling reactions at room temperature (desired to avoid the thermal *Z* to *E* isomerization).^{8-10,19} For instance, Fu *et al.* described the coupling of aryl chlorides and bromides, with arylboronic acids at room temperature.²⁰ As expected, higher conversions were found when aryl bromides were employed. These conditions were chosen to start the test with phosphine **3** (Scheme 3. 2). The reaction was performed at r. t. using THF as solvent, 0.5 % of $\text{Pd}_2(\text{dba})_3$, and 1.2 % of azomonophosphine **3**. The base used in this study was 3.3 equivalents of dry KF. In this first attempt, however, no conversion was observed, neither using *E*-**3** nor when the irradiation of the phosphine was done

during one hour before adding it to the reaction mixture. No conversion was obtained either using phosphine **23** (Figure 3. 3), reported in literature as active with very similar substrates and the same reaction conditions.²⁰



Scheme 3. 2. Suzuki cross-coupling reaction performed.

For similar substrates, but at different reaction conditions, Buchwald *et al.* found that biaryl type phosphines **21** and **22** (Figure 3. 3) were very active for the catalysis of unactivated aryl chlorides, even at room temperature, with very low catalyst loadings.¹⁷

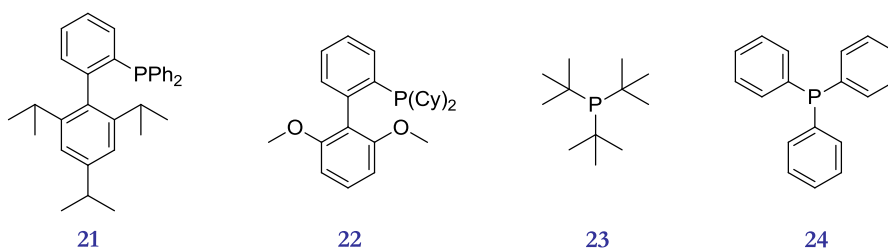


Figure 3. 3. Phosphines used for the optimization of r. t. Suzuki reaction.

Several reaction conditions were tested, changing ratios of reactants, palladium source, and base (KF or K₃PO₄). The optimized conditions resulted slightly different from the ones described by the Buchwald *et al.*, *i.e.* they used the less reactive aryl chloride (instead of aryl bromide), and Pd(OAc)₂ as metal source. In the optimized reaction conditions for the azophosphines, Pd₂(dba)₃ was used.²¹ The results obtained with several ligands using these conditions are summarized in Table 3. 1.

Ligand **22** was unreactive, unlike ligand **21** (Table 3. 1, entries 1 and 2). This was a surprising result, because phosphine **22** was known to perform the reaction on unactivated aryl chlorides and bromides (according to published results).¹⁹ Phosphine **21** was prepared at a later stage aiming at higher stability and lower synthetic costs (in

their search for future industrial applications) but Buchwald *et al.* postulated that ligand **22** is more effective in the reaction, especially for extremely bulky substrates.¹⁷ Surprisingly, in our hands phosphine **22** did not present any activity, not even after 24 h of reaction time, but instead phosphine **21** gave 87 % conversion after 3.5 h and reached full conversion at 17 h.

Ligand **3** was tested using the optimized reaction conditions (Table 3. 1, entries 3 and 4). The catalysis was performed both with the most stable *E-3* form and with the irradiated one (enriched in *Z-3*). Unfortunately, in none of the cases activity was observed.

Table 3. 1. Results obtained for the Suzuki cross-coupling with several phosphines.

Ligand	Entry	Irradiation	Conversion (%)			
			30 min	3.5 h	17 h	24 h
21	1	no	10	87	100	100
22	2	no	0	0	0	0
3	3	no	0	3	3	3
	4	before	1	3	3	4
7	5	no	0	0 ^a	9	9
	6	during	0	0 ^a	57	64
24	7	no	2	3 ^a	6	7
	8	during	16	28 ^a	65	65

Conditions: r.t., 24 h reaction, [Pd] = 1.25 mM, K₃PO₄/boronic acid/Br-toluene/P/Pd = 2400/1200/800/6/1. THF = 2 mL. ^a Sample analyzed after 2 h.

The main problem of performing the reaction at low temperatures, such as r. t., is that long reaction times are required to reach conversion (24 hours experiments are common). At this time interval, it was found previously that most of the *Z* azophosphine reverts to its *E* form for any of the ligands (see chapter 2), so the possible changes in activity observed due to the isomerization will become less evident. For that reason an experimental setup was developed in which the sample

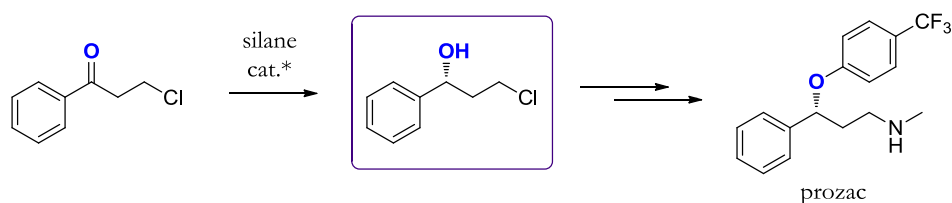
can be irradiated during catalysis (as mentioned before). A quartz reactor was used, that permits simultaneous reaction and irradiation ($\lambda = 350$ nm). Under these conditions, azodiphosphine **7** was chosen to perform the catalysis, as it gave 9 % conversion without irradiation (Table 3. 1, entries 5 and 6). Whilst *E-7* did not reach significant conversion after 24 h., when irradiation takes place during the catalysis the activity was much higher, reaching 57 % conversion after 17 h and 64 % after 24 h.

A control reaction was performed using triphenylphosphine **24** as ligand (Table 3. 1, entries 7 and 8) to discard background reactions not related to azobenzene. The results revealed that the same enhancing effect observed for azophosphine **7** was taking place; almost no activity was observed without irradiation, and around 65 % conversion was measured after 24 hours with irradiation. In fact, König *et al.* found a similar effect which they attributed to the local heating of the catalyst with P-ligands that contain extended π -conjugated aromatic systems, but not for triphenylphosphine.²² The results of these authors corroborate that irradiation affects the palladium Suzuki C–C cross coupling reaction, although their interpretation of “local catalyst heating” needs further refinement.

The results obtained in the Suzuki cross-coupling reaction suggests that eventually this reaction resulted not to be appropriate to test the azophosphines. There were temperature and time limitations, and the impossibility to irradiate during catalysis due to a light-induced activation observed even for triphenylphosphine.

3.2.2. RHODIUM CATALYZED HYDROSILYLATION OF KETONES

Hydrosilylation involves the reaction of an unsaturated bond such as alkenes, alkynes, and ketones with a silane. The product of reaction of ketones generates alcohols upon hydrolysis. The chiral version of the reaction is used to synthesize pharmaceutical products, as prozac (Scheme 3. 3).²³ It is also one of the fastest reactions known in homogeneous catalysis, it takes place at room temperature, and sometimes full conversion is observed in only a few minutes.



Scheme 3. 3. Synthesis of prozac via hydroxylation.

Although this reaction has been widely studied, the mechanism is somewhat controversial, as depending on the substrates used, the results change dramatically. However, there is a general mechanism proposed in 1975 by Ojima *et al.*, which is the most commonly accepted.²⁴ They discovered the activity of Wilkinson's complex in the hydrosilylation of carbonyl compounds.^{25,26} They based their mechanistic investigations on the isolation of the product obtained from an oxidative addition of triethylsilane to Wilkinson's catalyst, $[\text{RhH}(\text{PPh}_3)_2(\text{SiEt}_3)\text{Cl}]$.²⁷ The intermediate isolated was assumed to be the first reaction intermediate of the catalytic cycle (Figure 3. 4). The cycle starts with an oxidative addition of the hydrosilane to the Rh^{I} complex, obtaining the silyl metal hydride Rh^{III} compound. Then, the end-on coordination of the ketone leads to the insertion of the ketone carbonyl function into the $\text{Rh}-\text{Si}$ bond. The initial Rh^{I} species is recovered with a reductive elimination that liberates the silyl ether.

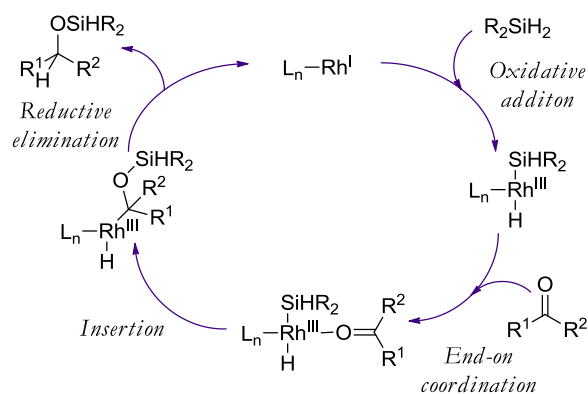


Figure 3. 4. General catalytic cycle of the Rh catalyzed hydrosilylation of ketones.

After that proposal, many efforts have been devoted to clarify the results obtained for specific regio- and enantio- induction when particular conditions are used,^{28–30} and some recent studies suggest alternative mechanisms for certain specific substrates or ligands.^{31–33} It is beyond the scope of this manuscript to make an extensive study of the mechanism of this reaction.

Initially, this catalysis was done with rhodium-phosphine systems, such as Wilkinson's catalyst based on triphenylphosphine,^{25,26} as mentioned previously, or other phosphines.^{34–39} A few years later oxazolines (specially bisoxazolines) became the most popular ligands due to the good activities and enantioselectivities obtained.^{40–46} Several oxazoline-phosphine chelate ligands were developed,^{47–49} and there are few examples with P,N ligands^{50–52} or pyridines.^{53–55} It was not until a few years ago that BSPs were applied to hydrosilylation catalysis. Several BSP ligands (as for instance the one depicted in Figure 3. 5) were tested in hydrosilylation using several silanes and ketones.^{56,57} The authors could not find a good correlation between the activity and the *cone angle* or the *basicity*, but they observed a very good enhancement of the reaction rate when these ligands were used compared to monophosphines such as **23** or triphenylphosphine **24**. This rate enhancement was attributed to the “deep bowl” formed around the phosphorus atom. It produces a large steric hindrance around the metal, generating that only one phosphine can be coordinated per metal centre. As a result, an excess of phosphine does not deactivate the system, as observed when smaller phosphines are used.⁵⁸ This reaction is the ideal reaction to test azophosphines (as **3**), which are expected to generate a bowl after isomerization of the azo bonds. As hindered BSPs had been already investigated in literature, the results obtained with the azophosphines can be compared to those reported, and one can study if the effect of isomerization translates in an effect in catalysis.^{56,57}

In the case of hydrosilylation the catalysis is fast enough to allow irradiation of the ligand only prior to catalysis. Additionally, it is worth mentioning that radical activation induced by light is known for hydrosilylation reactions,⁵⁹ also with platinum catalyst.^{60,61}

assuming that during this short time the phosphine *Z* isomer content stays the same in the irradiated samples. The results obtained are summarized in Table 3. 2.

Table 3. 2. Distribution of products obtained in the hydrosilylation of acetophenone with diphenyl silane.

Ligand	Entry	Acetophenone (%)	26 (%)	27 (%)
<i>E-2</i>	1	8	92	0
<i>Z-2</i>	2	2	94	4
<i>E-3</i>	3	14	51	35
<i>Z-3</i>	4	14	54	32
<i>E-7</i>	5	2	96	2
<i>Z-7</i>	6	6	92	2
24	7	4	96	0
25	8	8	89	3

Conditions: r.t., 10 min catalyst preformation, 30 min reaction, [Rh] = 10 mM, silane/acetophenone/P/Rh = 100/100/2/1. THF = 1 mL. *Z* denotes the mixture of isomers, enriched in the *Z* one, obtained after irradiation.

Several azophosphines (in both *E* and *Z* forms), triphenylphosphine **24** and BSP **25** were tested in the reaction.⁶² Unfortunately, by comparing the results obtained one can conclude that there was no difference in conversions between the *E* and the *Z* isomers of the azophosphines in any case. Additionally, the azophosphines with only one azo moiety in the structure presented nearly full conversion and a product distribution comparable to that of **24** and **25**.

High conversions (around 90 %) at 30 minutes of reaction are observed in all cases, which indicates that the system is too active to compare activities and shorter reaction times or more diluted samples would be required.

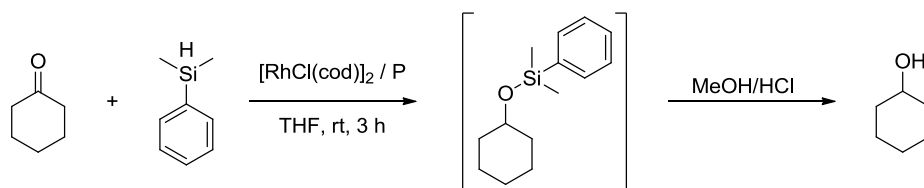
The most surprising result is the one obtained with azophosphine **3** (Table 3. 2, entries 3 and 4). Even though there was no difference in the conversion obtained between the two experiments performed with this phosphine (*E-3* and *Z-3*), the

outcome contrasts with those obtained for all other ligands. It presents a significant inversion in the selectivity towards the silyl enol ether **27**.

The ratio between **26** and **27** has not been widely studied in literature. Furthermore, **27** is frequently ignored, because in most of the occasions the analysis of the results is performed on the alcohols (hydrolyzed samples) and **27**, if present, is reverted to acetophenone. However, this compound can be interesting and useful as an intermediate for C–C or C–X bond forming reactions.⁶³ The synthesis of such silyl enol ethers is usually done through the *O*-silylation of lithium enolates. Rhodium dehydrogenative silylation of ketones offers an attractive alternative since hydrogen is the only by-product generated and no base is required.

Hydrosilylation of cyclohexanone

BSP ligands were also tested with the use of other substrates in literature, for example, in the hydrosilylation of cyclohexanone with dimethylphenylsilane (Scheme 3. 5).⁵⁷



Scheme 3. 5. Hydrosilylation of cyclohexanone with dimethylphenylsilane.

Azophosphines were tested using conditions similar to the ones reported in the literature for the hydrosilylation with BSP. The same substrate and silane were employed, but $[\text{Rh}(\mu\text{-Cl})(\text{cod})]_2$ was used instead of $[\text{RhCl}(\text{C}_2\text{H}_4)_2]_2$, (because of the good activities obtained with this precursor in the reaction explained previously), and THF instead of benzene, due to increased solubility of azo substituted ligands. The reaction time employed to preform the catalyst was 10 min and the reactions were done at room temperature. After 3 hours, a sample was hydrolyzed with a 1 % solution of HCl in methanol to obtain the alcohol. An aliquot was analyzed by GC.

The results obtained are summarized in Table 3. 3 (standard deviations are included).

Table 3. 3. Summary of the results obtained in the hydrosilylation of cyclohexanone.

Ligand	Entry	Conversion (%) ^a	σ^b
<i>E</i> -2	1	9	8
<i>Z</i> -2	2	3	3

<i>E</i> -3	3	36	13
<i>Z</i> -3	4	36	13

<i>E</i> -7	5	0	0
<i>Z</i> -7	6	4	4

24	7	0	0

25	8	36	27

Conditions: r.t., 10 min catalyst preformation, 3 h reaction, [Rh] = 10 mM, silane/cyclohexanone/P/Rh = 120/100/2/1. THF = 1 mL. ^a Averaged conversion.

^b Standard deviation.

This specific catalytic reaction showed a pronounced lack of reproducibility. This effect was also noticed previously by some authors,^{64,65} and it was attributed to the variable amount of water present in the system, or changes in the gas pressure when hydrogen is generated.⁶⁵ There is no clear explanation, but this lack of reproducibility is also evident from the results presented in table Table 3. 3, and this should be taken into account when interpreting these results.

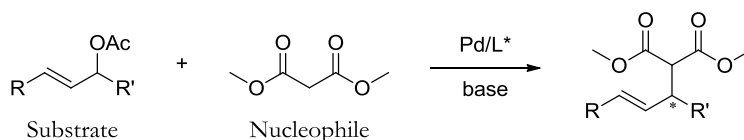
No differences in activity were observed in the catalysis (or lack of it) when the *E* form or the *Z* form of the azophosphines was used. In the case of the azophosphines with only one azo moiety in the structure, no conversion was noticed. The same was observed for triphenylphosphine 24. These results are in agreement with the ones reported by Tsuji *et al.*⁵⁷ In spite of the differences between our experimental conditions and the ones reported by the authors, the main trends are similar. When two equivalents of phosphine per rhodium centre were used, with less hindered phosphines, no activity of the catalyst was observed. This can be attributed to the formation of inactive species formed by coordination of more than one phosphine to

the metal.

As was observed in the hydrosilylation of acetophenone, ligand **3** presented different behaviour from the rest of the azophosphines tested (Table 3. 3, entries 3 and 4. The conversion measured was 36 %, irrespective of irradiation. This result was also observed for BSP **25**. One might conclude that phosphine **3** resembles a BSP, even when the azo is present in its *E* form, as was tentatively suggested by the MM2 calculations outlined in chapter 2. If so, both isomers are bulky enough to allow the coordination of only one P ligand to the rhodium complex (as happens for the BSP). As a result, similar conversions are observed for *E*-**3**, *Z*-**3** and **25**.

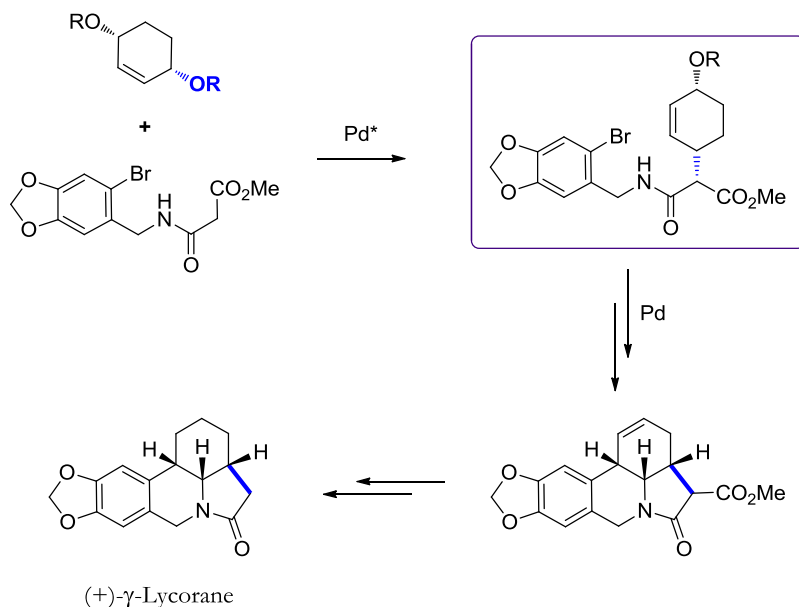
3.2.3. PALLADIUM CATALYZED ALLYLIC ALKYLATION

The formation of a new C–C bond via the palladium catalyzed allylic alkylation is an important tool in organic chemistry. The reaction involves palladium mediated nucleophilic substitution of an allylic substrate that incorporates a leaving group (usually acetate). Scheme 3. 6 represents the reaction with a generic substrate and a nucleophile to form a new carbon–carbon bond (among all the possible products that can be obtained, only one of them is depicted as an example).



Scheme 3. 6. Simplified model reaction of a palladium catalyzed allylic alkylation.

A huge number of synthetic examples have been published with special focus on the asymmetric variants.^{66–68} It is a useful synthetic tool in modern organic synthesis, and it has found applications in the synthesis of natural products, for example the alkaloid (+)- γ -Lycorane (Scheme 3. 7),^{69,70} which in addition to the desymmetrizing step contains two more palladium catalyzed coupling reactions. Surprisingly, industrial applications, if any, are rare.



Scheme 3. 7. Synthesis of (+)- γ -Lycorane, involving a palladium catalyzed allylic alkylation.

The first reaction of a π -allylpalladium chloride complex with nucleophiles was performed by Tsuji *et al.* in 1965.⁷¹ Trost *et al.* developed the asymmetric version.⁷² Many research groups have comprehensively studied the reaction, for example to achieve high regio- and stereoselectivity of the catalysis with a large variety of ligands and substrates.^{66–68,73} The asymmetric nucleophilic substitution of 1,3-diphenylallyl acetate has often been used as a model reaction to test chiral bidentate ligands in asymmetric allylic alkylation.^{74–76}

The mechanism of the catalytic cycle and the structures of its intermediates has been studied extensively. In spite of the complexity, one of the mechanisms proposed has succeeded in explaining the majority of the results. Having a look at the general mechanism suggested, it can be noticed that several products can be obtained depending on the regio- and enantiodiscrimination.⁷⁷

The catalytic cycle starts with the complexation of the alkene to Pd(0), followed by the ionization of the leaving group, resulting in a π -allylpalladium(II) intermediate which will undergo the addition of the nucleophile. Depending on the

stereochemistry of C3, the ionization (or oxidative addition) leads to the R and R' *syn* or *anti* π -allylpalladium intermediate. In the initial intermediate the R group at C1 will occupy a *syn* position, as the starting alkene has a *trans* (*E*) structure. *Syn* and *anti* configurations can be interchanged via π - σ rearrangements. The nucleophile can attack at C1 or C3, depending on the stereoisomer, the ligand, the solvent, the anions and the nucleophile. The final product is obtained after decomplexation of the substituted allyl product and the initial Pd(0) species is recovered to start the cycle again (Figure 3. 6).

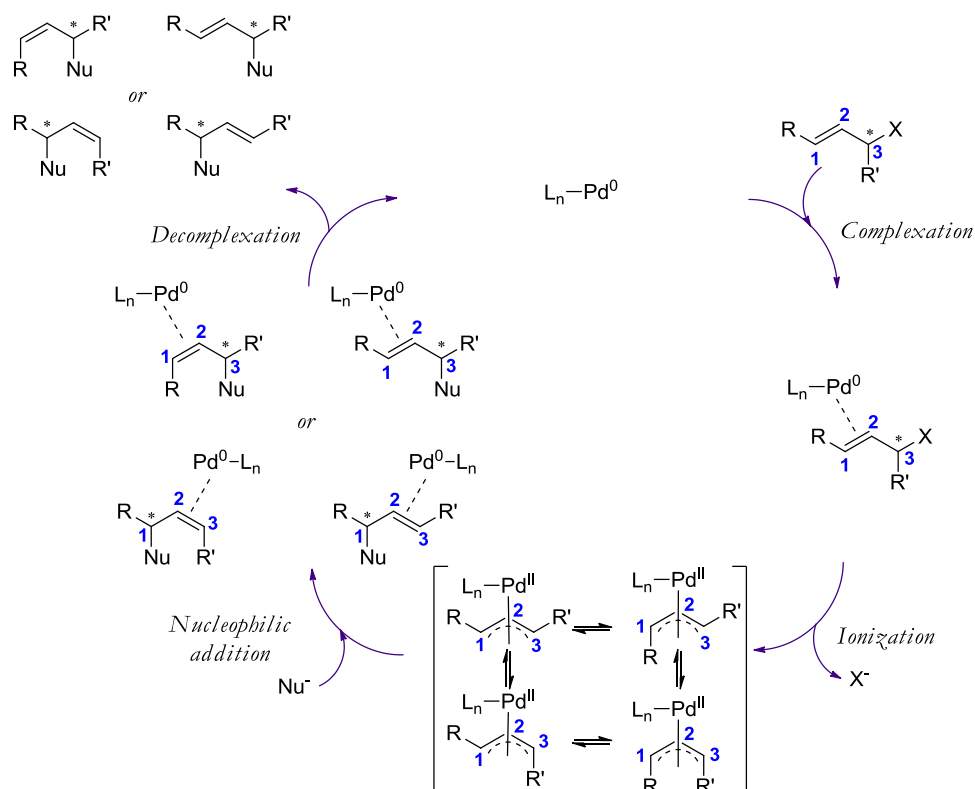
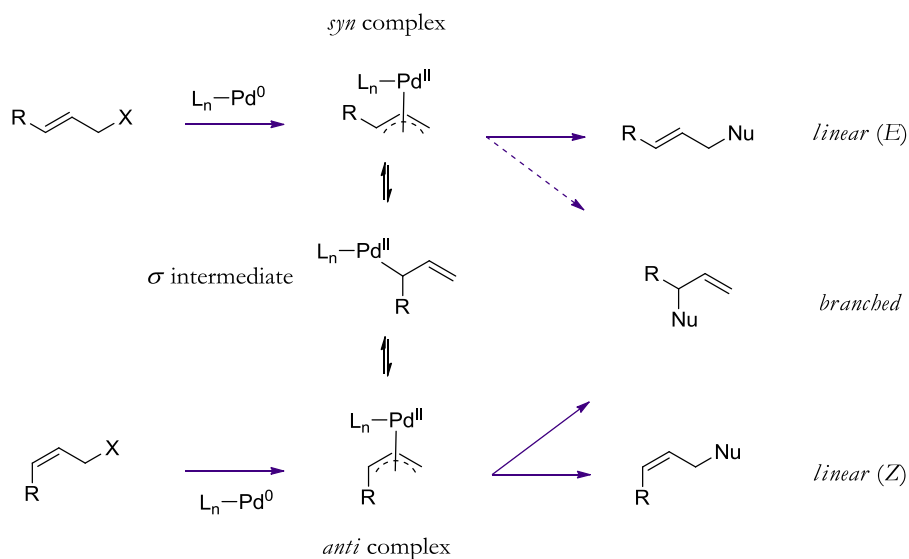


Figure 3. 6. General catalytic cycle for the palladium catalyzed allylic alkylation.

As a result, a range of products can be obtained from this relatively simple reaction, differing in regioselectivity and stereoselectivity involving *cis-trans* (*E-Z*) isomers and enantiomers.^{78,79}

In Scheme 3. 8 the formation of the *syn* and *anti* intermediates and their interconversion is depicted in more detail. When the substituent on C3 (*i. e.* R') is a hydrogen atom, depending on the position that the nucleophilic attack occurs, the linear (either with the double bond in a *Z* or *E* conformation) or the branched products will be formed.



Scheme 3. 8. Formation of regioisomers via *syn-anti* equilibrium.

The palladium catalyzed allylic alkylation using a chiral azo-containing P,N ligand was published by Kudo *et al.* (Figure 1. 13, **C**, chapter 1).⁸⁰ They studied whether the isomerization of the azobenzene affects the results of the catalysis and they did not observe differences in the catalytic performance between the azobenzene isomers. No explanation was found for this behaviour, but it might be due to the structure of this particular ligand. One nitrogen atom belonging to the azo double bond may coordinate to the metal during the catalysis, and this can inhibit the light induced isomerization of the azobenzene group. They only studied the azobenzene isomerization for the free ligand, and no isomerization studies were carried out in presence of palladium.

Before testing the azophosphines, some experiments were done to optimize the

catalytic conditions. The use of two different solvents (THF or DCM) was studied, and better activities were always observed for DCM. Also different palladium loadings (from 0.5 to 2.5 %) were tested. The ligands used for the optimization were the well-known triphenylphosphine (**24**), Xantphos (**28**) and dppf (**29**, Figure 3. 7).

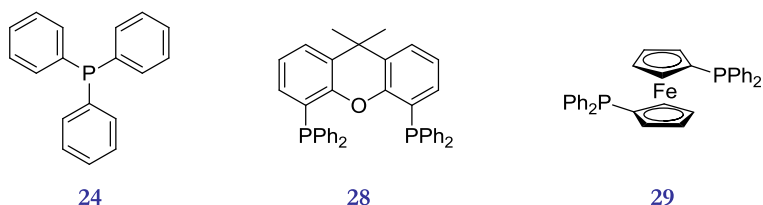


Figure 3. 7. Phosphines used to optimize the catalytic conditions for allylic alkylation.

Different substrates and nucleophiles were explored (depicted in Figure 3. 8). Substrates **30** and **31** will lead to different regioisomers, *linear* and *branched*.⁸¹ In addition, substrates **31** and **32** can also yield *trans* (*E*) and *cis* (*Z*) *linear* stereoisomers. However, some studies pointed out that the final geometry of the double bond depends strongly on the initial substrate used.^{79,82–84} In the case that the substrate has an *E* conformation, the final product is also the *E* one. On the other hand, when the substrate presents a *Z* conformation, the major product is the *Z* isomer, but a mixture of different ratios of *E* and *Z* products can be obtained. In this study **31** and **32** were used as *E* isomers, so the final product for the *linear* regioisomer was also the *E* one.

Usually the allylic alkylation is done at high temperatures to favour higher conversion and rates. However, to test the azophosphines it is necessary to perform the catalysis at room temperature to ensure a long enough lifetime of the *Z* isomer. Relatively few examples in literature using this condition were found,^{84–89} and the ones reported concerned mainly the use of diphosphines. Only in one example triphenylphosphine was used, which served as reference for this study.⁹⁰ The initial conditions were set based in this report from Anderson *et al.* and subsequently slight modifications yielded the optimized procedure. The substrates used in this study were **30**, *E*-**31** and *E*-**32**, and the nucleophile is compound **38**. The palladium source was the dimer [Pd(μ -Cl)(allyl)]₂.

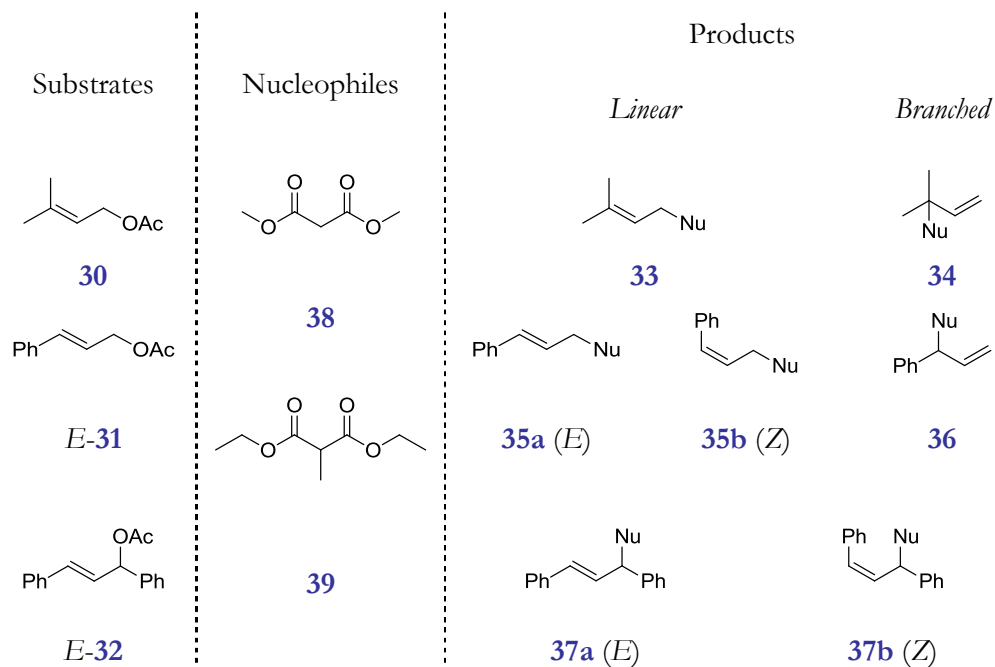


Figure 3. 8. List of the substrates and nucleophiles used in the allylic alkylation and possible products.

The results obtained using triphenylphosphine **24** were compared with the published ones,⁹⁰ which are 86 % yield after 2.5 hours of reaction with substrate **32** and nucleophile **38**, using 2.5 % of palladium. In contrast to the reported conversions, we obtained 100 % conversion for the same amount of palladium loading and only 1 h reaction (entry 1, Table 3. 4). The difference between the experiments is that higher concentrations were used to perform the catalysis in this study. Complete conversion was also obtained for substrate *E*-**31**, even when only 1 % of catalyst loading was used (Table 3. 4, entries 1 and 4).

In the case of diphosphine **28** good conversions were obtained when 1 and 2.5 % of palladium was used, but when the amount of metal was reduced to 0.5 % only substrate *E*-**32** gave an acceptable conversion. Complete conversions were obtained in all cases with the use of dppf (**29**).

Table 3. 4. Optimization of catalyst loading in the allylic alkylation of several substrates with nucleophile **38** using commercial ligands **24**, **28**, and **29**.

Entry	Ligand	Conversion (%)			l/b ratio		
		30	<i>E</i> - 31	<i>E</i> - 32	30	31	32
2.5 % Pd	24	0	100	100	-	18.6	-
	28	100	100	100	0.07	17.1	-
	29	100	100	100	0.91	8.5	-
1 % Pd	24	0	100	-	-	18.3	-
	28	77	100	100	0.02	18.2	-
	29	100	100	100	0.81	8.8	-
0.5 % Pd	28	0	0	90	-	-	-
	29	100	100	100	0.89	9.5	-

Conditions: r.t., 30 min catalyst preformation, 1 h reaction, [substrate] = 40 mM, BSA/nucleophile/substrate = 300/300/100. DCM = 14 mL. P/Pd = 2/1.

As regards the l/b ratio, substrate *E*-**31** gave mainly the *linear* isomer while substrate **30** gave the *branched* isomer preferentially, for all the conditions tested.

From these results and due to the limited availability of the azophosphine ligands the best compromise was to use 1 % of metal loading for future experiments.

Azomonophosphines **1**, **2**, and **3** were tested using the selected conditions. Only substrates **30** and *E*-**31** were considered because the ligands under study are achiral, and we were interested in comparing regioselectivity and/or activity. Substrate *E*-**32** was included in the initial screening of conditions because it will be considered, together with *E*-**31**, in the future for chiral versions of the azophosphines.

Unexpectedly, when the *meta* substituted azophosphines (**2** and **3**) were used no activity was observed in the allylic alkylation. An additional test with 2.5 % palladium loading was performed, and with phosphine **3** for substrate *E*-**31**, and nucleophile **38** a small conversion (12 %, and a *linear* to *branched* ratio of 7) was measured after 24 hours. No conversion was achieved in 1h.

In contrast, when the *para* substituted azomonophosphine **1** was used, moderate

to full conversion was observed. The results with ligand **1** are summarized in Table 3.5.

Table 3.5. Results obtained for monophosphine **1** in allylic alkylation of substrate *E*-**31**.

Entry	Nucleophile	1-E		1-Z	
		Conversion (%)	l/b	Conversion (%)	l/b
1	38	32	13	83	14
2	39	9	12	2	11

Conditions: r.t., 30 min catalyst preformation, 1 h reaction, [substrate] = 40 mM, BSA/nucleophile/substrate/P/Pd = 300/300/100/2/1. DCM = 14 mL.

In the case of nucleophile **39**, almost no activity was observed after 1 h reaction, but with nucleophile **38** a high activity was measured for azophosphine **1** in the *Z* form, and moderate activity for the *E* isomer. Compared with triphenylphosphine both *E*-**1** and irradiated **1** showed low conversion, while the l/b ratio remained similar. It can be assessed that the irradiated form of **1** gives a behavior similar to the one observed for phosphines **24** and **28**.

Regarding the lack of reactivity of monophosphines **2** and **3**, one possible explanation could be that due to its *meta* position the azo nitrogen atom is not an innocent atom as it might coordinate to palladium. Alternatively, the absence of reactivity could be due to activation of the carbon in between the nitrogen atom and phosphorus atom, giving metallation of the carbon to palladium, as is well-known for azobenzenes.⁹¹⁻⁹⁴ In any of these situations the ligand would act as a chelate (either neutral P,N or anionic P,C), instead of acting as monodentate. The reason why such systems are inactive is unclear, (P,N ligands are known to be active in allylic alkylation) but the blockage of the active sites due to the formation of the double chelate is a tentative explanation.

Although no convincing explanation for the difference in activity of phosphine **1** with and without irradiation could be found, this is a starting point for future developments.

The results obtained when diphosphines **7** and **8** were tested in the reaction are represented in Figure 3. 9 and Table 3. 6.

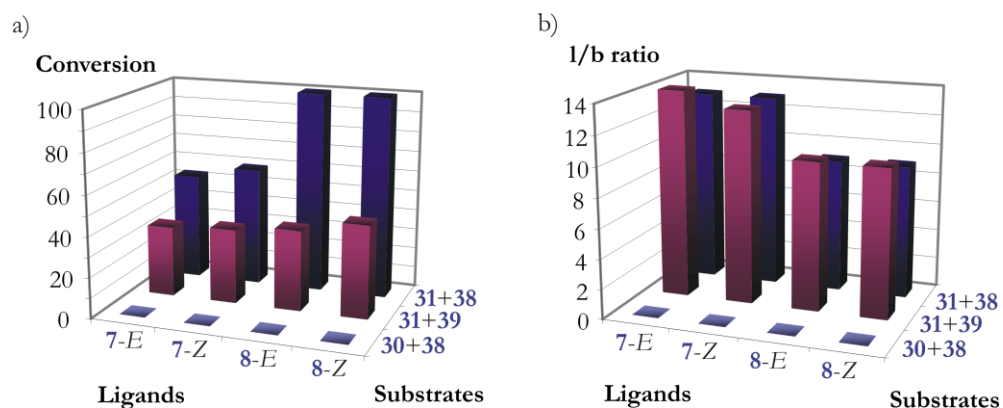


Figure 3. 9. Representation of the results obtained in allylic alkylation with diphosphines **7** and **8**.

As a general trend one can say that substrate **30** gave no conversion, but moderate to full conversion was obtained for substrate *E*-**31**. No remarkable effect of the irradiation was noticed, neither on the activity nor on the regioselectivity in any case. The major product observed was always the *linear* one **35a** with l/b ratios similar to those obtained with ligand **1**.

Table 3. 6. Results obtained for azodiphosphines **7** and **8** in allylic alkylation of substrates and nucleophiles *E*-**31**+**38**, **30**+**38**, *E*-**31**+**39**.

	Entry	Substrates	7- <i>E</i>	7- <i>Z</i>	8- <i>E</i>	8- <i>Z</i>
Conversion (%)	1	31 + 38	53	59	100	100
	2	30 + 38	0	0	0	0
	3	31 + 39	35	37	40	46
l/b	4	31 + 38	13	13	9	9
	5	30 + 38	-	-	-	-
	6	31 + 39	14	13	10	10

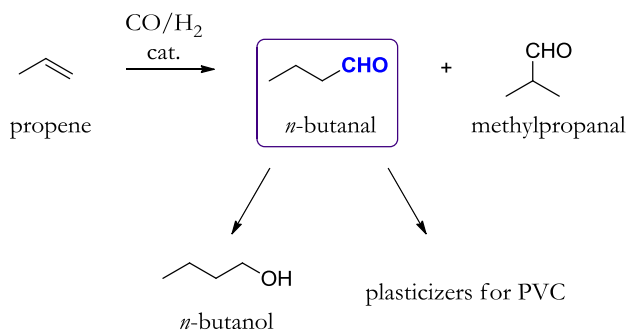
Conditions: r.t., 30 min catalyst preformation, 1 h reaction, [substrate] = 40 mM, BSA/nucleophile/substrate/P/Pd = 300/300/100/2/1. DCM = 14 mL.

These results of **7** and **8** are not in concordance with the ones observed for monophosphines **2** and **3**, as diphosphines **7** and **8** also have the azo group in the *meta* position.

Comparing the results obtained for the azodiphosphines with the ones obtained with the model ligands **24**, **28** and **29**, one can see that **7** and **8** behave similarly to **24**, *i.e.*, for 1 % of palladium and the combination of **31+38** full or moderate conversion are obtained (entry 1, Table 3. 6; entry 4 and 5, Table 3. 4), but the regioselectivity is slightly lower for the azodiphosphines; the lack of activity for substrate **30+38** confirms that these ligands behave as monophosphines (**24**).

3.2.4. RHODIUM CATALYZED HYDROFORMYLATION

Alkene hydroformylation is one of the most important homogeneously catalyzed reactions. It is used in industry to convert alkenes into aldehydes. Its applications concern a wide range of products: from the manufacture of butanal to detergents alcohols, to the synthesis of fine chemical intermediates for pharmaceutical uses.⁹⁵

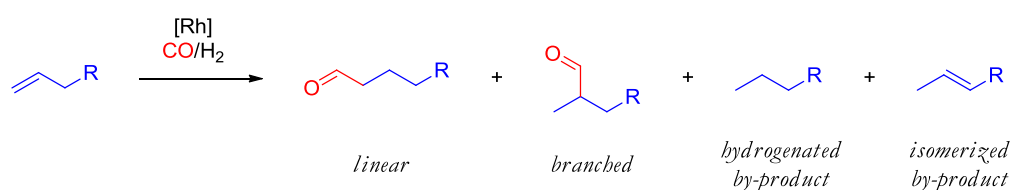


Scheme 3. 9. Schematization of the major industrial uses of hydroformylation.

Butanal is converted to dimers via condensation and hydrogenation and the resulting branched C₈ alcohols are used in dioctyl phthalates (DOPs, mainly for PVC) and C₁₂₋₁₃ aldehydes are converted to detergent alcohols.⁹⁶ One of the most important products in this approach is the linear *n*-butanal (Scheme 3. 9), which, in

addition to the application in DOPs, is used as butanol in butyl acrylates, as butanol solvent, etc.

The discovery of the hydroformylation reaction is attributed to Otto Roelen in the 40s.⁹⁷ He discovered accidentally the formation of aldehydes from alkenes while performing the Fischer-Tropsch process (this process converts carbon monoxide into higher hydrocarbons via heterogeneous catalysis). He discovered that hydroformylation was a homogeneous reaction catalyzed by molecular cobalt carbonyls,⁹⁸ but soon it was demonstrated that rhodium leads to faster and more selective catalysts.⁹⁹ The ligands used in this reaction have been mainly phosphorus containing ones, either monodentate or bidentates.



Scheme 3. 10. Hydroformylation of terminal alkenes.

The reaction of terminal alkenes with a mixture of 1:1 CO:H₂ (*syngas*) to obtain aldehydes can generate different products (Scheme 3. 10). Besides the isomeric *linear* and the *branched* aldehyde, also hydrogenation can take place resulting in the corresponding alkane, and isomerization of the double bond may occur to give internal alkenes.

Many experimental and theoretical methods have been developed to rationalize the hydroformylation catalytic cycle, its intermediates, and its products.^{100,101} The accepted mechanism is the so-called dissociative mechanism described by Wilkinson in 1968 (Figure 3. 10), while the associative one described by the same authors involving 20-electron species, has been discarded in view of experimental and theoretical results.¹⁰²

In many catalyst systems, a species of the formula [RhH(CO)₂(P)₂] (**A/B**, Figure 3. 10) is the resting state of the catalyst.¹⁰³ The catalytic cycle involves an alternation between 18 and 16-electron species. Subsequently CO dissociation, and association of

alkene to obtain **E**. After migratory insertion of the alkene into the Rh–H bond and association of CO, species **H** undergoes a CO migratory insertion into the Rh–alkyl bond, and oxidative addition of H₂. Further reductive elimination results in the aldehyde product and the recovery of **A/B** or **C/D** species.

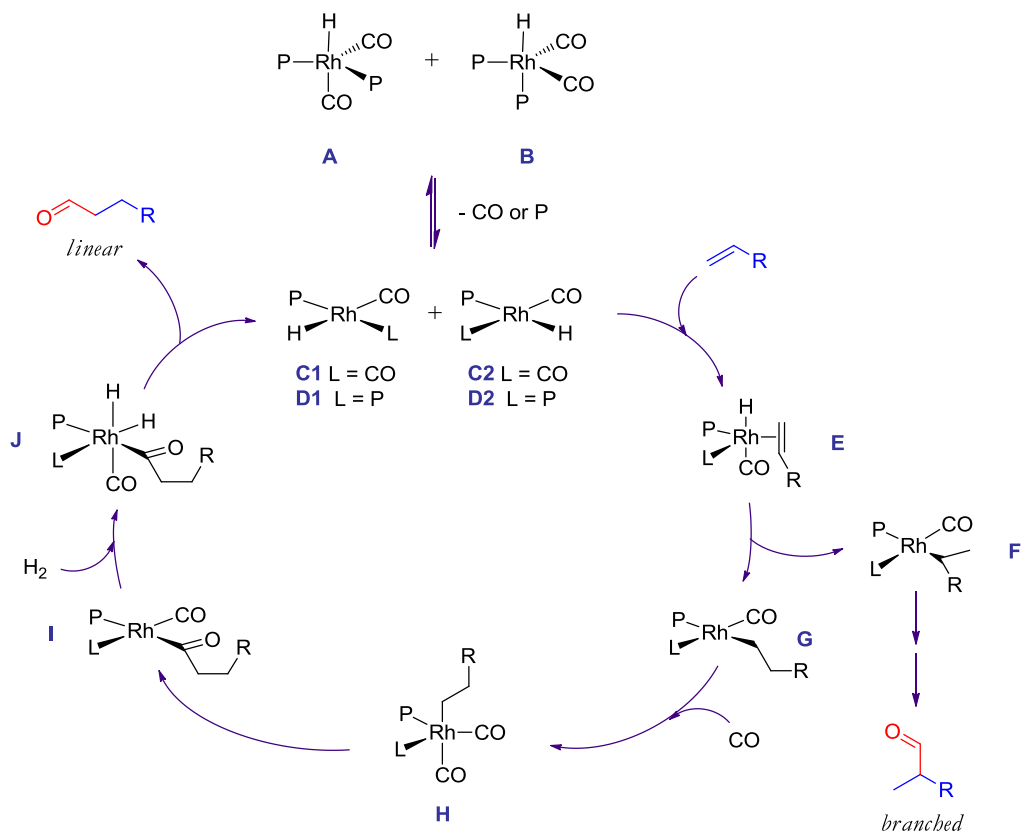


Figure 3. 10. Simplified catalytic cycle for the rhodium hydroformylation.

The regioselectivity of the process is explained by the formation of two different 16-electron intermediates (compounds **D1** and **D2**, Figure 3. 10) that stem from two different 18-electron resting states respectively (compounds **A** and **B**) which contain the two phosphines in two equatorial or in equatorial-axial position each.¹⁰⁴ The formation of the ratio of **A** and **B** depends on the steric and electronic properties of the ligands. It has been well documented that **A** (equatorial-equatorial) leads primarily

to linear alkyl species (and thus *linear* aldehydes) and **B** (equatorial-axial) to a mixture of *branched* and *linear* alkyl species. In all rhodium complexes with trigonal bipyramidal geometry and bearing a hydride, the hydrogen atom is located in an axial position.¹⁰⁵ In Figure 3. 10 the whole catalytic cycle toward *linear* aldehydes starting from rhodium-alkyl intermediate **G** has been described in detail. An analogous one starting from the branched alkyl rhodium complex **F** rendering the *branched* product is assumed.

By using diphosphines the formation of either one or the other isomeric species **A** or **B** can be favoured. Several authors have found a good correlation between the *natural bite angle* of the diphosphines and the selectivity of the catalysis.^{106–108} Monophosphines lead to a high proportion of **B**,^{103,109} furthermore dissociation of a monophosphine from **B** will give the more reactive intermediate **C**, which shows low selectivity for the *linear* aldehyde.

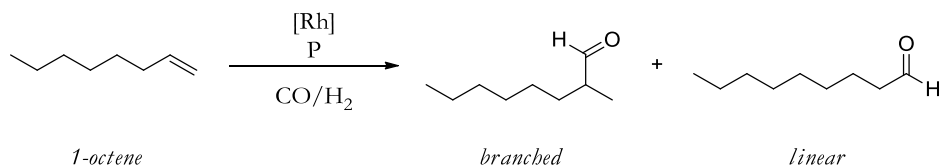
Activity is mainly controlled by electronic parameters, electron-poor ligands lead to more active catalysts.^{110,111}

In summary, usually when monophosphines are used, the system is more active, but less selective. The opposite happens for chelating diphosphines, where the activity decreases. For wide bite angle ligands ($\beta_n > 110^\circ$) the selectivity increases towards the linear aldehyde, and for small bite angle ligands ($\beta_n < 90^\circ$) the selectivity slightly decreases.

Our interest in the application of azophosphines in the hydroformylation of 1-octene (Scheme 3. 11) is to investigate if the irradiation of the catalyst, expected to generate a change in the steric properties of the ligands, affects the catalysis. Due to the experimental restrictions explained previously for azophosphines (room temperature and low pressure conditions) low-pressure operation conditions had to be developed.

The initial experiments by Wilkinson were conducted at atmospheric pressures, using $[\text{RhH}(\text{CO})(\text{PPh}_3)_3]$ as the catalyst.¹¹² Only one example has been found in recent literature where the reaction is performed at room temperature and under 1 bar of *syngas*. In this report, Breit *et al.* demonstrated that it is possible to use these mild conditions to perform the hydroformylation of several substrates.¹¹³ Reaction times, however, are longer than the conventional ones (temperatures between 80 and

100 °C and CO/H₂ pressure between 20 and 40 bar, where the reaction usually takes place in few hours). Reaction times as long as 20 hours have been reported. For such a long reaction time, the sample needs to be irradiated during catalysis to maintain a large proportion of ligand in its *Z* isomeric form.



Scheme 3. 11. Rhodium hydroformylation of 1-octene.

Triphenylphosphine, **24**, was used as ligand to optimize the reaction conditions based on the ones described by Breit *et al.*¹¹³ Two different metal precursors (**40**: [Rh(CO)₂(acac)]; **41**: [Rh(μ -OMe)(cod)]₂)¹¹⁴ were used. Incubation times (which is the time, before adding the substrate, in which the metal and ligand are reacted under CO/H₂ to form the active species **A/B**), solvents, and P/M ratio were also varied.

The best compromise found was using the conditions where the solvent was DCM, the ratio of phosphorus/metal was 3/1, incubation time of 30 min, and the metal precursor was [Rh(μ -OMe)(cod)]₂. The conversion in this case for PPh₃ was 21 % and the l/b ratio 3.3.

Regarding the azophosphine with three azo moieties in the structure **3**, no conversion was obtained under the reaction conditions optimized, so alternative reaction conditions were also tried at low pressure, such as using THF as solvent, rhodium precursor **40**, and P/Rh ratio 2/1 and 5/1, but they did not result also in activity either.

For that reason, it was decided to test **3** at 80 °C and 20 bar *syngas* (standard hydroformylation reaction conditions)¹⁰⁷ although we knew we could not apply the isomerized form of the ligand at these conditions. Under high pressure conditions ligand **3** should behave as a regular phosphine. Still no productivity was observed. This result suggests that the deactivation of the catalyst is inherent to the ligand.

Table 3. 7. Results obtained in the hydroformylation of 1-octene using azodiphosphine **7**.

Ligand	Entry	Conversion (%)	l/b ratio
<i>E-7</i>	1	23	5
<i>Z-7</i>	2	2	6

No hydrogenation nor isomerisation products were detected. Conditions: r.t., 20 h reaction, [Rh] = 6.5 mM, 1-octene/P/Rh = 150/3/1. 1 atm CO/H₂. DCM = 3 mL. Irradiation of the phosphine before catalysis, during catalyst incubation and during catalysis ($\lambda = 350$ nm).

Diphosphine **7** was also tested in 1-octene hydroformylation. In the case of *E-7*, a moderate activity was observed (23 %), and almost no conversion was measured for *Z-7* (Table 3. 7). No deactivation is observed with this ligand (at least when it is in the *E* form). As mentioned before, usually chelating ligands lead to lower activities in this reaction compared to their monodentate counterparts. One possible explanation for the observed difference in activities when ligand *E-7* is used could be that the ligand is coordinated in a monodentate manner (either to only one metal or to two different ones). This would be in agreement with the large P–P distance envisaged for this ligand. Instead, when the phosphine is irradiated and the double bond adopts a *Z* conformation, the two phosphorus atoms are placed close enough to act as a chelate. Surprisingly, no effect on the selectivity is observed.

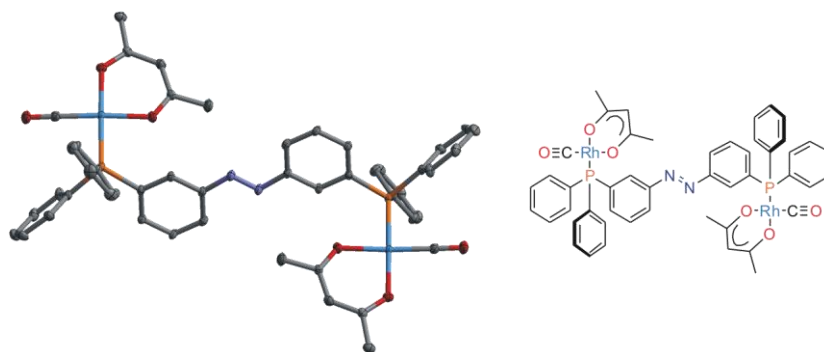


Figure 3. 11. X-Ray structure of [Rh₂(CO)₂(acac)₂(*E-7*)].

The expected coordinating behaviour of *E-7* is confirmed by an X-Ray structure

of a rhodium complex. Single crystals suitable to determine its molecular structure by X-Ray diffraction were obtained by reaction of the phosphine *E-7* with one equivalent of $[\text{Rh}(\text{CO})_2(\text{acac})]$ (Figure 3. 11). In the figure the phosphine presents an extended conformation, and the two phosphorus atoms are coordinated to different metal centres, with the ligand acting as a bridge. All the efforts to obtain crystals of a complex containing *Z-7*, unfortunately, were not successful.

Previous reports were found in literature in which irradiation during hydroformylation reaction produced an enhancement of the activity,^{115–117} (as happened also in the Suzuki cross-coupling). In the hydroformylation experiments studied in this chapter just the opposite effect was observed, which reinforces the idea of a chelating species being responsible for the low activity observed when the *Z* form of the diphosphine was used.

NMR studies

Several NMR experiments were done to test the coordination properties of the azophosphines under catalytic conditions.

Initially, azophosphine **2** was chosen as simple model to identify the metal complexes assembled. *In situ* high pressure NMR experiments were done by mixing two equivalents of phosphine **2** with $[\text{Rh}(\text{CO})_2(\text{acac})]$ and dissolved in toluene- D_8 under argon. The orange solution was then pressurized to 20 bar of CO/H_2 and $^{31}\text{P}\{^1\text{H}\}$ -NMR were recorded at different temperatures. To study the species obtained after isomerization of the ligand, the sample was depressurized, irradiated for one hour and pressurized again. In the next paragraphs some aspects of the results obtained will be discussed.

In all $^{31}\text{P}\{^1\text{H}\}$ -NMR spectra recorded with the phosphine complexes, singlets around 28.0 ppm were observed, which correspond to phosphine oxides. When the NMR of the initial complex was measured at room temperature (under argon), very broad signals were observed (Figure 3. 12, a), at low temperatures ($-40\text{ }^\circ\text{C}$) a broad doublet appeared at 31.4 ppm with a coupling constant $^1J(\text{P-Rh})$ of around 139 Hz (Figure 3. 12, b). This signal can be attributed to a $[\text{RhP}_4]^+$ cationic species, as

obtained for PPh₃, but using a P/Rh ratio > 4 (doublet at 32.4 ppm, $^1J(\text{P-Rh}) = 133$ Hz).^{118,119} The assignment to a species such as [Rh(acac)(CO)P₂] was discarded, as this is described in literature as a doublet at 11.7 ppm with $^1J(\text{P-Rh})$ of 90.9 Hz for Xantene based ligands.¹²⁰ The rest of the signals of the NMR spectrum were very broad and almost indistinguishable from the noise, which suggests that a lot of equilibria were involved between complexed and free phosphine.

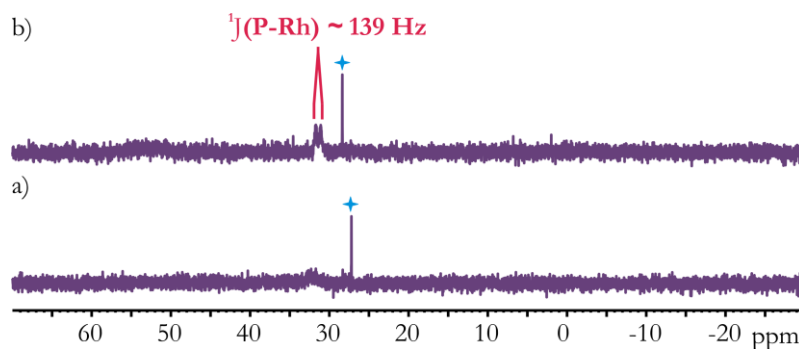


Figure 3. 12. *In situ* $^{31}\text{P}\{^1\text{H}\}$ -NMR of phosphine **2** with [Rh(CO)₂(acac)] in toluene-D₈ under argon. a) at 25 °C and b) at -40 °C.

When the sample was pressurized with 20 bar of CO/H₂, new signals appeared in the $^{31}\text{P}\{^1\text{H}\}$ -NMR spectra (Figure 3. 13, a). A sharp doublet at 40.8 ppm with a coupling constant $^1J(\text{P-Rh})$ of 139, and two broad doublets at 36.9 and 30.4 ppm (with $^1J(\text{P-Rh})$ around 117 and 144 Hz respectively) were observed. These new signals could be resolved when decreasing the temperature to 0 °C (Figure 3. 13, b).

When the sample was measured at 0 °C (Figure 3. 13, b), in addition to the free phosphine oxide observed and a very broad signal for a small amount of free phosphine around -2.4 ppm, several well defined signals appeared. To explain these new signals, all the possible species that could be formed under these conditions should be considered. The co-existence of several species is proposed, and the possible equilibria involved are depicted in Scheme 3. 12.

The signals with their corresponding Rh-P coupling constants are listed in Table 3. 8, and the enlarged spectrum with the assignment of the proposed species is shown in Figure 3. 14.

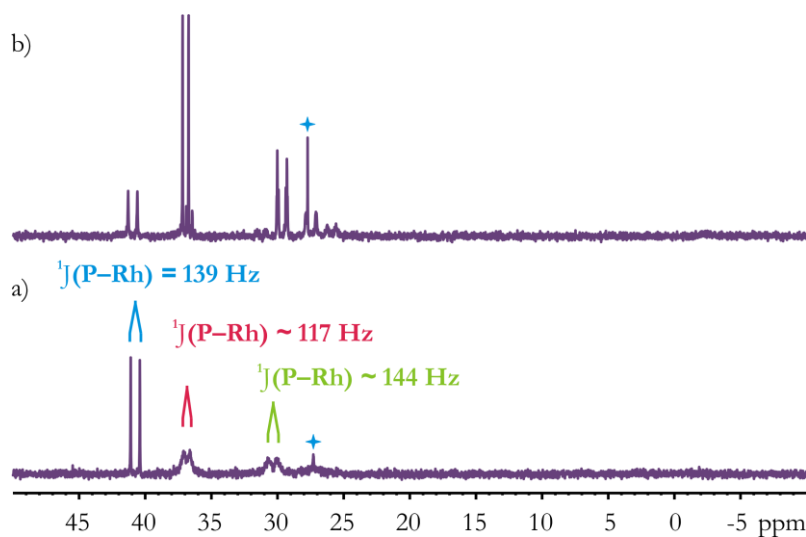
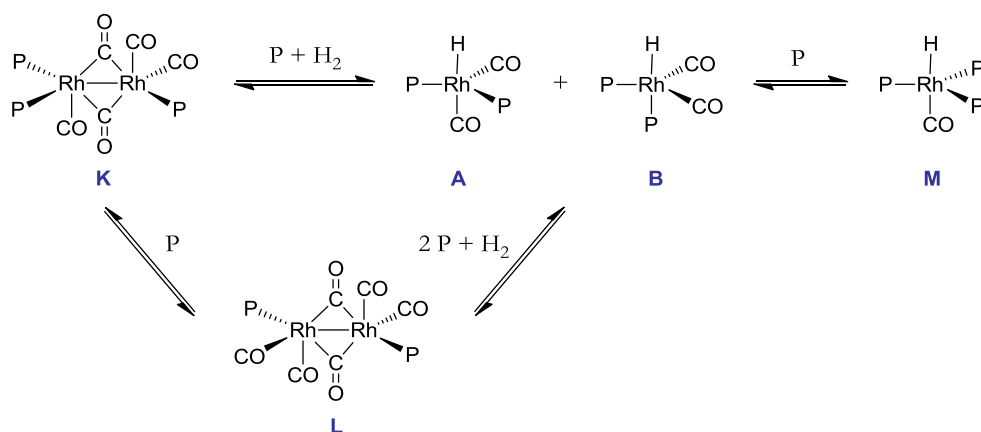


Figure 3. 13. *In situ* $^{31}\text{P}\{^1\text{H}\}$ -NMR of phosphine **2** with $[\text{Rh}(\text{CO})_2(\text{acac})]$ in toluene- D_8 under 20 bar of CO/H_2 . a) at 25 °C and b) at 0 °C.

The major species observed was a doublet at 36.9 ppm, with a $^1\text{J}(\text{P-Rh})$ of 92 Hz. This signal was attributed to the mixture of **A** plus **B** (Scheme 3. 12). In the case of PPh_3 , these two isomeric species are known to be in fast exchange on the NMR timescale and characterized as a 85/15 ratio (**A/B**).¹⁰³



Scheme 3. 12. Equilibria between the possible species formed.

The presence of this **A/B** mixture is also visible in the hydride region of the ^1H -NMR spectra. The hydride signal appeared as a small doublet at -8.8 ppm, with a $^1J(\text{H-Rh})$ of 3.8 Hz. Values of $^1J(\text{H-Rh})$ in the range of 3-7 Hz are characteristic of $[\text{RhH}(\text{CO})_2\text{P}_2]$ **A/B** species.¹⁰³ It was not possible to observe the $^2J(\text{H-P})$, as would be expected for this system. Usually the signal appears as a multiplet showing an averaged $^2J(\text{H-P})$ value which serves as indication of the **A/B** ratio as the range of the individual values of $^2J(\text{H-P})$ in *cis* and *trans* relative positions.¹¹⁰ The opposite sign of the $^2J(\text{H-P}_{\text{eq}})$ and $^2J(\text{H-P}_{\text{ax}})$ and the **A/B** ratio may further reduce the average coupling constant.^{103,121}

Additionally, a doublet of low intensity was observed at 36.7 ppm with $^1J(\text{P-Rh})$ of 92 Hz. The chemical shift and coupling constant value are similar to those of the previous **A/B** mixture, one can think that a small amount of **2** occurs in its *Z* form, and thus this doublet could correspond to a $[\text{RhH}(\text{CO})_2\text{P}_2\text{EPZ}]$ species as a mixture of equatorial-equatorial, equatorial-axial equilibrium (*vide infra*).

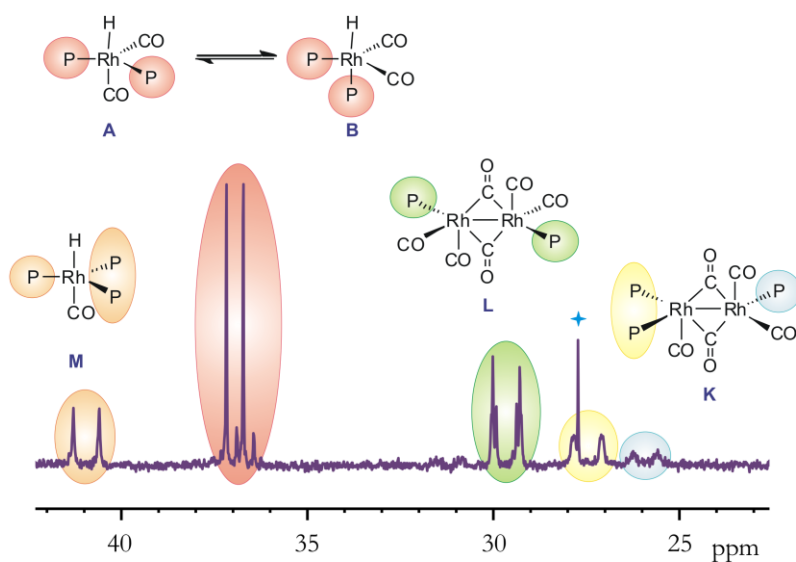


Figure 3. 14. Species observed in the *in situ* $^{31}\text{P}\{^1\text{H}\}$ -NMR of phosphine **2** with $[\text{Rh}(\text{CO})_2(\text{acac})]$ in toluene- D_8 under 20 bar of CO/H_2 at 0°C .

At 40.9 ppm a doublet with $^1J(\text{P-Rh})$ of 141 Hz was observed. This signal was

attributed to a trigonal bipyramidal hydrido carbonyl rhodium species with three phosphines in the equatorial position (**M**).^{122,123} Unfortunately we were unable to observe the signal of the corresponding hydride in the ¹H-NMR spectra, that would confirm the assignment.

Below 30 ppm, signals were detected, assigned to dimeric species. The value of the coupling constants and intensities matches with species **K**, which has an asymmetric substitution on each rhodium atom. This type of dimers was first reported by Wilkinson^{124,125} and characterized later by Chan,¹²⁶ and were discussed in many subsequent papers.^{127–130} At 27.5 ppm a signal was observed that was attributed to the two phosphines coordinated to the same rhodium atom, and with half intensity at 26.0 ppm appeared the phosphorus signal attributed to the phosphine coordinated to the other rhodium atom of the dimer. This species presents an AA'BXX' spin system in the ³¹P{¹H}-NMR spectrum, but unfortunately the signals were not sufficiently well enough resolved to allow accurate measurement of P–P coupling constants.

Table 3. 8. ³¹P{¹H}-NMR spectra data of the *in situ* ³¹P{¹H}-NMR of phosphine **2** with [Rh(CO)₂(acac)] in toluene-D₈ under 20 bar of CO/H₂ at 0 °C.

Entry	Species	δ [ppm]	¹ J(P–Rh) [Hz]
1	M	40.9	141
2	A + B [RhH(CO) ₂ P _E P _E]	36.9	92
3	A + B [RhH(CO) ₂ P _E P _Z]	36.7	92
4	L	29.7	<i>vide infra</i>
5	K	27.5	152
6		26.0	134

The signal at 29.7 ppm belongs to a dimer (**L**) with only one phosphine on each rhodium atom. The existence of only one signal for the two phosphorus nuclei of the

complex evidences that these atoms are chemically equivalent. This species exhibits a second order AA'XX' spin system in the $^{31}\text{P}\{^1\text{H}\}$ -NMR spectrum, which can be satisfactorily simulated (Figure 3. 15) being $^1J(\text{P-Rh}) = 140.63$ Hz, $^3J(\text{P-Rh}) = 6.21$ Hz and $^4J(\text{P-P}) = 27.42$ Hz.¹³¹

The presence of the dimeric species (**K**, **L**) strongly depends on the concentration.¹²⁹ The presence of these dimers can be considered as an artefact due to the high concentrations required for the NMR spectra, but one can assume that their concentration at catalytic conditions (approximately one order of magnitude lower) is so small that they can be neglected.

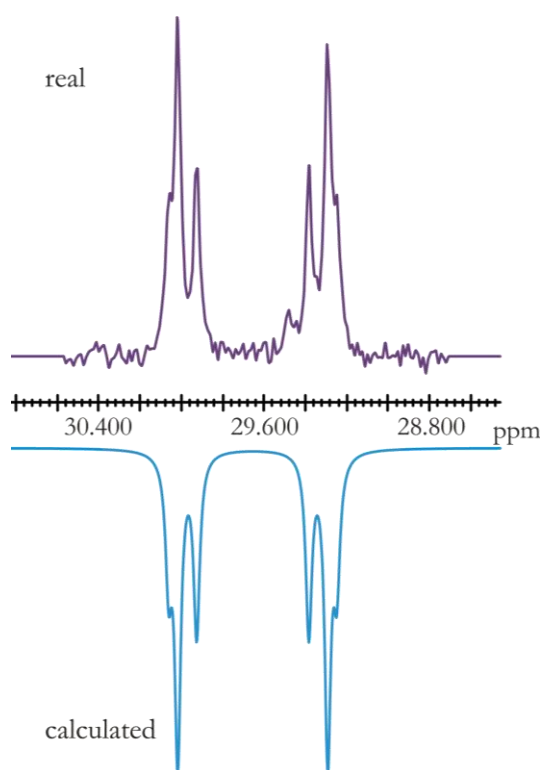


Figure 3. 15. Experimental and calculated spectrum of dimer **L** in the *in situ* $^{31}\text{P}\{^1\text{H}\}$ -NMR of phosphine **2** with $[\text{Rh}(\text{CO})_2(\text{acac})]$ in toluene- D_8 under 20 bar of CO/H_2 at 0 °C.

After measuring all the NMR experiments described previously, the sample was

depressurized and irradiated during 1 h ($\lambda = 350$ nm). After that, it was pressurized again to 20 bar of CO/H₂ and ³¹P{¹H}-NMR were measured at different temperatures.

Very broad signals were observed in the ³¹P{¹H}-NMR at room temperature, mainly due to the many species in equilibria.

The resolution of some signals was achieved at 0 °C. The ³¹P{¹H}-NMR was compared with the previous one (before irradiation) (Figure 3. 16, a and b). Around 36.0 and 37.0 ppm a set of signals was observed, attributed to mixture of species **A/B** in equilibrium (Table 3. 9). All the species have the same value of ¹J(P–Rh) of 92 Hz. The doublet observed at 36.9 ppm belongs to [RhH(CO)₂P_EP_E] species (as observed in the spectra before irradiation), while the doublet at 36.2 ppm was attributed to [RhH(CO)₂P_ZP_Z] species. The signals corresponding to these species could be satisfactory simulated (Figure 3. 16, c).

Table 3. 9. ³¹P{¹H}-NMR spectra data obtained from the simulation of the species **A+B** in the *in situ* ³¹P{¹H}-NMR of phosphine **2** with [Rh(CO)₂(acac)] in toluene-D₈ under 20 bar of CO/H₂ at 0 °C after irradiation.

Entry	Species	δ [ppm]	¹ J(P–Rh) [Hz]	² J(P _E –P _Z) [Hz]
1	A + B [RhH(CO) ₂ P _E P _E]	36.9	92	-
2	A + B [RhH(CO) ₂ P _E P _Z]	P _E 36.7 P _Z 36.5	92	165
3	A + B [RhH(CO) ₂ P _Z P _Z]	36.2	92	-

The signals corresponding to the complex with the two different isomers of the phosphine [RhH(CO)₂P_EP_Z] presented a second order ABX spin system in the ³¹P{¹H}-NMR spectra. This signal was satisfactory simulated (Table 3. 9, Figure 3. 16, c),¹³¹ showing four lines in the spectra. The signal corresponding to the phosphine in an *E* fashion appears at 36.7 ppm, and the phosphine in *Z* manner at 36.5 ppm. Both

phosphines present the coupling constants values $^1J(\text{P-Rh})$ of 92 Hz and $^2J(\text{P}_E\text{-P}_Z)$ of 165 Hz.

Probably due to the mixture of species and exchanges taking place at rates sufficiently high to broaden the ^1H signals, it was very difficult to observe the signal that corresponds to the hydrides in the ^1H -NMR, and only at $-70\text{ }^\circ\text{C}$ a broad doublet appeared at -8.7 ppm .

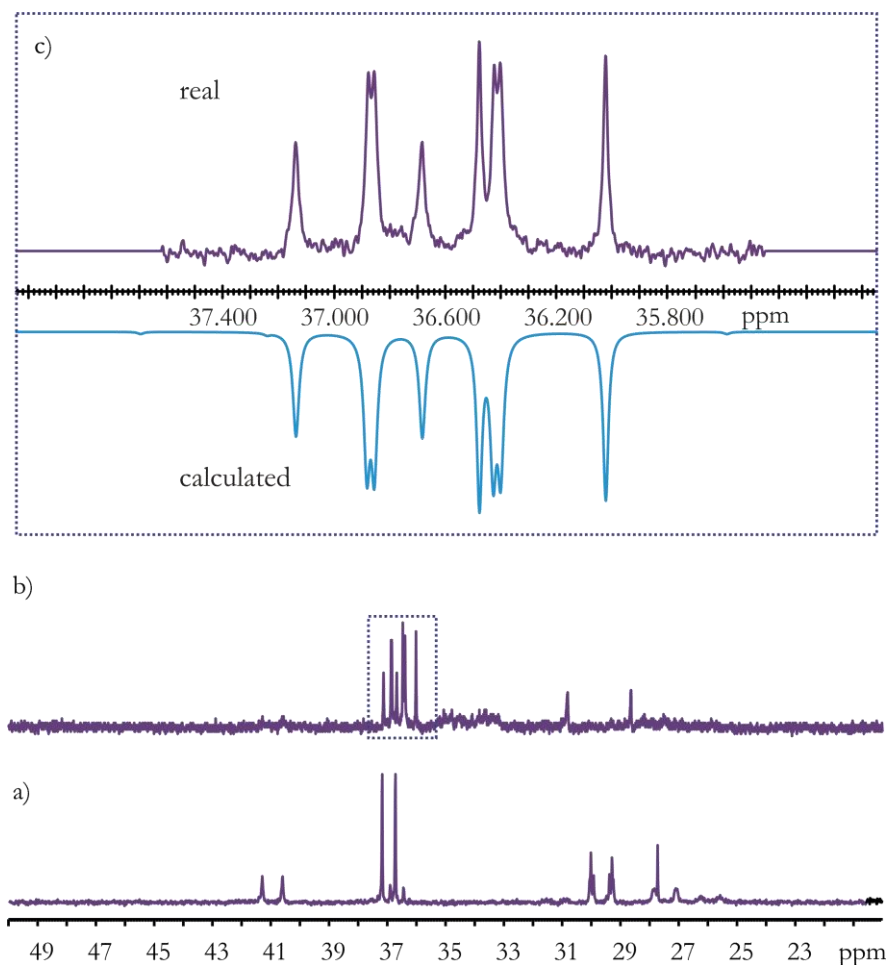


Figure 3. 16. *In situ* $^{31}\text{P}\{^1\text{H}\}$ -NMR of phosphine **2** with $[\text{Rh}(\text{CO})_2(\text{acac})]$ in toluene- D_8 under 20 bar of CO/H_2 at $0\text{ }^\circ\text{C}$. a) before irradiation; b) after irradiation and c) experimental and calculated spectrum of the mixture of species $[\text{RhH}(\text{CO})_2\text{P}_E\text{P}_E]$, $[\text{RhH}(\text{CO})_2\text{P}_E\text{P}_Z]$ and $[\text{RhH}(\text{CO})_2\text{P}_Z\text{P}_Z]$.

Once all the species with the azophosphine were identified, the possible formation of the active species from $[\text{Rh}(\mu\text{-OMe})(\text{cod})]_2$ at low pressure of CO/H_2 was studied. Triphenylphosphine **24** was chosen as model to form and identify all the possible rhodium complexes. A sample with four equivalents of the phosphine **24** per $[\text{Rh}(\mu\text{-OMe})(\text{cod})]_2$ precursor in toluene- D_8 was prepared. The yellow solution was subjected to CO/H_2 bubbling for 5 min. Then $^{31}\text{P}\{^1\text{H}\}$ -NMR spectra were recorded at different temperatures. All the spectra showed broad signals and only when the temperature was lowered to 0°C some of them were resolved (Figure 3. 17).

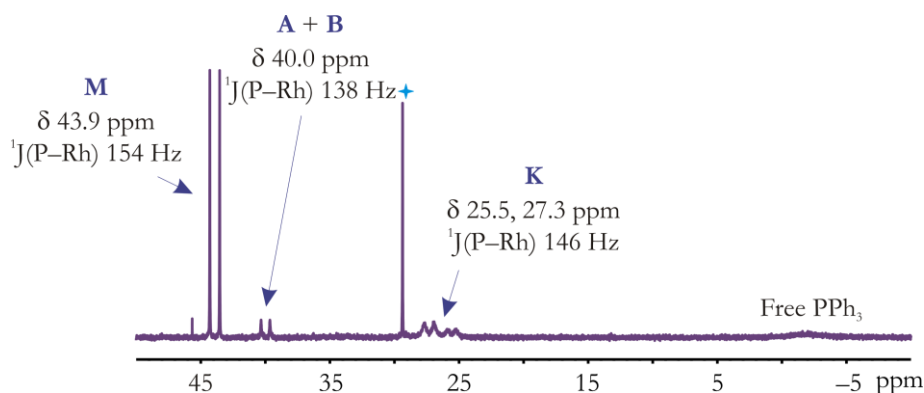


Figure 3. 17. *In situ* $^{31}\text{P}\{^1\text{H}\}$ -NMR of phosphine **24** with $[\text{Rh}(\mu\text{-OMe})(\text{cod})]_2$ in toluene- D_8 under 1 atm of CO/H_2 at 0°C .

In the $^{31}\text{P}\{^1\text{H}\}$ -NMR spectrum, five sets of signals were observed. Around -2.0 ppm a very broad band appeared due to the free phosphine, and at 29.4 ppm the phosphine oxide showed as a sharp singlet. Two minor species identified as **K** were located at 25.5 and 27.3 ppm (due to the broadness of the signal, an equilibrium with other dimeric species could be proposed as well). The mixture **A/B** (*vide supra*) appeared as a doublet at 40.0 ppm. The major species was the one labelled as **M**, with three phosphines in equatorial positions.

The presence of the hydride containing species was confirmed by ^1H -NMR. In the hydride region two signals were identified: at -8.9 ppm a doublet with $^1\text{J}(\text{H-Rh})$ of 3.8 Hz corresponding to **A/B** (*vide supra*), and at -9.3 ppm a quadruplet with $^2\text{J}(\text{H-P})$ of 14 Hz assigned to **M**.^{103,109} The latter signal resulted in a sharp singlet

when the $^1\text{H}\{^{31}\text{P}\}$ -NMR was recorded, while the former remained unmodified. The assignment of the hydride signals to the different species was supported by a 2D ^1H - ^{31}P HMQC experiment performed at -70°C .

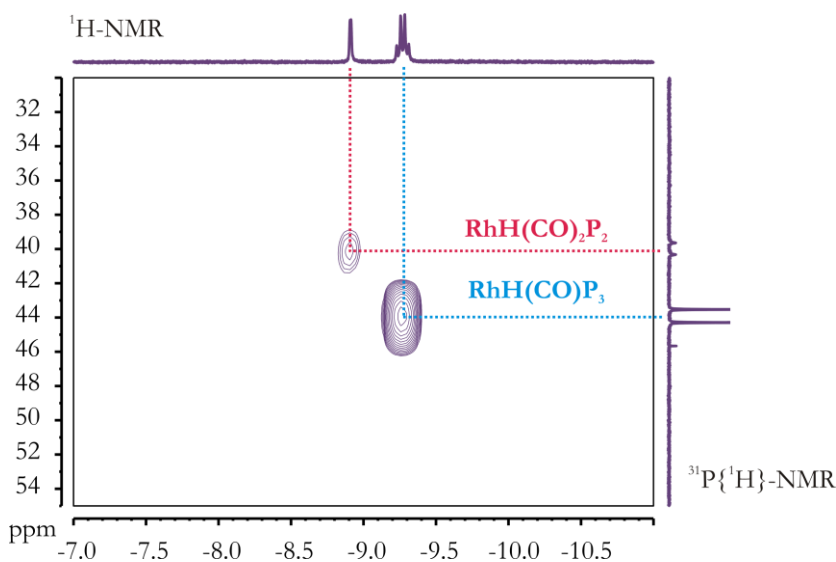


Figure 3. 18. *In situ* 2D ^1H - ^{31}P HMQC experiment of phosphine **24** with $[\text{Rh}(\mu\text{-OMe})(\text{cod})]_2$ under 1 atm of CO/H_2 at -70°C .

A few coupling constants do not show up in these hydride signals. One possible explanation could be that they are hidden by the width of the signals. If this is true it means that $^1\text{J}(\text{H-Rh}) < 2$ Hz for complex $[\text{RhH}(\text{CO})\text{P}_3]$, **M**, as reported by Brown;¹⁰⁹ and a surprisingly low value, not found in literature of $^2\text{J}(\text{P-H}) < 1$ Hz for $[\text{RhH}(\text{CO})_2\text{P}_2]$. This fact is in agreement with the previous observations for the hydride species of azophosphine **2**, (*vide supra*) but we do not have a convincing explanation.

When the same experiment was done with azomonophosphine **3**, only mixtures of broad signals were observed in the $^{31}\text{P}\{^1\text{H}\}$ -NMR spectra. None of them resembled the active species or the previously identified dimers. We decided to increase the CO/H_2 pressure to 20 bar, to favour the formation of the active species, and only a doublet appeared at 38.4 ppm with $^1\text{J}(\text{P-Rh})$ of 92 Hz. The chemical shift and the coupling constant was very similar to that previously described as $[\text{RhH}(\text{CO})_2\text{P}_2]$

(A/B) for the azophosphine **2**. However, no hydride was observed in the ^1H -NMR spectrum. For this new signal a species with P,N chelating type of coordination is tentatively proposed. Then, the extra equivalents of chelating ligand generates a lack of coordination metal sites available to the substrate, which explains the lack of activity of azomonophosphine **3**, even when high pressure conditions were used.

The situation is more complicated when diphosphines were considered. Two equivalents of azodiphosphine **7** per $[\text{Rh}(\mu\text{-OMe})(\text{cod})]_2$ precursor were dissolved in toluene- D_8 and the solution was subjected to CO/H_2 bubbling for 5 min prior to $^{31}\text{P}\{^1\text{H}\}$ -NMR measurements (Figure 3. 19, a). Apart from the signal of the phosphine oxide, very broad signals were obtained. As the phosphine is present in an “extended” *E* conformation, any of the species detected should be attributed to a complex in which the ligand acts as a bridge between two rhodium atoms or as a monodentate (with one free or oxidized phosphorus atom). As all the signals were very broad, it is concluded that all species are implicated in rapid equilibria (involving free and coordinated phosphine). For that reason, all the assignments proposed in the next discussion are very tentative.

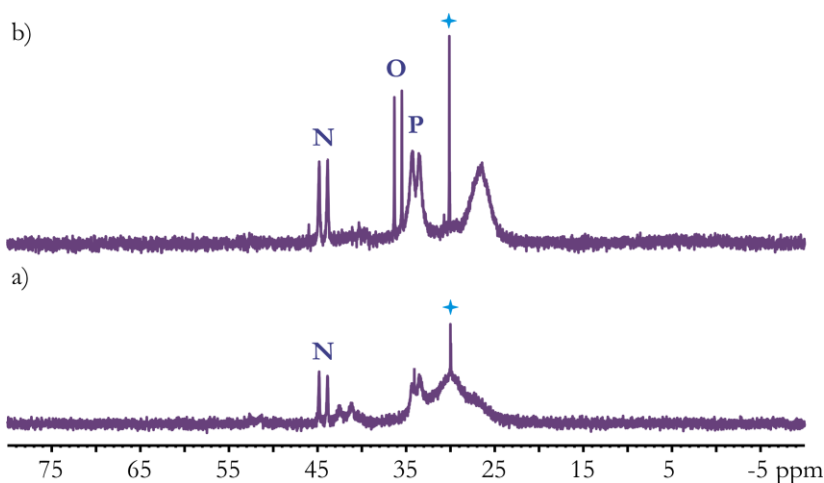


Figure 3. 19. *In situ* $^{31}\text{P}\{^1\text{H}\}$ -NMR of phosphine **7** with $[\text{Rh}(\mu\text{-OMe})(\text{cod})]_2$ in CD_2Cl_2 under 1 atm of CO/H_2 at 25 °C; a) with *E*-**7**, and b) with *Z*-**7**.

Only one small sharp doublet was identified at 44.3 ppm with $^1\text{J}(\text{P-Rh})$ of 153 Hz, which is characteristic of trigonal bipyramidal rhodium(I) carbonyl species with

three phosphines in equatorial positions.^{122–123} This signal was attributed tentatively to a dimeric species in which two diphosphines are acting as a bridge between two rhodium atoms. Another phosphine is coordinated to each rhodium, having one phosphorus atom bonded to the metal and the other one free (**N**, Figure 3. 20), but species of higher nuclearity cannot be discarded (**Q**).

The rest of the signals should be due to mixtures of dimeric and oligomeric species with the CO bridges between the rhodium atoms. There are many possibilities, and some of them are depicted in Figure 3. 20 (aryl substituents are omitted for clarity).

In the ¹H-NMR, a very broad signal around –9.5 ppm is observed, which suggests that there are several species containing a hydride rapidly equilibrating.

Some of the proposed species are depicted in Figure 3. 20.

When the same experiment was done but the phosphine was irradiated before adding it to the metal precursor (enriched *Z-7*), apart from broad signals detected and the previous described dimer at 44.3 ppm, a new doublet was observed at 35.9 ppm with ¹J(P–Rh) of 137 Hz (Figure 3. 19, b). This signal is characteristic of the presence of an active species, such as **O** depicted in Figure 3. 20.

Another new broad doublet was observed at 33.9 ppm with a coupling constant of ¹J(P–Rh) of 127 Hz. Due to the broadness of the signal a dimer with two phosphines acting as a bridge was proposed. There are many possibilities in the coordination pattern. Each rhodium has two CO and one hydride (**P**, Figure 3. 20). The phosphines can be coordinated to each rhodium atom either in equatorial or in axial position. At the same time, this species **P** can combine the phosphines in both *Z*, or both in *E* or one in *Z* and the other in *E* conformation that will lead to many possible, exchanging compounds which makes the doublet very broad. Some of these species are depicted in Figure 3. 20. *A priori*, all the pentacoordinated hydrido carbonyl Rh(I) can be expected to be active in hydroformylation (as for instance **O** and **P**).

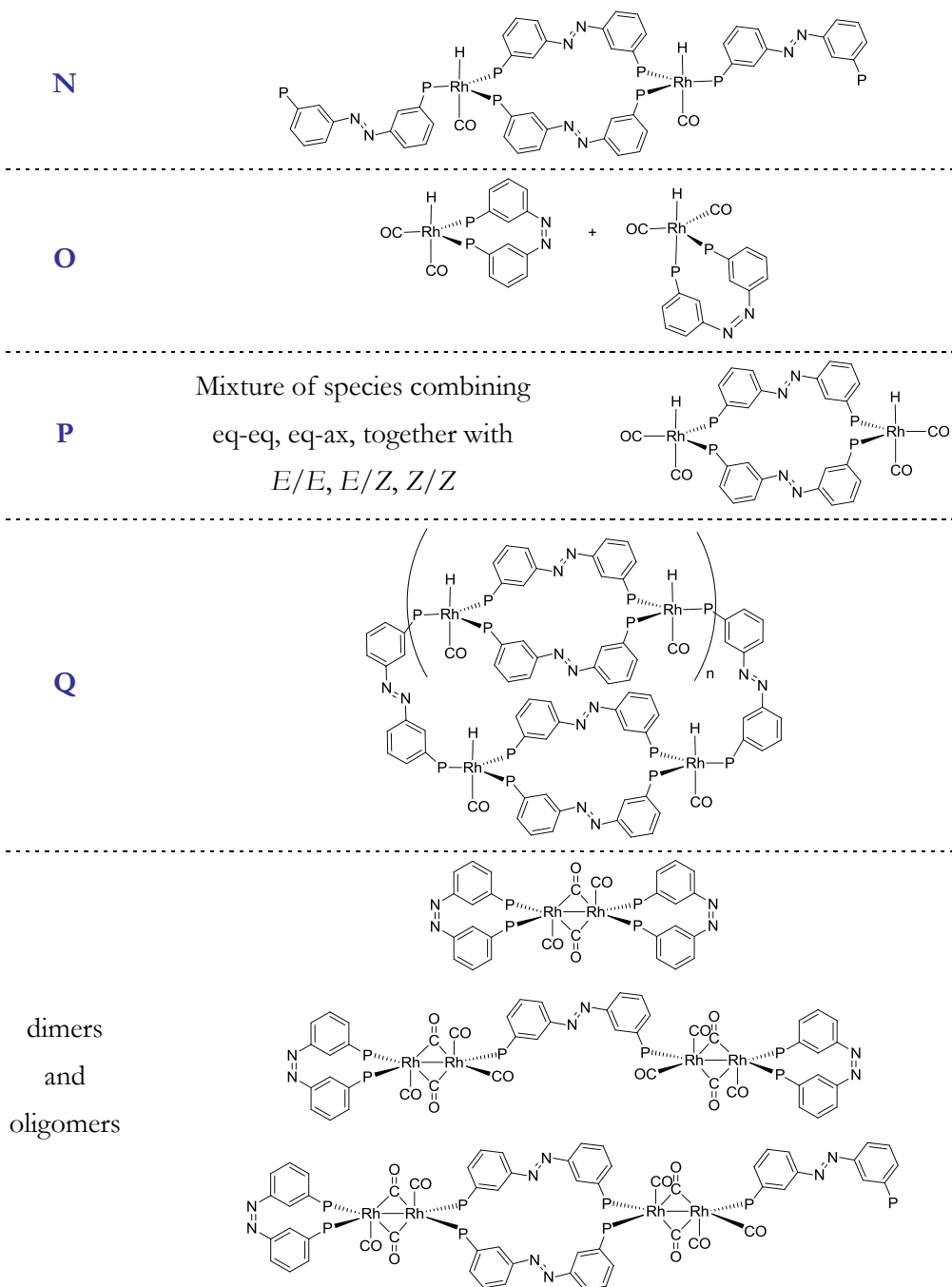


Figure 3. 20. Species proposed to be observed in the *in situ* $^{31}\text{P}\{^1\text{H}\}$ -NMR of phosphine **7** with $[\text{Rh}(\mu\text{-OMe})(\text{cod})_2]$ in CD_2Cl_2 under CO/H_2 at 25 °C.

3.3. CONCLUDING REMARKS

In this chapter the azobenzene based phosphines have been tested in a few catalytic reactions to check their robustness towards catalysis conditions. Furthermore, the effect of the isomerization on the catalytic reactions has been explored. One key question was whether the irradiated monodentate azophosphines would show a BSP like behaviour in catalysis.

When the irradiation is maintained during the catalytic event, in some cases side reactions can take place, through completely different mechanism from the conventional one. This is the case encountered in the palladium catalyzed Suzuki cross-coupling reaction.

Regarding hydrosilylation of acetophenone, azophosphine **3** gave results different from those usually described in literature for this reaction; instead of the usual regioselectivity observed in almost all the studies reported previously, this phosphine led to a major percentage of the silyl enol ether **27**. The rest of the phosphines, which only have one azo moiety in the structure, and also BSP **25** presented normal regioselectivities. Thus the behaviour of **3** is not like BSP like. This might suggest that an electronic effect due to the three azo moieties in the structure may be operative.

As regards the hydrosilylation of cyclohexanone, comparison of the results obtained for the azophosphines with those of BSP show that only ligand **3** presented a similar behaviour in this instance, which could be attributed to a steric effect due to the high steric hindrance around the metal. Furthermore, the same result was noticed for the *E* form and the *Z* form of **3**, which was assigned to the flexibility of the system, making that even if all the three azo units are in an *E* form, the *cone angle* can be large, thus generating a BSP type ligand.

In the palladium catalyzed allylic alkylation the outcomes of the monophosphines were very different from the ones obtained for the diphosphines. Different results were found amongst the mono-azophosphines, for which depending on whether the substitution of the aromatic ring is at the *meta* or *para* position, no activity or moderate conversions were found respectively. When *para* substituted phosphine **1** was used in the irradiated form, an enhancement of the activity was observed, but a

satisfactory explanation for this behaviour could not be given.

The studies in rhodium catalyzed hydroformylation of 1-octene learnt that phosphine **7** behaved differently depending on the azo isomer used. If the *E* isomer was used, the phosphine acted as a bridge between two metals, which resulted in a more active catalytic system than that employing the *Z* isomer. The *Z* isomer acts as a chelating ligand, which usually leads to a decrease in activity.

All the studies done in Part I evidenced that the initial idea to generate changes in catalysis by structural changes in the ligands caused by irradiation can indeed be put into practice. The use of these simple phosphines allowed their use in several catalytic systems and their reactivity towards irradiation could be investigated. One well explained outcome in catalysis in which the irradiation led to different results is the rhodium catalyzed hydroformylation with ligand **7**. This behaviour resulted from the change of the structure of the ligand upon irradiation. This encourages us to design more systems that are more rigid in the *E* form or *Z* form, or both, to favour more pronounced effects in catalysis caused by irradiation.

One might also consider designs implying the use of chiral moieties in the structures, for asymmetric allylic alkylation, as enantioselectivity may be more sensitive to small changes than regioselectivity studied so far.

References and notes

1. Miyaura, N.; Suzuki, A. *Chem. Rev.* **1995**, *95*, 2457.
2. Hassan, J.; Sevignon, M.; Gozzi, C.; Schulz, E.; Lemaire, M. *Chem. Rev.* **2002**, *102*, 1359.
3. Bellina, F.; Carpita, A.; Rossi, R. *Synthesis* **2004**, 2419.
4. Smith, G. B.; Dezeny, G. C.; Hughes, D. L.; King, A. O.; Verhoeven, T. R. *J. Org. Chem.* **1994**, *59*, 8151.
5. Nicolaou, K. C.; Ramanjulu, J. M.; Natarajan, S.; Brase, S.; Li, H.; Boddy, C. N. C.; Rubsam, F. *Chem. Commun.* **1997**, 1899.
6. Miyaura, N.; Yanagi, T.; Suzuki, A. *Synth. Commun.* **1981**, *11*, 513.
7. Wright, S. W.; Hageman, D. L.; McClure, L. D. *J. Org. Chem.* **1994**, *59*, 6095.
8. Wolfe, J. P.; Singer, R. A.; Yang, B. H.; Buchwald, S. L. *J. Am. Chem. Soc.* **1999**, *121*, 9550.
9. Mohanty, S.; Suresh, D.; Balakrishna, M. S.; Mague, J. T. *Tetrahedron* **2008**, *64*, 240.
10. Liu, S. Y.; Choi, M. J.; Fu, G. C. *Chem. Commun.* **2001**, 2408.
11. Miyaura, N.; Yamada, K.; Suzuki, A. *Tetrahedron Lett.* **1979**, 3437.
12. Martin, R.; Buchwald, S. L. *Acc. Chem. Res.* **2008**, *41*, 1461.
13. Suzuki, A. *Chem. Commun.* **2005**, 4759.
14. Braga, A. A. C.; Morgon, N. H.; Ujaque, G.; Maseras, F. J. *Am. Chem. Soc.* **2005**, *127*, 9298.
15. Miyaura, N. *J. Organomet. Chem.* **2002**, *653*, 54.
16. Littke, A. F.; Fu, G. C. *Angew. Chem., Int. Ed.* **2002**, *41*, 4176.
17. Barder, T. E.; Walker, S. D.; Martinelli, J. R.; Buchwald, S. L. *J. Am. Chem. Soc.* **2005**, *127*, 4685.
18. Ohta, H.; Tokunaga, M.; Obora, Y.; Iwai, T.; Iwasawa, T.; Fujihara, T.; Tsuji, Y. *Org. Lett.* **2007**, *9*, 89.
19. Walker, S. D.; Barder, T. E.; Martinelli, J. R.; Buchwald, S. L. *Angew. Chem., Int. Ed.* **2004**, *43*, 1871.
20. Littke, A. F.; Dai, C.; Fu, G. C. *J. Am. Chem. Soc.* **2000**, *122*, 4020.
21. Dr. Ruben Martin is kindly acknowledged for his helpful comments and providing ligands 21, 22 and 23.
22. Imperato, G.; Konig, B. *ChemSuschem* **2008**, *1*, 993.
23. Lipshutz, B. H.; Lower, A.; Kucejko, R. J.; Noson, K. *Org. Lett.* **2006**, *8*, 2969.
24. Ojima, I.; Nihonyanagi, M.; Kogure, T.; Kumagai, M.; Horiuchi, S.; Nakatsugawa, K.; Nagai, Y. *J. Organomet. Chem.* **1975**, *94*, 449.
25. Ojima, I.; Nihonyanagi, M.; Nagai, Y. *J. Chem. Soc., Chem. Commun.* **1972**, 938.
26. Ojima, I.; Nihonyanagi, M.; Kogure, T.; Nagai, Y. *Bull. Chem. Soc. Jpn.* **1972**, *45*, 3506.
27. Haszeldine, R. N.; Parish, R. V.; Parry, D. J. *J. Chem. Soc.* **1969**, 683.
28. Zheng, G. Z.; Chan, T. H. *Organometallics* **1995**, *14*, 70.
29. Ojima, I.; Kogure, T.; Kumagai, M.; Horiuchi, S.; Sato, T. *J. Organomet. Chem.* **1976**, *122*, 83.
30. Brunner, H.; Brandl, P. *Tetrahedron: Asymmetry* **1991**, *2*, 919.

31. Goikhman, R.; Milstein, D. *Chem.--Eur. J.* **2005**, *11*, 2983.
32. Schneider, N.; Finger, M.; Haferkemper, C.; Bellemin-Laponnaz, S.; Hofmann, P.; Gade, L. H. *Chem.--Eur. J.* **2009**, *15*, 11515.
33. Schneider, N.; Finger, M.; Haferkemper, C.; Bellemin-Laponnaz, S.; Hofmann, P.; Gade, L. H. *Angew. Chem., Int. Ed.* **2009**, *48*, 1609.
34. Ojima, I.; Kogure, T. *Chem. Lett.* **1973**, 541.
35. Corriu, R. J. P.; Moreau, J. J. E. *J. Chem. Soc., Chem. Commun.* **1973**, 38.
36. Ojima, I.; Nagai, Y. *Chem. Lett.* **1974**, 223.
37. Corriu, R. J. P.; Moreau, J. J. E. *J. Organomet. Chem.* **1974**, *64*, C51.
38. Yamamoto, K.; Hayashi, T.; Kumada, M. *J. Organomet. Chem.* **1973**, *54*, C45.
39. Hayashi, T.; Yamamoto, K.; Kumada, M. *Tetrahedron Lett.* **1974**, 4405.
40. Nishiyama, H.; Sakaguchi, H.; Nakamura, T.; Horihata, M.; Kondo, M.; Itoh, K. *Organometallics* **1989**, *8*, 846.
41. Nishiyama, H.; Kondo, M.; Nakamura, T.; Itoh, K. *Organometallics* **1991**, *10*, 500.
42. Nishiyama, H.; Yamaguchi, S.; Kondo, M.; Itoh, K. *J. Org. Chem.* **1992**, *57*, 4306.
43. Imai, Y.; Zhang, W. B.; Kida, T.; Nakatsuji, Y.; Ikeda, I. *Tetrahedron: Asymmetry* **1996**, *7*, 2453.
44. Brunner, H.; Storiko, R.; Nuber, B. *Tetrahedron: Asymmetry* **1998**, *9*, 407.
45. Brunner, H.; Obermann, U. *Chem. Ber.* **1989**, *122*, 499.
46. Balavoine, G.; Clinet, J. C.; Lellouche, I. *Tetrahedron Lett.* **1989**, *30*, 5141.
47. Langer, T.; Janssen, J.; Helmchen, G. *Tetrahedron: Asymmetry* **1996**, *7*, 1599.
48. Sudo, A.; Yoshida, H.; Saigo, K. *Tetrahedron: Asymmetry* **1997**, *8*, 3205.
49. Lee, S.; Lim, C. W. *Bull. Korean Chem. Soc.* **2001**, *22*, 231.
50. Tao, B. T.; Fu, G. C. *Angew. Chem., Int. Ed.* **2002**, *41*, 3892.
51. Brunner, H.; Weber, H. *Chem. Ber.* **1985**, *118*, 3380.
52. Hayashi, T.; Hayashi, C.; Uozumi, Y. *Tetrahedron: Asymmetry* **1995**, *6*, 2503.
53. Chelucci, G.; Gladiali, S.; Sanna, M. G.; Brunner, H. *Tetrahedron: Asymmetry* **2000**, *11*, 3419.
54. Brunner, H.; Kurzinger, A. *J. Organomet. Chem.* **1988**, *346*, 413.
55. Brunner, H.; Riepl, G. *Angew. Chem., Int. Ed.* **1982**, *21*, 377.
56. Niyomura, O.; Tokunaga, M.; Obora, Y.; Iwasawa, T.; Tsuji, Y. *Angew. Chem., Int. Ed.* **2003**, *42*, 1287.
57. Niyomura, O.; Iwasawa, T.; Sawada, N.; Tokunaga, M.; Obora, Y.; Tsuji, Y. *Organometallics* **2005**, *24*, 3468.
58. Ochida, A.; Sawamura, M. *Chem.--Asian J.* **2007**, *2*, 609.
59. Sakakura, T.; Tokunaga, Y.; Sodeyama, T.; Tanaka, M. *Chem. Lett.* **1987**, 2375.
60. Wang, F.; Neckers, D. C. *J. Organomet. Chem.* **2003**, *665*, 1.
61. Jakubek, V.; Lees, A. J. *Inorg. Chem.* **2004**, *43*, 6869.
62. Dr. Mathieu Tschan is kindly acknowledge for providing BSP 25.
63. Thiot, C.; Wagner, A.; Mioskowski, C. *Org. Lett.* **2006**, *8*, 5939.
64. Ito, H.; Kato, T.; Sawamura, M. *Chem.--Asian J.* **2007**, *2*, 1436.
65. Comte, V.; Balan, C.; Le Gendre, P.; Moise, C. *Chem. Commun.* **2007**, 713.
66. Trost, B. M. *Chem. Pharm. Bull.* **2002**, *50*, 1.

67. Trost, B. M.; VanVranken, D. L. *Chem. Rev.* **1996**, *96*, 395.
68. Trost, B. M. *J. Org. Chem.* **2004**, *69*, 5813.
69. Yoshizaki, H.; Satoh, H.; Sato, Y.; Nukui, S.; Shibasaki, M.; Mori, M. *J. Org. Chem.* **1995**, *60*, 2016.
70. Chapsal, B. D.; Ojima, I. *Org. Lett.* **2006**, *8*, 1395.
71. Tsuji, J.; Takahashi, H.; Morikawa, M. *Tetrahedron Lett.* **1965**, 4387.
72. Trost, B. M.; Dietsche, T. J. *J. Am. Chem. Soc.* **1973**, *95*, 8200.
73. Trost, B. M.; Toste, F. D. *J. Am. Chem. Soc.* **1999**, *121*, 4545.
74. Helmchen, G.; Pfaltz, A. *Acc. Chem. Res.* **2000**, *33*, 336.
75. Deerenberg, S.; Schrekker, H. S.; van Strijdonck, G. P. F.; Kamer, P. C. J.; van Leeuwen, P. W. N. M.; Fraanje, J.; Goubitz, K. *J. Org. Chem.* **2000**, *65*, 4810.
76. Maxwell, A. C.; Franc, C.; Pouchain, L.; Muller-Bunz, H.; Guiry, P. J. *Org. Biomol. Chem.* **2008**, *6*, 3848.
77. Trost, B. M.; Crawley, M. L. *Chem. Rev.* **2003**, *103*, 2921.
78. Blacker, A. J.; Clarke, M. L.; Loft, M. S.; Williams, J. M. J. *Org. Lett.* **1999**, *1*, 1969.
79. Kazmaier, U.; Stolz, D.; Kramer, K.; Zumpe, F. L. *Chem.--Eur. J.* **2008**, *14*, 1322.
80. Kawamura, M.; Kiyotake, R.; Kudo, K. *Chirality* **2002**, *14*, 724.
81. van Haaren, R. J.; Goubitz, K.; Fraanje, J.; van Strijdonck, G. P. F.; Oevering, H.; Coussens, B.; Reek, J. N. H.; Kamer, P. C. J.; van Leeuwen, P. W. N. M. *Inorg. Chem.* **2001**, *40*, 3363.
82. Sjogren, M. P. T.; Hansson, S.; Akermark, B.; Vitagliano, A. *Organometallics* **1994**, *13*, 1963.
83. Kazmaier, U.; Zumpe, F. L. *Angew. Chem., Int. Ed.* **2000**, *39*, 802.
84. van Haaren, R. J.; van Strijdonck, G. P. F.; Oevering, H.; Reek, J. N. H.; Kamer, P. C. J.; van Leeuwen, P. W. N. M. *Eur. J. Inorg. Chem.* **2001**, 837.
85. Hayashi, T.; Kawatsura, M.; Uozumi, Y. *J. Am. Chem. Soc.* **1998**, *120*, 1681.
86. Evans, L. A.; Fey, N.; Harvey, J. N.; Hose, D.; Lloyd-Jones, G. C.; Murray, P.; Orpen, A. G.; Osborne, R.; Owen-Smith, G. J. J.; Purdie, M. J. *J. Am. Chem. Soc.* **2008**, *130*, 14471.
87. van Haaren, R. J.; Zuidema, E.; Fraanje, J.; Goubitz, K.; Kamer, P. C. J.; van Leeuwen, P. W. N. M.; van Strijdonck, G. P. F. *C. R. Chim.* **2002**, *5*, 431.
88. Ahn, K. H.; Cho, C. W.; Park, J. W.; Lee, S. W. *Tetrahedron: Asymmetry* **1997**, *8*, 1179.
89. Ogasawara, M.; Takizawa, K.; Hayashi, T. *Organometallics* **2002**, *21*, 4853.
90. Anderson, J. C.; Osborne, J. *Tetrahedron: Asymmetry* **2005**, *16*, 931.
91. Ghedini, M.; Crispini, A. *Comments Inorg. Chem.* **1999**, *21*, 53.
92. Ghedini, M.; Aiello, I.; Crispini, A.; Golemme, A.; La Deda, M.; Pucci, D. *Coord. Chem. Rev.* **2006**, *250*, 1373.
93. Babic, D.; Curic, M.; Molcanov, K.; Ilc, G.; Plavec, J. *Inorg. Chem.* **2008**, *47*, 10446.
94. Shin, R. Y. C.; Goh, C. L.; Goh, L. Y.; Webster, R. D.; Li, Y. X. *Eur. J. Inorg. Chem.* **2009**, 2282.
95. Siegel, H.; Himmele, W. *Angew. Chem., Int. Ed.* **1980**, *19*, 178.
96. van Leeuwen, P. W. N. M.; Claver, C. *Rhodium Catalyzed Hydroformylation*; Kluwer Academic Publishers, **2000**.

97. Feisst, W.; Neweling, H.; Roelen, O., US Patent 2238726, **1941**.
98. Slauch, L. H.; Mullineau, R. D. *J. Organomet. Chem.* **1968**, *13*, 469.
99. Osborn, J. A.; Wilkinso, G.; Young, J. F. *Chem. Commun.* **1965**, 17.
100. Kamer, P. C. J.; van Rooy, A.; Schoemaker, G. C.; van Leeuwen, P. W. N. M. *Coord. Chem. Rev.* **2004**, *248*, 2409.
101. Zuidema, E.; Escorihuela, L.; Eichelsheim, T.; Carbo, J. J.; Bo, C.; Kamer, P. C. J.; Van Leeuwen, P. W. N. M. *Chem.-Eur. J.* **2008**, *14*, 1843.
102. Evans, D.; Osborn, J. A.; Wilkinson, G. *J. Chem. Soc. (A)*, **1968**, 3133.
103. Brown, J. M.; Kent, A. G. *J. Chem. Soc., Perkin Trans. 2* **1987**, 1597.
104. Casey, C. P.; Petrovich, L. M. *J. Am. Chem. Soc.* **1995**, *117*, 6007.
105. Buisman, G. J. H.; van der Veen, L. A.; Kamer, P. C. J.; van Leeuwen, P. W. N. M. *Organometallics* **1997**, *16*, 5681.
106. Casey, C. P.; Whiteker, G. T. *Isr. J. Chem.* **1990**, *30*, 299.
107. Kranenburg, M.; van der Burgt, Y. E. M.; Kamer, P. C. J.; van Leeuwen, P. W. N. M.; Goubitz, K.; Fraanje, J. *Organometallics* **1995**, *14*, 3081.
108. Casey, C. P.; Whiteker, G. T.; Melville, M. G.; Petrovich, L. M.; Gavney, J. A., Jr.; Powell, D. R. *J. Am. Chem. Soc.* **1992**, *114*, 5535.
109. Brown, J. M.; Canning, L. R.; Kent, A. G.; Sidebottom, P. J. *J. Chem. Soc., Chem. Commun.* **1982**, 721.
110. Van der Veen, L. A.; Boele, M. D. K.; Bregman, F. R.; Kamer, P. C. J.; Van Leeuwen, P. W. N. M.; Goubitz, K.; Fraanje, J.; Schenk, H.; Bo, C. *J. Am. Chem. Soc.* **1998**, *120*, 11616.
111. Freixa, Z.; Van Leeuwen, P. W. N. M. *Dalton Trans.* **2003**, 1890.
112. Brown, C. K.; Wilkinso, G. *J. Chem. Soc.* **1970**, 2753.
113. Seiche, W.; Schuschkowski, A.; Breit, B. *Adv. Synth. Catal.* **2005**, *347*, 1488.
114. Uson, R.; Oro, L. A.; Cabeza, J. A. *Inorg. Synth.* **1985**, *23*, 126.
115. Mirbach, M. J.; Topalsavoglu, N.; Phu, T. N.; Mirbach, M. F.; Saus, A. *Angew. Chem., Int. Ed.* **1981**, *20*, 381.
116. Saus, A.; Phu, T. N.; Mirbach, M. J.; Mirbach, M. F. *J. Mol. Catal.* **1983**, *18*, 117.
117. Willner, I.; Maida, R. *J. Chem. Soc., Chem. Commun.* **1988**, 876.
118. Long, J. A.; Marder, T. B.; Behnken, P. E.; Hawthorne, M. F. *J. Am. Chem. Soc.* **1984**, *106*, 2979.
119. Vinas, C.; Flores, M. A.; Nunez, R.; Teixidor, F.; Kivekas, R.; Sillanpaa, R. *Organometallics* **1998**, *17*, 2278.
120. Buhling, A.; Kamer, P. C. J.; van Leeuwen, P. W. N. M.; Elgersma, J. W.; Goubitz, K.; Fraanje, J. *Organometallics* **1997**, *16*, 3027.
121. Baker, M. V.; Field, L. D. *Inorg. Chem.* **1987**, *26*, 2010.
122. Hughes, O. R.; Young, D. A. *J. Am. Chem. Soc.* **1981**, *103*, 6636.
123. Varshavskii, Y. S.; Cherkasova, T. G.; Podkorytov, I. S.; Korlyukov, A. A.; Khrustalev, V. N.; Nikol'skii, A. B. *Russ. J. Coord. Chem.* **2005**, *31*, 121.
124. Evans, D.; Yagupsky, G.; Wilkinso, G. *J. Chem. Soc. (A)*, **1968**, 2660.
125. Yagupsky, M.; Brown, C. K.; Yagupsky, G.; Wilkinso, G. *J. Chem. Soc. (A)*, **1970**, 937.
126. Chan, A. S. C.; Shieh, H. S.; Hill, J. R. *J. Chem. Soc., Chem. Commun.* **1983**, 688.

127. James, B. R.; Mahajan, D.; Rettig, S. J.; Williams, G. M. *Organometallics* **1983**, *2*, 1452.
128. Castellanos-Paez, A.; Castillon, S.; Claver, C.; van Leeuwen, P. W. N. M.; de Lange, W. G. J. *Organometallics* **1998**, *17*, 2543.
129. Bianchini, C.; Lee, H. M.; Meli, A.; Vizza, F. *Organometallics* **2000**, *19*, 849.
130. Freixa, Z.; Pereira, M. M.; Pais, A. A. C. C.; Bayon, J. C. J. *Chem. Soc., Dalton Trans.* **1999**, 3245.
131. Simulation performed using gNMR software v4.1.

UNIVERSITAT ROVIRA I VIRGILI
SWITCHABLE AND TUNABLE LIGANDS FOR HOMOGENEOUS CATALYSIS
Maria Dolores Segarra Maset
ISBN:978-84-693-7666-9/DL:T-1755-2010

CHAPTER 4

EXPERIMENTAL

4.1. GENERAL PROCEDURES

Unless otherwise stated, all preparations were carried out under an inert atmosphere of argon using standard Schlenk techniques. All reagents were obtained from commercial suppliers and used without further purification. Solvents were purified using SPS-400-6 from Innovative Technologies, Inc.

Routine ^1H -, $^{13}\text{C}\{^1\text{H}\}$ - and $^{31}\text{P}\{^1\text{H}\}$ -NMR spectra were recorded on a Bruker Avance 400 Ultrashield spectrometer (400.1 MHz for ^1H -, 100.6 MHz for $^{13}\text{C}\{^1\text{H}\}$ - and 162.0 MHz for $^{31}\text{P}\{^1\text{H}\}$ -NMR), or Bruker Avance 500 Ultrashield spectrometer (500.1 MHz for ^1H -, 125.7 MHz for $^{13}\text{C}\{^1\text{H}\}$ - and 202.5 MHz for $^{31}\text{P}\{^1\text{H}\}$ -NMR). Chemical shifts, δ , are given in ppm, relative to TMS (^1H , ^{13}C) and 85% H_3PO_4 (^{31}P). Coupling constants, J , are given in Hz.

Mass spectra were recorded on a Waters LCT Premier ESI-TOF spectrometer, or on a Waters GTC spectrometer.

UV-vis experiments were conducted with a temperature controlled Double beam UV-vis spectrophotometer Shimadzu UV-2401 PC with a 1 mm quartz cell.

Gas chromatography analyses were performed on an Agilent Technologies 6890N/G1530N apparatus equipped with a FID detector and HP-5 column (length 30 m, internal diameter 0.32 mm, film thickness 0.25 μm), gas carrier was He.

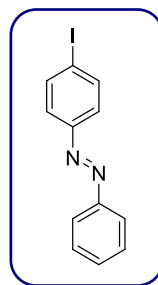
The measured crystals that were unstable under atmosphere conditions were prepared under inert conditions immersed in perfluoropolyether as protecting oil for manipulation. Crystal structure determination was carried out using a Bruker-Nonius diffractometer equipped with a APPEX 2 4K CCD area detector, a FR591 rotating anode with MoK α radiation, Montel mirrors as monochromator and a Kryoflex low temperature device ($T = -173$ °C). Full sphere data collection omega and phi scans. Programs used: Data collection Apex2 V2008.6-1 (Bruker-Nonius 2008), data reduction Saint + Version 7.60A (Bruker AXS 2008) and absorption correction SADABS V. 2008-1 (2008). Crystal structure solution was achieved using direct methods as implemented in SHELXTL Version 6.10 (Sheldrick, Universität Göttingen, Germany, 2000) and visualized using XP program. Missing atoms were subsequently located from difference Fourier synthesis and added to the atom list. Least-squares refinement on F² using all measured intensities was carried out using the program SHELXTL-97-UNIX VERSION.

4.2. SYNTHESIS

(*E*)-4-Iodoazobenzene (**14**)

4-iodoaniline (1.97 g, 9 mmol) was mixed with nitrosobenzene (0.96 g, 9 mmol) in 35 mL of acetic acid. The mixture was stirred at room temperature and the progress of the reaction was monitored by TLC. When no starting material was observed, the mixture was poured into 100 mL of water, and partitioned between diethyl ether and water. The aqueous layer was washed with diethyl ether twice. The organic layers were collected, dried over MgSO₄, filtered, and concentrated to dryness. The solid was dissolved in a 1:1 mixture of dichloromethane and hexane and filtered over basic alumina. The orange solution was concentrated to obtain 2.3 g of an orange powder (83 % yield).

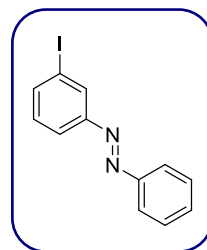
¹H-NMR (CDCl₃, 400.1 MHz) δ (ppm): 7.5 (m, 3H), 7.66 (m, 2H), 7.87 (m, 2H), 7.91 (m, 2H); ¹³C{¹H}-NMR (CDCl₃, 100.6 MHz) δ (ppm): 97.65, 122.98, 124.48, 129.16, 131.36, 138.36, 151.65, 152.46. HR-MS (ESI+ve): m/z calcd for C₁₂ H₁₀ N₂ I



$([M+H]^+)$ 308.9889, found 308.9890.

(E)-3-Iodoazobenzene (15)

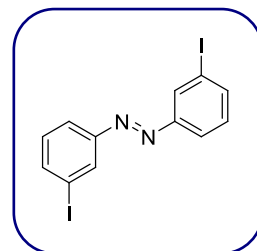
3-iodoaniline (4.82 g, 22 mmol) was mixed with nitrosobenzene (2.36 g, 22 mmol) in 85 mL of acetic acid. The mixture was stirred at room temperature and the progress of the reaction was monitored by TLC. When no starting material was observed, the mixture was partitioned between ethyl acetate and water. The organics were collected, dried over $MgSO_4$, filtered and concentrated to dryness. The solid was dissolved in dichloromethane and filtered over basic alumina. The orange solution was concentrated to obtain 5.9 g of an orange powder (87 % yield).



1H -NMR (CD_2Cl_2 , 400.1 MHz) δ (ppm): 7.29 (t, $J = 7.9$ Hz, 1H), 7.54 (m, 3H), 7.83 (ddd, $J = 7.8$ Hz, $J = 1.7$ Hz, $J = 1.1$ Hz, 1H), 7.93 (m, 3H), 8.26 (t, $J = 1.7$ Hz, 1H); $^{13}C\{^1H\}$ -NMR (CD_2Cl_2 , 100.6 MHz) δ (ppm): 94.42, 122.96, 123.54, 129.18, 130.51, 130.74, 131.55, 139.57, 152.34, 153.41. HR-MS (ESI+ve): m/z calcd for $C_{12}H_{10}N_2I$ ($[M+H]^+$) 308.9889, found 308.9903.

(E)-1,2-bis(3-iodophenyl)diazene (13)

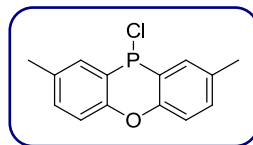
3-iodoaniline (10.79 g, 49.27 mmol) was dissolved in 300 mL of toluene. Activated MnO_2 was added (23.84 g, 274.22 mmol) and the mixture was refluxed and the progress of the reaction was monitored by TLC. When all the starting material was consumed, the crude reaction was cooled to room temperature, filtered over basic alumina, and the alumina washed with dichloromethane. The organic fraction was collected and concentrated to obtain 10.1 g of an orange product (94 % yield).



1H -NMR ($CDCl_3$, 400.1 MHz) δ (ppm): 7.27 (t, $J = 7.8$ Hz, 2H), 7.82 (d, $J = 7.8$ Hz, 2H), 7.91 (d, $J = 7.8$ Hz, 2H), 8.24 (s, 2H); $^{13}C\{^1H\}$ -NMR ($CDCl_3$, 100.6 MHz) δ (ppm): 94.58, 123.77, 130.72, 130.74, 140.02, 153.05. HR-MS (ESI+ve): m/z calcd for $C_{12}H_9N_2I_2$ ($[M+H]^+$) 434.8855, found 434.8870.

2,7-dimethyl-10-chlorophenoxaphosphin (19)

p-Tolylether (4.9 g, 24.71 mmol), AlCl₃ (4.9 g, 36.76 mmol) and PCl₃ (12.5 mL, 143.32 mmol) were refluxed for 8 hours. Then, the excess of PCl₃ was distilled off. The residue was

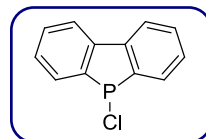


suspended in 50 mL of toluene and cooled to 0 °C. Pyridine (6 mL, 74.13 mmol) was added slowly and the mixture was stirred for 1 hour. The salts formed were filtered over celite, and the celite was washed with toluene. The solvent was removed under vacuum to obtain 3.98 g of the product as yellowish powder (61 % yield).

¹H-NMR (CDCl₃, 400.1 MHz) δ (ppm): 2.04 (s, 6H), 6.95 (dd, J = 8.5, J = 2.0 Hz, 2H), 7.16 (d, J = 8.5 Hz, 2H), 7.52 (dd, J = 2.0 Hz, J = 11.7 Hz, 2H); ³¹P{¹H}-NMR (CDCl₃, 162.0 MHz) δ (ppm): 38.76.¹

5-chloro-dibenzo[b,d]phosphole (20)

2,2'-dibromobiphenyl (7.1 g, 22.76 mmol) was dissolved in 100 mL of dried diethyl ether. The solution was cooled to 0 °C and *n*-BuLi 2.5 M in hexanes (19 mL, 47.49 mmol) was added dropwise. After 1 hour and 30 minutes, the mixture was frozen



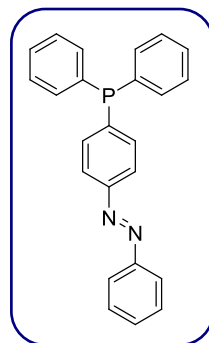
with liquid nitrogen and PCl₃ (aprox. 19 mL, 115.38 mmol) was distilled directly on to the frozen reaction mixture. It was warmed to -110 °C and homogenized quickly upon thawing. The reaction was left stirring overnight. The solvent and excess of PCl₃ was removed under vacuum. The remaining salts were extracted with 130 mL of hot hexanes. The solvent was removed to obtain 3.4 g of yellow product (68 % yield).

¹H-NMR (C₆D₆, 400.1 MHz) δ (ppm): 7.02 (ddt, J = 7.3 Hz, J = 1.0 Hz, J = 3.0 Hz, 2H), 7.14 (t, J = 7.5 Hz, 2H), 7.40 (d, J = 7.6 Hz, 2H), 7.64 (dd, J = 7.3 Hz, J = 4.0 Hz, 2H); ³¹P{¹H}-NMR (C₆D₆, 162.0 MHz) δ (ppm): 71.28.²

(E)-4-(diphenylphosphino)azobenzene (1)

HPPH₂ (0.46 g, 2.5 mmol) was dissolved in 8 mL of CH₃CN, and added to a mixture of **14** (0.75 g, 2.4 mmol) and Pd(OAc)₂ (0.016 g, 0.07 mmol). To the solution NEt₃ (0.35 mL, 2.5 mmol) was added, and the reaction mixture was stirred at 85 °C overnight. The dark orange mixture was cooled to room temperature and the solvent was removed. Orange needles of pure product were obtained after recrystallization from EtOH (0.65 g, 74 % yield).

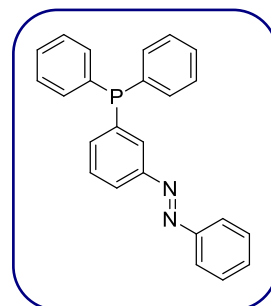
¹H{³¹P}-NMR (CDCl₃, 400.1 MHz) δ (ppm): 7.36 (m, 10H), 7.43 (d, J = 8.3 Hz, 2H), 7.50 (m, 3H), 7.86 (d, J = 8.3 Hz, 2H), 7.91 (br d, J = 6.8 Hz, 2H); ³¹P{¹H}-NMR (CDCl₃, 162.0 MHz) δ (ppm): -1.97; ¹³C{¹H}-NMR (CDCl₃, 100.6 MHz) δ (ppm): 122.63, 122.70, 122.91, 128.66 (d, J = 6.6 Hz), 129.06 (d, J = 8.8 Hz), 131.15, 133.92 (d, J = 19.7 Hz), 134.18 (d, J = 19.7 Hz), 136.61 (d, J = 10.2 Hz), 141.28 (d, J = 13.17 Hz), 152.60, 152.69. HR-MS (ESI+ve): m/z calcd for C₂₄ H₁₉ N₂ P ([M+H]⁺) 367.1364, found 367.1370.



(E)-3-(diphenylphosphino)azobenzene(2)

HPPH₂ (0.75 g, 4 mmol) was dissolved in 10 mL of CH₃CN, and added to a mixture of **15** (1.25 g, 4 mmol) and Pd(OAc)₂ (0.022 g, 0.1 mmol). To the solution NEt₃ (0.57 mL, 4 mmol) was added, and the reaction mixture was stirred at 85°C overnight. The dark orange mixture was cooled to room temperature and the solvent was removed. The pure product was obtained as an orange powder after recrystallization from EtOH (0.81 g, 58 % yield).

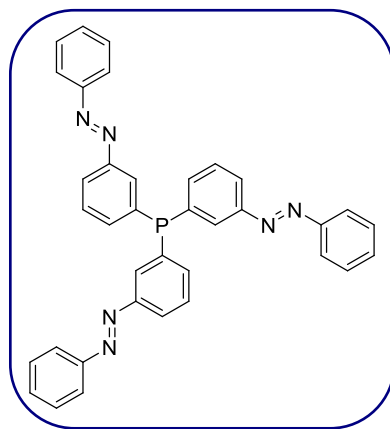
¹H{³¹P}-NMR (CDCl₃, 400.1 MHz) δ (ppm): 7.36 (m, 11H), 7.49 (m, 3H), 7.87 (br d, J = 7.3 Hz, 2H), 7.92 (br s, 1H); ³¹P{¹H}-NMR (CDCl₃, 162.0 MHz) δ (ppm): -1.92; ¹³C{¹H}-NMR (CDCl₃, 100.6 MHz) δ (ppm): 121.98, 122.89, 128.63 (d, J = 6.8 Hz), 128.93, 129.07, 129.17 (d, J = 20.1 Hz), 129.24 (d, J = 6.2 Hz), 131.12, 133.84 (d, J = 19.7 Hz), 135.97 (d, J = 18.1 Hz), 136.69 (d, J = 10.8 Hz), 138.92 (d, J = 13.1 Hz), 152.57, 152.61 (d, J = 7.3 Hz). HR-MS (ESI+ve): m/z calcd for C₂₄ H₁₉ N₂ P



$([M+H]^+)$ 367.1364, found 367.1357.

tris(3-((*E*)-phenyldiazenyl)phenyl)phosphine (**3**)

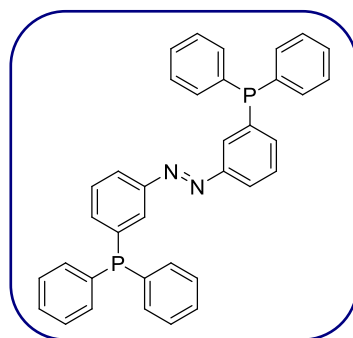
15 (2.05 g, 6.65 mmol) was dissolved in 35 mL of THF. At $-95\text{ }^\circ\text{C}$, *n*-BuLi 1.6 M in hexanes (4.17 mL, 6.67 mmol) was added, and the mixture was stirred during 25 min. Then, PCl_3 (193 μL , 2.22 mmol) was added and the dark mixture was left stirring overnight to reach slowly room temperature. The orange solution obtained was concentrated and diluted in CH_2Cl_2 . After filtration over basic alumina, the solvent was removed to obtain 0.68 g of the product as an orange powder (54 % yield).



$^1\text{H}\{^{31}\text{P}\}$ -NMR (CDCl_3 , 400.1 MHz) δ (ppm): 7.49 (m, 15H), 7.87 (m, $J = 8.3$ Hz, 6H), 7.92 (m, $J = 7.3$ Hz, 3H), 8.04 (br s, 3H); $^{31}\text{P}\{^1\text{H}\}$ -NMR (CDCl_3 , 162.0 MHz) δ (ppm): -1.94 ; $^{13}\text{C}\{^1\text{H}\}$ -NMR (CDCl_3 , 100.6 MHz) δ (ppm): 122.45, 122.96, 129.07, 129.36 (d, $J = 22.1$ Hz), 129.54 (d, $J = 6.6$ Hz), 131.20, 136.08 (d, $J = 17.8$ Hz), 137.91 (d, $J = 12.9$ Hz), 152.54, 152.74 (d, $J = 7.5$ Hz). HR-MS (ESI): m/z calcd for $\text{C}_{36}\text{H}_{28}\text{N}_6\text{P}$ ($[M+H]^+$) 575.2113, found 575.2120.

(*E*)-1,2-bis(3-(diphenylphosphino)phenyl)diazene (**7**)

13 (2.01 g, 4.63 mmol) was dissolved in 35 mL of THF. At $-95\text{ }^\circ\text{C}$, *n*-BuLi 1.6 M in hexanes (8.64 mL, 13.82 mmol) was added, and the mixture was stirred during 15 min. Then, ClPPH_2 (1.65 mL, 9.19 mmol) was added and the dark mixture was left stirring overnight to reach slowly room temperature. The orange solution obtained was concentrated and dissolved in CH_2Cl_2 . After filtration over basic alumina, the solvent was removed to obtain 1.41 g of the product as an orange solid

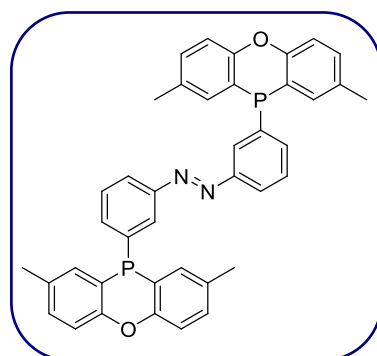


(55 % yield).

$^1\text{H}\{^{31}\text{P}\}$ -NMR (CDCl_3 , 500.1 MHz) δ (ppm): 7.37 (m, $J = 8.6$ Hz, 22H), 7.46 (t, $J = 7.9$ Hz, 2H), 7.81 (d, $J = 8.6$ Hz, 2H), 7.86 (br s, 2H); $^{31}\text{P}\{^1\text{H}\}$ -NMR (CDCl_3 , 202.5 MHz) δ (ppm): -2.16; $^{13}\text{C}\{^1\text{H}\}$ -NMR (CDCl_3 , 125.7 MHz) δ (ppm): 122.06, 128.66 (d, $J = 5.8$ Hz), 128.95, 129.14 (d, $J = 14.8$ Hz), 129.25, 133.83 (d, $J = 20.3$ Hz), 136.12 (d, $J = 19.4$ Hz), 136.66 (d, $J = 11.1$ Hz), 138.94 (d, $J = 13.9$ Hz), 152.52 (d, $J = 7.2$ Hz). HR-MS (ESI): m/z calcd for $\text{C}_{36} \text{H}_{29} \text{N}_2 \text{P}_2$ ($[\text{M}+\text{H}]^+$) 551.1806, found 551.1785.

(*E*)-1,2-bis(3-(2,8-dimethyl-10H-phenoxaphosphinin-10-yl)phenyl)diazene (**8**)

13 (1.49 g, 3.43 mmol) was dissolved in 30 mL of THF. At -95 °C, *n*-BuLi 1.6 M in hexanes (6.4 mL, 10.4 mmol) was added, and the mixture was stirred during 15 min. Then, ClMePOP (**19**) (2 g, 6.85 mmol) was dissolved in 20 mL of THF under Ar and added to the crude dark mixture. It was left stirring to reach slowly room temperature overnight. The orange solution obtained was concentrated and



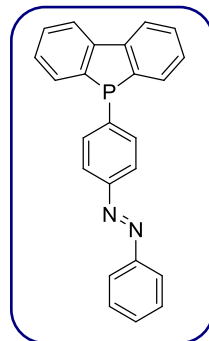
subjected to basic alumina chromatography, using as eluent a mixture of dichloromethane:hexane (1:4), and increasing slowly the polarity of the mixture. 1.83 g of the product were obtained as an orange solid (84 % yield).

$^1\text{H}\{^{31}\text{P}\}$ -NMR (CDCl_3 , 500.1 MHz) δ (ppm): 2.32 (s, 12H), 7.09 (d, $J = 8.3$ Hz, 4H), 7.18 (dd, $J = 8.3$ Hz, $J = 1.8$ Hz, 4H), 7.28 (m, 2H), 7.30 (d, $J = 7.6$ Hz, 2H), 7.33 (d, $J = 1.8$ Hz, 4H), 7.65 (m, 2H), 7.8 (br s, 2H); $^{31}\text{P}\{^1\text{H}\}$ -NMR (CDCl_3 , 202.5 MHz) δ (ppm): -50.53; $^{13}\text{C}\{^1\text{H}\}$ -NMR (CDCl_3 , 125.7 MHz) δ (ppm): 20.62, 117.42 (d, $J = 2.8$ Hz), 117.64, 121.77, 127.56 (d, $J = 24.1$ Hz), 129.22 (d, $J = 5.9$ Hz), 131.94, 133.00 (d, $J = 11.7$ Hz), 134.35 (d, $J = 15.8$ Hz), 134.99 (d, $J = 35.4$ Hz), 142.22 (d, $J = 24.3$ Hz), 152.39 (d, $J = 7.5$ Hz), 153.39. HR-MS (ESI): m/z calcd for $\text{C}_{40} \text{H}_{33} \text{N}_2 \text{O}_2 \text{P}_2$ ($[\text{M}+\text{H}]^+$) 635.2017, found 635.2024.

(*E*)-1-(4-(5H-benzo[*b*]phosphindol-5-yl)phenyl)-2-phenyldiazene (**6**)

14 (0.48 g, 1.56 mmol) was dissolved in 30 mL of THF and cooled to $-95\text{ }^{\circ}\text{C}$. *n*-BuLi 1.6 M in hexanes (1.02 mL, 1.66 mmol) was added and the mixture was stirred for 15 min. A solution of **20** (0.38 g, 1.73 mmol) in 10 mL of THF was added at $-95\text{ }^{\circ}\text{C}$. The mixture was then stirred at r.t. for 3 hours. The solvent was removed under vacuum and the residue partitioned between diethyl ether and water. The organics were concentrated, and the residue was dissolved in the minimum amount of dichloromethane and subjected to column chromatography (basic alumina) using a mixture of hexane:dichloromethane (1:1). The yield was too low to be determined.

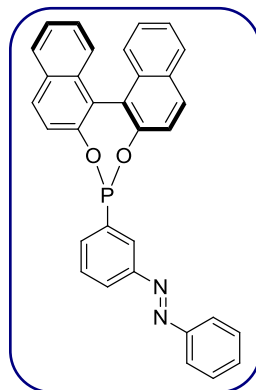
$^1\text{H-NMR}$ (CDCl_3 , 400.1 MHz) δ (ppm): 7.36 (ddt, $J = 7.3\text{ Hz}$, $J = 1.0\text{ Hz}$, $J = 3.0\text{ Hz}$, 2H), 7.4–7.6 (m, 8H), 7.70 (m, 3H), 7.80 (m, 2H), 7.98 (d, $J = 7.8\text{ Hz}$, 2H); $^{31}\text{P}\{^1\text{H}\}$ -NMR (CDCl_3 , 162.0 MHz) δ (ppm): -7.77 .



(*E*)-1-(3-(dinaphtho[2,1-*d*:1',2'-*f*][1,3,2]dioxaphosphepin-4-yl)phenyl)-2-phenyldiazene (**9**)

15 (1.32 g, 4.28 mmol) was dissolved in 30 mL of THF and cooled to $-95\text{ }^{\circ}\text{C}$. *n*-BuLi 1.6 M in hexanes (2.68 mL, 4.28 mmol) was added and the mixture was stirred for 20 min. A solution of bis(dimethylamino)chlorophosphine (0.66 g, 4.28 mmol) in 5 mL of THF was added and the mixture was left stirring overnight. The solvent was removed and the residue was dissolved in toluene and filtered over celite. (*R*)-(+)-binaphthol (1.22 g, 4.27 mmol) was added and the mixture was refluxed for 15 hours. After that the solvent was removed and the product was recrystallized from hot diethyl ether. The yield was too low to be determined.

$^1\text{H-NMR}$ (CDCl_3 , 400.1 MHz) δ (ppm): 7.36 (ddt, $J = 7.3\text{ Hz}$, $J = 1.0\text{ Hz}$, $J = 3.0\text{ Hz}$, 2H), 7.4–7.6 (m, 8H), 7.70 (m, 3H), 7.80 (m, 2H), 7.98 (d, $J = 7.8\text{ Hz}$, 2H); $^{31}\text{P}\{^1\text{H}\}$ -NMR (CDCl_3 , 162.0 MHz) δ (ppm): -7.77 .



4.3. PHOTOCHEMICAL PROCESSES

In a quartz vessel equipped with an internal cold finger cooling system, the solid azophosphine was introduced and dissolved under inert atmosphere in the appropriate solvent. Then, the sample was irradiated for 1 hour using a photochemical reactor (Rayonet RPR-200) equipped with 16 lamps (350 nm, 24 watts approx.). Quartz NMR tubes were used when necessary.

4.4. UV-VIS STUDIES

A solution $1 \cdot 10^{-3} \text{M}$ of the sample was prepared and irradiated as described in section 4.3. Then, 1 mL was transferred to the UV cell and the UV-vis spectra were recorded every 30 min during 48 h, keeping the temperature constant at 25 °C.

In the case of phosphine **3**, the concentration of the sample was three times lower, because the molecule has three chromophoric groups.

4.5. CATALYSIS

Palladium catalyzed Suzuki cross-coupling

Method A: In a flame-dried Schlenk flask 172.8 mg (1 mmol) of 4-bromotoluene (dried over molecular sieves), 4.6 mg (0.005 mmol) of $\text{Pd}_2(\text{dba})_3$, 193.7 mg (3.3 mmol) of KF and 137.0 mg (1.1 mmol) of phenylboronic acid were added. The Schlenk flask was purged with argon and then the appropriate amount of phosphine (0.012 mmol) dissolved in 2 mL of dried THF (this solution was previously irradiated as described in 4.3, if necessary) was added under Ar. Several aliquots were taken at regular intervals of time, and filtered over a pad of silica using CH_2Cl_2 as eluent. The analysis was performed by GC. The analysis conditions and retention times are described in Table 4. 1.

Method B: In a flame dried Schlenk flask 0.345 g (2 mmol) of 4-bromotoluene (dried over molecular sieves), 4.6 mg (0.005 mmol) of $\text{Pd}_2(\text{dba})_3$, 1.297 g (6 mmol) of K_3PO_4 and 0.372 g (3 mmol) of phenyl boronic acid were added. The Schlenk flask was purged and then the appropriate amount of phosphine (0.015 mmol) dissolved in 2 mL of dried THF (this solution was previously irradiated as described in 4.3) was added under Ar. Several samples were taken along time, filtered over a pad of silica using CH_2Cl_2 as eluent. The analysis was done by GC. The analysis conditions and retention times are described in Table 4. 1. If the reaction has to be irradiated during the catalysis, a quartz Schlenk vessel was used equipped with a cooling finger and a thermometer to maintain the temperature at 25 °C during the catalysis.

Table 4. 1. Analysis conditions for the determination of the conversion in the palladium catalyzed Suzuki cross-coupling reaction by GC.

	Retention time (min)
bromotoluene	8.4
phenyltoluene	16.0

T_{inj} 280 °C; T_{aux} 300 °C; Flow 4.0 mL/min; split 100:1; Ramp: 50 °C (5 min), 10 °C/min up to 320 °C (5 min).

Rhodium catalyzed hydrosilylation of ketones

Hydrosilylation of acetophenone: The appropriate amount of phosphine was dissolved in 1 mL of THF. When required, this solution was irradiated, and added under inert atmosphere to a Schlenk flask containing $[\text{Rh}(\mu\text{-Cl})(\text{cod})_2]$ (2.5 mg, 0.005 mmol). The mixture was stirred during 10 min. Acetophenone (120 μL , 1 mmol) and diphenylsilane (200 μL , 1 mmol) were added, and the reaction mixture was left at room temperature during 30 min. The analysis was performed by $^1\text{H-NMR}$ on the concentrated residue of the reaction dissolved in 0.8 mL of CDCl_3 .

Hydrosilylation of cyclohexanone: The appropriate amount of phosphine was dissolved in 1 mL of THF. When required, the phosphine solution was irradiated, and

added to to a Schlenk flask containing $[\text{Rh}(\mu\text{-Cl})(\text{cod})]_2$ (2.5 mg, 0.005 mmol) under inert atmosphere. The mixture was stirred during 10 min. Decane (internal standard, 49 μL , 0.25 mmol), cyclohexanone (105 μL , 1 mmol) and dimethylphenylsilane (188 μL , 1.2 mmol) were added, and the reaction mixture was left at room temperature during 3 h. Hydrolysis of an aliquot of the crude mixture was done diluting with a solution of MeOH 1 % in HCl, and the analysis of the conversion was done by GC analysis. The analysis conditions and retention times are described in Table 4. 2.

Table 4. 2. Analysis conditions for the determination of the conversion in the hydrosilylation of cyclohexanone by GC.

	Retention time (min)
cyclohexanol	6.8
cyclohexanone	7.2
decane	12.0

T_{inj} 220 °C; T_{aux} 230 °C; Flow 1.0 mL/min; split 100:1; Ramp: 70 °C (10 min), 5 °C/min up to 120 °C, 30 °C/min up to 320 °C (5 min).

Palladium catalyzed allylic alkylation

General procedure: Stock solutions of metal precursor $[\text{Pd}(\mu\text{-Cl})(\text{C}_3\text{H}_5)]_2$ and phosphine were prepared under argon (phosphine solution was irradiated as described in 4.3 when needed). The required amounts of these solutions to obtain 0.5, 1 or 2.5 % of metal and P/M ratio 2/1, were placed in the vessels of a Radley Carousel 12 Place Reaction Station, and the necessary amount of solvent was added to reach 14 mL of total volume. The solutions were stirred for 30 min at room temperature under argon to preform the catalyst. After that, 0.1 mL of decane (0.55 mmol), the appropriate amount of **30** or **31** (0.55 mmol), the appropriate amount of **38** or **39** (1.64 mmol), 381 μL of BSA (1.64 mmol), and a pinch of potassium acetate (approximately 5 mg) were added to the vessels. The mixtures were stirred at room

temperature. Samples were taken after 1 h, filtered over a pad of basic alumina using Et₂O as eluent and analyzed by GC. The analysis conditions and retention times are described in the next tables for each combination of acetate and malonate, except for the cases that used acetate **32**, for which the analysis was done by ¹H-NMR.

Table 4. 3. Analysis conditions for the determination of the conversion and regioselectivity in the allylic alkylation of reactants **30** and **38** by GC

	Retention time (min)
30	3.8
38	3.9
decane	4.8
Branched product 34	8.0
Linear product 33	9.4

T_{inj} 260 °C; T_{aux} 300 °C; Flow 2.7 mL/min; split 50:1; Ramp: from 50 °C – 10 °C/min up to 150 °C, 50 °C/min up to 250 °C (2 min).

Table 4. 4. Analysis conditions for the determination of the conversion and regioselectivity in the allylic alkylation of reactants **30** and **39** by GC.

	Retention time (min)
30	3.8
decane	4.8
39	6.3
Branched product 34	10.6
Linear product 33	11.0

T_{inj} 260 °C; T_{aux} 300 °C; Flow 2.7 mL/min; split 50:1; Ramp: from 50 °C – 10 °C/min up to 150 °C, 50 °C/min up to 250 °C (2 min).

Table 4. 5. Analysis conditions for the determination of the conversion and regioselectivity in the allylic alkylation of reactants **31** and **38** by GC.

	Retention time (min)
38	2.4
decane	2.8
31	5.2
Branched product 36	6.1
Linear product 35	6.9

T_{inj} 300 °C; T_{aux} 300 °C; Flow 2.6 mL/min; split 50:1; Ramp: from 60 °C – 30 °C/min up to 300 °C (2 min).

Table 4. 6. Analysis conditions for the determination of the conversion and regioselectivity in the allylic alkylation of reactants **31** and **39** by GC.

	Retention time (min)
decane	2.8
39	3.3
31	5.2
Branched product 36	6.7
Linear product 35	7.4

T_{inj} 300 °C; T_{aux} 300 °C; Flow 2.6 mL/min; split 50:1; Ramp: from 60 °C – 30 °C/min up to 300 °C (2 min).

Rhodium catalyzed hydroformylation

General procedure: In a flame-dried Schlenk flask 4.7 mg (0.0097 mmol) of **41**, and the necessary amount of phosphine was added in 3 mL of dichloromethane or THF under argon (the solution was irradiated previously if needed). Then the mixture was saturated with CO/H₂ and stirred under syngas during 30 min. After that, 0.57 mL of decane (3 mmol) and 0.47 mL of 1-octene (3 mmol) were added and the mixture was

left stirring at room temperature under CO/H₂ atmosphere during 20 h. If the reaction required irradiation during the catalysis, then a quartz Schlenk vessel was used equipped with a cooling finger and a thermometer to maintain a constant temperature during the catalysis. The analysis was done by GC. The analysis conditions and retention times are described in Table 4. 7.

Hydroformylation under CO/H₂ pressure: In a 25 mL stainless steel reactor (SS316Ti) under inert atmosphere 2.06 mg (0.008 mmol) of [Rh(acac)(CO)₂] and 46 mg of **3** (0.08 mmol) were dissolved in 6 mL of THF then the reactor was pressurized to 18 bar of CO/H₂ to preform the catalyst during 1.5 h at 80 °C. In a Schlenk flask 1.05 mL of decane (5.36 mmol) and 0.86 mL of 1-octene (5.36 mmol) were dissolved in 2 mL of THF under argon. This solution was added to the reactor, and then it was left stirring at 80 °C and 20 bar of CO/H₂ during 7 h. The analysis was done by GC. The analysis conditions and retention times are described in Table 4. 7.

Table 4. 7. Analysis conditions for the determination of the conversion and regioselectivity in the hydroformylation of 1-octene by GC.

	Retention time (min)
1-octene	4.7
decane	8.8
Branched aldehyde (2-methyloctanal)	9.6
Linear aldehyde (nonanal)	10.0

T_{inj} 260 °C; T_{aux} 300 °C; Flow 2.9 mL/min; split 100:1; Ramp: from 35 °C (5 min), 20 °C/min up to 150 °C (10 min).

4.6. HP-NMR

The sample was prepared in a Schlenk flask with toluene-D₈. 0.3 mL of the solution was transferred to a High Pressure NMR (HP-NMR) sapphire tube under argon. The system was purged twice with 10 bar of CO/H₂ and then pressurized to 20 bar of CO/H₂.

References and notes

1. Herwig, J.; Bohnen, H.; Skutta, P.; Sturm, S.; Van Leeuwen, P. W. N. M.; Bronger, R.. PCY. Int. Appl. WO Patent 2002-EP1380, **2002** (to Celanese).
2. Teunissen, H. T.; Hansen, C. B.; Bickelhaupt, F. *Phosphorus, Sulfur Silicon Relat. Elem.* **1996**, *118*, 309.

UNIVERSITAT ROVIRA I VIRGILI
SWITCHABLE AND TUNABLE LIGANDS FOR HOMOGENEOUS CATALYSIS
Maria Dolores Segarra Maset
ISBN:978-84-693-7666-9/DL:T-1755-2010

PART II

SUPRAMOLECULAR, TUNABLE DIPHOSPHINES

UNIVERSITAT ROVIRA I VIRGILI
SWITCHABLE AND TUNABLE LIGANDS FOR HOMOGENEOUS CATALYSIS
Maria Dolores Segarra Maset
ISBN:978-84-693-7666-9/DL:T-1755-2010

CHAPTER 5

INTRODUCTION

Descriptors of diphosphines

In transition metal catalysis, the properties of the ligands have an enormous effect on the reactivity of metal complexes, and hence, on the activity and selectivity of the catalytic processes. Therefore, describing ligand properties and finding a relation between these descriptors and the results observed in the catalytic reaction are challenging tasks. After having achieved this, these meaningful descriptors can be used as a tool for the rational design of ligands. Although far from being accomplished for most of the reactions, several advances have been achieved since the initial efforts in the late 60s.^{1,2}

Usually, the descriptors used to define or classify ligands according to their properties can be classified roughly in two main categories: electronic and steric parameters.³

The systematic study of electronic properties of phosphine ligands was initiated by Tolman who introduced the so called Tolman's electronic parameter (χ).⁴⁻⁶ The phosphorus ligands were studied by looking at the electron donating or accepting properties of the P atom towards a metal, indirectly measured through the symmetric stretching frequency of the carbonyls in $\text{Ni}(\text{CO})_3\text{L}$. This measurement was based on the methodology developed some years earlier by Horrocks and Strohmeier.^{7,8} Several

other authors investigated the effect of phosphine basicity on metal complexes,^{9,10} simply by modifying the substituents on the phosphorus.

Steric effects of ligands have been studied more extensively, and in an effort to quantify steric properties of phosphines several parameters have been defined such as Tolman's *cone angle* (θ),^{4,11} the *solid angle*,¹² and the *pocket angle*.^{4,13}

Undoubtedly, for diphosphine ligands the most commonly used parameter is the *natural bite angle* (β_n) which was defined in 1990 by Casey and Whiteker as "the preferred chelation angle determined by ligand backbone constraints only and not by the valence angles of the metal" (Figure 5. 1).¹⁴ This definition is based on steric restrictions of the diphosphine, which are clearly more demanding than those of monophosphines, due to the presence of a backbone that places the two phosphorus atoms at a specific distance and relative orientation.

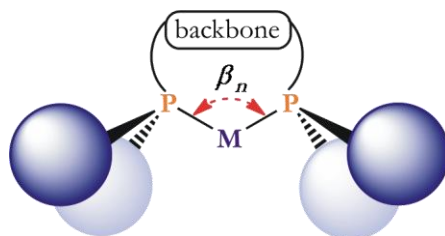


Figure 5. 1. Representation of the *natural bite angle* (β_n) for diphosphines.

The *natural bite angle* is calculated by using molecular mechanics. A dummy metal atom is used to direct the two lone pairs of the atoms to the dummy metal to simulate chelation (Figure 5. 2). As the *natural bite angle* was developed to justify effects on rhodium catalyzed hydroformylation, the M–P bond length is set at 2.315 Å, which is the typical distance found in crystal structures of Rh-phosphine complexes. Using this approach, a good correlation has been found between calculated *bite angles* and the trends of averaged values found in literature from crystal structures.¹⁵

Another important parameter related to the *natural bite angle*, also introduced by Casey, is the *flexibility range*. It is defined as the accessible range of P–M–P angles within less than 3 kcal mol⁻¹ excess strain energy from the energy minimum (located at the *natural bite angle*). Thus, using simple molecular mechanics, insight into the

preferred chelation angle and the rigidity of a diphosphine can be obtained. The next step is to find a correlation between the *bite angle* and the activity and selectivity of a catalytic process. This can be achieved examining the catalytic cycle, and studying how the diphosphine influences the transition states of the key steps of the mechanism. Concerning the *bite angle*, two different effects can be distinguished: the *steric bite angle effect* and the *electronic bite angle effect*.¹⁶ Sometimes one of them governs the reactivity of a given catalytic system, but the separate analysis of both contributions is rather complicated if not impossible. For example, while the regioselectivity in rhodium hydroformylation is controlled by *steric bite angle effects*, the activity is more related to *electronic bite angle effects*.

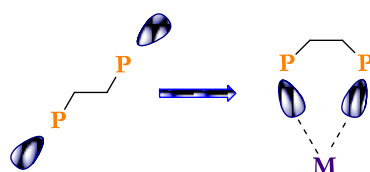


Figure 5. 2. Effect of the “dummy metal atom”.

To better understand these steric and electronic bite angle effects, two examples will be presented.

The *steric bite angle effect* can be studied in the rhodium catalyzed hydroformylation of alkenes. In several publications it was established that the use of wide *bite angle* diphosphines increased the regioselectivity towards the *linear* aldehyde.¹⁷ Later on, this effect was explained by the preferential formation of the *equatorial-equatorial (ee)* isomer compared to the *equatorial-axial (ea)* isomer (see 3.2.4) in the trigonal bipyramidal active species. This isomer distribution was found to favour the formation of the *linear* aldehyde. Diphosphines with a *natural bite angle* around 120° coordinate in an *ee* manner while diphosphines with smaller (about 90°) *bite angles* occupy *ea* sites. In order to enhance the coordination of the chelating ligand in an *ee* manner, a family of diphosphines based on a xanthene-related backbone was designed by van Leeuwen *et al.*¹⁸ These Xantphos ligands (Figure 5. 3) with rigid heteroaromatic skeletons presented *natural bite angle* values around 110–120°, which favoured the formation of the *ee* conformer.

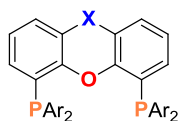


Figure 5. 3. Generic structure for the Xantphos type diphosphines.

It should be noted that the trigonal bipyramidal $\text{HRh}(\text{CO})_2(\text{PP})$ resting state is not directly involved in the key step that determines the regioselectivity of the catalytic event, as what really counts in the determination of the selectivity is the difference in the activation barriers of the insertion reaction leading to linear and branched products.¹⁸⁻²³ Nevertheless, the structure of the hydride resting state appears to be highly indicative of the steric hindrance brought about by the ligand in the transition state.

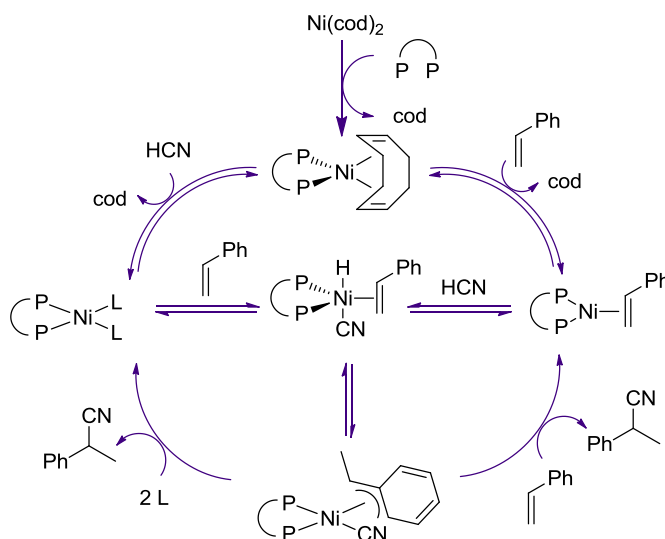
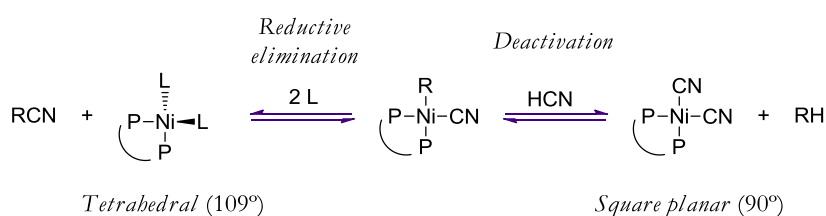


Figure 5. 4. Simplified catalytic cycle for styrene hydrocyanation.

The *electronic bite angle effect* is observed when due to phosphine *bite angle* restrictions, modifications are induced in the metal hybridization (forcing a specific coordination mode). To exemplify the *electronic bite angle effect*, the nickel catalyzed hydrocyanation can be considered. At industrial scale, DuPont commercialised the

double addition of HCN to butadiene for the production of adiponitrile (NC(CH₂)₄CN), a precursor of nylon-6,6 and polyurethanes.²⁴ However, this reaction is not very popular due to the high toxicity of HCN. Figure 5. 4 represents a simplified catalytic cycle for the hydrocyanation of styrene using diphosphines as ligands.

The rate determining step of this cycle is the reductive elimination that renders the desired alkyl cyanide. This reductive elimination generates a tetrahedral species that continues the catalytic cycle. In the presence of an excess of HCN, the reaction is in competition with a deactivation reaction that renders an inactive square planar species with two cyanides and the diphosphine (Scheme 5. 1).



Scheme 5. 1. Reductive elimination and deactivation competitive reactions in the nickel catalyzed hydrocyanation.

The activity of the reaction can be improved by using diphosphines with wide bite angles, which stabilize tetrahedral species with respect to square planar ones. This destabilization of square-planar intermediates accelerates reductive elimination. In particular, SiXantphos, with a *bite angle* of 105° turned out to be an outstanding ligand for this reaction, increasing the activity of the catalyst compared to diphosphines with preferred *bite angle* value far from 109°.^{25,26}

These two examples, chosen to illustrate *steric* and *electronic bite angle* effects, are permitted analysis of the two effects separately. Usually it is difficult to explain the behaviour of a catalytic system using only one of the extremes. For the rational design of ligands towards higher activities and selectivities, *electronic* and *steric bite angle* effects have to be considered together.^{27,28}

Biaryl based diphosphines

Several strategies have been developed to control and modify the *natural bite angle* of diphosphines. Among them, a smart approximation is the one developed by Zhang *et al.*, based on a biaryl backbone.²⁹ They used diphosphines carrying phosphorus donors in the 2,2' positions of the biaryl backbone. These diphosphines are susceptible to changes in the *bite angle* by slight modifications on the *dibedral angle* (θ) defined by the two aryl rings (Figure 5. 5). Csp²–Csp² rotation in these biaryl moieties causes only small energy changes within a wide range of *dibedral angles*.

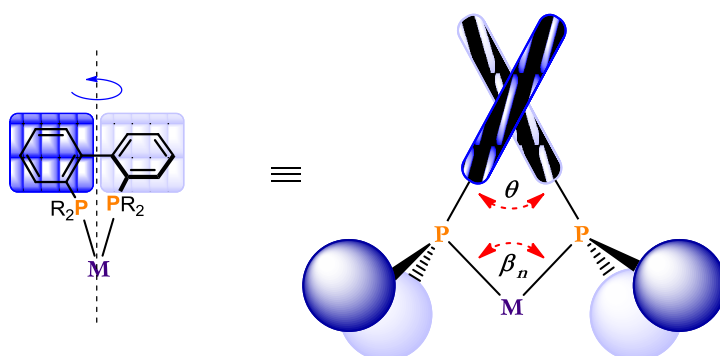


Figure 5. 5. Influence of the *dibedral angle* (θ) on the *bite angle* (β_n) in biaryl based diphosphines.

The control of the *dibedral angle* θ in this so-called TunaPhos (or TunePhos) family of diphosphines is achieved by introducing in the 6,6' positions of the biaryl an α - ω dioxyhydrocarbyl bridge. Each diphosphine has a different bridge length linking the biaryl groups (Figure 5. 6), and depending on the number of carbons (n), the *dibedral angle* of each ligand will be determined, which is reflected in their *natural bite angle* values. Furthermore, several attempts to correlate the *dibedral angle* and the *bite angle* were carried out by Zhang *et al.* using MM2 calculations.^{29,30}

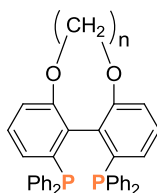


Figure 5. 6. Representation of the TunaPhos type diphosphines.

Tropos or atropos?

In addition to the possibility to modify the *bite angle* of the diphosphines based on this scaffold, biaryl backbones are very interesting due to the chiral *atropisomerism* inherent to the molecule.³¹ The existence of chirality due to an axial axis was first described by Christie and Kenner in 1922,³² although the term *atropisomerism* was introduced by Kuhn some years later when defining the restricted rotation around any single bond.^{33,34}



Figure 5. 7. Picture of the three sisters of destiny in Greek mythology. “A Golden Thread” by J. M. Strudwick, 1885, Tate Museum, London.

The word *tropos* comes from Greek mythology and it means “turn” (obviously, the “a” in *atropos* means “not”). *Atropos* derives its meaning from one of the three sisters that control the destiny of a person (Figure 5. 7): *Klotho*, *Lakbesis* and *Atropos* responsible for spinning the thread at the beginning of one’s life, measure the length, and cut the thread of one’s life, respectively. So *Atropos*, whose name means “she who

cannot be turned”, when applied to a molecule with an axial chiral axis refers to the restriction of the turn, blocking the interconversion of the enantiomers.³⁵

The rotation around the single bond that joins the two aromatic rings in the biaryl moiety is responsible for the existence of two *atropisomers*.³⁶ Oki defined that two conformers are recognized as *atropisomers*, *i.e.* physically separable species when, at a defined temperature, they have a half-life of at least 1000 s (which represents the following minimum free energy barrier at the respective temperatures: $\Delta G_{200\text{K}}^\ddagger = 61.6$ kJ mol⁻¹, $\Delta G_{300\text{K}}^\ddagger = 93.5$ kJ mol⁻¹, $\Delta G_{350\text{K}}^\ddagger = 109$ kJ mol⁻¹). The energy barrier to convert one substituted biaryl *atropisomer* into the other depends on several factors: the temperature, the substitution on carbons adjacent to the axial bond, the existence of bridges (and its rigidity) between the two aromatic moieties, and external stimuli (for example, photochemical induction).^{37–42} When the energy of interconversion is low enough as to make the enantiomer separation impracticable, the system presents a *tropos* nature (the complete turn around the single Csp²–Csp² bond is not restricted). On the other hand, when the two atropisomeric forms can be isolated separately, they present an *atropos* nature (the turn now is restricted).

When two substituents are located in the *ortho* 2,2' position of the biphenyl moiety, *atropisomerism* is only observed if both groups are bulky enough to restrict the rotation (for example, molecule **A** in Figure 5. 8, where $\Delta G_{332\text{K}}^\ddagger = 109$ kJ mol⁻¹).⁴³

A different possibility to obtain an *atropos* biphenyl due to steric effects of the substituents, is to have the substitution of three bulky groups in the *ortho* positions to the biaryl bond (*i.e.*, 2,2' and 6 positions) are necessary. For example, molecule **B** in Figure 5. 8 presents a $\Delta G_{383\text{K}}^\ddagger = 125$ kJ mol⁻¹,^{34,44} but also the bulkiness of the substituents determines the possible racemization between the isomers.

An additional option to obtain *atropisomers* is the substitution at the 2,2' and 3,3' positions. If the substituents in the *meta* positions are sufficiently bulky, it is possible to achieve restricted rotation of the biphenyl by the so-called *buttressing effect*.^{45,46} For example, in molecule **C** of Figure 5. 8 the rotation of the molecule costs more energy when the substituent in *meta* position is an iodine atom ($\Delta G_{298\text{K}}^\ddagger = 126$ kJ mol⁻¹) instead of a hydrogen atom ($\Delta G_{298\text{K}}^\ddagger = 98$ kJ mol⁻¹).^{34,47}

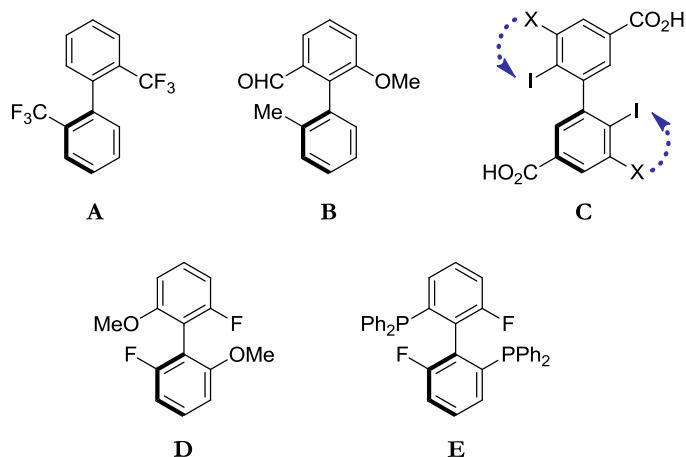


Figure 5. 8. Different substitution patterns to achieve an *atropis* biaryl molecule.

The best way to ensure an *atropis* biaryl system is to functionalize the biphenyl moiety in both the 2,2' and the 6,6' positions. For instance, molecule **D**, depicted in Figure 5. 8, shows a $\Delta G^{\ddagger}_{298\text{K}} = 66.9 \text{ kJ mol}^{-1}$,⁴⁸ and diphosphine **E** (Figure 5. 8) has a rotational barrier of $\Delta G^{\ddagger}_{483\text{K}} > 146 \text{ kJ mol}^{-1}$.⁴⁹

Atropisomerism to construct chiral diphosphines

Several approaches have been developed to take benefit of the *atropis* nature of substituted biaryls to construct chiral phosphorus ligands. For example the *buttressing effect* strategy was applied by Müller *et al.* to obtain chiral phosphinines. The calculated rotational barrier for the ligand depicted in Figure 5. 9 was found to be $\Delta G^{\ddagger}_{298\text{K}} = 116 \text{ kJ mol}^{-1}$.⁵⁰

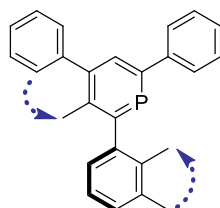
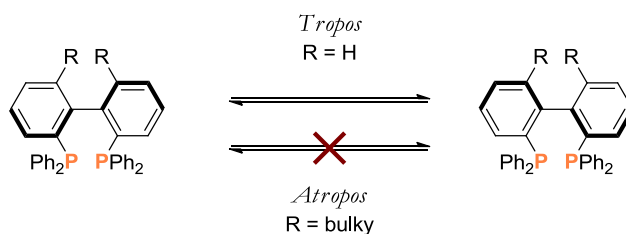


Figure 5. 9. Chiral phosphinine developed by Müller *et al.*

The simplest diphosphine based on biaryl skeleton is 2,2'-bis(diphenylphosphino)biphenyl (Biphep, R = H, Scheme 5. 2), which presents a $\Delta G^\ddagger_{398K} = 89.0 \text{ kJ mol}^{-1}$.⁴⁹ This means that Biphep, although the separate *atropoisomers* can be isolated at low temperature, they will racemize with a half-life time at room temperature of approximately 900 s.

Some options to obtain chiral ligands are the use of substituents in 6,6'-positions (Scheme 5. 2) or the introduction of a bridge between the two aromatic moieties to restrict the rotation and differentiate the two *atropoisomers*.



Scheme 5. 2. *Atropisomerism* of biphenyl diphosphines.

In the next paragraphs, some examples that make use of the biaryl *atropisomerism* to construct chiral ligands and their application will be discussed.

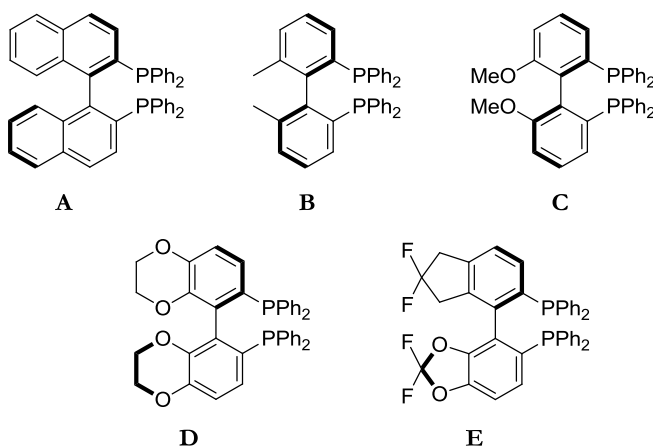
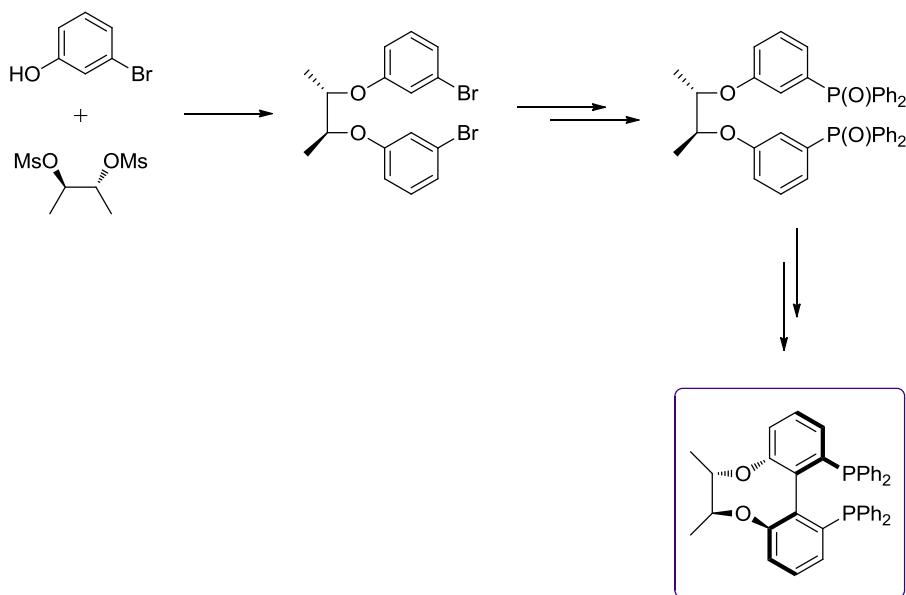


Figure 5. 10. Some chiral *atropis* diphosphines: **(A)** (R)-BINAP; **(B)** (R)-BIPHEMP; **(C)** (R)-MeO-BIPHEP; **(D)** (R)-SYNPHOS and **(E)** (R)-DIFLUORPHOS.

As mentioned before, the restriction between the two *atropisomers* can be achieved by introducing a substituent in the 6,6' position of the biaryl diphosphine scaffold. Some examples found in literature make use of just a methyl or methoxy group (Figure 5. 10),⁵¹⁻⁵⁵ but also aromatic rings can be employed, as in BINAP based on a binaphthyl backbone (Figure 5. 10). BINAP turned out to be very useful in many asymmetric catalytic reactions and it forms the basis for the construction of numerous chiral ligands.^{56,57}



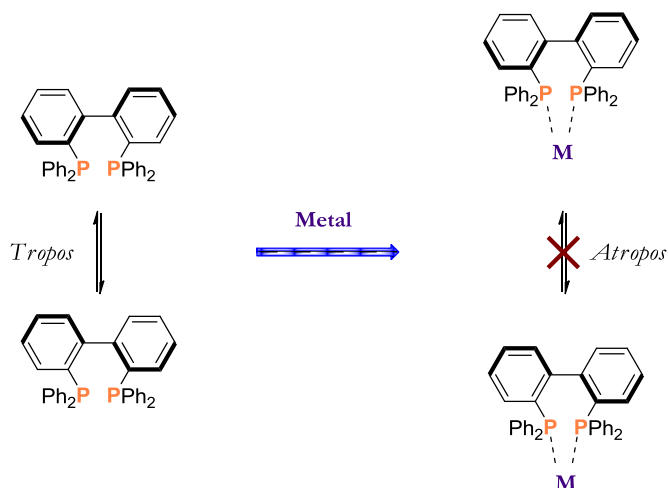
Scheme 5. 3. Simplified diastereoselective synthesis of a chiral *atropis* diphosphine.

Another strategy that has been already mentioned in this chapter is the use of a bridge as an additional linker between the two aryl units to restrict the rotation (TunaPhos). The isolation of one of the *atropisomers* is achieved by converting them to diastereoisomers (separable by precipitation) via metal coordination with the aid of an enantiopure co-ligand (usually diamine).⁵² After decoordination, the enantiopure *atropisomer* can be functionalized with a bridge to fix the Csp²-Csp² rotation. When different carbon bridge length are used, the dihedral angle also changes, and some authors studied how these variations affect to the enantioselectivity results in

asymmetric reactions.^{29,30,58,59}

Several authors used chiral carbon bridges.⁶⁰ If the bridge is used in an enantiopure form, also two different diastereoisomers can be generated. A smart strategy has been developed to synthesize one the products diastereoselectively as the Csp²–Csp² single bond is generated with the chiral bridge already present in the molecule. Using this methodology, one of the two *atropisomers* can be obtained selectively (Scheme 5. 3).^{61–65}

The examples described until now, include the bulky substituent or the bridge in the 6,6' position of the biaryl skeleton. Alternatively, the restriction of the rotation can also be achieved via the phosphorus atoms, *viz.* by coordinating to a metal centre (Scheme 5. 4).

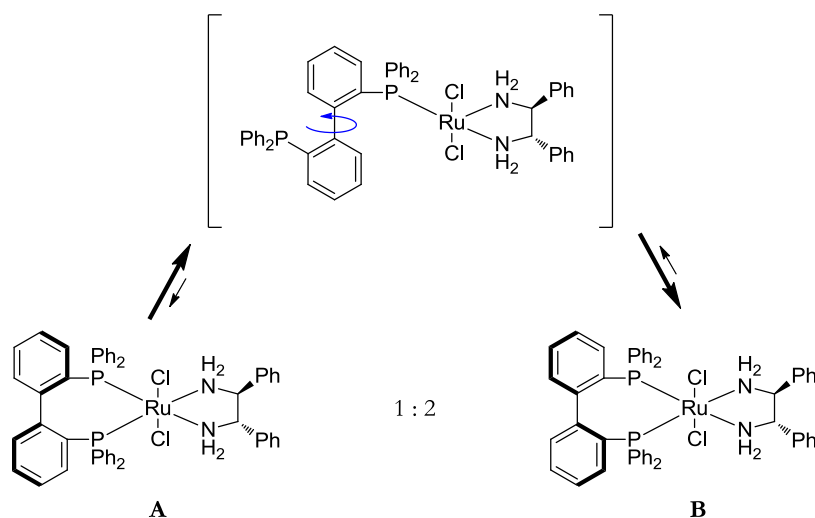


Scheme 5. 4. Generation of the two *atropis* enantiomers by metal coordination.

If an additional chiral ligand is introduced in such complexes, then diastereoisomers are generated (as mentioned before). One option is to use chiral and enantiopure co-ligands coordinated to the same metal. The analysis described before for the chiral bridge also applies in this case; two different diastereoisomers can be obtained. The use of chiral diamines as co-ligand is common in ruthenium-diphosphine complexes for asymmetric hydrogenation. The enantiopure diamine coordinates to the metal that is already coordinated to the biaryl diphosphine, and

two *atropodiastereoisomers* can be distinguished, which are interconverted via metal decoordination and further turn around the biaryl bond, as all the steps involved are in equilibrium (Scheme 5. 5).⁶⁶ A good chiral induction from the diamine to the biaryl diphosphine moiety may be achieved when one of the diastereoisomers is markedly more stable than the other.⁶⁷⁻⁶⁹

An alternative manner to transmit chirality to the *tropos* biaryl moiety was explored by Leitner *et al.* They successfully combined a biaryl type diphosphine with chiral ionic liquids (cILs), based on amino acid cations. They tested these systems in rhodium-catalyzed asymmetric hydrogenation.⁷⁰ The same authors were able to improve the enantiomeric excess results by using cILs with a racemic mixture of the *atropos* BINAP!⁷¹ This strategy has a major drawback in that the source of chirality is the solvent, and this is certainly not economically viable at a large scale.



Scheme 5. 5. Equilibrium of isomerization of the *atropodiastereoisomers*: **(A)** [(*R*)-biphep-Ru-(*S,S*)-dpen] and **(B)** [(*S*)-biphep-Ru-(*S,S*)-dpen].

Recently, Vidal-Ferran *et al.* reported the formation of a supramolecular complex that combines a *tropos* biphenol with a chiral diamine.⁷² The hydrogen bond formation between the amine moieties and the alcohols allows the generation of diastereomerically enriched supramolecular complexes. Depending on the substituents

of the chiral source the variations in the effectiveness of the chiral induction on the biaryl was studied.

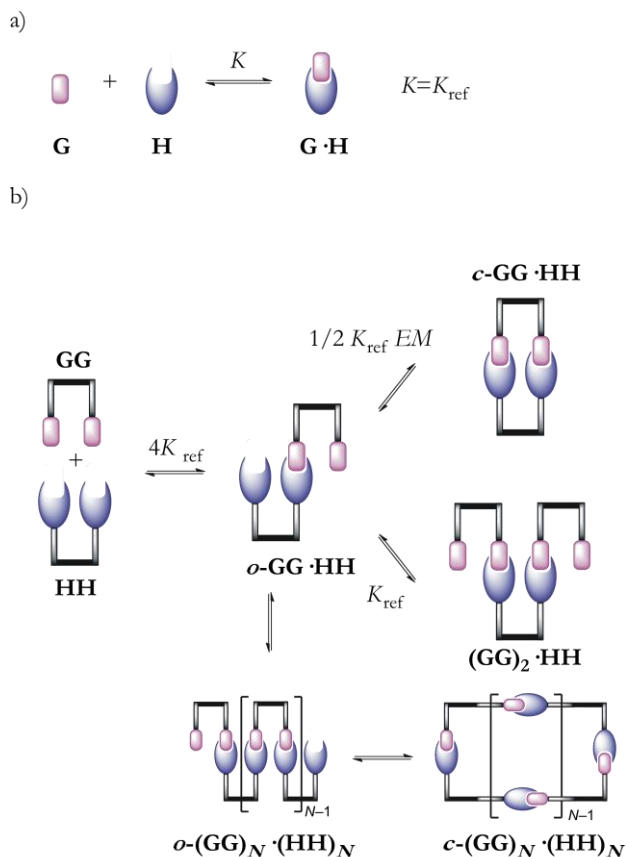
Simultaneously to Vidal-Ferran *et al.*, and following a similar approach, we developed the project explained in part II of this thesis, which involves the use of supramolecular interactions to induce chirality in a *tropos* biaryl diphosphine. To facilitate the discussion, a few concepts about supramolecular chemistry will be introduced first.

A glance at supramolecular concepts

Supramolecular chemistry is a relatively young field that is highly interdisciplinary. It covers the chemical, physical and biological features of the chemical entities of greater complexity than molecules themselves. These supramolecular entities are held together and organized by means of intermolecular (and intramolecular) non-covalent binding interactions.^{73,74} Various types of interactions may be distinguished, that present different degrees of strength and directionality: metal-ligand coordination (which can reach a strength of several hundreds of kJ mol^{-1}), electrostatic forces (from 100 to 500 kJ mol^{-1}), hydrogen bonding (from 15 up to 120 kJ mol^{-1}), van der Waals interactions (up to 30 kJ mol^{-1}), etc. Thus, their strengths range from weak or moderate as in hydrogen bonds, to strong or very strong for metal-ligand coordination.⁷⁵

Nature makes use of supramolecular interactions to build its structures and to drive the processes occurring in living organisms. These complicated structures are governed by specific interactions that enable the unique result “desired by nature” and do not allow misunderstandings in the processes.

In recent years, many efforts have been employed to design synthetic molecular receptors inspired by motifs found in nature. Pursuing stabilities and specificities similar to the ones encountered in natural assemblies, multiple binding sites in the host are used to recognize the counterparts in the guest and generate self-assembled structures.^{76–78} To characterize and define these systems, two terms are crucial: *multivalency* and *effective molarity*.



Scheme 5. 6. Schematic representation of the possible equilibria involved in
 a) a monovalent system; b) a divalent system.

The concept *multivalency* refers to the simultaneous interaction between multiple functionalities on one entity and complementary functionalities on another entity.^{79,80} Therefore, the valency of an entity is the number of separate connections that it can form through host-guest interactions between entities bearing the complementary functionalities. In this part II of the thesis divalent complexes are studied, *i.e.*, the self-assembly of well defined complexes whose dissociation requires the cleavage of two interactions. Depending on the size and the shape of the two entities involved, not only discrete structures, but also aggregates and polymeric species can be generated (Scheme 5. 6, b).

To quantify and predict the behaviour of such molecules one makes use of the *effective molarity* (EM).^{81,82}

When considering the model of two entities with two complementary binding sites (Scheme 5. 6, b)⁸³ the first intermolecular interaction will occur with the same strength as that between two monovalent species forming the “open” complex $\sigma\text{-GG}\cdot\text{HH}$. The second interaction can be treated as an intramolecular interaction (to form a discrete dimeric species, the “closed” complex $\epsilon\text{-GG}\cdot\text{HH}$) or as an intermolecular interaction (to form polymeric species $(\text{GG})_2\cdot\text{HH}$, $(\text{GG})_2\cdot(\text{HH})_2$, $\text{GG}\cdot(\text{HH})_2$, etc). In that case, the EM , defined in Eq. 5.1-5.2, reflects the advantage of an intramolecular interaction over the analogous intermolecular interaction, *i. e.*, the preferential formation of $\epsilon\text{-GG}\cdot\text{HH}$ versus $\sigma\text{-GG}\cdot\text{HH}$.

To estimate some data, one can consider a binding model consisting of only one binding site (Scheme 5. 6, a). The value of the association constant K of such system can be measured by conventional tools.⁷⁵ This K value will serve as a reference constant K_{ref} for the first intermolecular association of the two molecules. As a first approximation, the prediction of the overall stability of a divalent bimolecular system can be estimated as the sum of the individual interactions. If a deviation of the experimental result from the estimated one is observed, it is concluded that the system presents *cooperativity*. The *cooperativity* can be negative, if the first interaction disfavors the second; or positive, when the first interaction favors the next one. *Cooperativity* effects are well known in biochemistry,⁸⁴ and the most studied system is oxygen binding at haemoglobin.^{85,86} The concept has also been applied in artificial supramolecular systems and then each case has to be studied as each one will have its own properties,⁸⁷⁻⁹⁰ for example in self-assembly systems.⁹¹ However, a few general remarks can be developed.⁸³

$$EM = K_{\text{intra}} / K_{\text{inter}} \quad \text{Eq. 5.1}$$

$$\frac{1}{2} KEM = [\epsilon\text{-GG}\cdot\text{HH}] / [\sigma\text{-GG}\cdot\text{HH}] \quad \text{Eq. 5.2}$$

Desolvation is also an important phenomenon that must be taken into account when treating supramolecular interactions. In particular, this has been studied to

predict the apparent strength of hydrogen bonding interactions. To form an aggregate between two molecules in solution, one with a H-donor functional group (HD) and the other one with a H-acceptor group (A), first, one must break the interactions between the solutes and the solvent (Figure 5. 11). Using the approach developed by Hunter, it is possible to predict the magnitude of a hydrogen bond between a donor-acceptor couple by calculating first the free energy of hydrogen bonding interactions ($\Delta\Delta G_{\text{H-bond}}$) in the solvent. In Eq. 5.6, α and β are H-bond donor and H-bond acceptor constants for the solute molecules, and α_s and β_s are the same parameters for the solvent.⁹²

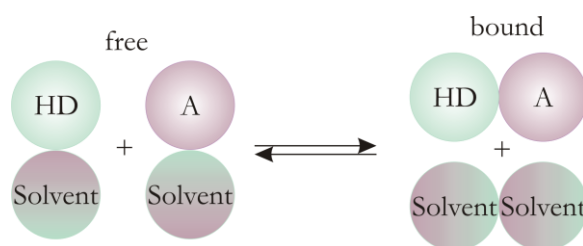


Figure 5. 11. Schematic representation of the equilibrium of formation of a complex between a H-donor and H-acceptor functionalized groups in solution. It involves the competition between solute-solute, solvent-solvent and solute-solvent interactions.

$$\Delta\Delta G_{\text{H-Bond}} = -(\alpha\beta + \alpha_s\beta_s) + (\alpha\beta_s + \alpha_s\beta) = -(\alpha - \alpha_s)(\beta - \beta_s) \quad \text{Eq. 5.3}$$

$$\log K = -(\Delta\Delta G_{\text{H-Bond}} + 6) / RT \quad \text{Eq. 5.4}$$

Thus the hydrogen bond free energy depends strongly on the solvent used. The values for α and β parameters have to be determined experimentally for each solvent. These values can serve as theoretical model and then one is able to predict the strength of the hydrogen bonds in different solvents.⁹²

General objectives of Part II

The aim of Part II is to make use of supramolecular interactions as a means to influence the axial chirality of biaryl *tropos* diphosphines. Apart from the phosphorus

atoms in positions 1,1', the biaryl backbone will include functional groups in the structure (suit)able to establish supramolecular interactions.

This substitution must not concern the 6,6' positions but the 5,5' positions, in order to have a prochiral *tropos* molecule.

Several chiral modifiers containing complementary functional groups will be explored in our search for an effective transmission of the chirality from the chiral modifiers to the diphosphines and eventually to the catalytic system.

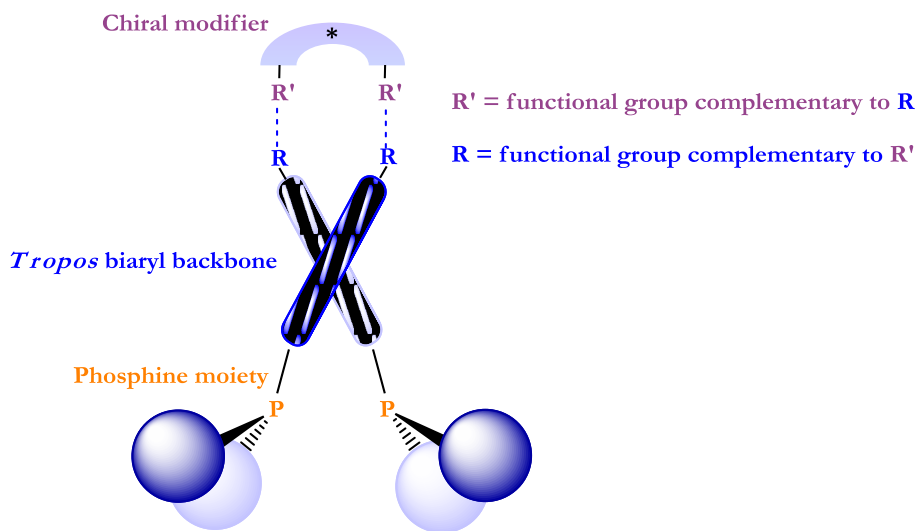


Figure 5. 12. Conceptual idea of the design of a tunable supramolecular system.

References and notes

1. Graham, W. A. G. *Inorg. Chem.* **1968**, *7*, 315.
2. Stewart, R. P.; Treichel, P. M. *Inorg. Chem.* **1968**, *7*, 1942.
3. van Leeuwen, P. W. N. M.; Freixa, Z.; Zuidema, E. *Phosphorus Ligands in Asymmetric Catalysis* **2008**, *3*, 1433.
4. Tolman, C. A. *Chem. Rev.* **1977**, *77*, 313.
5. Tolman, C. A. *J. Am. Chem. Soc.* **1970**, *92*, 2953.
6. Tolman, C. A. *J. Am. Chem. Soc.* **1970**, *92*, 2956.
7. Horrocks, W. D.; Taylor, R. C. *Inorg. Chem.* **1963**, *2*, 723.
8. Strohmeier, W.; Muller, F. J. *Chem. Ber.* **1967**, *100*, 2812.
9. Drago, R. S.; Joerg, S. J. *Am. Chem. Soc.* **1996**, *118*, 2654.
10. Joerg, S.; Drago, R. S.; Sales, J. *Organometallics* **1998**, *17*, 589.
11. Tolman, C. A.; Seidel, W. C.; Gosser, L. W. J. *Am. Chem. Soc.* **1974**, *96*, 53.
12. White, D.; Taverner, B. C.; Coville, N. J.; Wade, P. W. J. *Organomet. Chem.* **1995**, *495*, 41.
13. Koide, Y.; Bott, S. G.; Barron, A. R. *Organometallics* **1996**, *15*, 2213.
14. Casey, C. P.; Whiteker, G. T. *Isr. J. Chem.* **1990**, *30*, 299.
15. Dierkes, P.; van Leeuwen, P. W. N. M. *J. Chem. Soc., Dalton Trans.* **1999**, 1519.
16. Freixa, Z.; Van Leeuwen, P. W. N. M. *Dalton Trans.* **2003**, 1890.
17. Casey, C. P.; Whiteker, G. T.; Melville, M. G.; Petrovich, L. M.; Gavney, J. A., Jr.; Powell, D. R. *J. Am. Chem. Soc.* **1992**, *114*, 5535.
18. Kranenburg, M.; van der Burgt, Y. E. M.; Kamer, P. C. J.; van Leeuwen, P. W. N. M.; Goubitz, K.; Fraanje, J. *Organometallics* **1995**, *14*, 3081.
19. Casey, C. P.; Paulsen, E. L.; Beuttenmueller, E. W.; Proft, B. R.; Petrovich, L. M.; Matter, B. A.; Powell, D. R. *J. Am. Chem. Soc.* **1997**, *119*, 11817.
20. Van der Veen, L. A.; Boele, M. D. K.; Bregman, F. R.; Kamer, P. C. J.; Van Leeuwen, P. W. N. M.; Goubitz, K.; Fraanje, J.; Schenk, H.; Bo, C. J. *Am. Chem. Soc.* **1998**, *120*, 11616.
21. Van der Veen, L. A.; Keeven, P. H.; Schoemaker, G. C.; Reek, J. N. H.; Kamer, P. C. J.; Van Leeuwen, P. W. N. M.; Lutz, M.; Spek, A. L. *Organometallics* **2000**, *19*, 872.
22. Kamer, P. C. J.; van Leeuwen, P. W. N. M.; Reek, J. N. H. *Acc. Chem. Res.* **2001**, *34*, 895.
23. van der Veen, L. A.; Kamer, P. C. J.; van Leeuwen, P. W. N. M. *Cattech* **2002**, *6*, 116.
24. van Leeuwen, P. W. N. M. *Homogeneous Catalysis: Understanding the Art*; Kluwer Academic Publishers, **2004**.
25. Kranenburg, M.; Kamer, P. C. J.; van Leeuwen, P. W. N. M.; Vogt, D.; Keim, W. J. *Chem. Soc., Chem. Commun.* **1995**, 2177.
26. Goertz, W.; Keim, W.; Vogt, D.; Englert, U.; Boele, M. D. K.; van der Veen, L. A.; Kamer, P. C. J.; van Leeuwen, P. W. N. M. *J. Chem. Soc., Dalton Trans.* **1998**, 2981.
27. Oswald, A. A.; Hendriksen, D. E.; Kastrup, R. V.; Mozeleski, E. J. *Adv. Chem. Ser.* **1992**, 395.
28. Gillespie, J. A.; Dodds, D. L.; Kamer, P. C. J. *Dalton Trans.* **2010**, *39*, 2751.

29. Zhang, Z.; Qian, H.; Longmire, J.; Zhang, X. *J. Org. Chem.* **2000**, *65*, 6223.
30. Raghunath, M.; Zhang, X. M. *Tetrahedron Lett.* **2005**, *46*, 8213.
31. Adams, R.; Yuan, H. C. *Chem. Rev.* **1933**, *12*, 261.
32. Christie, G. H.; Kenner, J. J. *Chem. Soc.* **1922**, *121*, 614.
33. Kuhn, R. In *Stereochemie*; K. Freudenberg: **1933**, p 803.
34. Bringmann, G.; Mortimer, A. J. P.; Keller, P. A.; Gresser, M. J.; Garner, J.; Breuning, M. *Angew. Chem., Int. Ed.* **2005**, *44*, 5384.
35. Mikami, K.; Aikawa, K.; Yusa, Y.; Jodry, J. J.; Yamanaka, M. *Synlett* **2002**, 1561.
36. Oki, M. *Top. Stereochem.* **1983**, *14*, 1.
37. Hall, D. M.; Harris, M. M. *J. Chem. Soc.* **1960**, 490.
38. Bott, G.; Field, L. D.; Sternhell, S. *J. Am. Chem. Soc.* **1980**, *102*, 5618.
39. Grein, F. *J. Phys. Chem. A* **2002**, *106*, 3823.
40. Leroux, F. *ChemBioChem* **2004**, *5*, 644.
41. Oki, M.; Yamamoto, G. *Bull. Chem. Soc. Jpn.* **1971**, *44*, 266.
42. Mazzanti, A.; Lunazzi, L.; Minzoni, M.; Anderson, J. E. *J. Org. Chem.* **2006**, *71*, 5474.
43. Wolf, C.; Konig, W. A.; Roussel, C. *Liebigs Ann.* **1995**, 781.
44. Meyers, A. I.; Himmelsbach, R. J. *J. Am. Chem. Soc.* **1985**, *107*, 682.
45. Chien, S. L.; Adams, R. *J. Am. Chem. Soc.* **1934**, *56*, 1787.
46. Theilack, W.; Bohm, H. *Angew. Chem., Int. Ed.* **1967**, *6*, 251.
47. Rieger, M.; Westheimer, F. H. *J. Am. Chem. Soc.* **1950**, *72*, 19.
48. Hasaka, N.; Okigawa, M.; Kouno, I.; Kawano, N. *Bull. Chem. Soc. Jpn.* **1982**, *55*, 3828.
49. Desponds, O.; Schlosser, M. *Tetrahedron Lett.* **1996**, *37*, 47.
50. Mueller, C.; Pidko, E. A.; Totev, D.; Lutz, M.; Spek, A. L.; van Santen, R. A.; Vogt, D. *Dalton Trans.* **2007**, 5372.
51. Saito, T.; Yokozawa, T.; Ishizaki, T.; Moroi, T.; Sayo, N.; Miura, T.; Kumobayashi, H. *Adv. Synth. Catal.* **2001**, *343*, 264.
52. Schmid, R.; Cereghetti, M.; Heiser, B.; Schonholzer, P.; Hansen, H. J. *Helv. Chim. Acta* **1988**, *71*, 897.
53. Schmid, R.; Foricher, J.; Cereghetti, M.; Schonholzer, P. *Helv. Chim. Acta* **1991**, *74*, 370.
54. Schmid, R.; Broger, E. A.; Cereghetti, M.; Cramer, Y.; Foricher, J.; Lalonde, M.; Muller, R. K.; Scalone, M.; Schoettel, G.; Zutter, U. *Pure Appl. Chem.* **1996**, *68*, 131.
55. Jeulin, S.; de Paule, S. D.; Ratovelomanana-Vidal, V.; Genet, J. P.; Champion, N.; Dellis, P. *Proc. Natl. Acad. Sci. U. S. A.* **2004**, *101*, 5799.
56. Miyashita, A.; Takaya, H.; Souchi, T.; Noyori, R. *Tetrahedron* **1984**, *40*, 1245.
57. Noyori, R. *Angew. Chem., Int. Ed.* **2002**, *41*, 2008.
58. Wu, S.; Wang, W.; Tang, W.; Lin, M.; Zhang, X. *Org. Lett.* **2002**, *4*, 4495.
59. Lei, A. W.; He, M. S.; Wu, S. L.; Zhang, X. M. *Angew. Chem., Int. Ed.* **2002**, *41*, 3457.
60. Zou, Y. P.; Geng, H. L.; Zhang, W. C.; Yu, S. C.; Zhang, X. M. *Tetrahedron Lett.* **2009**, *50*, 5777.
61. Qiu, L.; Wu, J.; Chan, S.; Au-Yeung, T. T. L.; Ji, J.-X.; Guo, R.; Pai, C.-C.; Zhou, Z.; Li, X.; Fan, Q.-H.; Chan, A. S. C. *Proc. Natl. Acad. Sci. U. S. A.* **2004**, *101*, 5815.

62. Sun, X. F.; Li, W.; Hou, G. H.; Zhou, L.; Zhang, X. M. *Adv. Synth. Catal.* **2009**, *351*, 2553.
63. Wang, C. J.; Wang, C. B.; Chen, D.; Yang, G. F.; Wu, Z. S.; Zhang, X. M. *Tetrahedron Lett.* **2009**, *50*, 1038.
64. Sun, X. F.; Zhou, L.; Li, W.; Zhang, X. M. *J. Org. Chem.* **2008**, *73*, 1143.
65. Qiu, L.; Kwong, F. Y.; Wu, J.; Lam, W. H.; Chan, S.; Yu, W.-Y.; Li, Y.-M.; Guo, R.; Zhou, Z.; Chan, A. S. C. *J. Am. Chem. Soc.* **2006**, *128*, 5955.
66. Tudor, M. D.; Becker, J. J.; White, P. S.; Gagne, M. R. *Organometallics* **2000**, *19*, 4376.
67. Aikawa, K.; Mikami, K. *Angew. Chem., Int. Ed.* **2003**, *42*, 5455.
68. Mikami, K.; Aikawa, K.; Yusa, Y.; Hatano, M. *Org. Lett.* **2002**, *4*, 91.
69. Mikami, K.; Kakuno, H.; Aikawa, K. *Angew. Chem., Int. Ed.* **2005**, *44*, 7257.
70. Schmitkamp, M.; Chen, D.; Leitner, W.; Klankermayer, J.; Francio, G. *Chem. Commun.* **2007**, 4012.
71. Chen, D. J.; Schmitkamp, M.; Francio, G.; Klankermayer, J.; Leitner, W. *Angew. Chem., Int. Ed.* **2008**, *47*, 7339.
72. Etxebarria, J.; Degenbeck, H.; Felten, A. S.; Serres, S.; Nieto, N.; Vidal-Ferran, A. *J. Org. Chem.* **2009**, *74*, 8794.
73. Lehn, J. M. *Science* **1993**, *260*, 1762.
74. Lehn, J. M. *Proc. Natl. Acad. Sci. U. S. A.* **2002**, *99*, 4763.
75. Schalley, C.; Editor *Analytical Methods in Supramolecular Chemistry*; Wiley-VCH, **2007**.
76. Whitesides, G. M.; Mathias, J. P.; Seto, C. T. *Science* **1991**, *254*, 1312.
77. Lindsey, J. S. *New J. Chem.* **1991**, *15*, 153.
78. Philp, D.; Stoddart, J. F. *Angew. Chem., Int. Ed.* **1996**, *35*, 1155.
79. Mulder, A.; Huskens, J.; Reinhoudt, D. N. *Org. Biomol. Chem.* **2004**, *2*, 3409.
80. Mammen, M.; Choi, S. K.; Whitesides, G. M. *Angew. Chem., Int. Ed.* **1998**, *37*, 2755.
81. Mazor, M. H.; Wong, C. F.; Mccammon, J. A.; Deutch, J. M.; Whitesides, G. J. *Phys. Chem.* **1990**, *94*, 3807.
82. Cacciapaglia, R.; Di Stefano, S.; Mandolini, L. *Acc. Chem. Res.* **2004**, *37*, 113.
83. Hunter, C. A.; Anderson, H. L. *Angew. Chem., Int. Ed.* **2009**, *48*, 7488.
84. Whitty, A. *Nat. Chem. Biol.* **2008**, *4*, 435.
85. Perutz, M. F. *Q. Rev. Biophys.* **1989**, *22*, 139.
86. Eaton, W. A.; Henry, E. R.; Hofrichter, J.; Mozzarelli, A. *Nature Structural Biology* **1999**, *6*, 351.
87. Badjic, J. D.; Nelson, A.; Cantrill, S. J.; Turnbull, W. B.; Stoddart, J. F. *Acc. Chem. Res.* **2005**, *38*, 723.
88. Camara-Campos, A.; Hunter, C. A.; Tomas, S. *Proc. Natl. Acad. Sci. U. S. A.* **2006**, *103*, 3034.
89. Chekmeneva, E.; Hunter, C. A.; Packer, M. J.; Turega, S. M. *J. Am. Chem. Soc.* **2008**, *130*, 17718.
90. Hunter, C. A.; Ihekwaba, N.; Misuraca, M. C.; Segarra-Maset, M. D.; Turega, S. M. *Chem. Commun.* **2009**, 3964.
91. Ercolani, G. *J. Am. Chem. Soc.* **2003**, *125*, 16097.
92. Hunter, C. A. *Angew. Chem., Int. Ed.* **2004**, *43*, 5310.

UNIVERSITAT ROVIRA I VIRGILI
SWITCHABLE AND TUNABLE LIGANDS FOR HOMOGENEOUS CATALYSIS
Maria Dolores Segarra Maset
ISBN:978-84-693-7666-9/DL:T-1755-2010

CHAPTER 6

RESULTS AND DISCUSSION

6.1. INTRODUCTION AND OBJECTIVES

As mentioned in chapter 5, the aim of this part II is to make use of non covalent interactions to induce chirality to a biaryl diphosphine, and then apply this system in asymmetric catalysis. To achieve this goal, we will synthesize functionalized *tropos* biaryl diphosphines to be used as a receptor of chiral modifiers. Consequently, the biaryl backbone will include functional groups able to interact with complementary ones present in the chiral modifiers. Several supramolecular interactions can be used to construct this system.¹ Two approaches have been considered to form the supramolecular complex: one based on hydrogen bonds and another one that uses ionic interactions.

Both approaches have their own advantages and drawbacks. Hydrogen bonds are weaker than ionic interactions, but they provide high directionality due to the pairing of the orbitals between the H-donor and the H-acceptor. The ionic interaction, although being stronger, lacks the directionality, which hampers the design of sophisticated, predictable systems.

Among the possible functional groups for the construction of the supramolecular complexes via hydrogen bonds and ionic forces, the ones selected for this study are schematized in Figure 6. 1 and summarized in Table 6. 1.

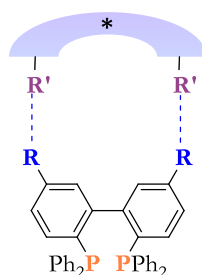


Figure 6. 1. Supramolecular chiral diphosphines constructed from functionalized biaryl backbones and chiral modifiers.

Table 6. 1. Functional groups considered for the design of the supramolecular diphosphines.

Entry	R	R'	Supramolecular interaction
1	- NH ₂		
2		- COOH	Hydrogen bond
3			
4	- SO ₃ ⁻	- NH ₃ ⁺	Ionic

The use of ionic interactions for the construction of supramolecular diphosphines has been successfully explored by our group in the past.²

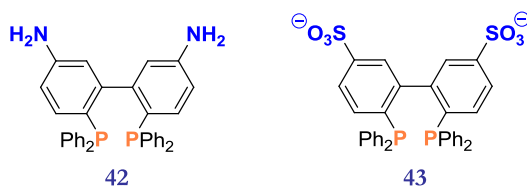


Figure 6. 2. Bis-amino and bis-sulfonate biaryl diphosphines.

The simplest interactions considered are the ones displayed in entries 1 and 4 of Table 6. 1 (the ones in entries 2 and 3 can be considered as derivatives of 1).

Accordingly, only biaryl diphosphines including amine (42) and sulfonate (43) groups will be considered initially (Figure 6. 2).

After the synthesis of the target phosphines, several modifiers (chiral inductors) will be considered to obtain insight in the affinity between the two fragments of the complexes. The modifiers envisaged to interact with diphosphine 42, through hydrogen bonds can be dicarboxylic acids, acquired from commercial sources. The diammonium salts necessary to interact with diphosphine 43 can be easily obtained from the parent diamines. The diamines also can be commercially available ones, or obtained from modifications of backbones that were synthesized before in our group. For instance, the diamine that renders diammonium 46, is derived from the SPAN backbone.³ The diammonium moieties used are presented in Figure 6. 3.

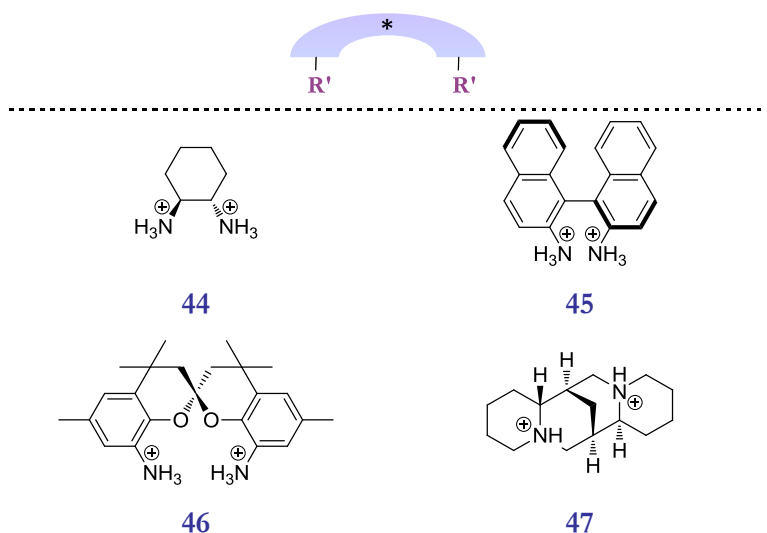


Figure 6. 3. Diammonium cations conceived as chiral modifiers of sulfonate diphosphine 43.

The determination of binding constants is usually not performed under inert conditions, which can be a handicap because phosphines oxidize easily in solution in presence of oxygen. For that reason, the initial evaluation of binding constants will be done using the phosphine precursors, instead of the oxygen sensitive ligands.

Finally, we will study the performance of the supramolecular assembly as a ligand

in asymmetric catalysis. The results will corroborate if there is an effective chiral induction from the modifier to the *tropos* diphosphines. The reaction chosen to evaluate the activity and enantioinduction is the asymmetric hydrogenation of dimethyl itaconate.

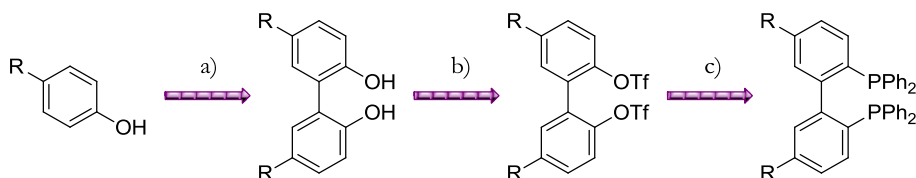
6.2. RESULTS AND DISCUSSION

6.2.1. SYNTHESIS OF THE FUNCTIONALIZED BIARYL PHOSPHINES

Initially, the retrosynthesis proposed for compounds **42** and **43** was inspired by the one reported by Genêt⁴ and Lemaire⁵ for the synthesis of chiral binaphthyl amine derivatives (Scheme 6. 1).

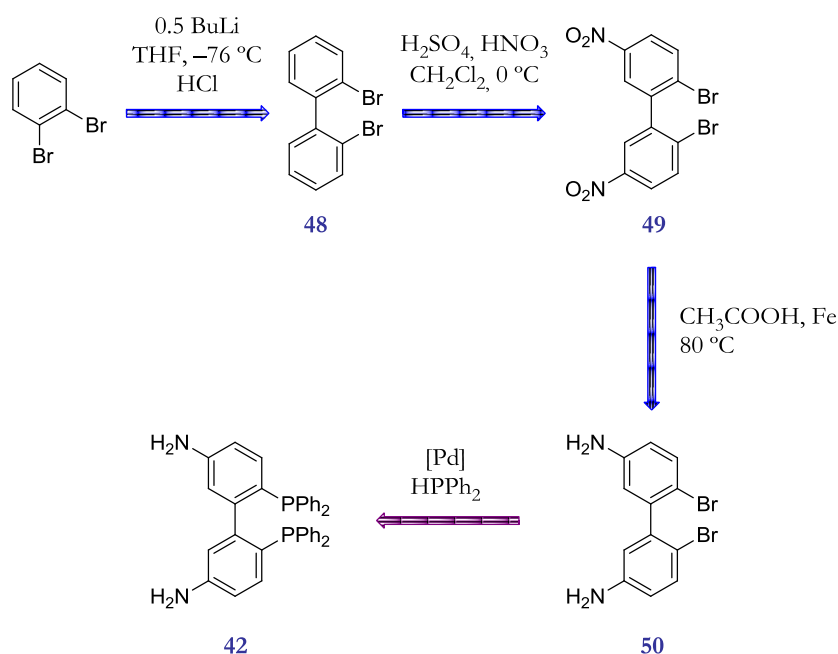
There is a large number of synthetic possibilities in literature to perform an aryl-aryl coupling reaction. Depending on the nature of the substrate, many metal catalyzed reactions can be applied, and often the optimization process for a specific structure is a matter of trial and error.⁶

Several methods from the ones described in literature were explored to synthesize the amine substituted bisphenol fragment. Mainly iron or copper mediated oxidative coupling of aryl alcohols were attempted, but the starting phenol or oxidized by-products were obtained in all cases. For that reason non metal catalyzed reactions were considered as alternative for the coupling reaction. The possibility to start from commercially available biaryl molecules was also explored.



Scheme 6. 1. Initial synthetic pathway proposed for the biaryl diphosphines.
Reactants: a) metal mediated oxidative coupling; b) Tf₂O, DCM, 0 °C; and c) HPPH₂, DABCO, NiCl₂dppe, DMF, 100 °C.

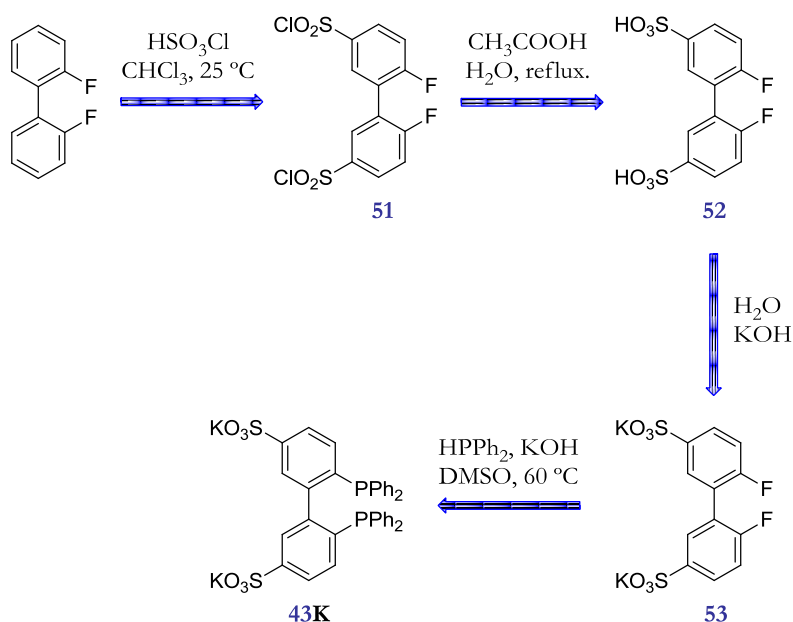
The alternative route proposed for the synthesis of diphosphine **42** is depicted in Scheme 6. 2. It starts from 1,2-dibromobenzene, to obtain via lithiation (using only half an equivalent of BuLi and *in situ* reaction with the remaining dibromo precursor) 2,2'-dibromobiphenyl **48** in moderate yield (44 %).^{7,8} Nitration of the biaryl moiety in the 5,5' position was performed using a mixture of nitric and sulphuric acids (the yield in this case was 47 %).⁸ For reduction of dinitro compound **49** to obtain diamine **50**, several reaction conditions were tried. Initially, it was performed using Pd/C with hydrogen. The product obtained in this case was (1,1'-biphenyl)-3,3'-diamine, which confirmed the reduction to the amine but also the undesired cleavage of the bromide atoms. Alternatively the reduction was attempted using Sn in a mixture of ethanol and hydrochloric acid under reflux. The formation of product **50** was observed, but it could not be isolated, due to the very low yield.⁹ The best result was obtained when iron in acetic acid at 80 °C was used. In only 30 min the formation of the product was accomplished with a moderate yield (22 %).¹⁰



Scheme 6. 2. Synthesis proposed for diphosphine **42**.

The last step is a palladium mediated P–C coupling reaction with diphenylphosphine to obtain compound **42**. This step was not performed due to the discouraging values of association constants envisaged for the hydrogen bonding based motifs (see 6.2.2.).

The synthesis of diphosphine **43** with potassium as counterion (**43K**) was already described in the literature by Stelzer *et al.*¹¹ It starts from the commercially available 2,2'-difluoro-1,1'-biphenyl, which reacts with chlorosulfonic acid to obtain the sulfochloride **51**. The next step is the hydrolysis to sulfonic acid **52** followed by neutralization to potassium salt **53**. The last step is the nucleophilic phosphination in superbasic medium to obtain sulfonated phosphine **43K** (Scheme 6. 3). Some problems were encountered to isolate diphosphine **43K** from the by-products obtained. For that reason it was decided to slightly modify the procedure. Addition of an excess of diphenylphosphine allowed increasing the conversion towards **43K**. The unreacted diphenylphosphine was converted to its oxide, from which **43K** can be easily separated. Using this methodology, the overall yield obtained (56 %) was better than the one reported by Stelzer (21 %).



Scheme 6. 3. Synthesis of diphosphine **43K**.

6.2.2. SUPRAMOLECULAR STUDIES

As explained before, phosphines are oxygen sensitive, especially in solution. If phosphine oxides were formed during measurements of the strength of the binding constant, it would interfere with the results. Unfortunately, performing these studies under inert conditions requires an extra effort that is not always feasible on a routine basis. For that reason, it was decided to start these studies using the more robust parent compounds, **50** (to study hydrogen bond interaction) and **53** (for ionic interaction).

Hydrogen bond interaction: prediction of binding constants

Divalent species **50** can form dimeric supramolecular complexes with dicarboxylic acids via multiple hydrogen bonds. However, as described in chapter 5, to characterize the divalent system the association constant of an analogue monovalent system has to be determined first, to set the reference association constant (K_{ref}).

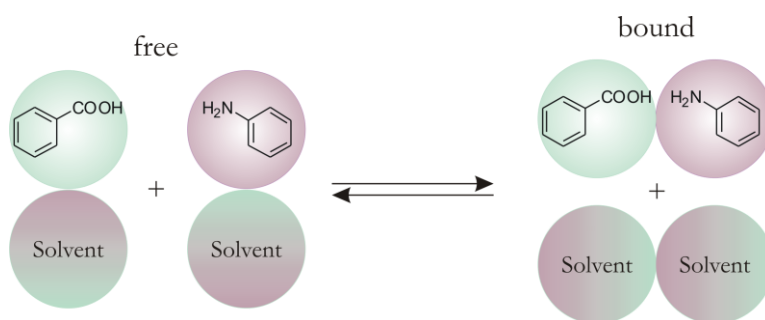


Figure 6. 4. Equilibrium between the free and bound species for the reference system to predict the association constants of the hydrogen bonded pair.

The monovalent equilibrium chosen for the determination of the K_{ref} for the hydrogen bond association was the one established between aniline and benzoic acid (Figure 6. 4). As described in chapter 5, it is possible to predict the magnitude of the

association constant for hydrogen bonding interactions by using the approximation developed by Hunter.¹²

The formation of a hydrogen bonded complex in solution can be interpreted as a competition between solute-solute, solute-solvent, and solvent-solvent interactions. With equations 5.3 and 5.4, and using the values of α and β reported (based on experimental values),^{13,14} the K_{pred} has been calculated for different solvents (Table 6.2).

$$\Delta\Delta G_{\text{H-Bond}} = -(\alpha\beta + \alpha_s\beta_s) + (\alpha\beta_s + \alpha_s\beta) = -(\alpha - \alpha_s)(\beta - \beta_s) \quad \text{Eq. 5.3}$$

$$\log K = -(\Delta\Delta G_{\text{H-Bond}} + 6) / RT \quad \text{Eq. 5.4}$$

Table 6.2. K_{pred} calculated for the reference system in different solvents.

solvent	α	β	α_s	β_s	K_{pred} (M ⁻¹)	polarity index
DMSO			0.8	8.9	$1.4 \cdot 10^{-3}$	7.2
acetone			1.5	5.8	$5.5 \cdot 10^{-2}$	5.1
methanol			2.7	5.8	$7.1 \cdot 10^{-2}$	5.1
THF			0.9	5.3	$8.6 \cdot 10^{-2}$	4
water	3.6	5.3	2.8	4.5	$1.1 \cdot 10^{-1}$	9
acetonitrile			1.7	4.7	$1.4 \cdot 10^{-1}$	5.8
chloroform			2.2	0.8	1.131	4.1
DCM			1.9	1.1	1.597	3.1
benzene			1	2.2	2.329	2.7
CCl ₄			1.4	0.6	5.939	1.6

From the results calculated it can be concluded that the association constants expected for the formation of a hydrogen bond between benzoic acid and aniline

were not very high in the range of solvents studied. Although there is not a linear correlation between the polarity of the solvent and the association constant, as expected a trend can be observed. The more polar the solvent, the lower is the association constant between the solutes.

The highest value for the K_{pred} for the complex (and strong enough to consider association in solution) is the one with the less polar solvent carbon tetrachloride. Unfortunately, compounds **50** and **42** are not soluble in carbon tetrachloride, and thus these studies could not be performed.

Consequently, our efforts focussed on the study of the ionic interaction and involved the precursor of diphosphine **43** (compound **53**) and several diammonium salts.

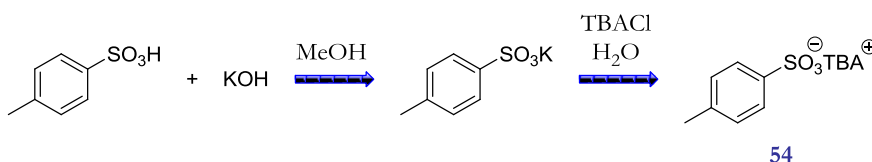
Ionic interaction: reference system and dilution experiments

Ionic interactions have not been characterized in as much detail as hydrogen bonds from a supramolecular point of view. There are no general α and β parameters to predict association constants, as there are many parameters that affect the binding affinity of charged species, such as size and shape of the ions, solvent polarity, counter-ion effects, salt concentration, etc. Consequently, each case has to be considered individually, and the strength of the interaction has to be experimentally determined. Some authors tried to characterize the binding behaviour for some onium salts^{15,16} and anions (mainly halides). They proposed that the ion can be characterized in terms of hydrogen bonding acidity or basicity,^{17–19} based on previous studies that pointed out the behaviour of halide anions as Lewis bases toward hydrogen bonding molecules.²⁰

It is expected that the ionic interaction between the two species involved in ion pairing will be strong in non-polar solvents (as happened in hydrogen bond interaction), which favours desolvation of the ions involved. One advantage of the formation of ion pairs compared to hydrogen bonding is that it is possible to modulate the solubility of the different components by changing the counter ion of the salt. By introducing a counter ion that contains more organic weight it is possible

to make the system soluble in less polar solvents, and then measure the binding constant in those solvents.

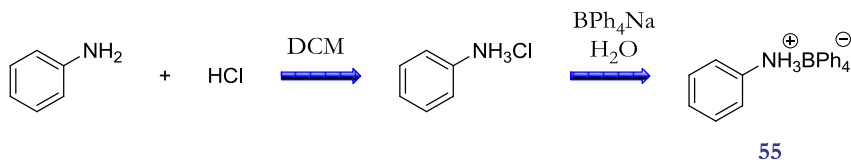
As explained before, to evaluate the binding constant of the ionic interaction, a model system with only one interaction to calculate the K_{ref} has to be characterized (see chapter 5). Regarding the ionic interaction, the anionic model considered was the tetrabutylammonium *p*-toluenesulfonate (**54**) and the cationic species the anilinium tetraphenylborate (**55**).



Scheme 6. 4. Change of the counterion to obtain the tetrabutylammonium sulfonate salt **54**, used as host for the reference system.

p-Toluenesulfonic acid was converted into the potassium *p*-toluenesulfonate salt by reacting it with KOH in methanol. The change of the counterion was performed by reaction in water with tetrabutylammonium chloride and subsequent extraction of the ion pair **54** with dichloromethane (Scheme 6. 4). All the reactions gave a quantitative yield.

In the case of the ammonium salts, the amines had to be protonated first by using HCl . After that, the counterion exchange was also feasible by precipitation from water when reacting with sodium tetraphenylborate to give **55** (Scheme 6. 5). The reactions were quantitative.



Scheme 6. 5. Change of the counterion to obtain the tetraphenylborate ammonium salt **55**, used as guest for the reference system.

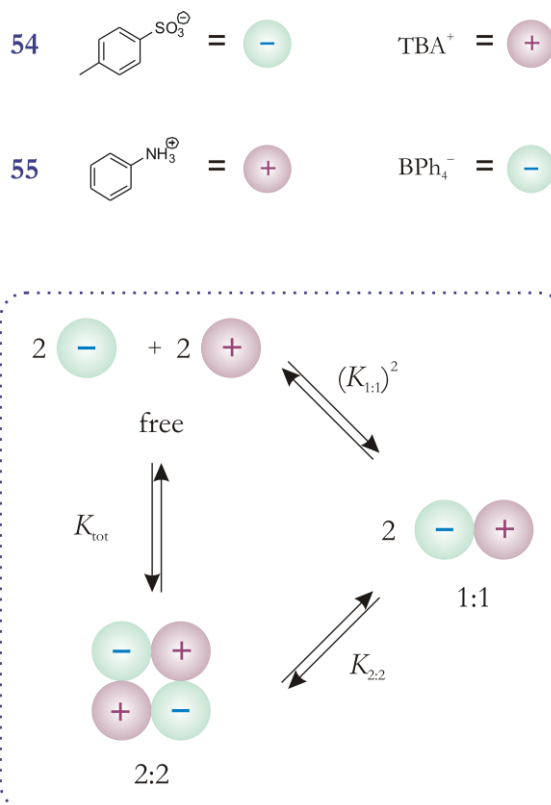


Figure 6. 5. Representation of the equilibria involved in the formation of ionic aggregates for ion pairs.

In solution, three situations can be considered: the presence of the species as separated ion pair, as close contact ion pair (denoted as 1:1 complex in Figure 6. 5) and the formation of higher aggregates (for example, the 2:2 complex in Figure 6. 5). To carry out the titrations, it is necessary to set the optimal concentration to work, to avoid (or minimize) the formation of higher stoichiometry aggregates of the ions subjected to study. For example, if one considers host **54** in solution (Figure 6. 5), it is preferable to have the ionic pair fully dissociated (separated ion pair), to facilitate the formation of the supramolecular complex with the modifier. If **54** would be involved in a close contact ion pair with its original counterion (1:1), one interaction has to be broken to form the host-guest couple. This situation, although less favourable than the separated ion pair can also render eventually the supramolecular complex. If a

higher aggregate is formed between the host and its original counterion (2:2), more interactions need to be broken to have the host free to associate with the guest, which will make the formation of the supramolecular complex more difficult.

Preliminary dilution $^1\text{H-NMR}$ experiments with **54** and **55** were independently performed. A concentration range from 2.6 mM to 239 mM was used for **54** and from 1.4 mM to 131 mM for **55**.

The data obtained for the dilution experiments were fitted to a binding model which considers the formation of a 1:1 species and a 2:2 species.²¹ The results are summarized in Table 6. 3 for both ion pairs. From the fitting K_{tot} and $K_{1:1}$ were obtained. $K_{2:2}$ was calculated according to equations 6.1–6.3.

$$K_{\text{tot}} = K_{1:1}^2 \cdot K_{2:2} \quad \text{Eq. 6.1}$$

$$\log K_{\text{tot}} = 2 \log K_{1:1} + \log K_{2:2} \quad \text{Eq. 6.2}$$

$$\log K_{2:2} = \log K_{\text{tot}} - 2 \log K_{1:1} \quad \text{Eq. 6.3}$$

Table 6. 3. Association constant values obtained from the dilution experiments of ion pairs **54** and **55** at 25 °C in CDCl_3 .

	54	55
$\log K_{1:1}$	7.992	5.155
$K_{1:1} (\text{M}^{-1})$	$9.81 \cdot 10^7$	$1.43 \cdot 10^5$
$\log K_{\text{tot}}$	15.132	10.329
$K_{\text{tot}} (\text{M}^{-3})$	$1.35 \cdot 10^{15}$	$2.13 \cdot 10^{10}$
$\log K_{2:2}$	-0.852	0.019
$K_{2:2} (\text{M}^{-1})$	0.14	1.05

As by NMR techniques only association constants values of 10^3 M^{-1} can be measured accurately, these values have to be considered as rough estimations. From the different values of K obtained,²² one can have an approximate idea of the behaviour of the system. From the speciation diagram constructed on the basis of the values obtained (Figure 6. 6), it is clear that a 1:1 species is predominant in the range of concentrations considered for both systems. As mentioned before, this is not the

most favourable situation to form the desired supramolecular complex, as the original cation-anion interaction has to be broken.

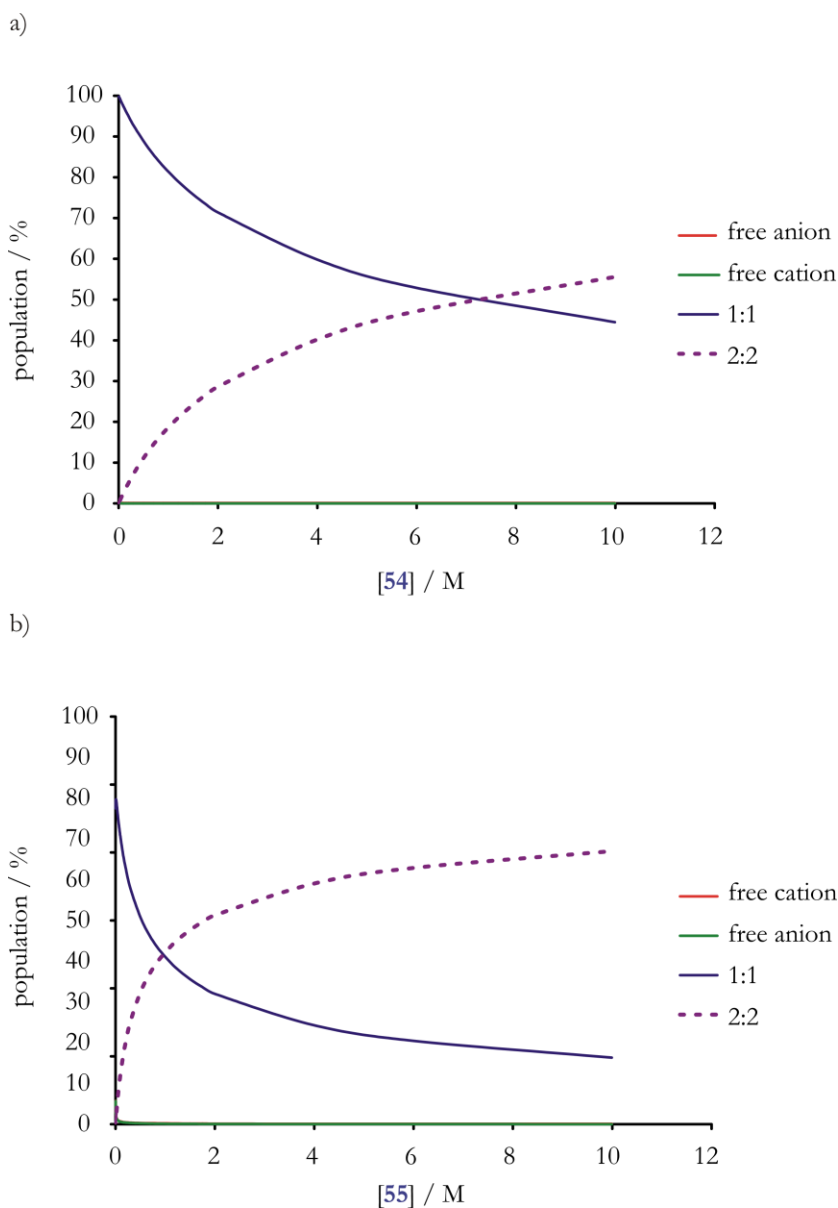


Figure 6. 6. Simulation of the speciation diagrams for the ionic pairs: a) **54** and b) **55**. Population of free cation and free anion is too low in all range to be appreciated.

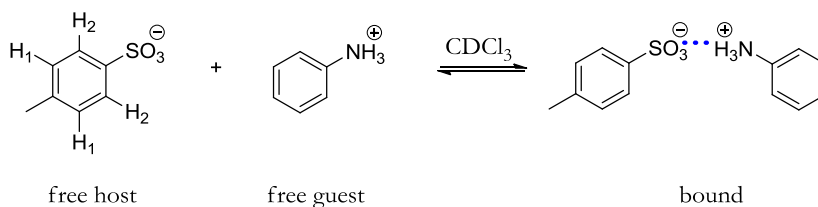
In the case of **54**, the 1:1 complex is the major species up to 7 M (approximately). For ionic pair **55**, however, the situation is less favourable, since at concentrations above 1 M the 2:2 complex is predominant. Unfortunately, the separate ion pair which is the ideal situation for the formation of the new assembly is not observed at any concentration.

Certainly, it is difficult to reach the desired conditions. Ideally separated ion pairs are wanted for the starting compounds (with spectator counterions) and the supramolecular complex occurring as a close ion pair.

After those considerations the reference constant (K_{ref}) was determined. The general procedure (by NMR) is having a solution of the host (from now on considered the anionic receptor **54**) of known concentration and use an aliquot of this parent solution, to prepare another solution that also includes the guest (considered from now on the cationic modifier, in this case **55**).

It has to be taken into account that all binding constants calculated for ionic interactions using this methodology, will be approximate values. This is due to the effects that the counter ions can produce in the media, such as it is the change in the ionic strength, which is neglected in this study and it can affect to the equilibria involved.

In the series of titrations performed, aliquots of the host solution that includes also the guest were added to the initial solution of the host. By using this methodology, the amount of guest increases with the successive additions, but the concentration of the host remains constant. This simplifies the calculations to fit the values obtained to certain equilibrium, and maintains the intensity of the signals of the host to follow by NMR techniques.



Scheme 6. 6. Species involved in the titration for the determination of the K_{ref} .

The species involved in the association are represented in Scheme 6. 6.

To determine an association constant, ideally one has to work with a value of the concentration of the host that is approximately the inverse of the association constant, and use a solution of the guest with a concentration at least ten times larger than the concentration used for the host. Regarding the hydrogen bonding associations, as discussed before, it is possible to have an approximate value of this constant using the α s and β s. However, for a system based on an ionic interaction it is not possible to estimate a value. Therefore, several preliminary experiments were done with solutions of host and guest of different concentrations, to have a rough idea of the value of the association constant. After those preliminary tests, two titrations were considered to determine the value of K_{ref} .

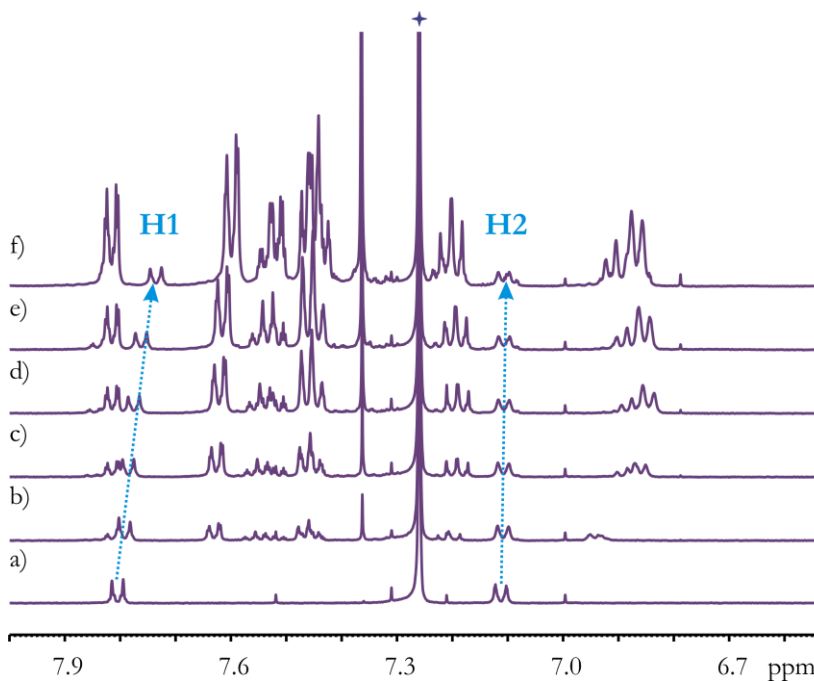


Figure 6. 7. Selected region of the ^1H -NMR titration of **54** with **55** in CDCl_3 at 25 $^\circ\text{C}$. a) **54**; b) **54** + 0.5 eq. of **55**; c) **54** + 1.1 eq. of **55**; d) **54** + 2 eq. of **55**; e) **54** + 3 eq. of **55**; f) **54** + 6 eq. of **55**. $[\text{54}] = 1.08 \text{ mM}$.

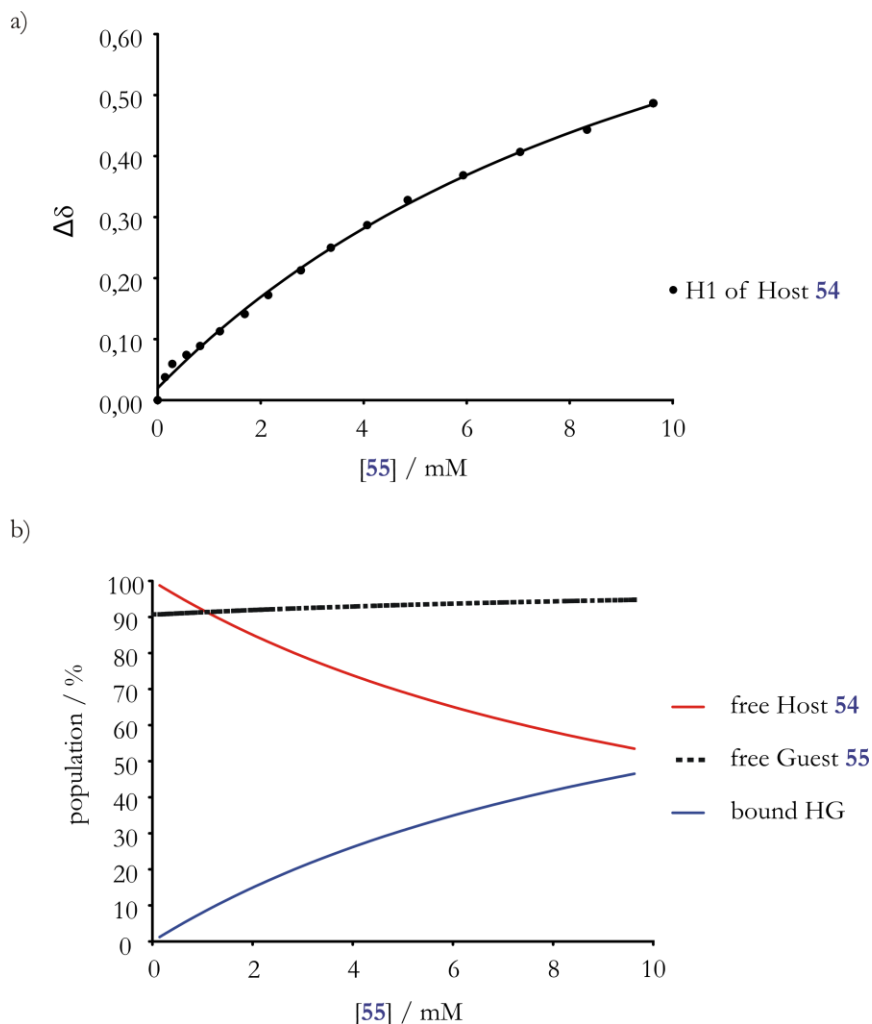


Figure 6. 8. a) Representation of the variation in the chemical shifts of the aromatic proton H1 of the host during the titration using **54** as host and **55** as guest. $[55]_i = 17.04$ mM. b) Representation of the speciation diagram. $[54] = 1.08$ mM. Population of H and HG calculated based on the mass balance $H + HG = H_{total}$; population of G calculated based on the mass balance $G + HG = G_{total}$.

In the first titration a solution 1.08 mM of host **54** in $CDCl_3$ was used to prepare a solution 17.04 mM of the guest. In the second titration, the concentration of the solution of the host **54** was 1.01 mM, and used to prepare the solution of the guest **55** 31.45 mM.

The titrations were done by $^1\text{H-NMR}$ and the shift of the signals of the host was followed while incremental equivalents of the guest were added. In Figure 6. 7 the $^1\text{H-NMR}$ spectra for different equivalents of guest are presented.

For protons H1 and H2 of the host (Scheme 6. 6), only one signal for each proton is observed in the $^1\text{H-NMR}$ during the titration. The equilibrium showed a fast exchange on the NMR timescale between the bound and free host: a unique signal that shifts depending on the proportion of free and bound species is observed for those protons. Hardly any shift was observed for H2, and therefore the variation on H1 was used for the fitting.

The fitting of the signals was done considering only the equilibrium of free **54**⁻ as host, free **55**⁺ as guest and the formation of the 1:1 ionic pair **54**·**55**, but neglecting the effect of the counterions, to simplify the model.

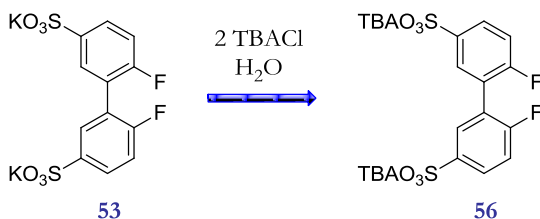
This way K_{ref} can be calculated as an average of the two values obtained from the fitting of both titrations (41 M^{-1} and 95 M^{-1}). As a result $K_{\text{ref}} = 68 \pm 27 \text{ M}^{-1}$.²³

One can notice in Figure 6. 7 (and in Figure 6. 8, a) an irregular trend in the variation of the NMR shift of the initial points. This irregularity is not very pronounced, and does not affect the fitting. A tentative explanation is that another equilibrium is present at the beginning of the titration, such as can be the dissociation of the 1:1 ion pairs of the host and the guest.

Ionic interaction: divalent system

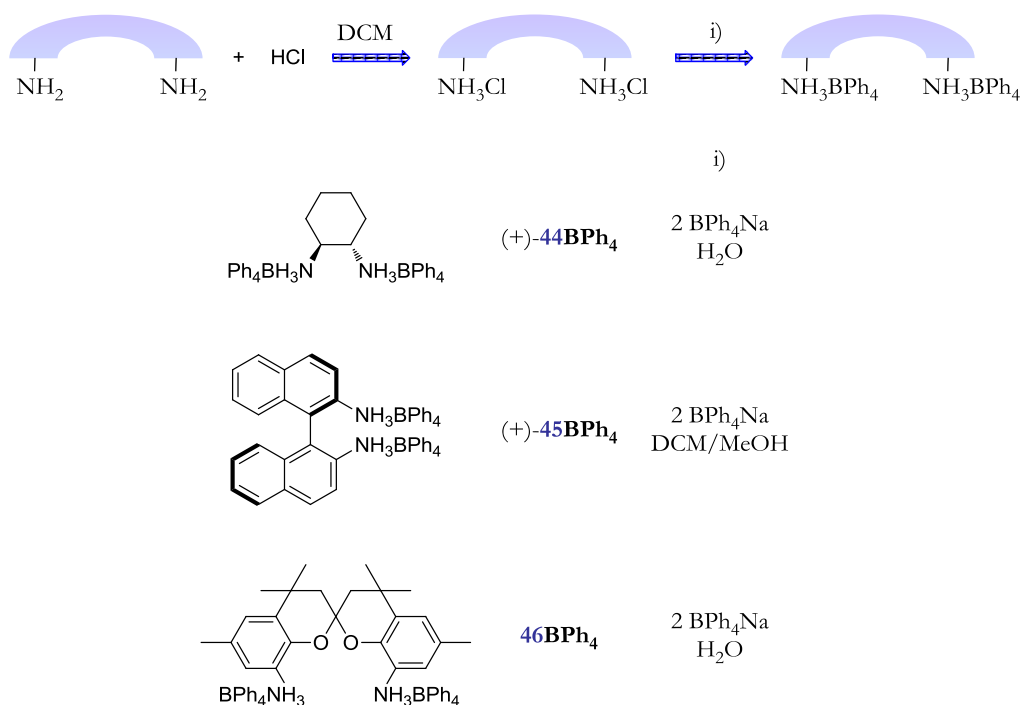
When the value of the reference monovalent system is set, the association constant between different modifiers (guests) with the anionic backbone (host) for the divalent model can be determined.

As explained previously, the studies to determine the binding constant were done with precursor **53** to preserve the air sensitive phosphine **43**. As described for the monovalent system the counterion of **53** was changed from K^+ to TBA^+ to increase its solubility. Sulfonated host **56** was obtained from **53** by mixing it with two equivalents of tetrabutylammonium chloride in water and extraction with DCM.



Scheme 6. 7. Change of the counterion to obtain the tetrabutylammonium sulfonate salt **56**, used as host for the divalent system.

The divalent counterions used as modifiers were those derived from **44**, **45** and **46**. In the case of the derivatives from the commercial (1*S*,2*S*)-(+)-1,2-diaminocyclohexane, ammonium chloride (+)-**44Cl** was obtained dissolving the corresponding diamine in DCM, adding HCl and removal of the solvent. (+)-**44BPh₄** was obtained by precipitation from water by adding two equivalents of NaBPh₄ to (+)-**44Cl** (Scheme 6. 8).

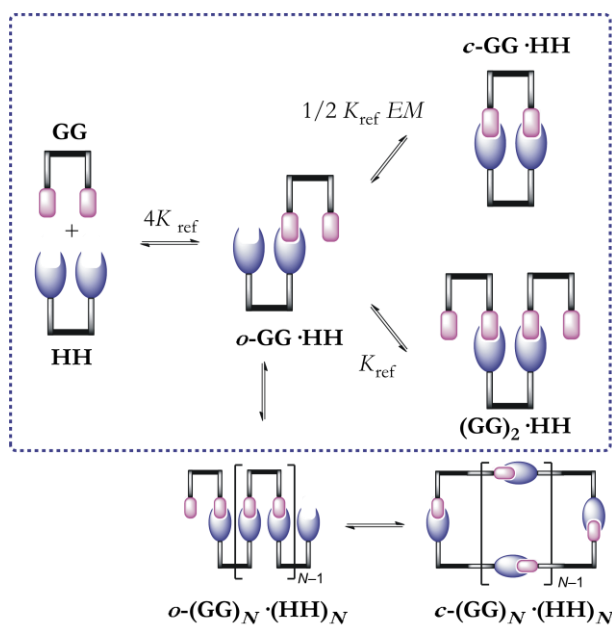


Scheme 6. 8. Counterion exchange for modifiers **44–46**.

For modifier **45**, the procedure was slightly different due to its different solubility. From the commercial (R)-(+)-2,2'-diamino-1,1'-binaphthalene, and following the previous described procedure, (+)-**45Cl** was obtained. The last step, anion exchange to obtain (+)-**45BPh₄**, was done in a mixture of DCM/MeOH by adding two equivalents NaBPh₄ and removing the solvent after filtration (Scheme 6. 8).

In the case of the racemic SPAN derivative **46**, again the first step was done as described for **44**, obtaining **46Cl**, but to have **46BPh₄** after adding the two equivalents of NaBPh₄ to **46Cl** (dissolved in water), the ionic pair **46BPh₄** was extracted from the reaction mixture with DCM (Scheme 6. 8).

The next step is to determine the binding constant for each modifier ((+)-**44BPh₄**, (+)-**45BPh₄**, and **46BPh₄**) with the biaryl receptor **56**. Each value will give an idea about the strength of the ionic interaction between each modifier with the biaryl backbone.



Scheme 6. 9. Schematic representation of the possible equilibria involved in a divalent system. If $[GG]_0 \gg [HH]_0$, only the species inside the box are populated.

To estimate the behaviour of each modifier towards the biaryl host, one useful parameter is the effective molarity (EM). Depending on this value one can say if the association of a divalent system as a discrete unit is preferred, or if the formation of oligomers will take place.

In Scheme 6. 9 all equilibria involved are presented.²⁴ To simplify the analysis, the formation of the oligomeric complexes $c\text{-}(\mathbf{GG})_N\cdot(\mathbf{HH})_N$ and $o\text{-}(\mathbf{GG})_N\cdot(\mathbf{HH})_N$ has been avoided by performing the titrations under conditions at which the guest (\mathbf{GG}) was always present in large excess, and the concentration of the host (\mathbf{HH}) was low ($[\mathbf{HH}] \ll 1/K_{\text{ref}}$, $[\mathbf{HH}] \ll 15$ mM). For that reason, only $o\text{-}\mathbf{GG}\cdot\mathbf{HH}$, $c\text{-}\mathbf{GG}\cdot\mathbf{HH}$ and $(\mathbf{GG})_2\cdot\mathbf{HH}$ should be considered in the analysis.

The titration experiments were done as described for the monovalent system: a stock solution of host **56** 1 mM in CDCl_3 was used to prepare solutions around 30 mM for each guest. The titrations were monitored by $^{19}\text{F}\{^1\text{H}\}$ -NMR spectroscopy, by looking at the chemical shift change of the fluorine atoms of the host. $^{19}\text{F}\{^1\text{H}\}$ -NMR spectroscopy was chosen due to the overlap of the host signals and the guest signals in the ^1H -NMR spectra.

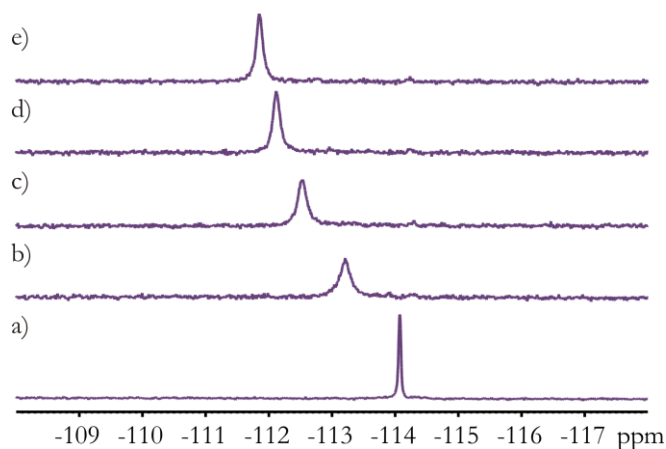


Figure 6. 9. Selected region of the $^{19}\text{F}\{^1\text{H}\}$ -NMR spectra during the titration of **56** with **46BPh₄** in CDCl_3 at 25 °C. a) **56**; b) **56** + 1 eq. of **46BPh₄**; c) **56** + 3 eq. of **46BPh₄**; d) **56** + 8 eq. of **46BPh₄**; e) **56** + 20 eq. of **46BPh₄**. $[\mathbf{56}] = 1.11$ mM.

In general a downfield shift was observed for the signal in the $^{19}\text{F}\{^1\text{H}\}$ -NMR

spectra while adding more guest. For example, Figure 6. 9 depicts the variation in the chemical shift during the titration of **56** with **46BPh₄** in CDCl₃.

As done previously to calculate K_{ref} , the effect of the counter ions was not considered in the fitting model.

The results were fitted to a simple 1:1 binding model (which includes ***o*-GG·HH** and ***c*-GG·HH**) for modifiers (+)-**44BPh₄** and **46BPh₄**. In the case of modifier (+)-**45BPh₄**, the data fitted better to a model that includes both 1:1 complex formation (including ***o*-GG·HH** and ***c*-GG·HH**) and 1:2 complex formation (**((GG)₂·HH**).

Therefore, when modifiers (+)-**44BPh₄** and **46BPh₄** were used, only one general binding constant for the 1:1 complexes was obtained ($K_{1:1}$), but from the fitting of the data obtained with the modifier (+)-**45BPh₄**, two association constants values were calculated ($K_{1:1}$ and $K_{1:2}$). Considering a *partially bound states* scenario,^{25–27} it is possible to analyze the population of each species. The value of EM can be estimated using the equations 6.4–6.11, based on K_{ref} .

The statistical numbers reflected in scheme 6.9 are calculated evaluating the symmetry of the molecules involved, taking in account the C_2 symmetry of the modifiers (guests) and the host molecule.^{24,28}

$$K(\mathbf{o}\text{-GG}\cdot\mathbf{HH}) = 4 K_{\text{ref}} \quad \text{Eq. 6.4}$$

$$K(\mathbf{((GG)}_2\cdot\mathbf{HH})) = 4 K_{\text{ref}}^2 \quad \text{Eq. 6.5}$$

$$K_{1:1} = K(\mathbf{c}\text{-GG}\cdot\mathbf{HH}) + K(\mathbf{o}\text{-GG}\cdot\mathbf{HH}) = 2 K_{\text{ref}}^2 EM + 4 K_{\text{ref}} \quad \text{Eq. 6.6}$$

$$K_{1:2} = K(\mathbf{((GG)}_2\cdot\mathbf{HH})) = 4 K_{\text{ref}}^2 \quad \text{Eq. 6.7}$$

In the case that one considers the formation of 1:1 complexes only, the EM is given by equation 6.6, which rearranges to Eq. 6.8:

$$EM = (K_{1:1} - 4 K_{\text{ref}}) / 2 K_{\text{ref}}^2 \quad \text{Eq. 6.8}$$

When both 1:1 complexes and 1:2 complexes are considered, the EM can be calculated from equations 6.6 and 6.7, giving equation 6.9.

$$EM = (2 K_{1:1} - 4 (K_{1:2}^{1/2})) / K_{1:2} \quad \text{Eq. 6.9}$$

The results are summarized in the Table 6. 4.

Table 6. 4. Values of the association constants and EM obtained in the titrations of backbone **56** with the different modifiers in $CDCl_3$ at r.t.

Entry	Modifier	$K_{1:1}$ (M ⁻¹)	$K_{1:2}$ (M ⁻²)	EM (M)	$K_{ref} \cdot EM$
1	(+)- 44BPh₄	423	-	0.02	1.11
2	(+)- 45BPh₄	3350	2710	2.39	162.89
3	46BPh₄	545	-	0.03	2.01

The value of $K_{ref} \cdot EM$ gives an idea about the stability of the different species involved in the equilibrium.²⁴ If $K_{ref} \cdot EM \ll 1$, the partially bound intermediate (**o-GG·HH**) is more stable than the cyclic complex (**c-GG·HH**). On the other hand, if $K_{ref} \cdot EM \gg 1$, the cyclic complex is more stable than the partially bound intermediate. The value obtained for modifier (+)-**45BPh₄** (Table 6. 4, entry 2) is clearly much higher than 1, which means that the open partially bound state **o-GG·HH** is scarcely populated. For modifiers (+)-**44BPh₄** and **46BPh₄** (Table 6. 4, entries 1 and 3, respectively) the value of $K_{ref} \cdot EM$ is close to 1, which means that there is no preferential formation of one of the two 1:1 species.

From these data, the relative distribution of the 1:1 species (**o-GG·HH** and **c-GG·HH**) can be determined using equations 6.10 and 6.11.²⁹ The populations obtained in each case are shown in Table 6. 5.

$$\text{population of } \mathbf{o-GG \cdot HH} = 4 K_{ref} / K_{1:1} \quad \text{Eq. 6.10}$$

$$\text{population of } \mathbf{c-GG \cdot HH} = (K_{1:1} - 4 K_{ref}) / K_{1:1} \quad \text{Eq. 6.11}$$

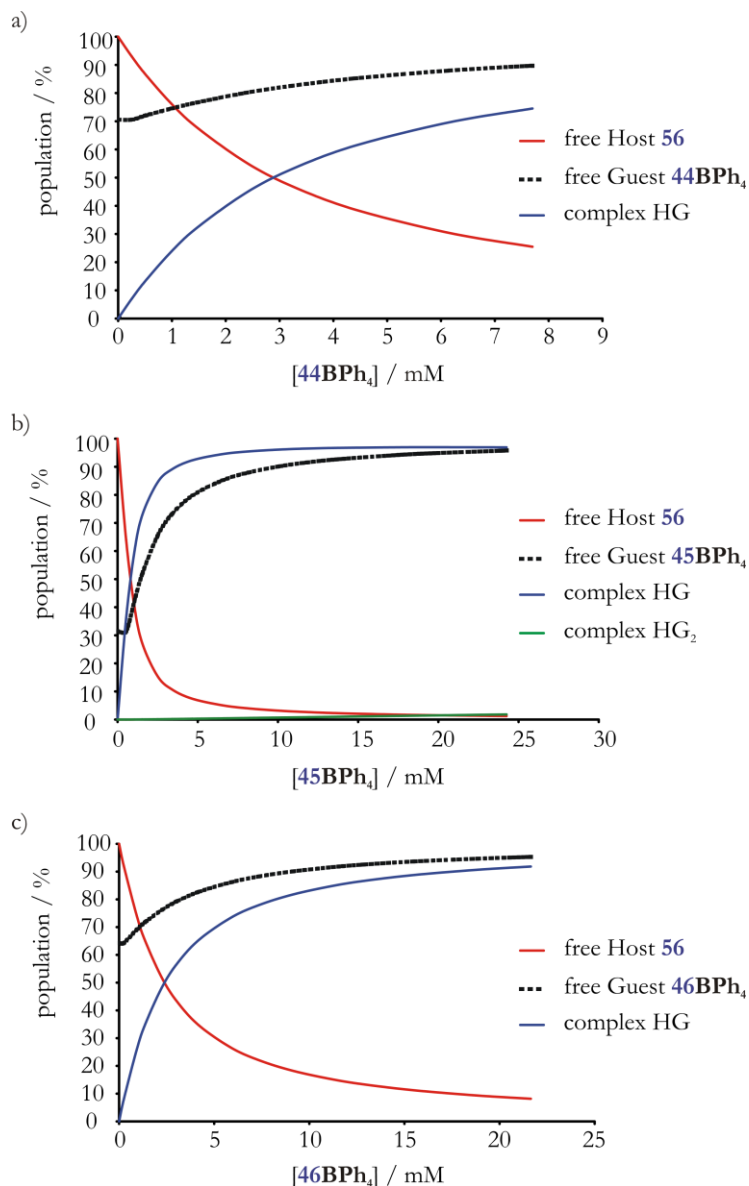
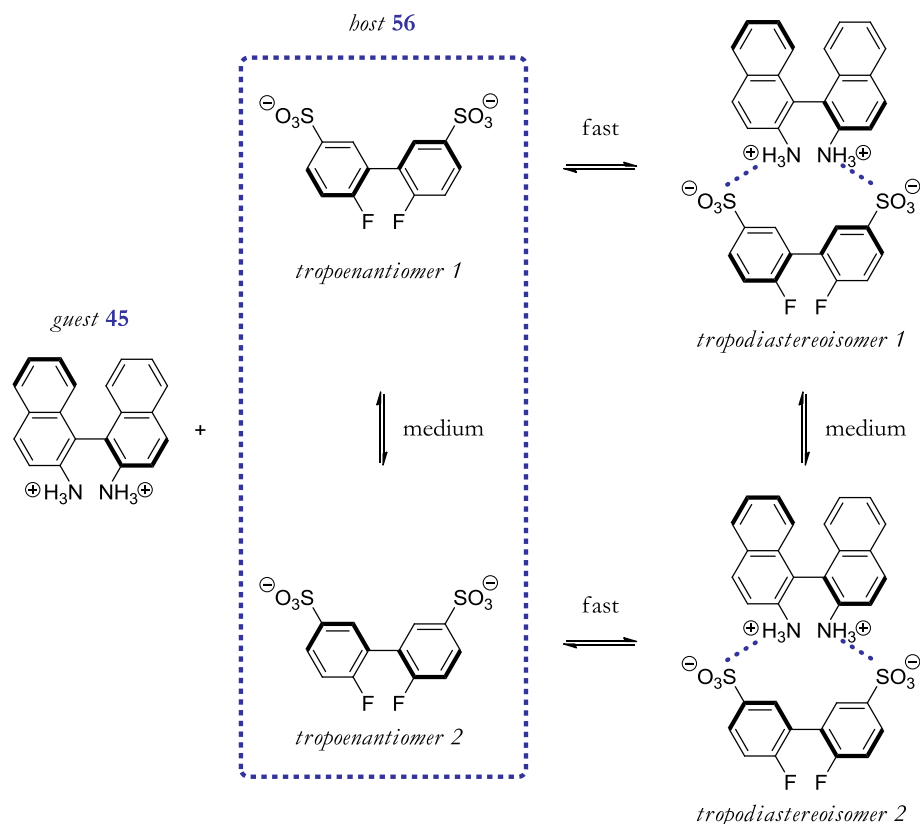


Figure 6. 10. Speciation diagrams for the titrations in CDCl₃ at r.t. of **56** with:
 a) **44BPh₄**, [**56**] = 1.06 mM; b) **45BPh₄**, [**56**] = 1.02 mM; and c) **46BPh₄**, [**56**] = 1.11 mM. For a) and c): population of H and HG calculated based on the mass balance $H + HG = H_{\text{total}}$; population of G calculated based on the mass balance $G + HG = G_{\text{total}}$. For b) population of H, HG and HG₂ calculated based on the mass balance $H + HG + HG_2 = H_{\text{total}}$; population of G calculated based on the mass balance $G + HG + 2 \cdot HG_2 = G_{\text{total}}$.

Table 6. 5. Populations calculated for the 1:1 species of host **56** and the different modifiers in CDCl₃ at r.t.

Entry	Modifier	population <i>o</i> -GG·HH	population <i>c</i> -GG·HH
1	(+)- 44BPh ₄	64 %	36 %
2	(+)- 45BPh ₄	8 %	92 %
3	46BPh ₄	50 %	50 %



Scheme 6. 10. Equilibria showing the two possible diastereoisomers formed by assembly between (R)-**45** and **56**.

Although all the binding constants obtained for the three modifiers were large enough to undergo association with the guest, for modifier (+)-**45BPh**₄ (the one

derived from the binaphthyl backbone) the calculated population of **c-GG·HH** is much larger than that of **o-GG·HH** (Table 6. 5, entry 2). This is in agreement with its value of $K_{\text{ref}} \cdot EM \gg 1$, as is to be expected (Table 6. 4, entry 2).

As a conclusion, the modifier that should associate with the host with the highest binding interaction and form a closed supramolecular structure is modifier **45**.

It is worthwhile to mention an effect observed in the $^{19}\text{F}\{^1\text{H}\}$ -NMR spectra when modifiers (+)-**44BPh₄** and (+)-**45BPh₄** were used. The initial narrow singlet undergoes a broadening and almost disappeared when 6 equivalents of the guest were added. The broadening of the signal can be attributed to the fact that more equilibria should be distinguished (Scheme 6. 10). The equilibrium involving the two free *tropoenantiomers* may occur with an intermediate rate on the NMR timescale (although faster than that of Biphep, see chapter 5). To study better the formation of both diastereoisomers, further studies with low temperature NMR experiments should be performed.

6.2.3. CATALYSIS: ASYMMETRIC HYDROGENATION

The low waste produced in the asymmetric hydrogenation (due to its atom economy) together with the high yields and enantioselectivities with low catalyst loadings, make this reaction a powerful tool for the production of a wide array of enantiomerically pure compounds.

The history of the metal catalyzed asymmetric hydrogenation of alkenes, ketones and imines to generate a new chiral carbon centre has evolved together with the history of the development of chiral ligands. The discovery of the facile hydrogenation of olefins in solution catalyzed by $\text{RhCl}(\text{PPh}_3)_3$ was made by Wilkinson *et al.* in 1966.³⁰ A couple of years later, the chiral version was developed for the asymmetric hydrogenation of prochiral olefins with the use of a phosphine having a chiral phosphorus centre. At that time, the enantioselectivity was still low. Knowles *et al.* employed the (–)-methylpropylphenylphosphine to obtain 3 % of enantioselectivity,³¹ and Horner *et al.* used the (+) enantiomer of the same phosphine to have only 4 % of enantioselectivity for similar substrates.³² After modifications of

the substituents on the P atom of the chiral phosphine, Knowles reached up to 90 % enantioselectivity on dehydroaminoacids in the early 70s.^{33,34} At the same time, Kagan *et al.* developed the chiral C_2 symmetric diphosphine DIOP (Figure 6. 11), which contains the source of chirality on its backbone.^{35,36}

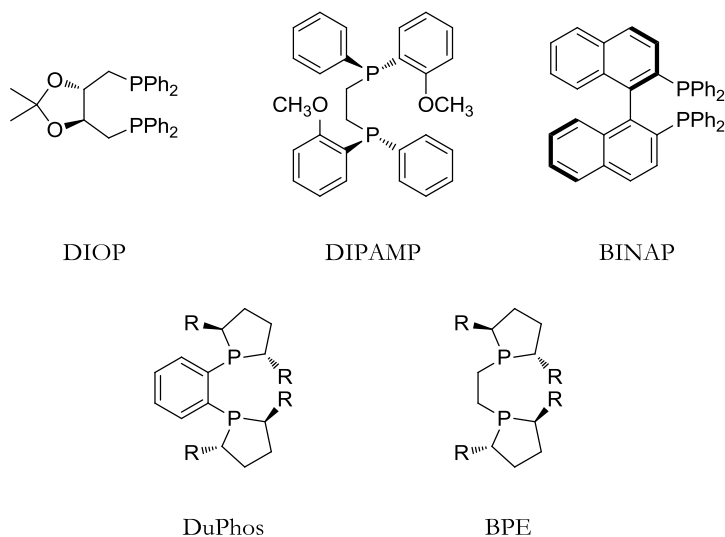


Figure 6. 11. Important chiral diphosphines developed for asymmetric hydrogenation.

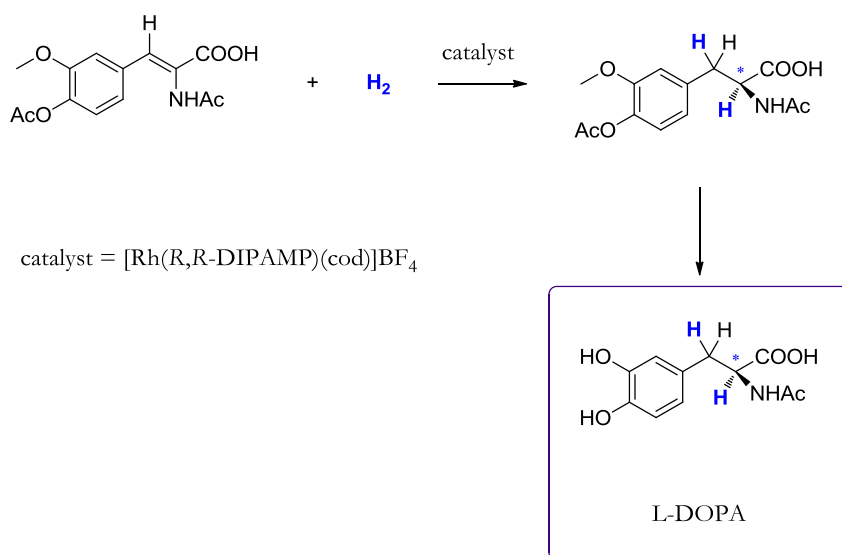
The development by Knowles of the synthesis at commercial scale of L-DOPA (a pharmaceutical product for the treatment of Parkinson's disease, Scheme 6. 11) at Monsanto by rhodium catalyzed hydrogenation was a real milestone.³⁷ The ligand used was the C_2 symmetric diphosphine DIPAMP (Figure 6. 11).^{38,39} But undoubtedly, the best diphosphine for the asymmetric hydrogenation of various substrates turned out to be the *atropis* BINAP (Figure 6. 11), developed by Noyori *et al.* in the 80s.^{40,41} The replacement of rhodium by ruthenium allowed to expand the scope of the hydrogenation reaction to C=N and C=O unsaturated substrates.⁴²

For their work in this field, Knowles and Noyori were awarded with the Nobel Prize in Chemistry in 2001 (together with Sharpless for his work on asymmetric epoxidation).^{43,44}

Another breakthrough was achieved in the 90s by Burk *et al.* with the application

of the chiral phospholanes DuPhos and BPE (Figure 6. 11) in the asymmetric hydrogenation of a wide scope of substrates, with high enantioselectivities (> 99 % ee).⁴⁵⁻⁴⁷

Nowadays, asymmetric hydrogenation is widely used to test the catalytic performance of new chiral ligands.^{48,49}



Scheme 6. 11. Asymmetric hydrogenation step in the industrial synthesis of L-DOPA.

There is not a general mechanism applicable for all the rhodium catalyzed asymmetric hydrogenation reactions. It has been proved that the structures of the intermediates formed during the catalysis depend directly on several parameters, for instance, the ligand employed, the substrates and the solvent. Earlier studies on hydrogenation mechanism were carried out by Wilkinson *et al.* They studied the reactivity of Wilkinson's catalyst towards olefins and H_2 pressure.^{30,50}

Important and systematic studies on the mechanism involving rhodium complexes have been performed by the groups of Halpern⁵¹⁻⁵⁵ and Brown.⁵⁶⁻⁶⁰ The mechanism proposed by Halpern for the asymmetric hydrogenation of enamides using a chiral diphosphine as ligand is one of the most frequently cited mechanisms

(Figure 6. 12).

The catalytic Rh(I) precursor **A** is hydrogenated to generate the species that starts the catalytic cycle (**B**). The coordination of the substrate in a reversible manner renders the two possible diastereoisomers **C1/D1**. The oxidative addition of dihydrogen to obtain the rhodium (III) dihydride **C2/D2** is the rate determining step. This step determines the enantioselectivity. After a migratory insertion of the coordinated alkene into one of the Rh–H bond generates the hydrido alkyl complex **C3/D3**. Reductive elimination liberates the hydrogenated products and the initial **B** species is regenerated to restart the cycle.⁵⁵

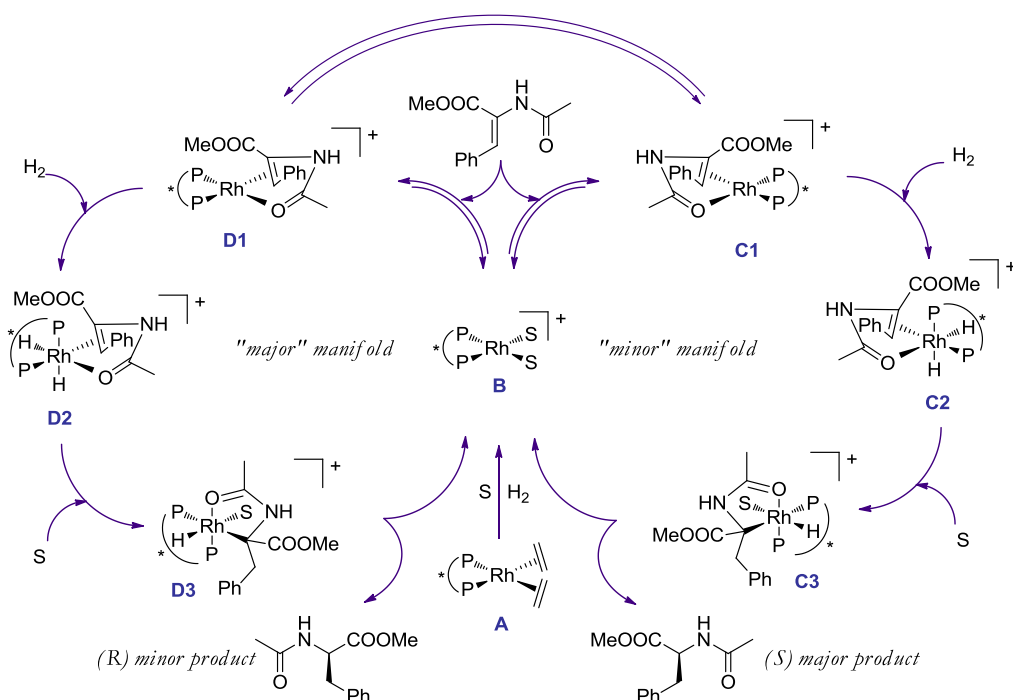


Figure 6. 12. Mechanism proposed by Halpern for the asymmetric hydrogenation.

The studies done by Halpern revealed that diastereoisomer **C1** is thermodynamically less stable than **D1**. *A priori*, it would be expected that the major product of the catalysis would be the enantiomer that comes from the more stable diastereoisomer **D1**, *i.e.*, enantiomer *R*. However, it was demonstrated that the

oxidative addition of dihydrogen to **C1** is much faster. Additionally, **C1** and **D1** can interconvert fast inter- and intramolecularly. As a result, the major product of the catalysis is the *S* enantiomer, which comes from the “minor” manifold of the cycle (anti lock-and-key postulate).^{52–55}

Later on, Landis *et al.* carried out theoretical calculations which support the anti lock-and-key postulate.^{61–64} Noyori proposed that the system involving BINAP-Rh complexes for the hydrogenation of enamides follows the Halpern mechanism.^{40,42}

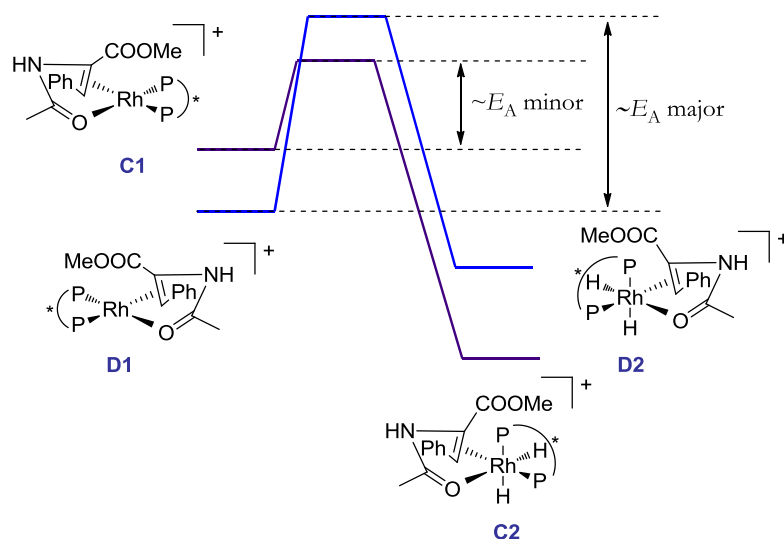


Figure 6. 13. Schematic reaction coordinates for the enantiodiscrimination in Halpern’s mechanism.

After realizing on the limitations of the initial mechanism to explain the results with the diphosphines with electron donating substituents, Gridnev and Imamoto proposed the so-called dihydride mechanism (Figure 6. 14).^{65–68} The main difference with the previous one is that the oxidative addition of the dihydride to the rhodium complex takes place before the coordination of the substrate forming a dihydride complex **E**. Then the substrate coordinates to the rhodium, followed by a migratory insertion to obtain **G**, which is the rate determining step. Finally the reductive elimination generates the hydrogenated product and the initial solvate complex **B**. The formation of one enantiomer preferentially depends on the stability of the

intermediate **G**, which strongly depends on the ligand properties. The detection of agostic dihydride intermediates formed prior to substrate addition was reported by Brown *et al.* (using a rhodium-phanephos complex),^{59,60} which supported the theory of the dihydride mechanism.

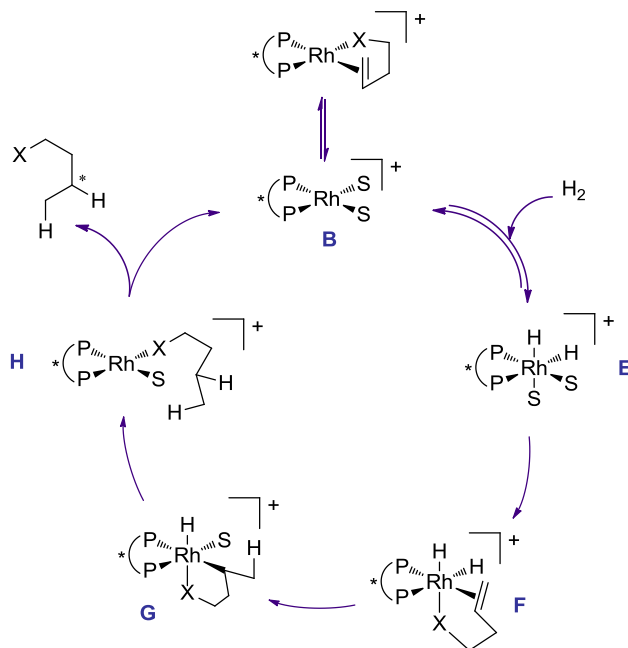
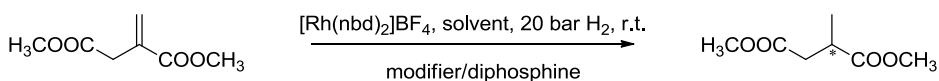


Figure 6. 14. Dihydride mechanism proposed by Gridnev for the asymmetric hydrogenation.

In fact the mechanism proposed by Gridnev and Imamonto does not discard completely the previous Halpern's mechanism already known; the mechanisms are interconnected via the common intermediate **B**.⁶⁷



Scheme 6. 12. Asymmetric hydrogenation of dimethyl itaconate.

The model reaction chosen to test the chiral supramolecular diphosphine was the

asymmetric hydrogenation of dimethyl itaconate (Scheme 6. 12).⁶⁹ Schmidt *et al.* studied the reactivity of the system rhodium/DIPAMP with dimethyl itaconate in methanol.⁷⁰ The NMR and X-Ray results that they obtained pointed out that the studied system followed the Halpern's mechanism.

For industrial applications, there is an increasing interest in the use of water-soluble organometallic catalysts. The reasons are the possibility to use of water as an environmentally benign solvent, together with the advantage of separation the product and catalyst in an aqueous-organic two phase system.⁷¹⁻⁷³ Furthermore, high conversions have been found for the asymmetric hydrogenation in methanol (and other polar solvents).^{74,75} Taking advantage of the high polarity (and solubility in polar solvents, and water) of both sulfonate and ammonium salts involved in the supramolecular system, the solvents selected to start the catalytic tests were methanol and a mixture of water/methanol (1/1).

Table 6. 6. Conversion obtained for the asymmetric hydrogenation of dimethyl itaconate using **43K** as ligand together with modifier **44** (combined with several counter ions) in MeOH.

Entry	Modifier	Conversion (%)
1	44 ^a	0
2	44Cl	2
3	44BPh₄	1
4	44BF₄	51

Conditions: r.t., 20 bar H₂. 10 min supramolecular complex formation, 5 min pre-catalyst formation, 1 h reaction, [Rh] = 3 mM, substrate/modifier/L/Rh = 250/1.05/1.05/1.

^a 1,2-diaminocyclohexane.

The hydrogenation was carried out by mixing in the selected solvent diphosphine **43K** with one equivalent of the corresponding modifier. After ten minutes (to guarantee the formation of the supramolecular complex), the metal precursor [Rh(nbd)₂]BF₄ was added. The *in situ* formation of the pre-catalyst [Rh(L)(nbd)]⁺ was considered to be complete within five minutes. Then, the substrate was added, and the reactor was pressurized to 20 bar of H₂. The experiments were run for 1h at r.t.

Initially, the effect of the counter ions of the ammonium salts on the activity was studied. 1,2-diaminecyclohexane (as a racemic mixture) was reacted with two equivalents of several acids to form its corresponding diammonium salts (see 6.2.2). **44BF₄**, **44Cl** and **44BPh₄** were tested in the asymmetric hydrogenation of dimethyl itaconate and the results are shown in Table 6. 6.

The best result was obtained when the counterion of the diammonium salt was BF₄⁻ (Table 6. 6, entry 4). When 1,2-diaminocyclohexane was used (instead of the diammonium salts, Table 6. 6, entry 1), no conversion was observed. This can be due to coordination of the diamine to rhodium as a co-ligand of the diphosphine, and deactivation of the catalyst. No activity was observed when using **44Cl**, which can be attributed to the possible coordination of Cl⁻ ions to Rh, blocking the catalyst. No satisfactory explanation, however, was found for the lack of reactivity of **44BPh₄** (Table 6. 6 entry 3). Therefore, BF₄⁻ was chosen as counterion to test the enantiopure modifiers.

Table 6. 7. Conversions and ee obtained for the asymmetric hydrogenation of dimethyl itaconate with chiral modifiers and **43K** in MeOH.

Entry	Modifier	Conversion (%)	ee (%), R)
1	(+)- 44BF₄	60	0
2	(+)- 45BF₄	96	12
3	(+)- 46BF₄	73	0
4	(-)- 47BF₄	78	0

Conditions: r.t., 20 bar H₂. 10 min supramolecular complex formation, 5 min catalyst preformation, 1 h reaction, [Rh] = 3 mM, substrate/modifier/L/Rh = 250/1.05/1.05/1.

Moderate to high conversions were obtained for all enantiopure modifiers tested. The best result was observed when (+)-**45BF₄** was used as modifier, with 96 % conversion and 12 % of ee (Table 6. 7, entry 2). Interestingly, we also observed in the previous supramolecular studies that modifier **45** was found to be the one with the best fitting towards **43K** to form the supramolecular **c-GG·HH** (1:1) complex (the binding constant of modifier **47** was not studied).

The formation of the supramolecular complex was carried out prior to formation of the metallic complex with the diphosphine. It was decided to invert the order of addition in the formation of the complexes to see if this affects the catalytic results. Thus, first the metal precursor was mixed with diphosphine **43K** and then the modifier was added. As in the previous example, an analysis of the influence of the counterion was performed on racemic modifiers.

Table 6. 8. Conversion and ee values obtained in the asymmetric hydrogenation of dimethyl itaconate using as ligand **43K** together with different modifiers in methanol. The chiral modifier is added after rhodium diphosphines complex formation.

Entry	Modifier	Conversion (%)	ee (% _R)
1	44^a	0	-
2	44Cl	0	-
3	44BPh₄	0	-
4	44BF₄	72	-

5	(+)- 44BF₄	88	0
6	(+)- 45BF₄	94	11
7	(+)- 46BF₄	100	1
8	(-)- 47BF₄	8	0

Conditions: r.t., 20 bar H₂. 10 min supramolecular complex formation, 5 min pre-catalyst formation, 1 h reaction, [Rh] = 3 mM, substrate/modifier/L/Rh = 250/1.05/1.05/1.

^a 1,2-diaminecyclohexane.

From these results, presented in Table 6. 8, it is noticed that no significant changes are observed when the order of addition is inverted. The main difference is the lower reactivity of (-)-**47BF₄**, but the other activities and ee's are very similar. The small ee obtained for **45** indicates that the initially formed racemic phosphine complex rearranges to give an excess of one of the two chiral conformations, which possibly involves dissociation of one of the phosphine groups of the bidentate.

An additional experiment was done changing the solvent to a 1:1 mixture of water/methanol to study the influence of the solvent. As in the previous examples,

the effect of the counterion is studied on racemic **44**. Results are summarized in Table 6. 9.

Table 6. 9. Conversion and ee values obtained in the asymmetric hydrogenation of dimethyl itaconate for different modifiers with **43K** in a 1:1 mixture of water/methanol.

Entry	Modifier	Conversion (%)	ee (% _R)
1	44Cl	50	-
2	44BF₄	77	-
3	44PF₆	96	-

4	(+)- 45BF₄	100	19

Conditions: r.t., 20 bar H₂. 10 min supramolecular complex formation, 5 min catalyst preformation, 1 h reaction, [Rh] = 3 mM, substrate/modifier/L/Rh = 250/1.05/1.05/1.

In this case, it was not possible to test the behaviour of **44BPh₄** because of the lack of solubility of this salt in the mixture of water/methanol. The stronger solvation of Cl⁻ in water reduces the inhibition observed in less polar media. **44PF₆** presented the highest activity found with modifier **44**. The best result with methanol in terms of enantioselectivity was found previously for (+)-**45BF₄**, and thus this system was tested also using the mixture of water/methanol, which resulted in a slightly higher activity and enantioselectivity.

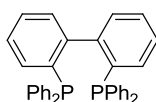


Figure 6. 15. Diphosphine **57**, used as control.

To ensure that the enantiomeric excess is due to the formation of the supramolecular interaction, a couple of additional tests were performed. Commercial *trans*-diphosphine **57** (BIPHEP), which does not have any functional group to interact with the modifier, was used instead of **43K**. As a control test, the catalysis was also done without any diphosphine, and only with diammonium salt (+)-**45BF₄**.

In all cases full conversion was reached. Unfortunately, when considering the options without formation of the supramolecular complex, *i.e.*, only using modifier (+)-**45BF**₄, or when this modifier was used in combination with diphosphine **57**, similar values of ee were obtained to those presented before.

Table 6. 10. Conversions and ee obtained for the asymmetric hydrogenation of dimethyl itaconate with using different diphosphines and modifier (+)-**45BF**₄ in MeOH.

Entry	Diphosphine	Modifier	Conversion (%)	ee (% _R)
1	43K	-	100	-
2	57	-	100	-
3	57	(+)- 45BF ₄	100	15
4	-	(+)- 45BF ₄	100	13

Conditions: r.t., 20 bar H₂. 10 min supramolecular complex formation, 5 min catalyst preformation, 1 h reaction, [Rh] = 3 mM, substrate/modifier/L/Rh = 250/1.05/1.05/1.

Unfortunately, these results evidence that the chiral induction observed in catalysis may not due to the formation of a supramolecular complex, but is inherent to an effect that the diammonium salt (+)-**45BF**₄ has in the media, such as the use of chiral ionic liquids has on the catalysis in the studies performed by Leitner.⁷⁶ In fact, very recently the same authors have described the use of a chiral borate anion based on a binaphthol moiety to induce ee in the asymmetric hydrogenation of dimethyl itaconate with a racemic BINAP/Rh complex.⁷⁷

Further supramolecular analysis

In view of the results obtained in catalysis, an additional titration trying to reproduce catalytic conditions was performed using as host diphosphine **43K** and (+)-**45BF**₄ as guest. The solvent was MeOD, and the concentration of host was 5 mM, similar to the ligand concentration used in catalysis. ³¹P{¹H}-NMR spectroscopy

was used to follow the variation in the chemical shift of the phosphorus atoms of the host as overlap of host signals with guest signals occurs in the ^1H -NMR spectra.

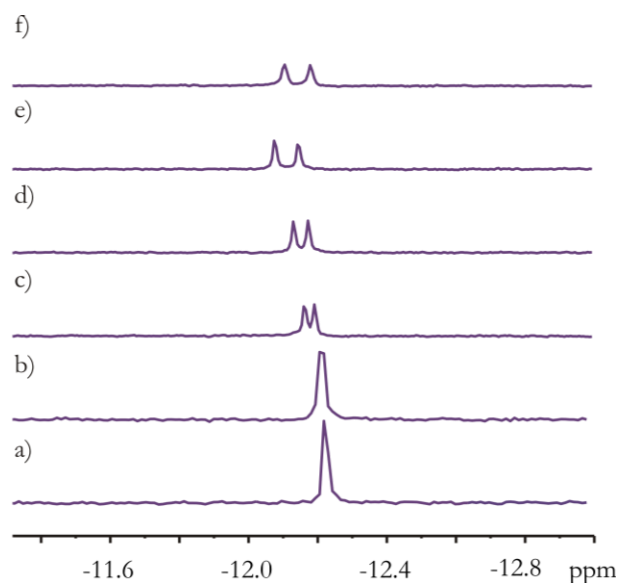


Figure 6. 16. Selected region of the $^{31}\text{P}\{^1\text{H}\}$ -NMR titration of **43K** with (R)-(+)-**45BF₄** in MeOD- D_4 at 25 °C. a) **43K**; b) **43K** + 0.5 eq. of (R)-(+)-**45BF₄**; c) **43K** + 0.8 eq. of (R)-(+)-**45BF₄**; d) **43K** + 1 eq. of (R)-(+)-**45BF₄**; e) **43K** + 2 eq. of (R)-(+)-**45BF₄**; f) **43K** + 6 eq. of (R)-(+)-**45BF₄**. [**43K**] = 5 mM.

Two $^{31}\text{P}\{^1\text{H}\}$ -NMR signals were observed upon successive additions of the chiral modifier (Figure 6. 16). This can be attributed to the fact that the equilibrium between free and complexed host is fast on the NMR timescale (as presented in Scheme 6. 13), while the interconversion of the two *tropo*enantiomers of host **43K** show slow exchange on the NMR timescale (Biphep's half-life time of the enantiomers may be as large as 15 min, see chapter 5). Thus, two signals are observed, which shift upon the addition of guest (the chemical shift is an averaged value between the ones of free and bound host). A doubling of the signal was also observed in the $^1\text{H}\{^{31}\text{P}\}$ -NMR for H1 (highlighted in Scheme 6. 13) of host **43K** (Figure 6. 18).

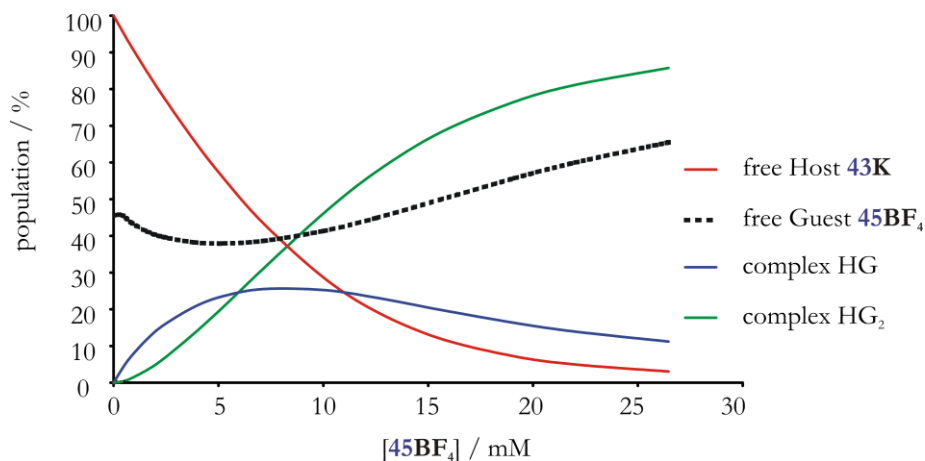
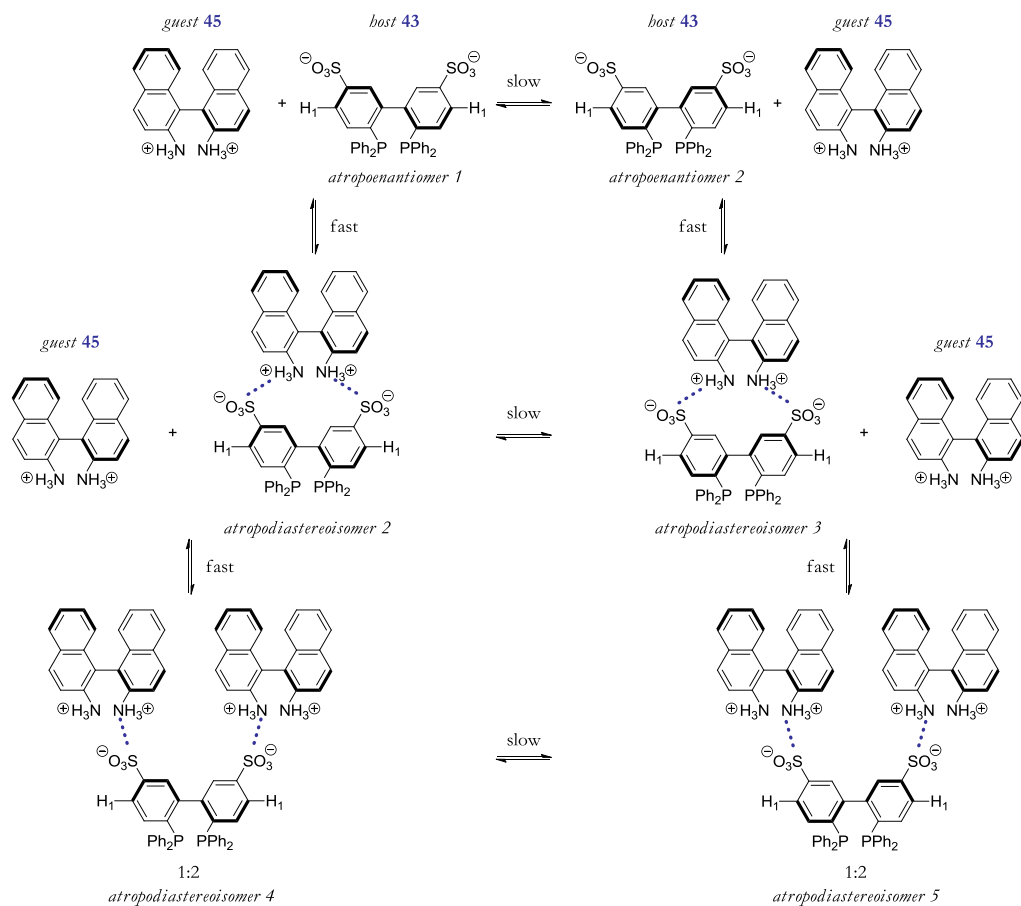


Figure 6. 17. Representation of the speciation diagram during the titration using **43K** as host and (+)-**45BF₄** as guest. [**43K**] = 5 mM. Population of H, HG and HG₂ calculated based on the mass balance $H + HG + HG_2 = H_{total}$; population of G calculated based on the mass balance $G + HG + 2 \cdot HG_2 = G_{total}$.

The two signals observed in the $^{31}\text{P}\{^1\text{H}\}$ -NMR were fitted to a binding model that supposes the formation of a 1:1 complex (which includes $\alpha\text{-GG}\cdot\text{HH}$ and $\text{c-GG}\cdot\text{HH}$) and a 1:2 complex. The association constants obtained for the fitting were $K_{1:1} = 213 \text{ M}^{-1}$ and $K_{1:2} = 94100 \text{ M}^{-2}$.

From the speciation diagram (Figure 6. 17), one can notice that at high guest concentration, the 1:2 species was the most populated one, while the 1:1 species is always the minor one. However, at the concentrations used in catalysis, where the host and guest are in equimolar ratio, one can observe that, in contrast with our previous observations when the system was studied in CDCl_3 , (Fig. 6. 10) the major species are the free host and free guest. This could explain the identical results obtained in catalysis for (+)-**45BF₄** with **43K** and unfunctionalized diphosphine **57**.

Having a look at the speciation diagram, one can notice that after addition of two equivalents of the guest, the 1:2 species starts to be predominant (Figure 6. 17). Furthermore, in the ^{31}P -NMR a change in the trend of the shift is observed when more than two equivalents of the guest are added (Figure 6. 16). This can be attributed to 1:2 complex formation.



Scheme 6. 13. Equilibria showing the possible diastereoisomers formed by assembly between (+)-45 and 43.

The fact that the same results were obtained in absence of phosphine indicates that the cations (+)-45 generate an extremely active and slightly enantioselective system for the hydrogenation which does not require phosphine coordination to the metal.

As a conclusion, we must say that, not surprisingly, the change from less polar solvents, as is chloroform, to polar ones (methanol for instance) produces a dramatic drop in the value of the association constant for the ionic assemblies.

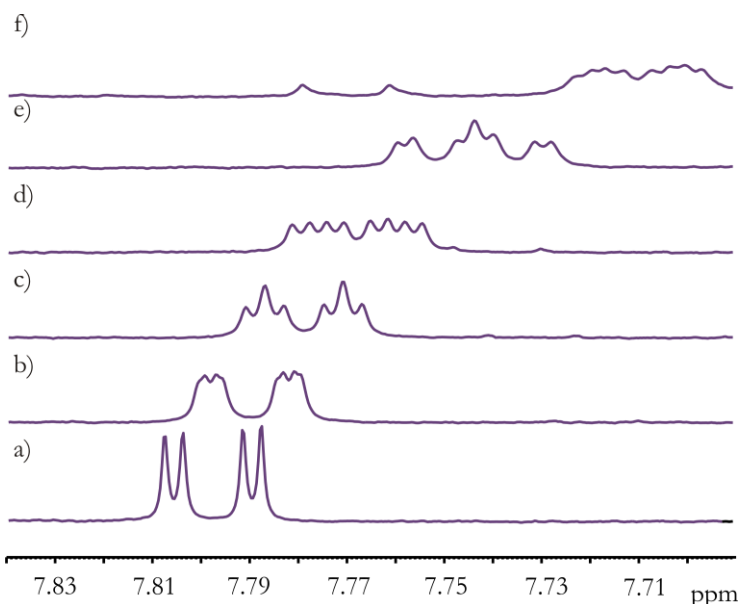


Figure 6. 18. Selected region of the $^1\text{H}\{^{31}\text{P}\}$ -NMR titration of **43K** with (R)-(+)-**45BF₄** in MeOD-D₄ at 25 °C. a) **43K**; b) **43K** + 0.5 eq. of (+)**45BF₄**; c) **43K** + 0.8 eq. of (+)**45BF₄**; d) **43K** + 1 eq. of (+)**45BF₄**; e) **43K** + 2 eq. of (+)**45BF₄**; f) **43K** + 6 eq. of (+)**45BF₄**. [**43K**] = 5 mM.

The use of organic solvents could be considered for future catalytic studies, to analyze if the enantioinduction from the chiral modifier to the *tropos* molecule can be achieved by ionic supramolecular interactions. Accordingly, the appropriate counterions, to solubilize the species in organic solvents, should be used.

6.3. CONCLUDING REMARKS

In this chapter we designed a system that takes benefit of supramolecular interactions to induce chirality to a *tropos* generic diphosphine.

Two supramolecular interactions were initially considered: hydrogen bonding and ionic interactions. The precursors of the biaryl diphosphines were synthesized to study the supramolecular properties of the forces involved.

Hydrogen bonding interaction was discarded due to the low binding interaction

for the systems considered when predicting the association constants using Hunter's approach.

Regarding the ionic interaction, three diammonium salts were used to study the interaction with the precursor of the sulfonate diphosphine **56**: **44BPh₄**, **45BPh₄** and **46BPh₄**. It was found that the combination of **56** with **45BPh₄** in CDCl₃, the major species present in the range of concentrations considered was the ring-closed dimer **c-GG·HH**, which was considered to be the one that would induce the highest chirality in the *tropos* backbone.

When performing the catalysis, the counterion of the diammonium salt played an important role in the activity of the asymmetric hydrogenation. The higher activity was found when using BF₄⁻ in methanol as solvent, and PF₆⁻ in a 1:1 mixture of methanol/water.

Enantioselectivity was only observed in catalysis when modifier **45** was involved. However, further catalytic experiments using the modifier without a diphosphine and also a diphosphine with no functional groups on the aryl backbone showed that the same ee values were obtained. This may be coincidental, or it may point to an induction mechanism different from the supramolecular ionic interaction considered initially.

Further NMR titrations under conditions similar to the catalytic ones demonstrated that the change to polar solvents has a detrimental effect on the supramolecular aggregate, and free host and free guest molecules are the major species present under these conditions. Consequently, for future work new approaches are needed. Several possibilities could be envisaged: the use of another type of supramolecular interaction, the use of more recognition points per molecule to increase the strength of the interaction, the use of less polar solvents, or the use of more extended biaryl systems as in VAPOL type ligands to obtain a more profound "embracing" of host and guest.

References and notes

1. Schneider, H. J. *Angew. Chem., Int. Ed.* **2009**, *48*, 3924.
2. Gulyas, H.; Benet-Buchholz, J.; Escudero-Adan, E. C.; Freixa, Z.; van Leeuwen, P. W. N. M. *Chem.-Eur. J.* **2007**, *13*, 3424.
3. Sala, X.; Suarez, E. J. G.; Freixa, Z.; Benet-Buchholz, J.; van Leeuwen, P. W. N. M. *Eur. J. Org. Chem.* **2008**, 6197.
4. Guerreiro, P.; Ratovelomanana-Vidal, V.; Genet, J. P.; Dellis, P. *Tetrahedron Lett.* **2001**, *42*, 3423.
5. Ter Halle, R.; Colasson, B.; Schulz, E.; Spagnol, M.; Lemaire, M. *Tetrahedron Lett.* **2000**, *41*, 643.
6. Hassan, J.; Sevignon, M.; Gozzi, C.; Schulz, E.; Lemaire, M. *Chem. Rev.* **2002**, *102*, 1359.
7. Gilman, H.; Gaj, B. J. *J. Org. Chem.* **1957**, *22*, 447.
8. Dougherty, T. K.; Lau, K. S. Y.; Hedberg, F. L. *J. Org. Chem.* **1983**, *48*, 5273.
9. Oldridge, L.; Kastler, M.; Muellen, K. *Chem. Commun.* **2006**, 885.
10. Parlow, J. J.; South, M. S. *Tetrahedron* **2003**, *59*, 7695.
11. Herd, O.; Hoff, D.; Kottsieper, K. W.; Liek, C.; Wenz, K.; Stelzer, O.; Sheldrick, W. S. *Inorg. Chem.* **2002**, *41*, 5034.
12. Hunter, C. A. *Angew. Chem., Int. Ed.* **2004**, *43*, 5310.
13. Abraham, M. H.; Grellier, P. L.; Prior, D. V.; Duce, P. P.; Morris, J. J.; Taylor, P. J. *J. Chem. Soc., Perkin Trans. 2* **1989**, 699.
14. Abraham, M. H.; Grellier, P. L.; Prior, D. V.; Morris, J. J.; Taylor, P. J. *J. Chem. Soc., Perkin Trans. 2* **1990**, 521.
15. Taylor, R. P.; Kuntz, I. D. *J. Am. Chem. Soc.* **1970**, *92*, 4813.
16. Kuntz, I. D., Jr.; Taylor, R. P. *J. Phys. Chem.* **1970**, *74*, 4573.
17. Singh, S.; Rao, C. N. R. *Trans. Faraday Soc.* **1966**, *62*, 3310.
18. Green, R. D.; Martin, J. S. J. *Am. Chem. Soc.* **1968**, *90*, 3659.
19. Abraham, M. H.; Zhao, Y. H. *J. Org. Chem.* **2004**, *69*, 4677.
20. Allerhand, A.; Schleyer, P. V. J. *Am. Chem. Soc.* **1963**, *85*, 1233.
21. The observed changes in chemical shift of the host signals as a function of guest concentration were analyzed using purpose-written software authored by Prof. C. A. Hunter, which yields the association constant, the bound chemical shift and the free chemical shift.
22. Simulation done with SPECFIT, v 3.0.36, Spectrum Software Associates.
23. Error given as standard deviation of both values.
24. Hunter, C. A.; Anderson, H. L. *Angew. Chem., Int. Ed.* **2009**, *48*, 7488.
25. Hunter, C. A.; Tomas, S. *Chem. Biol.* **2003**, *10*, 1023.
26. Williams, D. H.; Davies, N. L.; Koivisto, J. J. *J. Am. Chem. Soc.* **2004**, *126*, 14267.
27. Chekmeneva, E.; Hunter, C. A.; Packer, M. J.; Turega, S. M. *J. Am. Chem. Soc.* **2008**, *130*, 17718.
28. Bailey, W. F.; Monahan, A. S. *J. Chem. Educ.* **1978**, *55*, 489.

29. Misuraca, M.C.; Grecu, T.; Hunter, C.A.; Turega, S.M.; Garavini, V.; Segarra-Maset, M.D.; van Leeuwen P.W.N.M.; Freixa, Z. *In preparation*.
30. Osborn, J. A.; Jardine, F. H.; Young, J. F.; Wilkinson, G. *J. Chem. Soc.* **1966**, 1711.
31. Knowles, W. S.; Sabacky, M. J. *Chem. Commun.* **1968**, 1445.
32. Horner, L.; Siegel, H.; Buthe, H. *Angew. Chem., Int. Ed.* **1968**, 7, 942.
33. Knowles, W. S.; Vineyard, B. D.; Sabacky, M. J. *J. Chem. Soc., Chem. Commun.* **1972**, 10.
34. Knowles, W. S.; Sabacky, M. J.; Vineyard, B. D. *Adv. Chem. Ser.* **1974**, 274.
35. Dang, T. P.; Kagan, H. B. *J. Chem. Soc., Chem. Commun.* **1971**, 481.
36. Kagan, H. B.; Dang, T. P. *J. Am. Chem. Soc.* **1972**, 94, 6429.
37. Knowles, W. S. *J. Chem. Educ.* **1986**, 63, 222.
38. Knowles, W. S.; Sabacky, M. J.; Vineyard, B. D.; Weinkauff, D. J. *J. Am. Chem. Soc.* **1975**, 97, 2567.
39. Knowles, W. S. *Acc. Chem. Res.* **1983**, 16, 106.
40. Miyashita, A.; Yasuda, A.; Takaya, H.; Toriumi, K.; Ito, T.; Souchi, T.; Noyori, R. *J. Am. Chem. Soc.* **1980**, 102, 7932.
41. Miyashita, A.; Takaya, H.; Souchi, T.; Noyori, R. *Tetrahedron* **1984**, 40, 1245.
42. Noyori, R.; Kitamura, M.; Ohkuma, T. *Proc. Natl. Acad. Sci. U. S. A.* **2004**, 101, 5356.
43. Knowles, W. S. *Adv. Synth. Catal.* **2003**, 345, 3.
44. Noyori, R. *Angew. Chem., Int. Ed.* **2002**, 41, 2008.
45. Burk, M. J.; Feaster, J. E.; Harlow, R. L. *Organometallics* **1990**, 9, 2653.
46. Burk, M. J. *J. Am. Chem. Soc.* **1991**, 113, 8518.
47. Burk, M. J. *Acc. Chem. Res.* **2000**, 33, 363.
48. Knowles, W. S.; Noyori, R. *Acc. Chem. Res.* **2007**, 40, 1238.
49. Jaekel, C.; Paciello, R. *Chem. Rev. (Washington, DC, U. S.)* **2006**, 106, 2912.
50. Young, J. F.; Osborn, J. A.; Jardine, F. H.; Wilkinson, G. *Chem. Commun.* **1965**, 131.
51. Halpern, J.; Riley, D. P.; Chan, A. S. C.; Pluth, J. J. *J. Am. Chem. Soc.* **1977**, 99, 8055.
52. Halpern, J. *Science* **1982**, 217, 401.
53. Halpern, J. *New Front. Organomet. Inorg. Chem., Proc. China-Jpn.-U.S.A. Trilateral Semin., 2nd* **1984**, 269.
54. Halpern, J. *Asymmetric Synth.* **1985**, 5, 41.
55. Landis, C. R.; Halpern, J. *J. Am. Chem. Soc.* **1987**, 109, 1746.
56. Brown, J. M.; Chaloner, P. A. *J. Am. Chem. Soc.* **1980**, 102, 3040.
57. Brown, J. M.; Chaloner, P. A.; Parker, D. *Adv. Chem. Ser.* **1982**, 196, 355.
58. Brown, J. M.; Parker, D. *J. Org. Chem.* **1982**, 47, 2722.
59. Giernoth, R.; Heinrich, H.; Adams, N. J.; Deeth, R. J.; Bargon, J.; Brown, J. M. *J. Am. Chem. Soc.* **2000**, 122, 12381.
60. Heinrich, H.; Giernoth, R.; Bargon, J.; Brown, J. M. *Chem. Commun.* **2001**, 1296.
61. Landis, C. R.; Hilfenhaus, P.; Feldgus, S. *J. Am. Chem. Soc.* **1999**, 121, 8741.
62. Feldgus, S.; Landis, C. R. *J. Am. Chem. Soc.* **2000**, 122, 12714.
63. Landis, C. R.; Feldgus, S. *Angew. Chem., Int. Ed.* **2000**, 39, 2863.
64. Feldgus, S.; Landis, C. R. *Organometallics* **2001**, 20, 2374.
65. Gridnev, I. D.; Higashi, N.; Asakura, K.; Imamoto, T. *J. Am. Chem. Soc.* **2000**, 122, 7183.

66. Gridnev, I. D.; Higashi, N.; Imamoto, T. *Organometallics* **2001**, *20*, 4542.
67. Gridnev, I. D.; Imamoto, T. *Acc. Chem. Res.* **2004**, *37*, 633.
68. Gridnev, I. D.; Imamoto, T. *Chem. Commun.* **2009**, 7447.
69. Gergely, I.; Hegedus, C.; Gulyas, H.; Szollosy, A.; Monsees, A.; Riermeier, T.; Bakos, J. *Tetrahedron: Asymmetry* **2003**, *14*, 1087.
70. Schmidt, T.; Dai, Z.; Drexler, H. J.; Baumann, W.; Jager, C.; Pfeifer, D.; Heller, D. *Chem.--Eur. J.* **2008**, *14*, 4469.
71. Wan, K. T.; Davis, M. E. *J. Chem. Soc., Chem. Commun.* **1993**, 1262.
72. Schmid, R.; Broger, E. A.; Cereghetti, M.; Cramer, Y.; Foricher, J.; Lalonde, M.; Muller, R. K.; Scalone, M.; Schoettel, G.; Zutter, U. *Pure Appl. Chem.* **1996**, *68*, 131.
73. Grassert, I.; Kovacs, J.; Fuhrmann, H.; Oehme, G. *Adv. Synth. Catal.* **2002**, *344*, 312.
74. Gridnev, I. D.; Imamoto, T.; Hoge, G.; Kouchi, M.; Takahashi, H. *J. Am. Chem. Soc.* **2008**, *130*, 2560.
75. Zou, Y. P.; Geng, H. L.; Zhang, W. C.; Yu, S. C.; Zhang, X. M. *Tetrahedron Lett.* **2009**, *50*, 5777.
76. Schmitkamp, M.; Chen, D.; Leitner, W.; Klankermayer, J.; Francio, G. *Chem. Commun.* **2007**, 4012.
77. Chen, D. J.; Sundararaju, B.; Krause, R.; Klankermayer, J.; Dixneuf, P. H.; Leitner, W. *Chemcatchem* **2010**, *2*, 55.

UNIVERSITAT ROVIRA I VIRGILI
SWITCHABLE AND TUNABLE LIGANDS FOR HOMOGENEOUS CATALYSIS
Maria Dolores Segarra Maset
ISBN:978-84-693-7666-9/DL:T-1755-2010

CHAPTER 7

EXPERIMENTAL

7.1. GENERAL PROCEDURES

Unless otherwise stated, all preparations were carried out under an inert atmosphere of argon using standard Schlenk techniques. All reagents were obtained from commercial suppliers and used without further purification. Solvents were purified using SPS-400-6 from Innovative Technologies, Inc.

Routine ^1H -, $^{13}\text{C}\{^1\text{H}\}$ -, $^{31}\text{P}\{^1\text{H}\}$ -, and $^{19}\text{F}\{^1\text{H}\}$ -NMR spectra were recorded on a Bruker Avance 400 Ultrashield spectrometer (400.1 MHz for ^1H -, 100.6 MHz for $^{13}\text{C}\{^1\text{H}\}$ -, 162.0 MHz for $^{31}\text{P}\{^1\text{H}\}$ -, and 376.5 MHz for $^{19}\text{F}\{^1\text{H}\}$ -NMR), or Bruker Avance 500 Ultrashield spectrometer (500.1 MHz for ^1H -, 125.7 MHz for $^{13}\text{C}\{^1\text{H}\}$ - and 202.5 MHz for $^{31}\text{P}\{^1\text{H}\}$ -NMR). Chemical shifts, δ , are given in ppm, relative to TMS (^1H , ^{13}C), 85% H_3PO_4 (^{31}P), and CCl_3F (^{19}F). Coupling constants, J , are given in Hz.

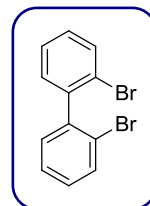
Mass spectra were recorded on a Waters LCT Premier ESI-TOF spectrometer, or in a Waters GTC spectrometer, or in a MALDI-TOF (Autoflex, Bruker Daltonics).

Gas chromatography analyses were performed on an Agilent Technologies 6890N/G1530N apparatus equipped with a FID detector and β -DEX 225 column (length 30 m, internal diameter 0.25 mm, film thickness 0.25 μm).

7.2. SYNTHESIS

2,2'-dibromo-1,1'-biphenyl (48)

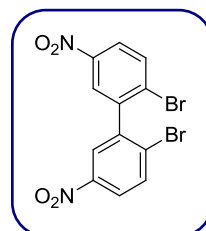
1,2-dibromobenzene (12.6 mL, 105.75 mmol) was dissolved in 250 mL of dried THF and cooled to $-79\text{ }^{\circ}\text{C}$. Then, *n*-BuLi (34.36 mL, 54.98 mmol, 1.6 M in hexanes) was added dropwise, and the reaction mixture was stirred while warming up slowly to r.t. After 2 h, 60 mL of HCl (36 % aq. soln.) were added and when the reaction reached room temperature the crude was partitioned 3x50 mL of Et₂O. The organics were collected, dried over MgSO₄ filtered and concentrated. The solid was recrystallized from EtOH to obtain 7.17 g of white needles (44 % yield).



¹H-NMR (CDCl₃, 400.1 MHz) δ (ppm): 7.27 (d, *J* = 7.3 Hz, 2H), 7.28 (m, 2H), 7.4 (m, 2H), 7.69 (d, *J* = 7.8 Hz, 2H); ¹³C{¹H} NMR (CDCl₃, 100.6 MHz) δ (ppm): 123.52, 127.12, 129.39, 130.98, 132.58, 142.06. GCMS (ESI+ve) *m/z* (% relative intensity): 310.0 ([C₁₂H₈⁷⁹Br₂]^{•+}, 100 %), 231.0 ([C₁₂H₈⁷⁹Br]⁺, 53 %), 152.0 ([C₁₂H₈]^{•+}, 25 %).¹⁻³

2,2'-dibromo-5,5'-dinitro-1,1'-biphenyl (49)

48 (7 g, 22.43 mmol) was dissolved in 28 mL of CH₂Cl₂ in a three-necked 250 mL round bottom flask and 116 mL of H₂SO₄ (96 % aq. soln.) were added. The mixture was cooled in an ice/water bath and then 36 mL of HNO₃ (65 % aq. soln.) were added dropwise via a dropping funnel. The mixture was left stirring to reach room temperature and then it was poured into 700 mL of water and extracted by 4x100 mL of CH₂Cl₂. The organics were collected, dried over MgSO₄, filtered and the filtrate concentrated to dryness. The residue was recrystallized from a mixture of acetone/ethanol (1:3) to obtain 4.25 g of yellowish crystals (47 % yield).



¹H-NMR (CDCl₃, 400.1 MHz) δ (ppm): 7.92 (d, *J* = 8.8 Hz, 2H), 8.15 (d, *J* = 2.6 Hz, 2H), 8.2 (dd, *J* = 8.8 Hz, *J* = 2.6 Hz, 2H); ¹³C{¹H} NMR (CDCl₃, 100.6 MHz) δ (ppm): 124.93, 125.66, 130.79, 134.16, 141.28, 147.11. HR-MS (MALDI-TOF): calcd

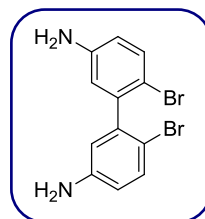
for $C_{12}H_6Br_2N_2O_4$ 399.8700, found 399.8681.³

6,6'-dibromo-(1,1'-biphenyl)-3,3'-diamine (50)

49 (3.67 g, 9.13 mmol) was dissolved in 75 mL of acetic acid glacial, Fe (powder, 5.1 g, 91.31 mmol) was added and the mixture was heated to 80 °C. After 30 min the mixture was filtered over Celite® 545 with diethyl ether and ethyl acetate. The organics were washed with water and brine, dried over $MgSO_4$ and filtered.

After removal of the solvent, the residue was subjected to silica chromatography using as eluent a mixture of ethyl acetate and hexane 1:1.5 (0.1 % v/v of NEt_3) to recover 0.69 g of pure product (22 % yield).

1H -NMR (CD_3CN , 400.1 MHz) δ (ppm): 7.07 (d, $J = 2.27$ Hz, 2H), 7.17 (dd, $J = 8.59$ Hz, $J = 2.27$ Hz, 2H), 7.68 (d, $J = 8.59$ Hz, 2H), 8.14 (br s, 4H); $^{13}C\{^1H\}$ -NMR (CD_3CN , 100.6 MHz) δ (ppm): 117.37, 122.12, 122.79, 133.68, 135.80, 142.16. HR-MS (ESI+ve): m/z calcd for $C_{12}H_{11}N_2Br_2$ ($[M+H]^+$) 340.9289, found 340.9274.

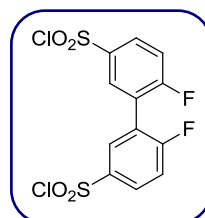


5,5'-bis(chlorosulfonyl)-2,2'-difluoro-1,1'-biphenyl (51)

2,2'-difluoro-1,1'-biphenyl (4.92 g, 25.87 mmol) was dissolved in 80 mL of chloroform and added dropwise to 21.21 mL of chlorosulfonic acid. It was stirred overnight at room temperature and after that the mixture was poured onto 30 g of ice. The aqueous layer was washed three times with 50 mL of chloroform

and the organics were washed with a saturated solution of $NaHCO_3$ in water. The solvent was removed under vacuum to obtain 7.92 g of a white solid. (79 % yield).

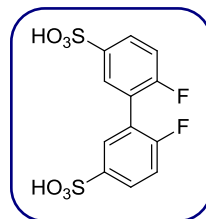
$^1H\{^{19}F\}$ -NMR ($CDCl_3$, 400.1 MHz) δ (ppm): 7.49 (d, $J = 8.8$ Hz, 2H), 8.16 (d, $J = 2.44$ Hz, 2H), 8.2 (dd, $J = 8.8$ Hz, $J = 2.44$ Hz, 2H); $^{19}F\{^1H\}$ -NMR ($CDCl_3$, 376.5 MHz) δ (ppm): -101.⁴



2,2'-difluoro-1,1'-biphenyl-5,5'-bis(sulfonic acid) (**52**)

51 (7.92 g, 20.45 mmol) was dispersed in 21 mL of water and heated to reflux. Then, 33 mL of acetic acid were added and after 2 hours the yellow dissolution was concentrated to obtain **52** in a quantitative yield.

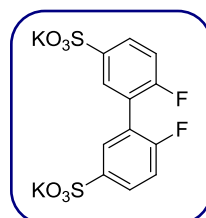
$^1\text{H}\{^{19}\text{F}\}$ -NMR (D_2O , 400.1 MHz) δ (ppm): 7.4 (d, $J = 8.3$ Hz, 2H), 7.9 (dd, $J = 8.3$ Hz, $J = 1.95$ Hz, 2H), 7.93 (d, $J = 1.95$ Hz, 2H); $^{19}\text{F}\{^1\text{H}\}$ -NMR (D_2O , 376.5 MHz) δ (ppm): -111.4



5,5'-bis(sulfonato)-2,2'-difluoro-1,1'-biphenyl dipotassium (**53**)

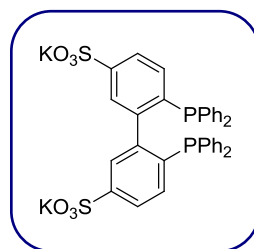
52 (7.16 g, 20.45 mmol) was dissolved in 30 mL of water. Then, solid KOH (2.3 g, 40.91 mmol) was added and the mixture was stirred at room temperature during 1 hour. After that, the solvent was removed under vacuum and the solid was recrystallized from a mixture of water/ethanol (1:2) to obtain 6.19 g of **53** (71 % yield).

$^1\text{H}\{^{19}\text{F}\}$ -NMR (DMSO, 400.1 MHz) δ (ppm): 7.3 (d, $J = 8.8$ Hz, 2H), 7.6 (d, $J = 2.44$ Hz, 2H), 7.69 (dd, $J = 8.8$ Hz, $J = 2.44$, 2H); $^{19}\text{F}\{^1\text{H}\}$ -NMR (DMSO, 376.5 MHz) δ (ppm): -115. MS (ESI-ve): m/z ($[\text{C}_{12}\text{H}_6\text{F}_2\text{O}_6\text{S}_2\text{K}]^-$) 387.0, m/z ($[\text{C}_{12}\text{H}_7\text{F}_2\text{O}_6\text{S}_2]^-$) 349.0, m/z ($[\text{C}_{12}\text{H}_6\text{F}_2\text{O}_6\text{S}_2]^{2-}$) 174.0.4



5,5'-bis(sulfonato)-2,2'-bis(diphenylphosphino)-1,1'-bi-phenyl dipotassium salt (**43**)

Diphenylphosphine (1.35 g, 7.25 mmol) was dissolved under Ar in 5 mL of dry and degassed DMSO. Then, KOH (0.41 g, 7.25 mmol) was added and the mixture was stirred at room temperature during 1 hour. Then, **53** (1.03 g, 2.42 mmol) was added and the crude mixture was heated to 70 °C during 20 hours. Finally, 20 mL of ethanol were added and a white precipitate appeared, which resulted in 1.82 g of **43** (99 % yield).



$^1\text{H}\{^{31}\text{P}\}$ -NMR (DMSO, 400.1 MHz) δ (ppm): 7.07 (d, $J = 8.3$ Hz, 2H), 7.13 (br s,

8H), 7.28 (br s, 6H), 7.34 (br s, 8H), 7.57 (d, $J = 7.55$ Hz, 2H); $^{31}\text{P}\{^1\text{H}\}$ -NMR (DMSO, 162.0 MHz) δ (ppm): -14.25. MS (ESI-ve): m/z ($[\text{C}_{36}\text{H}_{27}\text{O}_6\text{P}_2\text{S}_2]^-$) 680.9, m/z ($[\text{C}_{36}\text{H}_{26}\text{O}_6\text{P}_2\text{S}_2]^{2-}$) 339.9.⁴

General procedure for the synthesis of a tetrabutylammonium sulfonate salts

The corresponding sulfonic acid was dissolved in methanol. KOH (one equivalent per sulfonic group present in the starting compound), was added and the mixture was stirred for 1 hour. A white precipitate appeared, it was filtered and washed with methanol. The solid was dissolved in water and then TBACl (1 or 2 equivalents, depending on the number of functional groups) was added. After 2 hours stirring the final product was extracted from the aqueous layer with dichloromethane, obtaining the final salt as an oily product by evaporation of the solvent.

General procedure for the synthesis of a tetraphenylborate ammonium salts

The corresponding amine was dissolved in dichloromethane and HCl (1 or 2 equivalents, 1.25 M in methanol) was added dropwise. The mixture was stirred for 2 hours and after that the solvent was removed. The residue was dissolved in water and then NaBPh_4 (1 or 2 equivalents depending on the number of functional groups) was added. After 2 hours stirring the final product was extracted from the aqueous layer with dichloromethane, which gives the final salt by evaporation of the solvent.

7.3. NMR TITRATIONS

NMR dilution experiments: To 0.6 mL of the deuterated solvent (CDCl_3) in a NMR tube at r.t., aliquots of a solution (with concentration 0.2-0.3 M approximately) of the corresponding compound studied were added. After each addition the NMR tube was shaken to allow complete mixing of the solutions. The NMR spectra were recorded on a Bruker AMX400 spectrometer. The observed changes in chemical shift were analysed using purpose-written software (authored by Prof. C. A. Hunter) which yields the association constants, the bound chemical shift and the free chemical shift.

NMR titrations: Host solutions were prepared at a known concentration. If the association constant is estimated, the host solutions were prepared approximately $[H] = 1/K$. Guest stock solutions were prepared by dissolving the guest in a sample of the host solution (approximately, $[G] = 10 \cdot [H]$), so the concentration of the host was maintained constant throughout the titration. On addition of aliquots of the guest solution to the host solution contained in the NMR tube, it was thoroughly shaken to mix the solutions. The NMR spectra were recorded on a Bruker AMX400 spectrometer or in a Bruker Avance 500 Ultrashield spectrometer. The observed changes in chemical shift were analysed using purpose-written software (authored by Prof. C. A. Hunter) to calculate the association constants, the bound chemical shift and the free chemical shift.

7.4. CATALYSIS: ASYMMETRIC HYDROGENATION

General procedure: In a flame dried Schlenk vessel, diphosphine (0.021 mmol) and modifier (0.021 mmol) were mixed in 6 mL of the solvent for 10 minutes. The solution was transferred under Ar to a 25 mL stainless steel reactor (SS316Ti) that contains 7.5 mg (0.02 mmol) of $[Rh(nbd)_2]BF_4$ and stirred for 5 minutes. Under Ar, 700 μ L (5 mmol) of dimethyl itaconate were added. Then all was pressurized to 20 bar of H_2 and left reacting at room temperature during one hour. An aliquot was filtered over a small pad of silica, eluted with DCM and analyzed by GC (Table 7. 1).

The catalytic experiments were also performed either with an AMTEC SPR16 multiphase parallel reactor (suited to perform simultaneously four reactions) or HEL-CAT²⁴ multireactor (to perform up to 24 reactions in parallel). When the HEL was used, the reaction conditions were scaled down to 1 mL total reaction volume.

Table 7. 1. Analysis conditions for the determination by GC of the conversion and enantioselectivity in the hydrogenation of dimethyl itaconate.

	Retention time (min)
(<i>R</i>)-dimethyl 2-methylsuccinate	18.0
(<i>S</i>)-dimethyl 2-methylsuccinate	18.7
dimethyl itaconate	24.6

T_{inj} 220 °C; T_{aux} 240 °C; Flow 0.8 mL/min; split 80:1; Ramp: 95 °C (22 min), 5 °C/min up to 150 °C.

References and notes

1. Gilman, H.; Gaj, B. J. *J. Org. Chem.* **1957**, *22*, 447.
2. van Klink, G. P. M.; de Boer, H. J. R.; Schat, G.; Akkerman, O. S.; Bickelhaupt, F.; Spek, A. L. *Organometallics* **2002**, *21*, 2119.
3. Dougherty, T. K.; Lau, K. S. Y.; Hedberg, F. L. *J. Org. Chem.* **1983**, *48*, 5273.
4. Herd, O.; Hoff, D.; Kottsieper, K. W.; Liek, C.; Wenz, K.; Stelzer, O.; Sheldrick, W. S. *Inorg. Chem.* **2002**, *41*, 5034.

PART III

TRANS-BIDENTATE SUPRAMOLECULAR AND SWITCHABLE LIGANDS

UNIVERSITAT ROVIRA I VIRGILI
SWITCHABLE AND TUNABLE LIGANDS FOR HOMOGENEOUS CATALYSIS
Maria Dolores Segarra Maset
ISBN:978-84-693-7666-9/DL:T-1755-2010

CHAPTER 8

INTRODUCTION

A brief history about *trans*-bidentate ligands

The discovery by Wilkinson in the 60s of the catalytic activity of complex $\text{RhCl}(\text{PPh}_3)_3$ in homogeneous hydrogenation,^{1,2} motivated the development of homogeneous catalysis, and the use of phosphine ligands as modifiers. Initially, monodentate ligands were used, such as triphenylphosphine in Wilkinson's catalyst, but soon bidentate ligands were developed, showing higher stability in the corresponding complexes than similar monodentate ones.

The increased stability of bidentate ligands versus monodentate ones is due to the chelate effect, which has been characterized in terms of the entropy change involved in the chelation process.³ Initially, bidentate ligands formed *cis*-complexes in square planar geometries. The stability of *cis*-chelate complexes depends of the chelate ring size, and reaches a maximum for five-membered rings. Thus, chelating ligands found in early literature were based on short carbon chain backbones which stabilized such ring sizes. For instance, the first diphosphine described was 1,2-bis(diphenylphosphino)ethane (dppe).⁴

Furthermore, the use of bidentate ligands opened a door to new reactivities in catalytic processes. For example, when PPh_3 is used in palladium catalyzed carbonylation of ethene in methanol, methyl propionate is formed selectively. On the

contrary, when using 1,3-bis(diphenylphosphino)propane (dppp) a copolymer of ethene and carbon monoxide is obtained.⁵

The catalytic cycles of many catalytic processes involve intermediates having geometries with larger P–M–P angles than those stabilized by *cis* C₂ or C₃ bridged diphosphines. For instance, tetrahedral or trigonal bipyramidal geometries, which needed bidentate ligands able to reach 109° and 120° respectively (for equatorial-equatorial substitution in trigonal bipyramidal geometry). This fact triggered the development of wide bite angle diphosphines, and the term *natural bite angle*⁶ was coined (see chapter 5). For example, BISBI and Xantphos (Figure 8. 1) presented wide bite angles, and they show unprecedented reactivities in certain catalytic reactions compared with the traditional *cis*-diphosphines.^{7–9} For instance, Hayashi *et al.* found high selectivities and activities using dppf ligand in the palladium-catalyzed cross-coupling reaction of 2-butyilmagnesium chloride with bromobenzene, but the same reaction using dppe as ligand showed no activity.^{10,11}

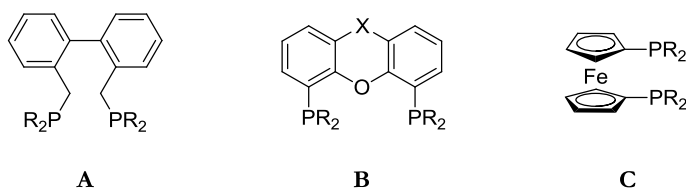


Figure 8. 1. Initial wide bite angle diphosphines: (A) BISBI, (B) Xantphos and (C) dppf.

Following the same reasoning, it seems evident that there was still one more possibility of coordination of a bidentate, *viz.* *trans*-chelation (bite angles of around 180°). The use of such *trans*-chelating ligands^{12,13} to generate transition metal catalyst could eventually render new catalytic pathways, compared to the traditional well-known catalytic systems based on *cis*- or wide *bite angle* ligands.

The first *trans*-complex with a diphosphine was synthesized in 1961.¹⁴ It consisted of a square planar nickel complex using a simple diphosphine with a long hydrocarbon chain as a backbone (Figure 8. 2). However, the flexibility of the skeleton of the diphosphine still allows formation of *cis*-complexes, or oligomers.¹⁵

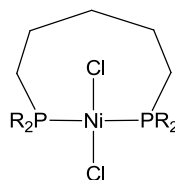


Figure 8. 2. First example reported of a *trans*-diphosphine complex.

The attention was then focused on the development of less flexible skeletons. Venanzi *et al.* designed an on purpose *trans*-ligand based on the phenanthrene molecule.¹⁶ This diphosphine was coined TRANSPHOS (Figure 8. 3, **A**), and numerous examples of *trans*-complexes have been described with it.¹⁷⁻²⁰

Another important family of diphosphines designed to achieve *trans*-coordination complexes is the so-called TRAP ligand (Figure 8. 3, **B**),²¹ constructed from two ferrocenyl units, although many of the catalytic reactions of TRAP are typical of *cis*-ligands. Furthermore chiral centers are incorporated in this structure, and it has been successfully applied to asymmetric catalysis.^{22,23}

Both examples achieved the desired *trans*-coordination, but *cis*-complex formation could not be discarded, and it has been claimed occasionally to justify some of the catalytic activities observed with TRAP ligands.

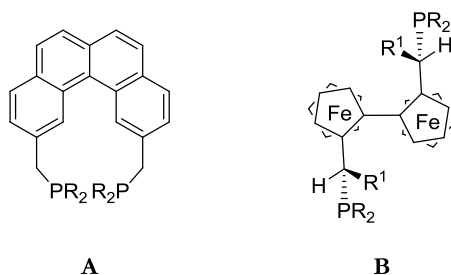


Figure 8. 3. Initial *trans*-diphosphines reported: **(A)** TRANSPHOS and **(B)** TRAP.

One of the backbones that emerged as a truly *trans*-coordinating ligand was SPANphos (Figure 8. 4).²⁴ Its structure is based on a bis-chromane unit containing a spiro carbon center with a global C_2 symmetry. The large skeleton, which places the phosphorus atoms at a large distance, is not as rigid as initially thought by the

authors.²⁵ Some years after the initial reports, they stated that SPANphos also forms *cis*-chelating complexes when the co-ligand used enforces *cis*-geometry.

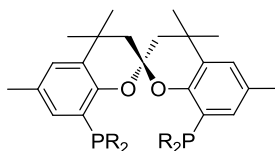


Figure 8. 4. General structure of SPANphos diphosphines.

Remarkable efforts were done by Süss-Fink *et al.* to achieve a *trans*-coordinating diphosphine. For instance, trying to avoid the *ortho* metallation in a palladium complex, the authors designed bis(3-((diphenylphosphino)methyl)-2,4,6-trimethylphenyl)methane (Figure 8. 5, **A**).²⁶ Additionally, based on the structures described by Trost *et al.*,^{27,28} Süss-Fink *et al.* developed a family of *trans*-diphosphines constructed from modular units, linked by amide and ester moieties (Figure 8. 5, **B**).^{29–32}

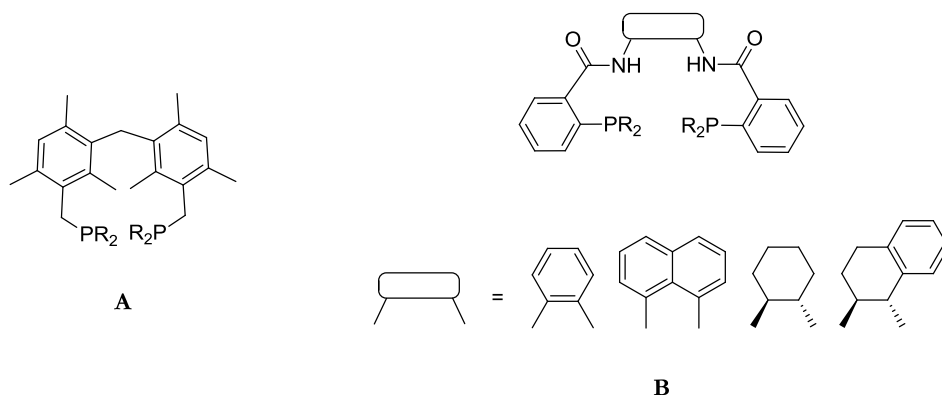


Figure 8. 5. Diphosphines designed by Süss-Fink *et al.* to achieve *trans*-coordination.

One striking example due to its sophisticated design is the one that involves the use of supramolecular structures, such as calix[4]arenes or cyclodextrins (Figure 8. 6). Matt *et al.* used these backbones to incorporate the phosphines in the upper or lower rim. Upon coordination, the metal is located close to a cavity, with the aim of

increasing selectivity in catalysis.³³⁻³⁹

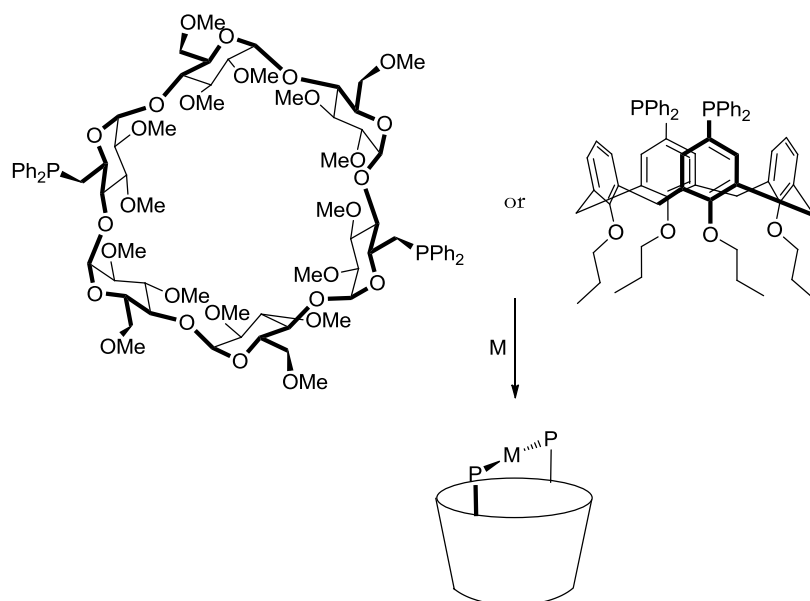


Figure 8. 6. Examples of *trans*-coordinating cyclodextrins and calix[4]arenes developed by Matt *et al.*

The last *trans*-diphosphine reported (to our knowledge) is based in the rigid anthracene backbone (Figure 8. 7), which locates the phosphorus atoms at the appropriate distance to form *trans*-palladium complexes. This diphosphine has been used in the carbonylative Suzuki coupling and methoxycarbonylation of aryl iodides and bromides. The authors attribute the high selectivity of the system to the deceleration of the reductive elimination step due to the *trans*-configuration of the complex.⁴⁰

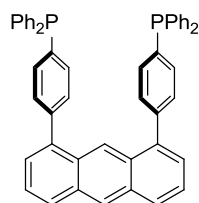


Figure 8. 7. *trans*-coordinating diphosphine based on anthracene backbone.

Some attempts to construct *trans*-hetero-bidentate ligands have been also developed. The first example was reported very early. In 1974, Chottard *et al.* described a square planar platinum complex with a *trans*-pyridine-olefin bidentate ligand (Figure 8. 8, **A**).⁴¹⁻⁴¹ It was not since last decades when designs involving *trans* P,N ligands were reported. In the two examples shown the hetero-bidentate ligand forms *trans*-complexes with palladium (Figure 8. 8, **B** and **C**).^{42,43}

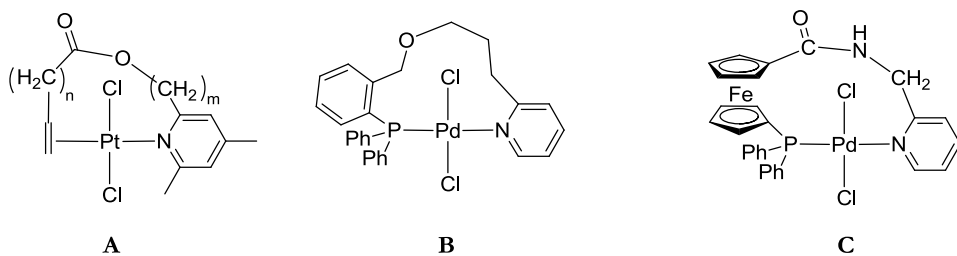


Figure 8. 8. Hetero-bidentate *trans*-chelating ligands.

trans-coordinating phosphinines and pyridines

One of the handicaps that present the previously designed phosphines is the flexibility of the large backbones employed. A strategy to avoid this flexibility is to restrict structural freedom, for instance constructing skeletons based exclusively on aromatic systems. This type of arrangement confines the structure into a bidimensional space, simplifying enormously the design. To ensure the planarity along the whole structure (including the lone pairs of the donor atoms used to coordinate to the metal) these donor atoms (P or N, for instance) can be incorporated into heteroaromatic rings. Then, phosphinine and pyridine ligands (with sp² hybridized donors) are generated. Based on this type of construction, it is relatively simple to envisage a backbone in which the lone pairs of the donor atoms point into the same direction to favour the formation of a *trans*-complex with a metal. This strategy, developed by Müller *et al.* was exemplified in diphosphinine **58**, depicted in Figure 8. 9.⁴⁴ This diphosphinine forms preferably *trans*-complexes, due to the linear orientation of the lone pairs in combination with an appropriate P–P distance. However, the authors found that the *cis*-coordination could also be enforced

with the use of a co-ligand such as norbornadiene (Figure 8. 9).⁴⁴ The *cis*-coordination mode was achieved through a Csp^2-Csp^2 rotation of the bond between the phosphinine and the adjacent aryl ring of the backbone and concomitant loss of planarity of the ligand.

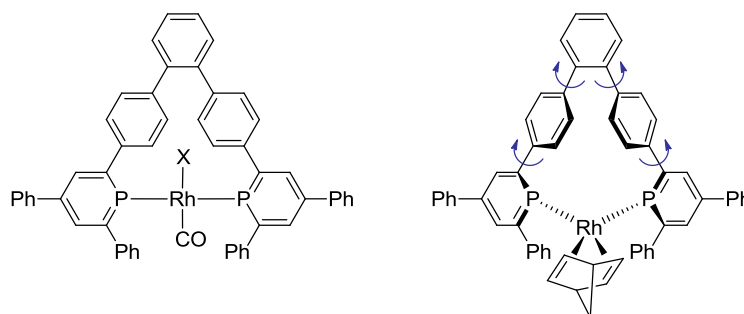


Figure 8. 9. *trans*- and *cis*- complexes with diphosphinine **58**. X = Cl or I.

A *trans*-bidentate pyridyl ligand was reported initially by Bosch *et al.*⁴⁵ The aromatic rings combined with alkyne moieties confer to the molecule the rigidity to place the nitrogen atoms at the appropriate distance to form *trans*-complexes (Figure 8. 10, **A**). Its *trans*-chelating properties toward different metal centres have been reported.^{46–48}

Figure 8. 10, **B** presents another example of a *trans*-chelating pyridyl ligand. In this complex, however, the ligand cannot be considered as a bidentate, since the alkyne moiety coordinates to the metal, and the ligand ends up as a tridentate ligand.⁴⁹

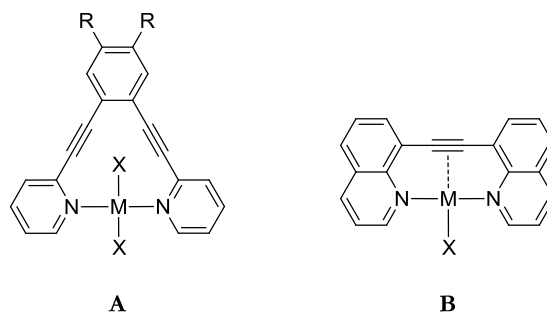


Figure 8. 10. *trans*-bidentate pyridyl ligands.

Supramolecular hydrogen bonding interactions to construct bidentate ligands

One strategy to construct libraries of bidentate ligands involves the synthesis of complementary monodentate ligands, which by pairwise combination generate a myriad of chelating ligands. This can be achieved by the formation of covalent bonds or by means of non-covalent, supramolecular interactions.⁵⁰

One of the most successful works in this field is the system designed by Breit *et al.* Initially, the authors generated a library of homo-bidentate ligands formed through hydrogen bonding associations between two monodentate phosphorus ligands (Figure 8. 11).^{51–55} It is known that 2-hydroxypyridine exists in equilibrium with its tautomer 2-pyridone. Dimerization of the tautomeric pair is favoured in aprotic solvents. Upon formation of the dimer, the phosphorus atoms can be found in the same direction, or pointing into opposite directions. To obtain a bidentate ligand, the phosphorus atoms have to point in the same direction, which is favoured through chelation to a metal. Ligands obtained with this strategy have been successfully applied in rhodium catalyzed hydroformylation of terminal alkenes, giving high regioselectivity towards the linear aldehyde.^{52,53} Recently, a chiral version of the system has been applied in asymmetric hydrogenation.^{54,55}

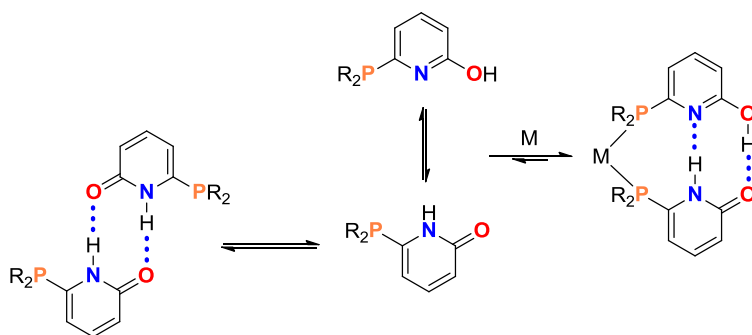


Figure 8. 11. Breit's strategy to form a homo-bidentate ligand through hydrogen bonding interactions.

Following the same strategy, Börner *et al.* used chiral cyclic phosphines substituted with the 2-hydroxypyridine moiety to apply in catalytic asymmetric

hydrogenation (Figure 8. 12).^{56,57} They compared the results obtained with protected alcohols, unable to form the hydrogen bonding interactions, to confirm that the enantioselectivities observed are due to the supramolecular bidentate ligand. The use of polar solvents also influenced the activity and enantioselectivity, demonstrating that the solvent competes for the hydrogen bonding association and changes the properties of the supramolecular chelate.

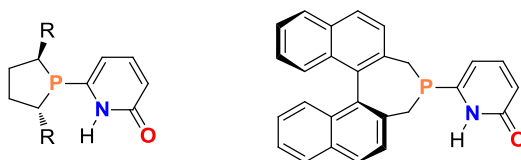


Figure 8. 12. Chiral cyclic phosphanes used by Börner *et al.* in asymmetric hydrogenation.

This strategy can not be applied to form hetero-bidentate ligands, because the lack of specificity in the supramolecular interaction could render (if steric or electronic effects are similar for both building blocks) the statistical distribution of the homo- and hetero- bidentate ligands mixture (Figure 8. 13).

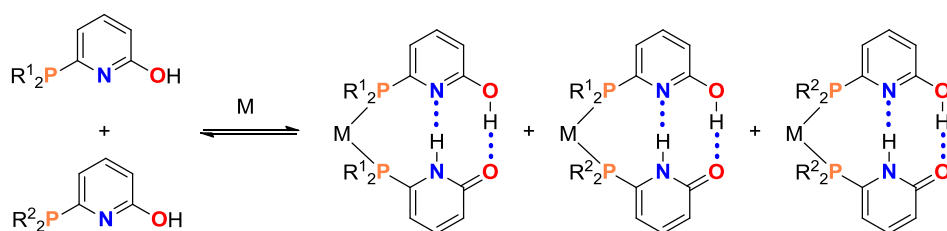


Figure 8. 13. Formation of the statistical distribution mixture when homo-interactions and hetero-phosphorus ligands are used.

Aiming to favour the formation of hetero-bidentate ligands, Breit *et al.* designed a system inspired on nature. The authors used the same hydrogen bonded motif found in the adenine-thymine DNA base pair to construct hetero-bidentate phosphorus ligands (Figure 8. 14).^{58,59}

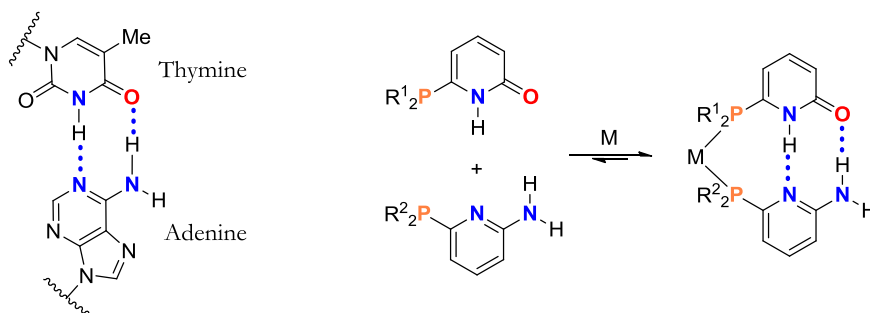


Figure 8. 14. Breit's strategy to form a hetero-bidentate ligand through hydrogen bonding interactions.

Although there are many examples that use supramolecular interactions to form *trans*-bidentate ligands, only one of them use hydrogen bonding interactions. Two papers appeared simultaneously describing the formation of hydrogen bonds between two urea-functionalized phosphorus ligands, a homo-bidentate ligand is achieved, which forms a *trans*-complex when coordinated to palladium or rhodium (Figure 8. 15).^{60–63} Apart from the direct formation of the hydrogen bonds between the urea moieties, an anion can serve as template between the two urea units.

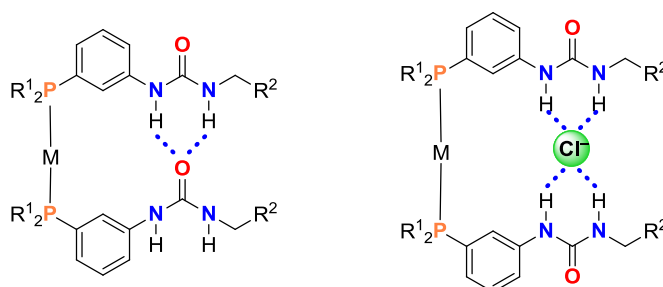


Figure 8. 15. Formation of *trans*-complexes through supramolecular interactions.

General objectives of Part III

The project developed in this part aims at the design and synthesis of *trans*-bidentate ligands.

Two strategies are applied for the construction of the ligands: the use of

supramolecular hydrogen bonding interactions and the use of switchable properties of an azobenzene moiety.

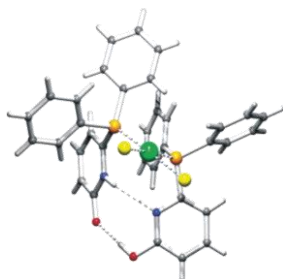


Figure 8. 16. X-Ray structure of *cis*-PtCl₂(6-diphenylphosphanyl-2-pyridone)₂ reported by Breit *et al.* The planarity of the hydrogen bonded motif can be appreciated.

The first strategy deals with the design of *trans*-coordinating supramolecular bisphosphinines, bispyridines and mixed phosphinine-pyridine ligands based on the use of hydrogen bonding interactions to construct bidentate ligands. Thus, units of monodentate phosphinines and pyridines are designed, which, after hydrogen bonding association, would render *trans*-bidentate ligands. This design has also the advantage of generating a library of extended ligands, further enlarged by the formation of homo- and hetero-combinations.

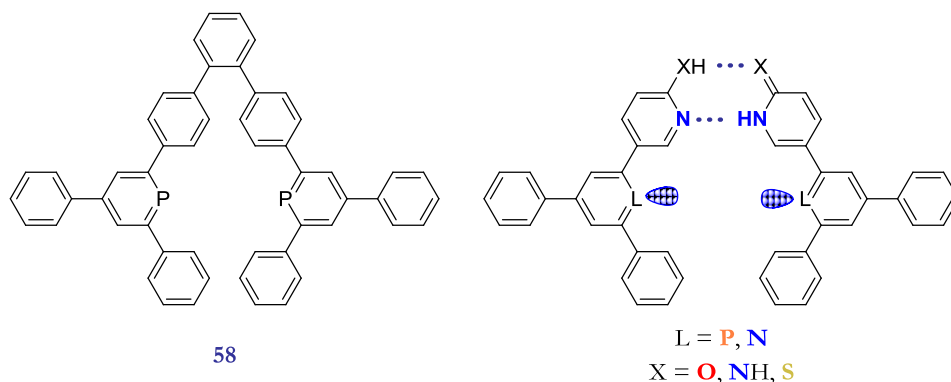


Figure 8. 17. *trans*-bidentate ligand formed by supramolecular hydrogen bonding interactions between two monodentate units. The planarity achieved in the supramolecular assembled ligand resembles the planar structure needed to form the *trans*-complexes with 58.

This design has the advantage that the formation of the hydrogen bonds between the two aromatic units adjacent to the phosphinine/pyridine moiety, should avoid the Csp^2-Csp^2 rotation (observed in the *trans*-diphoshinine **58**). This restriction is due to the high directionality needed to the formation of the hydrogen bonding interactions, which is noticed, for instance, in the X-Ray structures obtained by Breit *et al* for *cis*-PtCl₂(6-diphenylphosphanyl-2-pyridone)₂ (Figure 8. 16).⁵¹

The second strategy employed consists of designing switchable *trans*-coordinating phosphinines and pyridines by using rigid structures that contain the azobenzene moiety. When the azobenzene linker is in its *E* form, the structure is extended, so no chelating effect would be observed. Upon irradiation at the appropriate wavelength, the azobenzene will adopt the *Z* conformation, locating the donor atoms at the right distance to allow the lone pair pointing into the appropriate direction to coordinate in a *trans*-fashion to a metal.

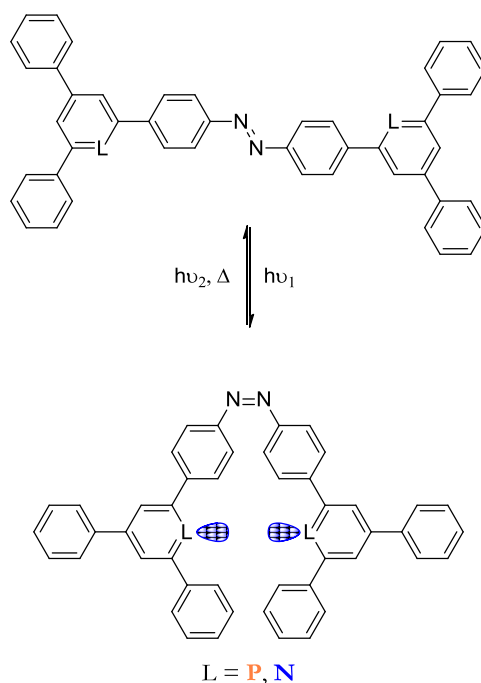


Figure 8. 18. Effect of the light on the switchable bidentate ligand.

References and notes

1. Young, J. F.; Osborn, J. A.; Jardine, F. H.; Wilkinson, G. *Chem. Commun.* **1965**, 131.
2. Osborn, J. A.; Jardine, F. H.; Young, J. F.; Wilkinson, G. *J. Chem. Soc.* **1966**, 1711.
3. Minahan, D. M. A.; Hill, W. E.; McAuliffe, C. A. *Coord. Chem. Rev.* **1984**, *55*, 31.
4. Levason, W.; McAuliffe, C. A. *Advan. Inorg. Chem. Radiochem.* **1972**, *14*, 173.
5. Drent, E.; Vanbroekhoven, J. A. M.; Doyle, M. J. *J. Organomet. Chem.* **1991**, *417*, 235.
6. Casey, C. P.; Whiteker, G. T. *Isr. J. Chem.* **1990**, *30*, 299.
7. Puckette, T. A.; Devon, T. J.; Phillips, G. W.; Stavinoha, J. L., Application: US Patent, 87-123407, **1989**.
8. Casey, C. P.; Whiteker, G. T.; Melville, M. G.; Petrovich, L. M.; Gavney, J. A., Jr.; Powell, D. R. *J. Am. Chem. Soc.* **1992**, *114*, 5535.
9. Kranenburg, M.; van der Burgt, Y. E. M.; Kamer, P. C. J.; van Leeuwen, P. W. N. M.; Goubitz, K.; Fraanje, J. *Organometallics* **1995**, *14*, 3081.
10. Hayashi, T.; Konishi, M.; Kumada, M. *Tetrahedron Lett.* **1979**, 1871.
11. Hayashi, T.; Konishi, M.; Kobori, Y.; Kumada, M.; Higuchi, T.; Hirotsu, K. *J. Am. Chem. Soc.* **1984**, *106*, 158.
12. Bessel, C. A.; Aggarwal, P.; Marschilok, A. C.; Takeuchi, K. *J. Chem. Rev.* **2001**, *101*, 1031.
13. Freixa, Z.; van Leeuwen, P. W. N. M. *Coord. Chem. Rev.* **2008**, *252*, 1755.
14. Issleib, K.; Hohlfeld, G. *Z. Anorg. Allg. Chem.* **1961**, *312*, 169.
15. Hill, W. E.; Minahan, D. M. A.; Taylor, J. G.; McAuliffe, C. A. *J. Am. Chem. Soc.* **1982**, *104*, 6001.
16. DeStefano, N. J.; Johnson, D. K.; Venanzi, L. M. *Angew. Chem.* **1974**, *86*, 133.
17. Destefano, N. J.; Johnson, D. K.; Lane, R. M.; Venanzi, L. M. *Helv. Chim. Acta* **1976**, *59*, 2674.
18. Holderegger, R.; Venanzi, L. M. *Helv. Chim. Acta* **1979**, *62*, 2154.
19. Holderegger, R.; Venanzi, L. M.; Bachechi, F.; Mura, P.; Zambonelli, L. *Helv. Chim. Acta* **1979**, *62*, 2159.
20. Bracher, G.; Kellenberger, B.; Venanzi, L. M.; Bachechi, F.; Zambonelli, L. *Helv. Chim. Acta* **1988**, *71*, 1442.
21. Sawamura, M.; Hamashima, H.; Ito, Y. *Tetrahedron: Asymmetry* **1991**, *2*, 593.
22. Sawamura, M.; Hamashima, H.; Ito, Y. *J. Am. Chem. Soc.* **1992**, *114*, 8295.
23. Sawamura, M.; Kuwano, R.; Ito, Y. *J. Am. Chem. Soc.* **1995**, *117*, 9602.
24. Freixa, Z.; Beentjes, M. S.; Batema, G. D.; Dieleman, C. B.; van Strijdonck, G. P. F.; Reek, J. N. H.; Kamer, P. C. J.; Fraanje, J.; Goubitz, K.; van Leeuwen, P. W. N. M. *Angew. Chem., Int. Ed.* **2003**, *42*, 1284.
25. Jimenez-Rodriguez, C.; Roca, F. X.; Bo, C.; Benet-Buchholz, J.; Escudero-Adan, E. C.; Freixa, Z.; van Leeuwen, P. W. N. M. *Dalton Trans.* **2005**, 268.
26. Chahen, L.; Therrien, B.; Suss-Fink, G. *J. Organomet. Chem.* **2006**, *691*, 4257.
27. Trost, B. M.; Vanvranken, D. L.; Bingel, C. *J. Am. Chem. Soc.* **1992**, *114*, 9327.
28. Trost, B. M.; Vanvranken, D. L. *Angew. Chem., Int. Ed.* **1992**, *31*, 228.

29. Thomas, C. M.; Mafua, R.; Therrien, B.; Rusanov, E.; Stoeckli-Evans, H.; Suss-Fink, G. *Chem.-Eur. J.* **2002**, *8*, 3343.
30. Burger, S.; Therrien, B.; Suss-Fink, G. *Eur. J. Inorg. Chem.* **2003**, 3099.
31. Burger, S.; Therrien, B.; Suss-Fink, G. *Helv. Chim. Acta* **2005**, *88*, 478.
32. Nasser, N.; Eisler, D. J.; Puddephatt, R. J. *Chem. Commun.* **2010**, *46*, 1953.
33. Wieser, C.; Matt, D.; Toupet, L.; Bourgeois, H.; Kintzinger, J. P. *J. Chem. Soc., Dalton Trans.* **1996**, 4041.
34. Wieser, C.; Matt, D.; Fischer, J.; Harriman, A. *J. Chem. Soc., Dalton Trans.* **1997**, 2391.
35. Wieser-Jeunesse, C.; Matt, D.; De Cian, A. *Angew. Chem., Int. Ed.* **1998**, *37*, 2861.
36. Armspach, D.; Matt, D. *Chem. Commun.* **1999**, 1073.
37. Engeldinger, E.; Armspach, D.; Matt, D.; Jones, P. G.; Welter, R. *Angew. Chem., Int. Ed.* **2002**, *41*, 2593.
38. Lejeune, M.; Jeunesse, C.; Matt, D.; Kyritsakas, N.; Welter, R.; Kintzinger, J. P. *J. Chem. Soc., Dalton Trans.* **2002**, 1642.
39. Jeunesse, C.; Armspach, D.; Matt, D. *Chem. Commun.* **2005**, 5603.
40. Kaganovsky, L.; Gelman, D.; Rueck-Braun, K. *J. Organomet. Chem.* **2009**, *695*, 260.
41. Chottard, J. C.; Mulliez, E.; Girault, J. P.; Mansuy, D. *J. Chem. Soc., Chem. Commun.* **1974**, 780.
42. Tani, K.; Yabuta, M.; Nakamura, S.; Yamagata, T. *J. Chem. Soc., Dalton Trans.* **1993**, 2781.
43. Kuhnert, J.; Dusek, M.; Demel, J.; Lang, H.; Stepnicka, P. *Dalton Trans.* **2007**, 2802.
44. Muller, C.; Freixa, Z.; Lutz, M.; Spek, A. L.; Vogt, D.; van Leeuwen, P. W. N. M. *Organometallics* **2008**, *27*, 834.
45. Bosch, E.; Barnes, C. L. *Inorg. Chem.* **2001**, *40*, 3097.
46. Kawano, T.; Kuwana, J.; Shinomaru, T.; Du, C. X.; Ueda, I. *Chem. Lett.* **2001**, 1230.
47. Fiscus, J. E.; Shotwell, S.; Layland, R. C.; Smith, M. D.; zur Loye, H. C.; Bunz, U. H. F. *Chem. Commun.* **2001**, 2674.
48. Hu, Y. Z.; Chamchoumis, C.; Grebowicz, J. S.; Thummel, R. P. *Inorg. Chem.* **2002**, *41*, 2296.
49. Greco, N. J.; Hysell, M.; Goldenberg, J. R.; Rheingold, A. L.; Tor, Y. *Dalton Trans.* **2006**, 2288.
50. van Leeuwen, P. W. N. *Supramolecular Catalysis*; Wiley-VCH, **2008**.
51. Breit, B.; Seiche, W. *J. Am. Chem. Soc.* **2003**, *125*, 6608.
52. Breit, B. *Angew. Chem., Int. Ed.* **2005**, *44*, 6816.
53. Seiche, W.; Schuschkowski, A.; Breit, B. *Adv. Synth. Catal.* **2005**, *347*, 1488.
54. Birkholz, M.-N.; Dubrovina, N. V.; Jiao, H.; Michalik, D.; Holz, J.; Paciello, R.; Breit, B.; Boerner, A. *Chem.-Eur. J.* **2007**, *13*, 5896.
55. Weis, M.; Waloch, C.; Seiche, W.; Breit, B. *J. Am. Chem. Soc.* **2006**, *128*, 4188.
56. Dubrovina, N. V.; Shuklov, I. A.; Birkholz, M. N.; Michalik, D.; Paciello, R.; Borner, A. *Adv. Synth. Catal.* **2007**, *349*, 2183.
57. Schaeffner, B.; Holz, J.; Verevkin, S. P.; Boerner, A. *Tetrahedron Lett.* **2008**, *49*, 768.
58. Breit, B.; Seiche, W. *Angew. Chem., Int. Ed.* **2005**, *44*, 1640.
59. Breit, B.; Seiche, W. *Pure Appl. Chem.* **2006**, *78*, 249.

60. Duckmanton, P. A.; Blake, A. J.; Love, J. B. *Inorg. Chem.* **2005**, *44*, 7708.
61. Knight, L. K.; Freixa, Z.; Van Leeuwen, P. W. N. M.; Reek, J. N. H. *Organometallics* **2006**, *25*, 954.
62. Sandee, A. J.; van der Burg, A. M.; Reek, J. N. H. *Chem. Commun.* **2007**, 864.
63. Meeuwissen, J.; Kuil, M.; van der Burg, A. M.; Sandee, A. J.; Reek, J. N. H. *Chem.--Eur. J.* **2009**, *15*, 10272.

UNIVERSITAT ROVIRA I VIRGILI
SWITCHABLE AND TUNABLE LIGANDS FOR HOMOGENEOUS CATALYSIS
Maria Dolores Segarra Maset
ISBN:978-84-693-7666-9/DL:T-1755-2010

CHAPTER 9

RESULTS AND DISCUSSION

9.1. INTRODUCTION AND OBJECTIVES

The project developed in this part aims at the design and synthesis of bidentate ligands able to coordinate in a *trans*-fashion to a metal.

The backbone used as inspiration to construct the ligands is the rigid phosphinine **58** (Figure 9. 1).¹ As explained in chapter 8, this phosphinine, previously developed by Dr. Müller in collaboration with our group, presents a preferential formation of *trans*-complexes. As advanced in the previous chapter, it is possible to maintain a similar backbone skeleton, but introducing several modifications in the structure. The donor atoms can be either phosphorus (as in **58**) or nitrogen.

The *trans*-bidentate ligands envisaged in this project are based on two different strategies to build the backbones: the use of hydrogen bonding supramolecular interactions or the incorporation of molecular switches (azobenzene) into the ligand backbone.

As done by Breit *et al.*,² supramolecular hydrogen bonding interactions can be used to hold together two monodentate ligands for the construction of a bidentate. Furthermore, taking advantage of the adenine-thymine base-pair complementarities one can form hetero-bidentate ligands based on a skeleton that resembles the backbone of ligand **58**. In this project, three different monodentate ligands are

As mentioned before, the second strategy to achieve *trans*-coordinating bidentate ligands is the use of the switchable properties of an azobenzene moiety. To construct the switchable *trans*-bidentate ligands, the azobenzene unit (presented in previous chapters) will be used to generate a backbone that structurally resembles **58** in its *Z* isomeric form. Bis-phosphinine **62** and bis-pyridine **63** (Figure 9. 3) are expected to act as *trans*-chelating ligands when the azo unit adopts the *Z* conformation, and to act as a bridging ligand between two metal centres when the azo moiety presents the *E* isomer.

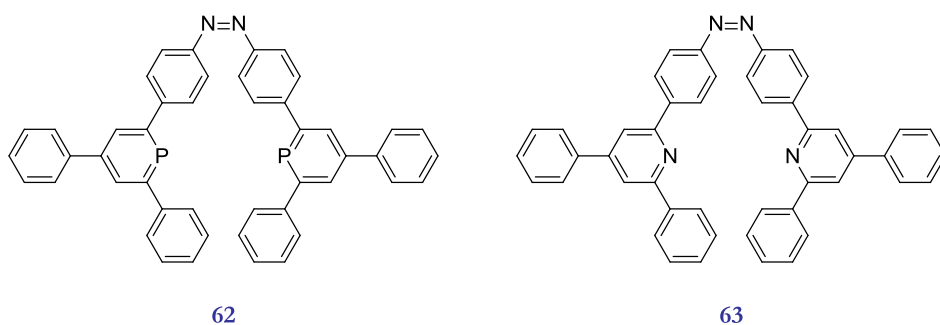


Figure 9. 3. Switchable *trans*-coordinating bis-phosphinine **62** and bis-pyridine **63**. The molecules are drawn in the *Z* conformation of the azo moiety to show the resemblance to backbone **58**.

In chapter 1 it was already discussed that the azobenzene *Z* isomer does not adopt a completely planar conformation, as one of the aromatic rings rotates 56° with respect to the $N=N-C$ plane. Although the planarity of the structure will be not preserved when **62** and **63** isomerize from the *E* to the *Z* conformation, it is expected that, due to the possible $C_{sp^2}-C_{sp^2}$ rotation of the adjacent aryl groups of the heteroaromatic rings, the *trans*-chelating coordination can be achieved (as observed for **58**).

It has to be mentioned that this is an ongoing project; current studies and future work will be discussed together with the preliminary synthetic results.

9.2. SYNTHESIS

9.2.1. SYNTHESIS OF THE SUPRAMOLECULAR LIGANDS

Three ligands have been synthesized, with complementary functional groups capable to form hydrogen bonding interactions. Thus, up to six *trans*-chelating ligands can be generated (taking into account both homo- and hetero-combinations).

The synthesis of each ligand will be discussed separately.

Hydroxyphosphinine **59**

The synthesis of this phosphinine started from the protected 5-bromo-2-methoxypyridine. Product **64** was obtained via lithiation, using *N,N*-dimethylacetamide as source of the ketone (39 % yield).³

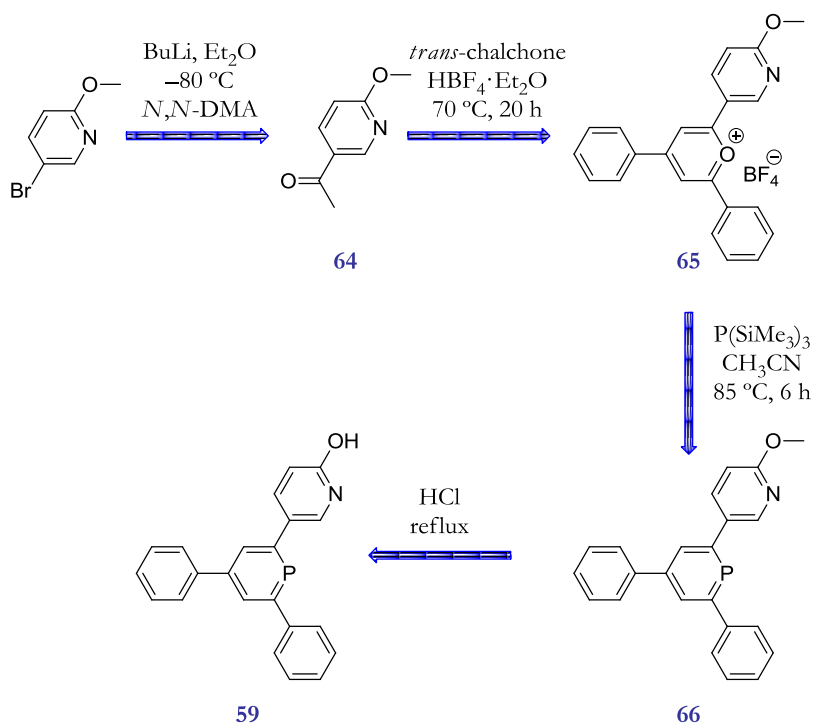
The next step was the synthesis of the pyrylium salt **65**. The synthesis of a triaryl-substituted pyrylium salt is usually performed by reaction of an aromatic ketone with two equivalents of *trans*-chalcone, in presence of tetrafluoroboric acid.⁴ Pyrylium salt **65** was prepared in 41 % yield by this methodology.

The synthesis of phosphinine **66** can be done using two different procedures. The first one involved the use of $P(CH_2OH)_3$ in pyridine at 125 °C during 3 h (20 % yield).^{5,6} The second methodology involved the use of $P(SiMe_3)_3$ in CH_3CN at 85 °C during longer time (6 h), resulting in slightly better yield (33%).^{4,7}

Crystals suitable for X-ray determination were obtained for compounds **65** and **66**. It is worth mentioning that for the first time both the structure of a phosphinine and that of its pyrylium salt precursor are obtained (Figure 9. 4).

In the structure of pyrylium salt **65**, the presence of BF_4^- as the counter ion can be observed. Also, the different shapes of the heteroaromatic central rings are noticed. In the case of **65**, the C–O distance is 1.36 Å, but in the case of **66** the C–P distance is larger (1.76 Å). In the case of the pyrylium salt, all the aromatic rings are coplanar, whilst for phosphinine **66** the aromatic rings are slightly out of the plane of

the central heteroaromatic one. In both structures one can observe that the functional groups needed for the construction of the hydrogen bonds (N and O), are located in the opposite direction from the one needed to form the bidentate ligand. However, the Csp^2-Csp^2 rotation through the bond formed between the heteroaromatic rings, would eventually allow the reorganization of the structure to form the supramolecular assembly. As occurred in the examples presented by Breit *et al.*,⁸ this is expected to be favoured upon metal coordination.



Scheme 9. 1. Synthetic route to phosphinine **59**.

The cleavage of the methoxy group was initially tried with BBr₃, as described previously for phosphinines substituted with methoxy groups.^{6,9} Unfortunately, with this method it was not possible to obtain phosphinine **59**, and mainly starting material was recovered. The deprotection was accomplished using hot HCl, which is a method

described to deprotect *ortho* methoxy pyridines,¹⁰ yielding 74 % of the phosphinine **59**.

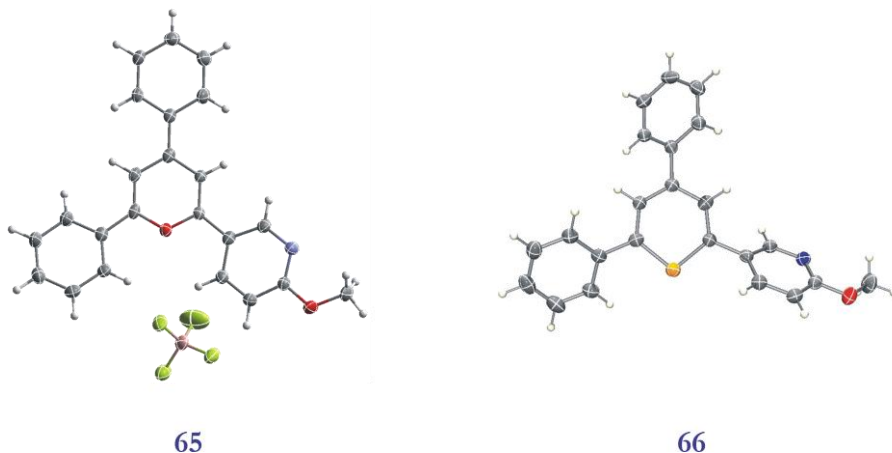


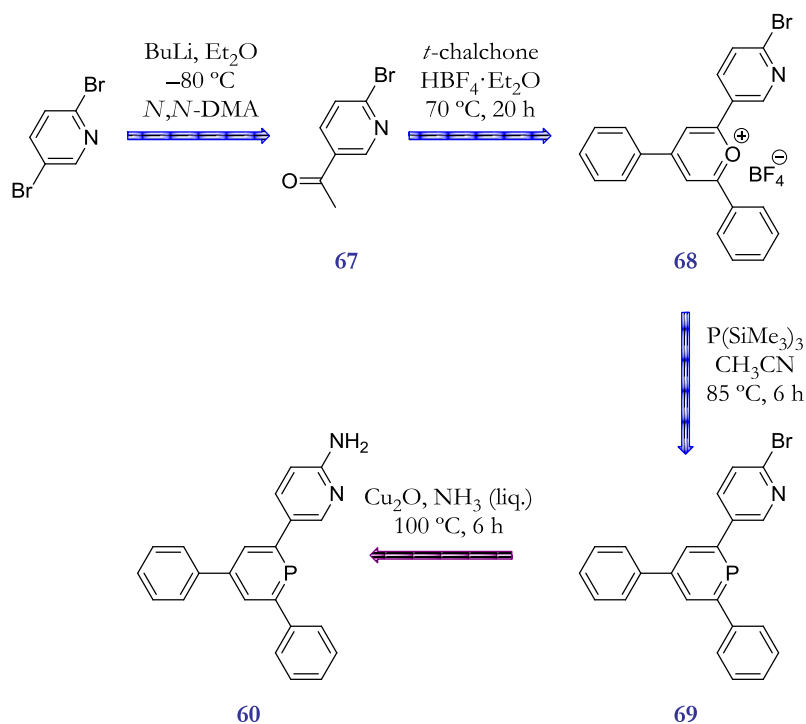
Figure 9. 4. X-Ray structures of pyrylium salt **65** and phosphinine **66**.

Aminophosphinine **60**

The synthesis was performed as described by Mashino *et al.* It starts from 2,5-dibromopyridine (BuLi, *N,N*-DMA) to obtain ketone **67**. This product was obtained in only 43% yield (versus the 50 % reported).³ Pyrylium salt **68** was produced from it using the general method described previously with a yield of only 16 %.⁴ In this case, the phosphinine **69** could only be obtained employing P(SiMe₃)₃ as phosphorus source with a 33 % yield.

The synthesis of the amine from the bromo derivative was described for several substituted bromo-pyridines by Lang *et al.* using copper as catalyst.¹¹ Initially, the reaction was assayed on a generic substrate (2-bromopyridine) with 0.5 % of Cu₂O, using ethylene glycol as solvent, saturated with NH₃, and heating in a stainless steel reactor to 100 °C for 6 h. Together with 2-aminopyridine (88 % yield), 2-(pyridin-2-yloxy)ethanol was obtained as by-product in 12 % yield. It was decided to carry out

the same procedure using 0.14 g of **69**, but unfortunately, in this case the formation of **60** was not observed.



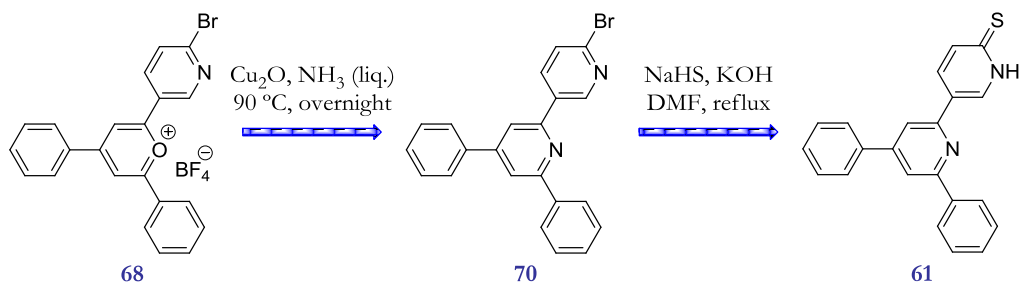
Scheme 9. 2. Synthetic route to phosphinine **60**.

Thiopyridine **61**

Applying the procedure described before (from Lang *et al.*),¹¹ which makes use of Cu₂O and ethylene glycol saturated with NH₃, on pyrylium salt **68** and heating to 90 °C overnight, pyridine **70** was obtained in 55 % yield. The molecular structure of this compound was confirmed by X-Ray crystallography (Figure 9. 5). This pyridine can easily be converted to thiopyridine **61** (82 % yield) using NaHS.¹²

In the X-Ray structure of compound **70** one can notice that all aromatic rings are positioned almost in the same plane. The N–C distance (1.34 Å) in the central

aromatic ring is smaller than the previous P–C and O–C ones. Also in this structure the pyridine moiety *ortho* functionalized is oriented in the opposite direction compared to the one needed to form the hydrogen bonding interactions.



Scheme 9.3. Synthetic route to thiopyridine **61**.

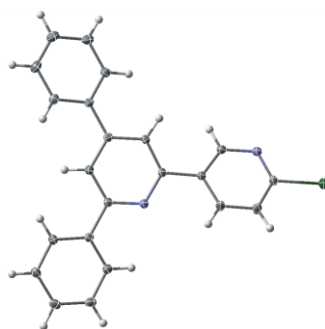


Figure 9.5. X-Ray structure of pyridine **70**.

The conversion of **69** to thiophosphinine could not be achieved, as the harsh conditions needed for the synthesis were not tolerated by the phosphinine moiety.

9.2.2. SYNTHESIS OF THE SWITCHABLE LIGANDS

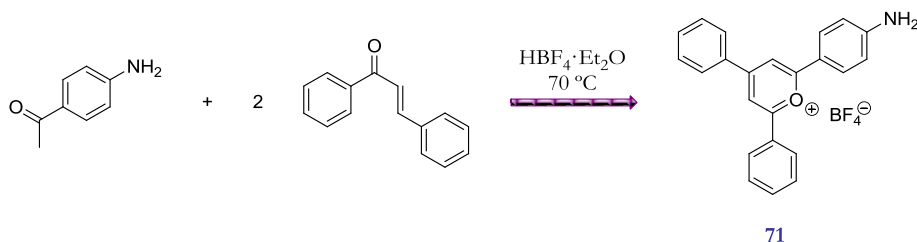
As described previously, by incorporating the switchable azobenzene moiety into structure of **58**, one can expect that after isomerization from the *E* to the *Z* form of

the N=N double bond, the donor atoms will display the appropriate distance between them to form *trans*-chelating complexes. Two bidentate ligands were designed: phosphinine **62** and pyridine **63**.

Switchable phosphinine **62**

To synthesize phosphinine **62**, the excerpts about azobenzene chemistry explained in chapter 2 have to be kept in mind. The synthesis of the azo moieties implies the use of harsh conditions, which will be incompatible with a phosphinine. For that reason two approaches were considered: either the synthesis of the pyrylium salt is done before introducing the azo functionality or the heterocycle is formed using azo benzene containing species.

Initially the synthesis of the pyrylium salt was tried by reacting 4-aminoacetophenone with *trans*-chalcone and HBF₄ (Et₂O, 70 °C) as described previously (Scheme 9. 4).⁴ Even when long reaction times were employed the extent of the reaction was very limited, and the small amount of the pyrylium salt **71** obtained hampered isolation and made this route not viable.



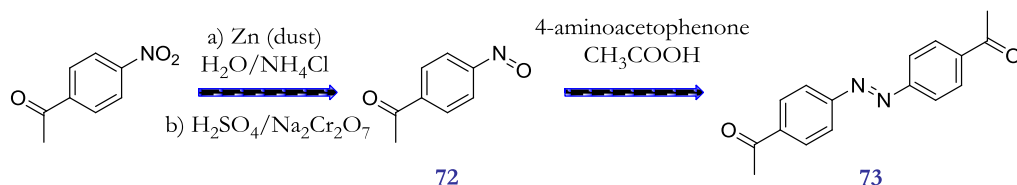
Scheme 9. 4. Initial attempt to synthesize pyrylium salt **71**.

Alternatively, the synthesis of the pyrylium salt after the synthesis of the azobenzene unit was attempted. To this end the synthesis of an azobenzene substituted with ketone moieties is required.

Several routes were explored to obtain azo-bis-ketone **73**. The first route started from 4-nitroacetophenone and used Bi in basic media. Using these reaction conditions only reduction of the nitro group to obtain 4-aminoacetophenone was

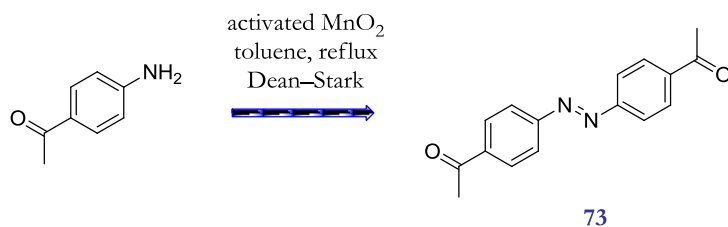
achieved.¹³

The next attempt to obtain **73** involved the synthesis of nitrosobenzene **72** from 4-nitroacetophenone using Zn.¹⁴ Reaction of **72** with 4-aminoacetophenone in acetic acid gave **73**, but in a low overall yield (17 %, Scheme 9. 5).¹⁵ It has to be mentioned that one of the reasons of the low yield may be its decomposition on the silica column when attempting its purification.



Scheme 9. 5. Synthesis of **73** through nitrosobenzene **72**.

The best route to obtain the envisaged bis-ketone diazobenzene was by a direct homocoupling of 4-nitroacetophenone using activated manganese dioxide in toluene under refluxing conditions (Scheme 9. 6).¹⁴ Compound **73** was obtained in a 67 % after purification over basic alumina.

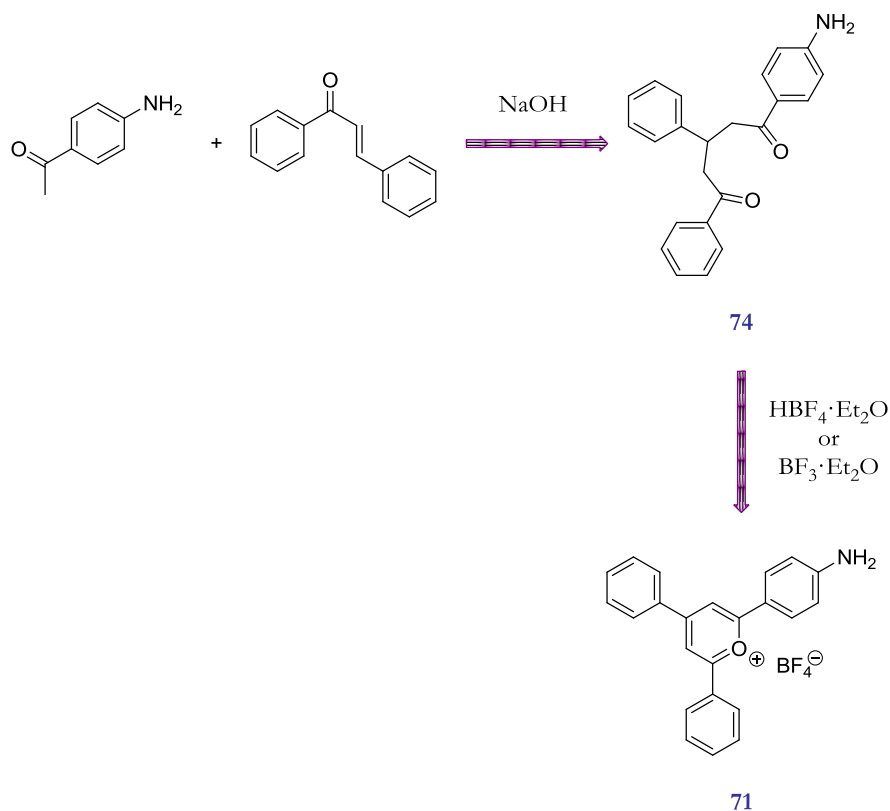


Scheme 9. 6. Synthesis of **73**.

Once the bis-ketone **73** was obtained, the synthesis of the bis-pyrylium salt was attempted. For that, **73** was reacted with four equivalents of *trans*-chalcone and HBF₄ (Et₂O, 70 °C). However, decomposition of the azo double bond was observed, and products similar to those obtained when trying to synthesize **71** were observed.

In the future, in an effort to solve the synthetic problems found to obtain azophosphinine **62**, alternative methodologies can be considered for the synthesis of

the pyrylium salt. It is possible to consider a two-step synthesis. In the first step, using one equivalent of *trans*-chalcone under basic conditions, 1,5-bis-ketone **74** could be obtained in a solvent free reaction. After that, the next equivalent of *trans*-chalcone under acid conditions would allow the cyclization of the diketone to afford the pyrylium salt (Scheme 9. 7).^{4,16}

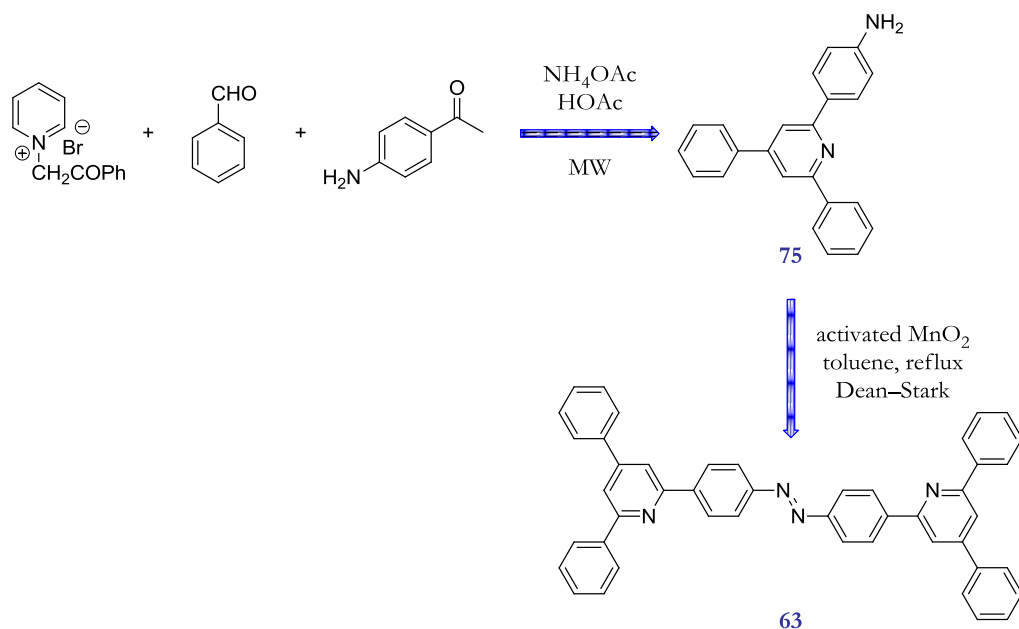


Scheme 9. 7. Synthesis proposed for pyrylium salt **71** through diketone **74** route.

Switchable pyridine **63**

For the synthesis of dipyrindine **63** a one-pot microwave-assisted synthesis was attempted to obtain 2,4,6-triarylpyridine **75**.¹⁷ The microwave-assisted synthesis allows shorter reaction times, compared to classical heating. The reaction starts with

the aromatic aldehyde and the acetophenone to give the chalcone, which immediately reacts with the pyridinium bromide in a Kröhnke type synthesis to obtain **75** in good yield (91 %).¹⁸



Scheme 9. 8. Synthesis of azodipyridine **63**.

Once **75** was obtained, azodipyridine **63** was synthesized using activated manganese dioxide under reflux with toluene (20 % yield).¹⁴

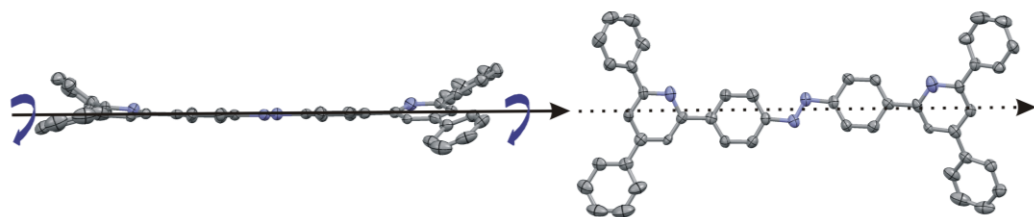


Figure 9. 6. X-Ray structure of azodipyridine **63**. H atoms are omitted for clarity.

Crystals of **63** suitable to X-Ray analysis were obtained by slow evaporation from

CH₂Cl₂. In Figure 9. 6 the high planarity of the azobenzene structure can be appreciated. As expected, the azobenzene double bond is present in its *E* isomeric form. The heteroaromatic rings and their aryl moieties are located slightly out of the plane that is formed by the azobenzene unit. Both N atoms of the pyridine rings are oriented in the same direction, and N–C distances are slightly higher (around 1.38 Å) than the ones observed for the previous compounds described here.

Currently, studies of the switchability and complex formation with this ligand are under development.

9.3. CONCLUDING REMARKS

Using the strategies learned in Part I and Part II of this thesis, *i.e.*, the use of switchable moieties and supramolecular interactions, new *trans*-coordinating chelate ligands have been designed and synthesized in Part III.

Regarding the use of hydrogen bonding interactions to construct *trans*-chelating ligands from two units, until now, only phosphinine **59** and pyridine **61** have been synthesized. The full set of *trans*-phosphininies, or pyridines to be assembled through hydrogen bonding interactions has not been obtained yet.

As this is an ongoing project, there are still many unsolved experimental and synthetic problems. For instance, the synthesis of a switchable phosphinine, which contains azobenzene remains elusive, although the synthesis of a switchable azo-bis-pyridine **63** has been successfully achieved.

As future work, further studies on coordination properties of the ligands have to be done, to confirm the ability of the ligands to form *trans*-chelating complexes.

References and notes

1. Muller, C.; Freixa, Z.; Lutz, M.; Spek, A. L.; Vogt, D.; van Leeuwen, P. W. N. M. *Organometallics* **2008**, *27*, 834.
2. Weis, M.; Waloch, C.; Seiche, W.; Breit, B. *J. Am. Chem. Soc.* **2006**, *128*, 4188.
3. Hatanaka, M.; Takahashi, K.; Nakamura, S.; Mashino, T. *Bioorg. Med. Chem.* **2005**, *13*, 6763.
4. Mueller, C.; Wasserberg, D.; Weemers, J. J. M.; Pidko, E. A.; Hoffmann, S.; Lutz, M.; Spek, A. L.; Meskers, S. C. J.; Janssen, R. A. J.; van Santen, R. A.; Vogt, D. *Chem.-Eur. J.* **2007**, *13*, 4548.
5. Ellis, J. W.; Harrison, K. N.; Hoye, P. A. T.; Orpen, A. G.; Pringle, P. G.; Smith, M. B. *Inorg. Chem.* **1992**, *31*, 3026.
6. Mueller, C.; Pidko, E. A.; Totev, D.; Lutz, M.; Spek, A. L.; van Santen, R. A.; Vogt, D. *Dalton Trans.* **2007**, 5372.
7. Niecke, E.; Westermann, H. *Synthesis* **1988**, 330.
8. Breit, B.; Seiche, W. *J. Am. Chem. Soc.* **2003**, *125*, 6608.
9. Muller, C.; Lopez, L. G.; Kooijman, H.; Spek, A. L.; Vogt, D. *Tetrahedron Lett.* **2006**, *47*, 2017.
10. Fang, Y. Q.; Yuen, J.; Lautens, M. *J. Org. Chem.* **2007**, *72*, 5152.
11. Lang, F.; Zewge, D.; Houpis, I. N.; Volante, R. P. *Tetrahedron Lett.* **2001**, *42*, 3251.
12. Wang, Q.; Day, P.; Griffiths, J.-P.; Nie, H.; Wallis, J. D. *New J. Chem.* **2006**, *30*, 1790.
13. Laskar, D. D.; Prajapati, D.; Sandhu, J. S. *Perkin 1* **2000**, 67.
14. Shine, H. J.; Zmuda, H.; Kwart, H.; Horgan, A. G.; Brechbiel, M. *J. Am. Chem. Soc.* **1982**, *104*, 5181.
15. Garlich-Zschoche, F. A.; Doetz, K. H. *Organometallics* **2007**, *26*, 4535.
16. Cave, G. W. V.; Raston, C. L. *J. Chem. Soc., Perkin Trans. 1* **2001**, 3258.
17. Yan, C. G.; Cai, X. M.; Wang, Q. F.; Wang, T. Y.; Zheng, M. *Org. Biomol. Chem.* **2007**, *5*, 945.
18. Krohnke, F. *Synthesis* **1976**, 1.

CHAPTER 10

EXPERIMENTAL

10.1. GENERAL PROCEDURES

Unless otherwise stated, all preparations were carried out under an inert atmosphere of argon using standard Schlenk techniques. All reagents were obtained from commercial suppliers and used without further purification. Solvents were purified using SPS-400-6 from Innovative Technologies, Inc.

Routine ^1H -, $^{13}\text{C}\{^1\text{H}\}$ -, $^{31}\text{P}\{^1\text{H}\}$ -, and $^{19}\text{F}\{^1\text{H}\}$ -NMR spectra were recorded on a Bruker Avance 400 Ultrashield spectrometer (400.1 MHz for ^1H -, 100.6 MHz for $^{13}\text{C}\{^1\text{H}\}$ -, 162.0 MHz for $^{31}\text{P}\{^1\text{H}\}$ -, and 376.5 MHz for $^{19}\text{F}\{^1\text{H}\}$ -NMR), or Bruker Avance 500 Ultrashield spectrometer (500.1 MHz for ^1H -, 125.7 MHz for $^{13}\text{C}\{^1\text{H}\}$ - and 202.5 MHz for $^{31}\text{P}\{^1\text{H}\}$ -NMR); or in a Varian Mercury 200 or Varian Mercury 400 NMR spectrometer. Chemical shifts, δ , are given in ppm, relative to TMS (^1H , ^{13}C), 85% H_3PO_4 (^{31}P), and CCl_3F (^{19}F). Coupling constants, J , are given in Hz.

Mass spectra were recorded on a Waters LCT Premier ESI-TOF spectrometer, or in a Waters GTC spectrometer.

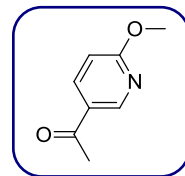
The measured crystals that were unstable under atmosphere conditions were prepared under inert conditions immersed in perfluoropolyether as protecting oil for manipulation. Crystal structure determination was carried out using a Bruker-Nonius diffractometer equipped with a APPEX 2 4K CCD area detector, a FR591 rotating

anode with $\text{MoK}\alpha$ radiation, Montel mirrors as monochromator and a Kryoflex low temperature device ($T = -173\text{ }^\circ\text{C}$). Full sphere data collection omega and phi scans; or in a Nonius Kappa CCD diffractometer with rotating anode (graphite monochromator, $\lambda = 0.71073\text{ \AA}$). Programs used: Data collection Apex2 V2008.6-1 (Bruker-Nonius 2008), data reduction Saint + Version 7.60A (Bruker AXS 2008) and absorption correction SADABS V. 2008-1 (2008). Crystal structure solution was achieved using direct methods as implemented in SHELXTL Version 6.10 (Sheldrick, Universität Göttingen (Germany), 2000) and visualized using XP program. Missing atoms were subsequently located from difference Fourier synthesis and added to the atom list. Least-squares refinement on F2 using all measured intensities was carried out using the program SHELXTL-97-UNIX VERSION.

10.2. SYNTHESIS

1-(6-methoxy-3-pyridyl)ethanone (64)

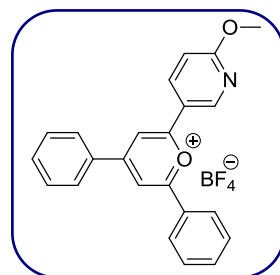
5-bromo-2-methoxypyridine (24.82 g, 132 mmol) was dissolved in 400 mL of dry diethyl ether. The solution was cooled down to $-80\text{ }^\circ\text{C}$ and *n*-BuLi (91 mL, 146 mmol, 1.6 M in hexanes) was added dropwise under Ar. The mixture was stirred at $-80\text{ }^\circ\text{C}$ for 1h. Then, at this temperature, *N,N*-dimethylacetamide (14.29 mL, 153.69 mmol, distilled over BaO) was added dropwise. The crude reaction was allowed to reach r.t. slowly. Then it was poured into 400 mL of a saturated solution of NH_4Cl . It was partitioned, and the aqueous layer was washed with Et_2O twice. The organics were collected and washed with brine, dried over MgSO_4 , filtered and concentrated to dryness. A yellow liquid was obtained which after standing overnight at r.t. crystallized. The crystalline compound was washed with hexane to yield 7.81 g of the product (39 % yield).



$^1\text{H-NMR}$ (CDCl_3 , 400.1 MHz) δ (ppm): 2.54 (s, 3H), 3.98 (s, 3H), 6.76 (d, $J = 8.7\text{ Hz}$, 1H), 8.11 (dd, $J = 8.7\text{ Hz}$, $J = 2.4\text{ Hz}$, 1H), 8.75 (d, $J = 2.4\text{ Hz}$, 1H).

2-(6-methoxy-3-pyridyl)-4,6-diphenylpyrylium tetrafluoroborate (**65**)

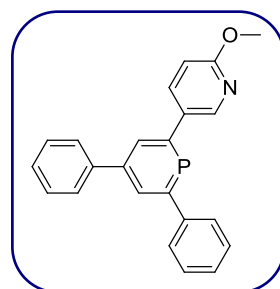
64 (7.81 g, 52 mmol) and *trans*-chalcone (21.53 g, 103 mmol) were dissolved in 5 mL of 1,2-dichloroethane and heated to 70 °C in an Ace Pressure Tube (Ace Glass Inc., 4-10 bar). $\text{HBF}_4 \cdot \text{Et}_2\text{O}$ (16.74 g, 103 mmol, 52 % ethereal solution) was added dropwise. It was stirred at 70 °C during 20 h. and an orange precipitate appeared. It was filtered, washed with Et_2O , and recrystallized from hot MeOH to render 9.00 g of the desired compound as orange crystals (41 % yield).



$^1\text{H}\{^{19}\text{F}\}$ -NMR (MeOD, 400.1 MHz) δ (ppm): 4.21 (s, 3H), 7.24 (d, $J = 8.5$ Hz, 1H), 7.85 (m, 4H), 7.93 (m, 2H), 8.49 (d, $J = 7.3$ Hz, 2H), 8.54 (d, $J = 7.3$ Hz, 2H), 8.79 (dd, $J = 8.5$ Hz, $J = 2.6$ Hz, 1H), 9.00 (d, $J = 1.6$ Hz, 1H), 9.02 (d, $J = 1.6$ Hz, 1H), 9.45 (d, $J = 2.6$ Hz, 1H); $^{19}\text{F}\{^1\text{H}\}$ -NMR (MeOD, 376.5 MHz) δ (ppm): -154.95, -155.00; 1,2 $^{13}\text{C}\{^1\text{H}\}$ -NMR (MeOD, 100.6 MHz) δ (ppm): 53.89, 112.15, 114.24, 114.38, 128.29, 129.25, 129.35, 129.87, 129.91, 134.90, 138.07, 149.81, 166.23, 168.29, 170.14, 170.61. HR-MS (ESI+ve): m/z calcd for $\text{C}_{23} \text{H}_{18} \text{N} \text{O}_2$ ($[\text{M}]^+$) 340.1338, found 340.1331.

2-(6-methoxy-3-pyridyl)-4,6-diphenyl- λ^3 -phosphinine (**66**)

METHOD A: In a flame dried Schlenk vessel **65** (3.0 g, 7 mmol) was partially dissolved in 20 mL of degassed CH_3CN . $\text{P}(\text{SiMe}_3)_3$ (3.7 g, 15 mmol) was added and the mixture was heated to 85 °C for 6 h. After that the solvent was removed under vacuum and the remaining brown powder was dissolved in 20 mL of CH_2Cl_2 . It was purified by silica column chromatography using diethyl ether/ethyl acetate (4:1) as eluent. After removing the solvent 0.8 g of the product as brown powder were obtained (33 % yield).



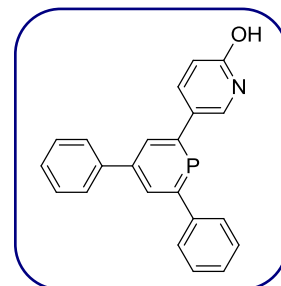
METHOD B: In a flame dried Schlenk vessel **65** (3.0 g, 7 mmol) and $\text{P}(\text{CH}_2\text{OH})_3$ (1.7 g, 14 mmol) were dissolved in 20 mL of distilled pyridine. The mixture was heated to 125 °C for 3 h. After that, the total reaction volume was reduced to half its original

volume under reduced pressure, and 25 mL of degassed water were added. The mixture was left under vigorous stirring overnight. The aqueous layer was removed and the organics concentrated to dryness. The solid residue was dissolved in a 1:1 mixture of petroleum ether and dichloromethane and filtered over silica. After removing the solvent, a 0.5 g of a dark yellow solid was obtained (20 % yield).

$^1\text{H}\{^{31}\text{P}\}$ -NMR (CDCl_3 , 500.1 MHz) δ (ppm): 4.01 (s, 3H), 6.87 (d, $J = 8.4$ Hz, 1H), 7.43 (m, 2H), 7.50 (m, 4H), 7.69 (d, $J = 7.7$ Hz, 2H), 7.74 (d, $J = 7.7$ Hz, 2H), 7.95 (dd, $J = 8.4$ Hz, $J = 2.6$ Hz, 1H), 8.11 (d, $J = 0.9$ Hz, 1H), 8.19 (d, $J = 0.9$ Hz, 1H), 8.54 (d, $J = 2.6$ Hz, 1H); $^{31}\text{P}\{^1\text{H}\}$ -NMR (CDCl_3 , 202.5 MHz) δ (ppm): 185.00; $^{13}\text{C}\{^1\text{H}\}$ -NMR (CDCl_3 , 125.7 MHz) δ (ppm): 110.98, 127.65, 127.76, 128.11, 128.98, 129.07, 131.31 (d, $J = 12.0$ Hz), 131.82 (d, $J = 12.0$ Hz), 137.89, 137.98, 142.01 (d, $J = 2.8$ Hz), 143.19 (d, $J = 24.0$ Hz), 144.38 (d, $J = 13.9$ Hz), 145.06 (d, $J = 13.9$ Hz), 164.22, 167.8 (d, $J = 51.8$ Hz), 171.94 (d, $J = 51.8$ Hz). HR-MS (ESI+ve): m/z calcd for $\text{C}_{23} \text{H}_{19} \text{N O P}$ ($[\text{M}+\text{H}]^+$) 356.1204, found 356.1215.

2-(6-hydroxy-3-pyridyl)-4,6-diphenyl- λ^3 -phosphinine (59)

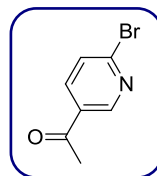
66 (1.5 g, 4.2 mmol) was dispersed in 100 mL of a degassed solution of HCl (3M, 300 mmol). The reaction mixture was refluxed for 24 h and then after cooling down to r.t. K_2CO_3 was added in portions to reach pH 9. The aqueous solution was extracted with CH_2Cl_2 . The organics were collected, dried over MgSO_4 , filtered and concentrated, to obtain 1.06 g of the product as pale orange solid (74 % yield).



$^1\text{H}\{^{31}\text{P}\}$ -NMR (CDCl_3 , 400.1 MHz) δ (ppm): 6.73 (m, 1H), 7.44 (m, 2H), 7.49 (m, 4H), 7.69 (m, 4H), 7.81 (m, 1H), 7.94 (m, 1H), 8.01 (m, 1H), 8.16 (d, $J = 4.8$ Hz, 1H), 12.77 (br s, 1H); $^{31}\text{P}\{^1\text{H}\}$ -NMR (CDCl_3 , 162.0 MHz) δ (ppm): 182.7. HR-MS (ESI+ve): m/z calcd for $\text{C}_{22} \text{H}_{17} \text{N O P}$ ($[\text{M}+\text{H}]^+$) 342.1048, found 342.1061.

1-(6-bromo-3-pyridyl)ethanone (**67**)

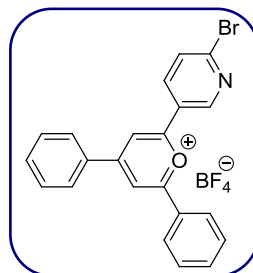
2,5-dibromopyridine (3.08 g, 13.0 mmol) was dissolved in 50 mL of dry diethyl ether. The solution was cooled down to $-80\text{ }^{\circ}\text{C}$ and *n*-BuLi (8.14 mL, 13.02 mmol, 1.6 M in hexanes) was added dropwise under Ar. The mixture was stirred at $-80\text{ }^{\circ}\text{C}$ for 30 min. Then, at this temperature, *N,N*-dimethylacetamide (1.4 mL, 15.06 mmol, distilled over BaO) was added dropwise. The crude reaction was allowed reach r.t. Then it was poured into 200 mL of NH_4Cl saturated solution. It was partitioned, and the aqueous layer was washed with 3x150 mL Et_2O . The organics were collected and washed with brine, dried over MgSO_4 , filtered and concentrated. The solid obtained was dissolved in the minimum amount of CH_2Cl_2 and purified by silica column chromatography using an initial mixture of eluents hexane/ethyl acetate 4:1 and increasing the polarity (1.13 g, 43 % yield).



^1H -NMR (CDCl_3 , 400.1 MHz) δ (ppm): 2.62 (s, 3H), 7.61 (d, $J = 8.4$ Hz, 1H), 8.07 (dd, $J = 8.4$ Hz, $J = 2.3$ Hz, 1H), 8.89 (d, $J = 2.3$ Hz, 1H); $^{13}\text{C}\{^1\text{H}\}$ -NMR (CDCl_3 , 125.7 MHz) δ (ppm): 26.74, 128.44, 131.48, 137.69, 146.98, 150.45, 195.60.³

2-(6-bromo-3-pyridyl)-4,6-diphenylpyrylium tetrafluoroborate (**68**)

67 (4.56 g, 22.8 mmol) and *trans*-chalcone (9.56 g, 45.9 mmol) were dissolved in 20 mL of 1,2-dichloroethane and heated to $70\text{ }^{\circ}\text{C}$ in an Ace Pressure Tube (Ace Glass Inc., 4-10 bar). $\text{HBF}_4 \cdot \text{Et}_2\text{O}$ (7.46 g, 46.1 mmol, 52 % ethereal solution) was added dropwise. It was stirred at $70\text{ }^{\circ}\text{C}$ for 48 h and a yellow precipitate appeared. It was filtered, washed with Et_2O , and recrystallized from hot MeOH to have 1.76 g of orange crystals (16 % yield).

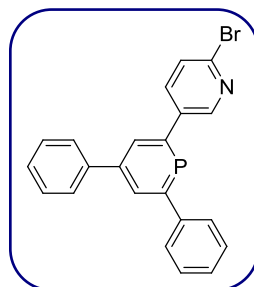


$^1\text{H}\{^{19}\text{F}\}$ -NMR (MeOD, 400.1 MHz) δ (ppm): 7.88 (m, 2H), 7.96 (m, 2H), 8.11 (d, $J = 8.5$ Hz, 1H), 8.54 (m, 2H), 8.63 (m, 2H), 8.79 (dd, $J = 8.5$ Hz, $J = 2.6$ Hz, 1H), 9.19 (s, 2H), 9.51 (d, $J = 2.6$ Hz, 1H); $^{19}\text{F}\{^1\text{H}\}$ -NMR (MeOD, 376.5 MHz) δ (ppm): -154.91 , -154.96 ;^{1,2} $^{13}\text{C}\{^1\text{H}\}$ -NMR (MeOD, 125.7 MHz) δ (ppm): 115.77, 115.89, 128.76, 129.25, 129.69, 129.99, 130.04, 135.49, 135.53, 137.82, 152.16, 152.33, 152.50.

HR-MS (ESI+ve): m/z calcd for $C_{22}H_{15}NOBr$ ($[M]^+$) 388.0337, found 388.0313.

2-(6-bromo-3-pyridyl)-4,6-diphenyl- λ^3 -phosphine (**69**)

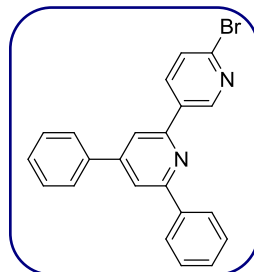
In a flame dried Schlenk vessel **68** (1.00 g, 2.1 mmol) was partially dissolved in 10 mL of degassed CH_3CN . $P(SiMe_3)_3$ (1.10 g, 4.4 mmol) was added and the mixture was heated to 85 °C for 6 h. The solvent was removed under vacuum and the remaining brown residue dissolved in 10 mL of CH_2Cl_2 . It was purified by means of silica column chromatography using a mixture of diethyl ether/ethyl acetate (4:1) as eluent. After removing the solvent 0.28 g of the product as brown powder were obtained (33 % yield).



$^1H\{^{31}P\}$ -NMR ($CDCl_3$, 500.1 MHz) δ (ppm): 7.45 (m, 2H), 7.51 (m, 4H), 7.60 (d, $J = 8.1$ Hz, 1H), 7.68 (m, 2H), 7.73 (m, 2H), 7.90 (dd, $J = 8.1$ Hz, $J = 2.6$ Hz, 1H), 8.12 (d, $J = 1.1$ Hz, 1H), 8.24 (d, $J = 1.1$ Hz, 1H), 8.71 (d, $J = 2.6$ Hz, 1H); $^{31}P\{^1H\}$ -NMR ($CDCl_3$, 202.5 MHz) δ (ppm): 187.42; $^{13}C\{^1H\}$ -NMR ($CDCl_3$, 125.7 MHz) δ (ppm): 127.64, 127.74, 127.77, 128.12, 128.32, 129.06, 131.81 (d, $J = 12.9$ Hz), 132.56 (d, $J = 12.0$ Hz), 137.37, 137.47, 141.6 (d, $J = 3.7$ Hz), 142.8 (d, $J = 24.0$ Hz), 144.74 (d, $J = 13.9$ Hz), 148.37 (d, $J = 12.95$ Hz), 166.04 (d, $J = 52.7$ Hz), 172.21 (d, $J = 51.8$ Hz). HR-MS (ESI+ve): m/z calcd for $C_{22}H_{16}NPBr$ ($[M+H]^+$) 404.0204, found 404.0209.

6'-bromo-4,6-diphenyl-2,3'-bipyridine (**70**)

68 (0.5 g, 1.0 mmol) was dissolved in a stainless steel reactor with 5 mL of ethylene glycol saturated with 1.9 g of NH_3 . The mixture was heated to 90 °C overnight. The solid obtained was filtered and washed with ether. It was dissolved in the minimum amount of CH_2Cl_2 and precipitated with diethyl ether. 0.22 g of a pale yellow product was obtained (55 % yield).

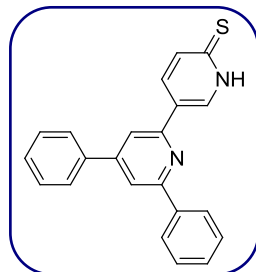


1H -NMR ($CDCl_3$, 400.1 MHz) δ (ppm): 7.48 (m, 2H), 7.54 (m, 4H), 7.63 (d, $J = 8.3$

Hz, 1H), 7.74 (m, 2H), 7.86 (d, $J = 1.1$ Hz, 1H), 7.95 (d, $J = 1.1$ Hz, 1H), 8.16 (m, 2H), 8.41 (dd, $J = 8.3$ Hz, $J = 2.5$ Hz, 1H), 9.11 (d, $J = 2.5$ Hz, 1H). HR-MS (ESI+ve): m/z calcd for $C_{22} H_{16} N_2 Br$ ($[M+H]^+$) 387.0497, found 387.0491.

4,6-diphenyl-[2,3'-bipyridine]-6'-(1'H)-thione (**61**)

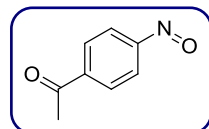
70 (0.22 g, 0.57 mmol) was added to a solution of NaHS (0.32 g, 5.74 mmol) in 12 mL of DMF. Then, KOH (0.10 g, 1.7 mmol) was added and the mixture was refluxed overnight. It was cooled down to r.t. and filtered off. The filtrate was concentrated to half of the initial volume and 50 mL of water were added. HCl 6 M was added until pH acid to litmus, and a yellow solid appeared. The solid was filtrated and dissolved in the minimum amount of CH_2Cl_2 , then it was washed twice with 50 mL of water. The organic layer was concentrated to dryness to obtain a 0.16 g of the product as yellow powder (82 % yield).



1H -NMR ($CDCl_3$, 400.1 MHz) δ (ppm): 7.49 (m, 2H), 7.53 (m, 4H), 7.72 (m, 4H), 7.90 (d, $J = 1.1$ Hz, 1H), 8.13 (m, 2H), 8.21 (dd, $J = 9.0$ Hz, $J = 1.9$ Hz, 1H), 8.52 (d, $J = 1.9$ Hz, 1H), 12.88 (br s, 1H). HR-MS (ESI+ve): m/z calcd for $C_{22} H_{17} N_2 S$ ($[M+H]^+$) 341.1112, found 341.1102.

1-(4-nitrosophenyl)ethanone (**72**)

4-nitroacetophenone (4.04 g, 24.5 mmol) was dispersed in a solution of NH_4Cl (1.50 g, 28.0 mmol) in 50 mL of water. Zn (dust, 3.81 g, 58.3 mmol) was added and after 1 h stirring at r.t.



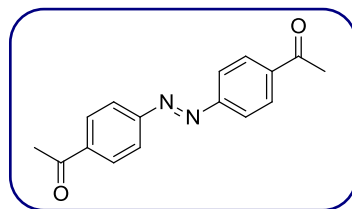
the mixture was filtered off, and the solid washed with 60 mL of hot water. To the aqueous solution, 20 g of ice were added, and a mixture of 7.5 mL of H_2SO_4 and 20 g of ice were added to it. The mixture was vigorously stirred and the temperature maintained at $0^\circ C$. A solution of sodium dichromate dihydrate (1.7 g, 5.7 mmol) in 8 mL of water was added and the yellow solid obtained was filtered to obtain 1.35 g of the product (37 % yield).

1H -NMR ($CDCl_3$, 400.1 MHz) δ (ppm): 2.69 (s, 3H), 7.96 (d, $J = 8.3$ Hz, 2H), 8.19 (d,

$J = 8.3$ Hz, 2H); $^{13}\text{C}\{^1\text{H}\}$ NMR (CDCl_3 , 100.6 MHz) δ (ppm): 27.13, 120.78, 129.71, 140.92, 163.99, 197.17.

(*E*)-4,4'-bis-aceto-azobenzene (**73**)

METHOD A: 4-aminoacetophenone (5.23 g, 38.7 mmol) was partially dissolved in 200 mL of dry toluene. Activated MnO_2 (18.76 g, 215.8 mmol) was added and the mixture was heated to reflux. After 48 h. the crude was filtered over basic alumina using CH_2Cl_2 to collect all the orange solution. The solvent was removed and the solid was subjected to column chromatography using basic alumina and a mixture of increasing polarity CH_2Cl_2 :hexane. 3.45 g of the product were obtained as orange powder (67 % yield).

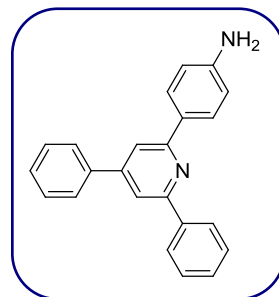


METHOD B: **72** (0.46 g, 3.1 mmol) and 4-aminoacetophenone (0.42 g, 3.1 mmol) were partially dissolved in in 20 mL of acetic acid. After 3 h, the solvent was removed under vacuum and subjected to silica column chromatography using a mixture of AcOEt:hexane (3:2, and the minimum amount of CH_2Cl_2 to solubilize the solid). 0.38 g of the orange product were obtained (46 %).

^1H -NMR (CDCl_3 , 400.1 MHz) δ (ppm): 2.67 (s, 6H), 8.01(d, $J = 8.7$ Hz, 4H), 8.12 (d, $J = 8.7$ Hz, 4H). HR-MS (ESI+ve): m/z calcd for $\text{C}_{16}\text{H}_{15}\text{N}_2\text{O}_2$ ($[\text{M}+\text{H}]^+$) 267.1134, found 267.1135.

4-(4,6-diphenyl-2-pyridyl)aniline (**75**)

In the following order: ammonium acetate (3.04 g, 39.43 mmol), *N*-phenylacetylpyridinium bromide (0.34 g, 1.22 mmol), 4-aminoacetophenone (0.14 g, 1 mmol), 2 mL of acetic acid, and benzaldehyde (102 μL , 1 mmol) were placed in a 100 mL round bottom flask. A condenser was adapted and then it was introduced in the MW apparatus (CEM Focused MicrowaveTM, Model Discover). The reaction was performed at 130 W for 2 min (T_{max} 140 $^\circ\text{C}$). After cooling the reaction mixture to

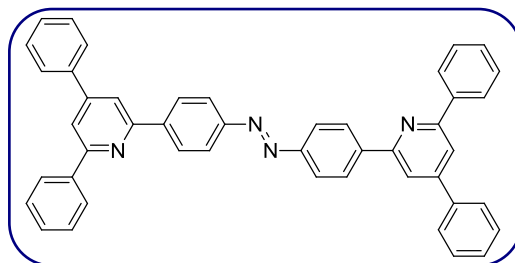


r.t., 50 mL of water were added and the reaction mixture was stirred for 1 h. The orange precipitate was filtered to obtain 0.29 g of the product (91 % yield).

$^1\text{H-NMR}$ (CD_2Cl_2 , 400.1 MHz) δ (ppm): 4.80 (br s, 2H), 6.56 (d, $J = 8.6$ Hz, 2H), 7.48 (m, 6H), 7.74 (d, $J = 7.1$ Hz, 2H), 7.79 (s, 2H), 8.06 (d, $J = 8.6$ Hz, 2H), 8.19 (d, $J = 7.1$ Hz, 2H). HR-MS (ESI+ve): m/z calcd for $\text{C}_{23} \text{H}_{19} \text{N}_2$ ($[\text{M}+\text{H}]^+$) 323.1548, found 323.1543.

(*E*)-1,2-bis(4-(4,6-diphenyl-2-pyridyl)phenyl)diazene (63)

75 (1.73 g, 5.4 mmol) was partially dissolved in 100 mL of toluene, activated MnO_2 (2.59 g, 29.8 mmol) was added and the mixture was heated to reflux, using a Dean–Stark. After 6 h, it was cooled to r.t. and filtered over basic



alumina, washing with CH_2Cl_2 . The organics were collected and the solvent removed to yield 0.35 g of product as orange powder. (20 % yield).

$^1\text{H-NMR}$ (CDCl_3 , 500.1 MHz) δ (ppm): 7.52 (m, 12H), 7.79 (d, $J = 7.33$ Hz, 4H), 7.95 (d, $J = 1.47$ Hz, 2H), 7.99 (d, $J = 1.47$ Hz, 2H), 8.12 (d, $J = 8.43$ Hz, 4H), 8.24 (d, $J = 7.33$ Hz, 4H), 8.41 (d, $J = 8.80$ Hz, 4H); $^{13}\text{C}\{^1\text{H}\}$ -NMR (CDCl_3 , 125.7 MHz) δ (ppm): 117.46, 117.66, 123.40, 127.18, 127.23, 127.90, 128.80, 129.11, 129.19, 129.21, 138.96, 139.50, 141.98, 150.45, 153.06, 156.49, 157.79. HR-MS (ESI+ve): m/z calcd for $\text{C}_{46} \text{H}_{33} \text{N}_4$ ($[\text{M}+\text{H}]^+$) 641.2705, found 641.2711.

References and notes

1. Atanassova, M. S.; Dimitrov, G. D. *Spectrochim. Acta, Part A* **2003**, *59*, 1655.
2. Hofstetter, C.; Pochapsky, T. C. *Magn. Reson. Chem.* **2000**, *38*, 90.
3. Hatanaka, M.; Takahashi, K.; Nakamura, S.; Mashino, T. *Bioorg. Med. Chem.* **2005**, *13*, 6763.

CONCLUDING REMARKS OF THE THESIS

According to the objectives presented, the concluding remarks of the Thesis are:

Part I

- A new series of azophosphines has been synthesized.
- Studies of irradiation on metal complexes containing these azophosphines demonstrated that the switchability of azobenzene was not quenched by metal coordination.
- The performance of the azophosphines in several catalytic reactions has been tested. It has been proved that activity in palladium catalyzed allylic alkylation and rhodium catalyzed hydroformylation is affected by light irradiation. However, no effect of the isomerization of the ligands was observed in the palladium catalyzed Suzuki cross-coupling and rhodium catalyzed hydrosilylation.

Part II

- A general *tropos* diphosphine backbone has been synthesized.
- A weak interaction has been predicted for the hypothetical assembly based on hydrogen bonding interactions between the diphosphine and the chiral modifiers. After evaluating the strength of the ionic supramolecular interaction, the system has been successfully characterized in terms of partially bound states.
- The chiral induction from the modifiers to the *tropos* diphosphine backbone has been tested in asymmetric hydrogenation. The unsatisfactory results could be explained by the fact that the system designed does not accomplish all the requirements to have an effective chiral induction by supramolecular ionic interactions.

Part III

- A set of monodentate phosphinine and pyridine ligands able to coordinate preferentially in a *trans*-fashion to a metal has been synthesized.
- A switchable azo-bis-pyridine ligand has been synthesized.

UNIVERSITAT ROVIRA I VIRGILI
SWITCHABLE AND TUNABLE LIGANDS FOR HOMOGENEOUS CATALYSIS
Maria Dolores Segarra Maset
ISBN:978-84-693-7666-9/DL:T-1755-2010

APPENDIX I

MM2 STRUCTURE OPTIMIZATIONS

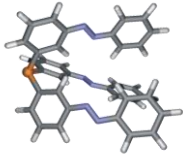
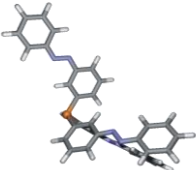
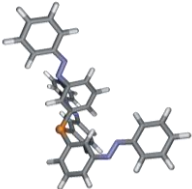
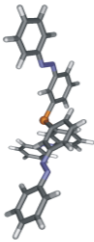
On account of the unexpected catalytic results obtained with ligand **3** (for instance in hydrosilylation reaction), it was decided to perform molecular mechanics calculations on monophosphine **3** to obtain an impression of the shape of the ligand. We envisaged a bowl-type structure after irradiation, especially for the *ZZZ-3* isomer, but also crowded structures were presumed for the *ZEE-3* and *ZZE-3* ligands. The thermodynamically most stable *EEE-3* isomer, however, was expected not to form a pocket and act as a common triphenylphosphine in catalysis. The visual effect is depicted in Figure 2. 4 (see chapter 2).

The catalytic results with this phosphine were not in agreement with this “ideal” behaviour, since the non-irradiated phosphine gave results similar to those obtained with BSP.

Rotation around the P–C bonds allows the azobenzene moiety (*meta* positioned) to move from the “back part of the phosphine” closer to the lone pair of the phosphorus atom. This is feasible in any of the isomers of phosphine **3** (*i.e.* *EEE*, *EEZ*, *ZZE*, *ZZZ*). Clearly, in this situation, the steric hindrance around the phosphorus coordination site will be more pronounced if the azobenzene is in a *Z* configuration. The question we are considering now, in view of the results, is if it is possible to generate a reasonable steric hindrance around the phosphorus lone pair when the three azobenzene moieties are present as *E* isomers.

Molecular mechanics calculations were done using MM2 force field,¹ as implemented in CAChe v. 6.1.1. Minimum energy conformations were located by using a block diagonal Newton–Raphson algorithm. Optimization continues until the energy change is less than 0.001 kcal/mol.

Table I. 1. Selected conformations and calculated energies of *EEE-3*.

Entry	Structures	Energy kcal/mol
1		-28.0 kcal/mol
2		-27.1 kcal/mol
3		-26.2 kcal/mol
4		-26.2 kcal/mol
5		-26.1 kcal/mol

Calculations on the *Z* isomers are not reported because the program used tends to convert the *Z* structure to the *E* form.

The more stable *EEE-3* structure is the one that places the three azo groups far from the P lone pair. However, the energy difference between the structures is less than 2 kcal/mol. Having a look on the structures, one can notice that structure 5 (Table I. 1) resembles a BSP with small depth (*d*) and large diameter (*l*), (see Figure 3. 2).

It was found in literature that, the energy barrier for the rotation through P–C bond for triphenylphosphine was calculated to be around 0.4–0.8 kcal/mol.²⁻⁴ For more sterically demanding monophosphines with bis-*meta* substituents in the aryl moieties, this rotation barrier energy was found to be 3.8 kcal/mol.³ For *EEE-3* phosphine, as it only has one substituent in the *meta* position, this energy is expected to be low enough to allow the rotation. The CAChe functionality to estimate rotational barriers gave values for the present compounds below 8 kcal/mol. Even at this value, rotation is extremely fast.

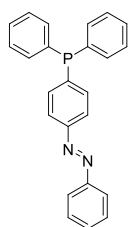
In conclusion, with *EEE-3* it is possible to generate a pseudo-BSP, which could be the cause for the behaviour of this phosphine in some of the catalytic experiments.

References and notes

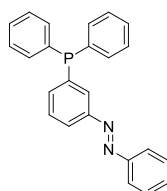
1. Bowen, J. P.; Allinger, N. L. *J. Org. Chem.* **1987**, *52*, 2937.
2. Polowin, J.; Mackie, S. C.; Baird, M. C. *Organometallics* **1992**, *11*, 3724.
3. Kreiter, R.; Gebbink, R. J. M. K.; van Koten, G. *Tetrahedron* **2003**, *59*, 3989.
4. Mislow, K. *Acc. Chem. Res.* **1976**, *9*, 26.

APPENDIX II

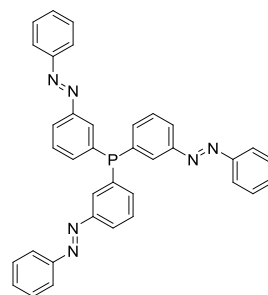
COMPOUNDS INDEX



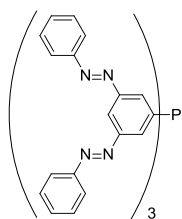
1



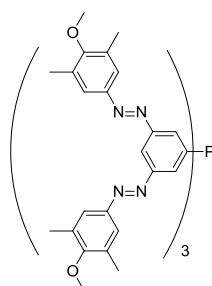
2



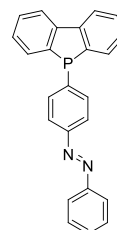
3



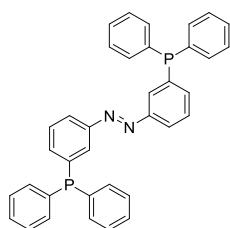
4



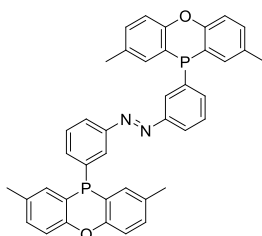
5



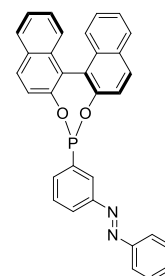
6



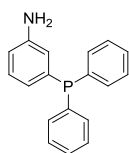
7



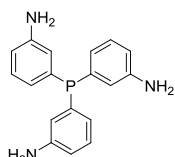
8



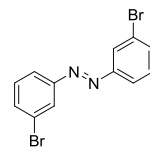
9



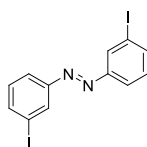
10



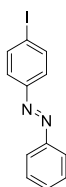
11



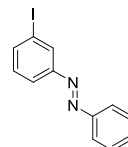
12



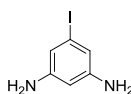
13



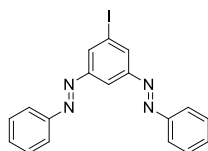
14



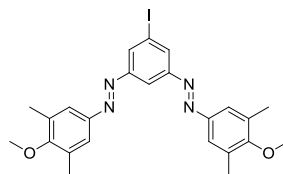
15



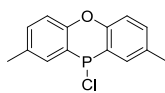
16



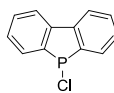
17



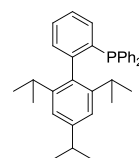
18



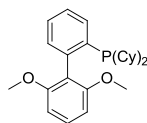
19



20



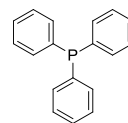
21



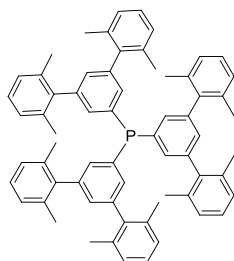
22



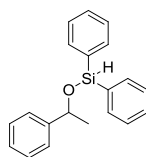
23



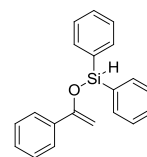
24



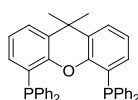
25



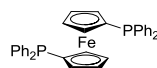
26



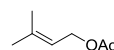
27



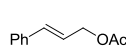
28



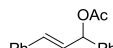
29



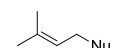
30



31



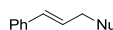
32



33



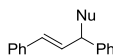
34



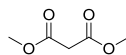
35



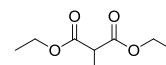
36



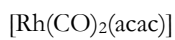
37



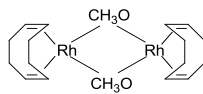
38



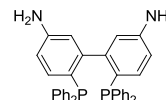
39



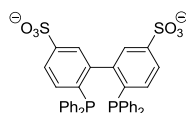
40



41



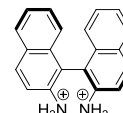
42



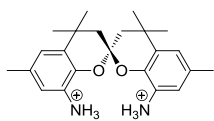
43



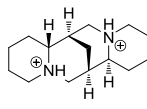
44



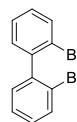
45



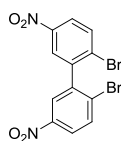
46



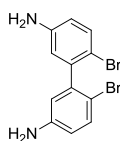
47



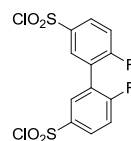
48



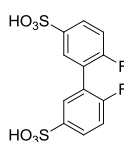
49



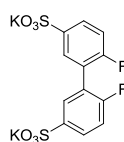
50



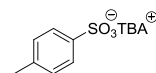
51



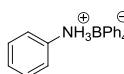
52



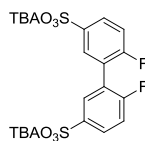
53



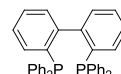
54



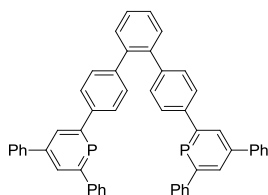
55



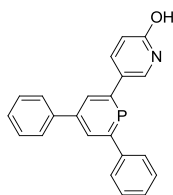
56



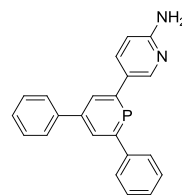
57



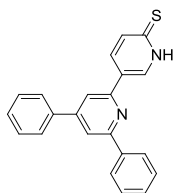
58



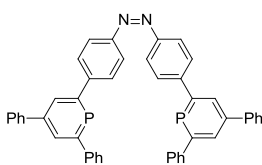
59



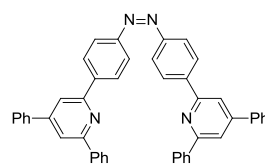
60



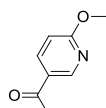
61



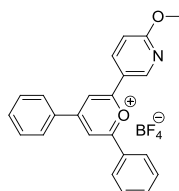
62



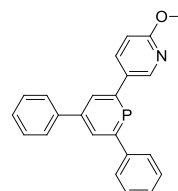
63



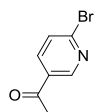
64



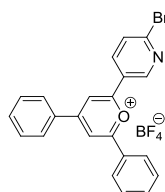
65



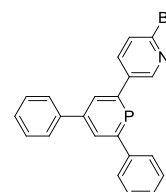
66



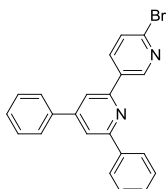
67



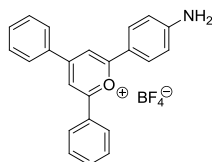
68



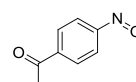
69



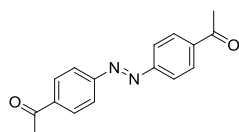
70



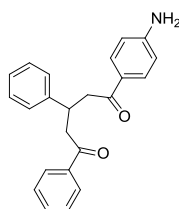
71



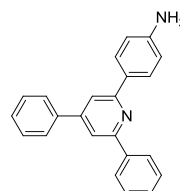
72



73



74



75

UNIVERSITAT ROVIRA I VIRGILI
SWITCHABLE AND TUNABLE LIGANDS FOR HOMOGENEOUS CATALYSIS
Maria Dolores Segarra Maset
ISBN:978-84-693-7666-9/DL:T-1755-2010

ABBREVIATIONS

Abs	absorbance
acac	acetylacetonate
aq. soln.	aqueous solution
Ar	aromatic
BSA	<i>N,O</i> -bis(trimethylsilyl)acetamide
BSP	bowl-shaped phosphine
calcd	calculated
cod	1,5-cyclooctadiene
cy	cyclohexyl
DABCO	1,4-diazabicyclo[2.2.2]octane
dba	dibenzylideneacetone
DBP	dibenzophosphole
DCM	dichloromethane
DMF	<i>N,N</i> -dimethylformamide
DMSO	dimethyl sulfoxide
DNA	deoxyribonucleic acid
DOP	dioctyl phthalate
dpen	1,2-diphenylethylenediamine
dppe	1,2-bis(diphenylphosphino)ethane
dppf	1,1'-bis(diphenylphosphino)ferrocene
e.e.	enantiomeric excess
GC	gas chromatography
ⁱPr	isopropyl
LSP	light switchable phosphine
MeOH	methanol
MePOP	2,8-dimethylphenoxaphosphine

Ms	methanesulfonyl
nbd	norbornadiene
ⁿBuLi	<i>n</i> -butyllithium
NMR	nuclear magnetic resonance
<i>N,N</i>-DMA	<i>N,N</i> -dimethylacetamide
OAc	acetate
OMe	methoxy
PVC	polyvinyl chloride
r.t.	room temperature
TBACl	tetrabutylammonium chloride
Tf	trifluoromethanesulfonyl
TMS	tetramethylsilane
TMEDA	<i>N,N,N',N'</i> -tetramethylethylenediamine
^tBuOK	potassium <i>tert</i> -butoxyde
^tBuOH	<i>tert</i> -butanol
THF	tetrahydrofuran
TLC	thin layer chromatography
UV	ultraviolet
UV-vis	ultraviolet-visible

NMR abbreviations

br	broad
d	doublet
dd	double doublet
ddt	double double triplet
m	multiplet
s	singlet
t	triplet

UNIVERSITAT ROVIRA I VIRGILI
SWITCHABLE AND TUNABLE LIGANDS FOR HOMOGENEOUS CATALYSIS
Maria Dolores Segarra Maset
ISBN:978-84-693-7666-9/DL:T-1755-2010

UNIVERSITAT ROVIRA I VIRGILI
SWITCHABLE AND TUNABLE LIGANDS FOR HOMOGENEOUS CATALYSIS
Maria Dolores Segarra Maset
ISBN:978-84-693-7666-9/DL:T-1755-2010